Alexandre Artur Pinho Rodrigues

Heteroclinic Phenomena

Departamento de Matemática
Faculdade de Ciências da Universidade do Porto
2011

Alexandre Artur Pinho Rodrigues

Heteroclinic Phenomena

Tese submetida à Faculdade de Ciências da Universidade do Porto para obtenção do grau de Doutor em Matemática

Agosto de 2011

U.PORTO

FACULDADE DE CIÊNCIAS
UNIVERSIDADE DO PORTO

You must have chaos within you to give birth to a dancing star.
Friedrich Nietzsche

Acknowledgement

Vai caminhando desamarrado
Dos nós e laços que o mundo faz
Vai abraçando desenleado
De outros abraços que a vida dá
(...)

Liberta o grito que trazes dentro
E a coragem e o amor
Mesmo que seja só um momento
Mesmo que traga alguma dor
Só isso faz brilhar o lume
Que hás-de levar até ao fim
E esse lume já ninguém pode
Nunca apagar dentro de ti

Mafalda Veiga, O Lume

I would like to express my gratitude to *Isabel Labouriau* and *Manuela Aguiar*, whithout whom this thesis would not have been written. They have generously given their time and guidance in writing this thesis. Their knowledge and patient advise have been invaluable. Thanks also for their continuing support and understanding.

I am grateful for the precious discussions and support of *Michael Field* and *Nikita Agarwal*, during my visit to the University of Houston (USA) and afterwards. I am also thankful to *Maria Carvalho* for keeping the door of her office always open to me. I dedicate this work to my *little star* and to my genuine friends which are always giving me support and unfailing encouragement.

My research had financial support from *Fundação para a Ciência e a Tecnologia* (FCT), Portugal, through the programs POCTI and POSI with European Union and national funding, from the grant SFRH/BD/28936/2006 of FCT and from NSF Grant DMS-0806321 (USA).

Resumo

O estudo de redes heteroclínicas pode ser visto como o centro organizador para a compreensão de dinâmicas complexas. Nos seis trabalhos que constituem esta tese, pretendemos investigar a dinâmica perto de redes heteroclínicas: nos artigos 1–5, os nós das redes heteroclínicas são selas-foco ou soluções periódicas não triviais. No artigo 6, estuda-se a dinâmica perto do produto de sistemas planares atractores. Em seguida, vamos descrever, de uma forma sumária, os principais conteúdos dos seis artigos.

No artigo 1, estabelece-se um mecanismo para a existência de *comutação heteroclínica* perto de uma rede mergulhada numa variedade tridimensional, cujos nós são soluções periódicas ou selas-foco. Recorrendo à transversalidade das variedades invariantes bidimensionais de nós consecutivos, provamos que perto da rede existem trajectórias que visitam as vizinhanças das selas, sombreando as ligações heteroclínicas da rede por qualquer ordem pré-determinada.

Usando dinâmica simbólica, no artigo 2 caracterizamos um outro fenómeno dinâmico que existe perto de um ciclo heteroclínico entre soluções periódicas: *ciclicidade caótica*; este fenómeno ocorre quando há trajectórias que seguem o ciclo, dando um qualquer número de voltas em torno das soluções periódicas. Sob condições genéricas, provamos a existência de *ciclicidade caótica* e encontramos um conjunto de condições iniciais, robusto e transitivo, cujas trajectórias seguem eternamente o ciclo. Na restrição a este conjunto, provamos que a discretização do campo é conjugada a um *Shift* de Markov associado a um alfabeto finito. Também generalizamos a técnica de *levantamento por rotação* de Aguiar, Castro and Labouriau (2006) e ilustramos os nossos resultados com simulações numéricas associadas a um exemplo concreto.

Invocando as noções de *comutação heteroclínica* perto de uma rede com nós de rotação, obtemos no artigo 3, evidências analíticas de que o modelo matemático estudado por Melbourne, Proctor and Rucklidge (2001) é relevante para o estudo das reversões do campo magnético da Terra. Apresentamos simulações de soluções do modelo, todas elas consistentes com o comportamento efectivo do campo magnético da Terra o qual, por sua vez, está documentado por vários estudos paleomagnéticos.

Os artigos 4 e 5 estão relacionados. No artigo 5, investigam-se os efeitos da adição de dois termos independentes que quebram a simetria na dinâmica perto de uma rede heteroclínica assimptoticamente estável. Quando uma simetria é quebrada, cada ciclo da rede

é substituído por uma solução periódica atractora. Quando a outra simetria é quebrada, surge um atractor contendo dois pontos de equilíbrio hiperbólicos, um conjunto hiperbólico básico não trivial e trajectórias heteroclínicas ligando transversalmente os dois pontos de equilíbrio. No artigo 4, contruimos explicitamente um campo de vectores numa esfera tridimensional, contendo um atractor com estas características. Perturbações genéricas deste campo de vectores têm ainda um atractor contendo um conjunto hiperbólico básico. Órbitas homoclínicas do tipo Shilnikov (1967) associadas a selas-foco emergem como um fenómeno de codimensão 2.

Finalmente, o artigo 6 é uma extensão dos resultados provados por Ashwin and Field (2005); apresentamos resultados gerais para o produto de atractores homoclínicos planares, os quais afirmam que o conjunto limite provável da bacia de atracção do produto de ciclos homoclínicos é a rede heteroclínica definida pela união dos atractores.

Nesta tese, tentando ao máximo expôr os assuntos de um modo auto-suficiente, apresentamos seis assuntos de investigação actuais relacionados com ciclos e redes heteroclínicos.

Abstract

Heteroclinic networks may be seen as the skeleton for the understanding of complicated dynamics. The six works in this thesis investigate the dynamics near heteroclinic networks; in articles [1–5] the nodes of the heteroclinic networks are either saddle-foci or non-trivial periodic solutions. In article 6, we study of the dynamics near the product of attracting planar systems. Below, we give a brief description of the contents of each of the six articles.

In article 1, we establish a mechanism for the existence of *switching* near a heteroclinic network embedded in a three-dimensional manifold whose nodes are either periodic solutions or saddle-foci. Asking for transversality of the connections that take place in two-dimensions, we prove that close to the network there are trajectories that visit neighbourhoods of the saddles following the heteroclinic connections of the network in any prescribed order.

Using symbolic dynamics, we characterize in article 2 another dynamical phenomenon existing near heteroclinic cycles of periodic solutions: *chaotic cycling*; it occurs when there are trajectories that follow the cycle making any prescribed bi-infinite sequence of turns near the periodic solutions. Under generic conditions, we prove the existence of *cycling* and we find a robust and transitive set of initial conditions whose trajectories follow the cycle for all time. Restricted to this set, we prove that the discretization is conjugate to a Markov shift over a finite alphabet. We also generalize the technique of *lifting by rotation* of Aguiar, Castro and Labouriau (2006) and we illustrate our results with numerical simulations on a concrete example.

Invoking the theoretical notion of *switching* near a network of rotating nodes, we obtain in article 3, analytical evidence that a mathematical model given by Melbourne, Proctor and Rucklidge (2001) is relevant for the study of georeversals. We also present numerical plots of solutions of the model, all of them consistent with the behaviour of the geomagnetic field documented by several paleomagnetic studies.

Articles 4 and 5 are related. In article 5, the effect of two independent forced symmetry breaking terms on the dynamics near an asymptotically stable heteroclinic network is investigated. When one symmetry is broken, each cycle on the network is replaced by an attracting periodic solution. When the other symmetry is broken, an attractor emerges, containing two hyperbolic equilibria, a non-trivial hyperbolic basic set and heteroclinic

trajectories connecting transverselly the two equilibria. In article 4, we construct explicitly a vector field on a three-dimensional sphere, with an attractor with these features. Generic perturbations of this vector field will still have an attractor containing a hyperbolic basic set. Homoclinic orbits of Shilnikov type (1967) associated to a saddle-focus bifurcate as a phenomenon of codimension 2.

Finally, article 6 gives an extension of the results proved by Ashwin and Field (2005): we present general results for the product of planar homoclinic attractors which state that the *likely limit set* of the basin of attraction of the product of two such attractors is always the heteroclinic network defined as the union of the attractors.

In this thesis we have endeavoured to make a self contained exposition bringing together six current research topics related to heteroclinic cycles and networks.

Contents

Introduction

C'est véritablement utile puisque c'est joli.
A. de Saint-Exupéry, Le Petit Prince

State of Art

Recent studies in several areas have emphasized ways in which heteroclinic cycles and networks associated to equilibria, periodic solutions and chaotic sets may be responsible for intermittent dynamics in nonlinear systems. Besides the interest on the study of heteroclinic networks themselves, the chaotic itinerancy which characterizes heteroclinic dynamics models a wide range of phenomena including economics and game theory [**4**] [1], neuronal networks - *bursting of neurons* [**20**], cryptography [**58**] and physics exemplified by the *Rayleigh-Bénard experiment* [**15**] and the geomagnetic field [**54**]. Heteroclinic networks may be seen as the skeleton for the understanding of complicated switching between physical states.

The definition of heteroclinic network emerged according to the particular examples under consideration. In the literature, there are many definitions of heteroclinic cycle and networks - see for instance Field [**21**] or Ashwin and Field [**12**]. Roughly speaking, a heteroclinic cycle is the union of hyperbolic invariant saddles (also called *nodes*) and solutions that connect them. A heteroclinic network is a connected union of heteroclinic cycles (possibly infinite in number), such that for any pair of nodes in the network, there is a sequence of heteroclinic connections connecting them. In [**12**], Ashwin and Field generalize the concept of heteroclinic network as a flow-invariant set that is indecomposable but not recurrent. Some properties of these sets are also derived. In this thesis, we allow n-dimensional connections between two nodes ξ_i and ξ_j ($n > 1$), which can be considered as a set of solutions bi-asymptotic to ξ_i and ξ_j, in negative and positive time, respectively. These heteroclinic connections are what Ashwin and Chossat [**11**] call a *continua of connections*.

[1] The list of references of the sections *Introduction* and *Discussion and Future Work* is on page 207; each article has its own list of references.

Generically in dynamical systems, heteroclinic networks involving equilibria are not structurally stable (in this thesis, we follow the classical definition of Shilnikov *et al* [**75**]: a system is *structurally stable* if every C^1-close system is topologically equivalent to it). In fact, the existence of heteroclinic networks involving at least one equilibrium is typically a phenomenon of codimension at least 1. Nevertheless, heteroclinic networks may occur robustly with respect to symmetric perturbations, even when the invariant manifolds of consecutive nodes are not transverse. Basically, this is due to the following property: symmetry forces the existence of fixed point subspaces, which are not destroyed under symmetric perturbations (see Field [**22**] or Golubitsky *et al* [**27**] for a systematic exposition of the theory of differential equations equivariant under a compact Lie group). It should be clear that generically the heteroclinic networks found in equivariant systems are not persistent under small symmetry breaking perturbations.

Robust heteroclinic networks also appear in the flow of differential equations which do not have symmetry but have invariant hyperplanes - this occurs in the case of population models in which the hyperplanes

$$\{(x_1, \ldots, x_n) \in \mathbf{R}^n : x_i = 0\}$$

should be flow-invariant (see Hofbauer [**33**] and Hofbauer and Sigmund [**38**]). It is also worth to read Aguiar *et al* [**3**], where heteroclinic networks appear in coupled cell systems without symmetry.

The dynamics near a stable heteroclinic cycle is well known and it is characterized by intermittency: a solution remaining near the cycle, spends long periods of time close to each node and makes fast transitions from one node to the next. Usually, in the presence of perfect symmetry, this stability is stronger: the solution approaches the cycle and the time spent near each saddle increases geometrically (*asymptotic stability*). A criterion for the asymptotic stability of a cycle has been given in 1984 by Dos Reis [**63**] and generalized by Krupa and Melbourne [**45, 46**]. Under small non-symmetric perturbations, this recurrence may persist even though the cycle might be destroyed (see Melbourne [**52**] or Kirk and Rucklidge [**42**] for instance), giving rise to the curious phenomenon of *intermittency*.

The rigorous analysis of the intermittent dynamics associated to the structure of the nonwandering sets close to heteroclinic networks is nowadays a big challenge. We refer to Homburg and Sandstede [**38**] for a wide overview of heteroclinic bifurcation and for details on the dynamics near heteroclinic structures.

A remarkable behaviour occurs near heteroclinic networks associated to equilibria whose linearization involves only real eigenvalues: the ω-limit of almost all trajectories[2] may be contained in a smaller heteroclinic network. This is the concept of *essential*

[2]in the sense of Lebesgue measure

asymptotic stability (see Brannath [**17**] and Melbourne [**53**]). In this setting, Kirk and Silber [**41**] gave one of the most famous examples of an essentially asymptotically stable network with two cycles, in $\mathbf{R}^4$; in their example, the authors prove that almost all trajectories approach one cycle. This is closely related to the conjecture of Ashwin and Chossat [**11**] that states that if Σ is a heteroclinic network associated to a finite number of equilibria whose linearization has only real eigenvalues, then the connections associated to the strongest expanding eigenvalues might determine a smaller attracting subnetwork. Partial answers to this problem have already been given: Ashwin and Chossat [**11**] in the case of homoclinic networks and Castro *et al* [**18**], in a quotient network using the notion of railroad switch. The works of Aguiar [**2**] and Aguiar and Castro [**4**] give also interesting insights into random trajectories shadowing the whole network in the conservative setting. The existence of such excursions does not contradict the conjecture of Ashwin and Chossat [**11**] since random trajectories and essential asymptotic stability may coexist.

Numerical simulations involving heteroclinic networks studied by Aguiar [**1**], in which the nodes are either saddle-foci or non-trivial closed trajectories (*rotating nodes*), suggested the existence of trajectories visiting the neighbourhood of the saddles repeatedly but in an irregular fashion. Numerically, it seems to be possible to shadow repeatedly the whole network in any possible (admissible) order through a unique trajectory. This behaviour is what we call hereafter *switching* and it will be strongly related to the existence of *shift dynamics* near the network.

The study of heteroclinic networks in three-dimensions involving saddle-focus began with L. P. Shilnikov who published a set of papers in the sixties ([**69, 71, 72**]). The author described the dynamics of the solutions near a homoclinic cycle associated to a non-resonant saddle-focus. Due to the spiralling geometry near saddle-foci equilibria, the analysis of cycles involving rotating nodes becomes difficult and this is probably why this subject was left almost untouched during more than 20 years.

During the eighties, P. Holmes [**34**] studied the dynamics near the *figure-eight* [3] using symbolic dynamics and he concluded that for any forward infinite sequence of loops, there is a trajectory following it. From 1984 onwards, the study of heteroclinic cycles with rotating nodes has resulted in many papers on the subject: Bykov [**16**], Glendinning and Sparrow [**25, 26**] and Tresser [**80**].

Recently, there has been a resurgence of interest on this topic: see for example Aguiar *et al* [**5**], Kirk and Rucklidge [**42**] or Postlethwaite and Dawes [**60**]. Related dynamics appears also in Ashwin *et al* [**14**], where the authors associated switching to a random process in the context of the geodynamo model, and in Armbruster *et al* [**10**] where this phenomenon appears after the addition of noise to a robust heteroclinic network. See

[3] Two-symmetric homoclinic loops in $\mathbf{R}^3$ associated to the same saddle-focus.

also Homburg and Knobloch [**36, 37**] or Jukes [**39**], where homoclinic bifurcations have been studied using a functional analytical approach due to Lin [**49**]. Till the beginning of this millennium only few authors have studied rigorously heteroclinic cycles involving non-trivial periodic solutions - see Knobloch [**43**] or more recently Rademacher [**61, 62**]; both authors used the Lin's method.

Overview of the Thesis

In the present thesis, we give a contribution to the understanding of the dynamics near heteroclinic networks involving saddle-foci and (non-trivial) periodic solutions as well as the product of planar heteroclinic networks. This thesis is organised in the form of six self contained articles plus an appendix to article 2. A discussion, with ideas for future work, is presented at the end.

Switching near a Network of Rotating Nodes. Motivated by the works [**1**], [**5**] and [**42**] we try to understand the mechanisms for shadowing all the admissible sequences of heteroclinic connections, through a unique solution of the differential equation. We address this issue in paper 1, where we prove the existence of *switching* for a class of three-dimensional systems. This phenomenon arises as a combination of transverse intersection of the invariant manifolds of the nodes and either the existence of either complex non-real eigenvalues of the linearization at the nodes or the existence of periodic solutions with real Floquet multipliers. We also give an example satisfying the conditions which entail switching. The existence of switching is accompanied by complex dynamics namely the existence of a *increasing nested sequence of suspended horseshoes* with the same shape as the network, accumulating on it.

Chaotic Double Cycling. Essentially motivated by the paper 1 and by a numerical example of a heteroclinic cycle involving three periodic solutions, we asked if there were trajectories that would follow the heteroclinic cycle making any prescribed number of turns near the nodes, for any given bi-infinite sequence of turns (from now on, this phenomenon will be called by *cycling*). This problem had already been studied by Koon *et al* [**44**] and by Moeckel [**55**], in the context of conservative systems (the later work has been developed in the context of the Poincaré's three-body problem). Rademacher [**61, 62**] obtained similar results for cycles involving one equilibrium and one periodic solution, using Lin's method.

In paper 2, in a small section transverse to a cycle of periodic solutions, we capture a robust and transitive set of initial conditions whose trajectories follow the cycle for negative and positive times. We obtain a conjugacy to a Markov shift which generalises that of Alekseev [**8**]. This conjugacy over a finite alphabet allows us to prove the existence

of a heteroclinic network with infinitely many cycles and chaotic dynamics near them, exhibiting themselves switching and cycling. The particular point of this work is that given a system of Poincaré sections transverse to the periodic solutions, it will be possible to code all trajectories that remain near the cycle for all time.

Generalizing the concept of *lifting by rotation* of a vector field of Aguiar *et al* [**6**], we construct explicitly a system of differential equations in $\mathbf{R}^6$ whose flow has a normaly hyperbolic attracting manifold containing a heteroclinic cycle with three periodic solutions. We give numerical evidence that the phenomenon of cycling holds in a perturbation of the vector field. In appendix 1, we review results on the center manifolds for heteroclinic cycles that have been used in article 2.

Switching near the Heteroclinic Model for the Geodynamo Problem. Geomagnetic reversals are one of the main interesting points of the geomagnetism, one of the most challenging phenomena in geophysics. Invoking the notions of *switching* and *cycling* near heteroclinic networks of rotating nodes presented in papers 1 and 2, we give analytical evidence that the mathematical model for the geomagnetic field given by Melbourne *et al* [**54**] is relevant for the study of georeversals and it explains its intermittent behaviour. Moreover, in paper 3, we explain the reason why the Earth's magnetic field flips from time to time.

The authors in [**54**] used symmetry to construct the model but the intermittent behaviour occurs only when it is broken. This subject touches another interesting problem in dynamical systems: the capture of the effects of *forced symmetry breaking* on heteroclinic cycles and networks, which has been pointed out by several authors (see for example Kirk and Rucklidge [**42**] and Sandstede and Scheel [**65**]). Later in paper 5, we investigate the effects of forced symmetry breaking.

Contracting Lorenz-like attractors close to symmetry. In the theory of autonomous differential equations of the type $\dot{x} = f(x)$, a basic step to study the asymptotic behaviour of trajectories, near an invariant compact set Λ, is to understand how the behaviour of df determines the dynamics of the flow. When $f|_\Lambda$ has hyperbolic structure, the theory started by S. Smale [**76, 77**] in the sixties is till today the paradigm for the study of such systems. The *spectral decomposition theorem* proved by Smale [**77**] gives a description of the non-wandering set of structurally stable systems as a finite union of disjoint, compact, maximal, flow-invariant and transitive sets. Each one of these *pieces* are well understood and this decomposition persists under small C^1–perturbations.

It is well known that, in the class of three-dimensional hyperbolic systems, a compact manifold Λ (containing equilibria or periodic solutions) is structurally stable if and only

if all the invariant manifolds of the nodes meet transversely. At this point, we would like to study dynamical properties of systems that are not C^1–structurally stable.

In 1963, E. Lorenz [**50**] studied the following system of differential equations associated to the evolution of the atmospheric dynamics:

$$\begin{cases} \dot{x} = \sigma(y - x) \\ \dot{y} = rx - y - xz \\ \dot{z} = xy - bz \end{cases} . \tag{1}$$

In its flow, for $\sigma = 10$, $r = 28$ and $b = \frac{8}{3}$, there is an attractor (often called *Lorenz butterfly*) containing [4]:

- an equilibrium point at the origin;
- periodic solutions accumulating on the equilibrium;
- a dense orbit.

The theory of hyperbolic systems cannot be applied to compact flow-invariant sets containing equilibria accumulated by regular trajectories [5]. This example is the paradigm of a *non-hyperbolic* attractor which cannot be destroyed by small C^1–perturbations (ie, it is C^1–*robust*). In order to understand the Lorenz equation, *geometric models* have been constructed independently by Afraimovich *et al* [**7**] and Guckenheimer and Williams [**30**]. The construction of these models is based on the properties suggested by numerics. A lot of papers describing the Lorenz equations have been written (for a general overview about the subject, see chapter 2 of Araújo and Pacífico [**9**]).

Starting in the nineties, the systematic theory that explains the coexistence of robust flow-invariant sets containing equilibria and non-trivial sets of closed trajectories accumulating on them, has been developed. In three dimensions, Morales *et al* [**56**] proved that robust sets containing equilibria are *singular hyperbolic sets*, *ie*, these sets have the main properties of the geometric Lorenz attractor. In the literature, there are several examples of dynamical systems possessing singular hyperbolic attractors (in the setting of fluid convection, Nguyen and Homburg [**57**] provide an interesting example).

A. Rovella [**64**] studied a different class of strange, non-robust and persistent attractors. More precisely, starting with a variation of the classical geometric Lorenz model (with respect to the eigenvalues at the origin), he proved that for a parameterized family of vector fields, there is an open and dense subset in the parameter space, in which the flows exhibit uniformly hyperbolic sets and singular attractors linking these sets. There are few explicit examples with non-robust but persistent sets. In paper 4, we construct explicitly a vector field on a three-dimensional sphere, with an attractor containing two

[4]Tucker [**81**] was the first who provided a computer assisted proof of the existence of such attractor.

[5]The hyperbolic splitting $E^u_p \oplus E^c_p \oplus E^s_p$ cannot be extended *continuously* from regular trajectories to equilibria.

saddle-foci, heteroclinic trajectories connecting them and a non-trivial hyperbolic basic set near the network. This attractor will not be *robustly transitive* under generic perturbations but it is persistent. Dynamical properties are also derived.

The vector field of paper 4 unfolds from an organizing center with $\mathbf{SO(2)} \times \mathbf{Z}_2$ – symmetry. The analysis of this bifurcation is the bridge with paper 5. There, we characterise the nonwandering points of the dynamics of a class of $(\mathbf{Z}_2 \oplus \mathbf{Z}_2)$ – equivariant systems in the neighbourhood of an attracting network (on a three-dimensional sphere) containing two saddle foci of different type. The two symmetries $\mathbf{Z}_2$ act differently on the sphere. When the first symmetry is broken, we prove that near each cycle, a unique hyperbolic attracting solution arises. When the second involution is broken, an explosion of non-trivial structures accumulating on the remaining heteroclinic network appears. Among these structures, there is a class of heteroclinic cycles often called *Bykov cycles*, and homoclinic cycles that bifurcate from them. These bifurcations also occours in the flow of the Lorenz equations (for $\sigma = 10$, $r \approx 30.475$ and $b \approx 2.623$) and have been studied by Glendinning and Sparrow [**26**], by Bykov [**16**] and by Lamb *et al* [**48**] for reversible systems.

We also show that, breaking gradually the two symmetries we get a wide range of behaviour, namely the appearance of homoclinic orbits, n-pulses, shift dynamics, and a cascade of Shilnikov's bifurcations. As far as possible we try to give the taxonomy of the dynamics which appears for all kinds of symmetry breaking. Doing a classical approach of composition of Poincaré maps, under an *open condition* on the parameters, we also find a suspension of a non-hyperbolic set near the heteroclinic cycle associated to *heteroclinic tangencies*. Although each individual tangency may be eliminated by small perturbations, slight perturbations do not allow to remove heteroclinic tangencies completely, being an interesting bridge between our work and that of Gonchenko *et al* [**28, 29**].

Product of Homoclinic Planar Attractors. In the context of game theory and the replicator equation, Sato *et al* [**67**] studied numerical examples of heteroclinic networks in the product of simplices. In the case of the Rock-Scissors-Paper game, the dynamics is dependent on the payoff matrices between the players. In this setting as well as in the context of coupled cell systems, it may be useful to know the dynamics of the uncoupled product system.

Motivated by problems in equivariant dynamics and connection selection in heteroclinic networks, Ashwin and Field [**12**] investigated the product of independent planar dynamics where one at least of the factors was a planar homoclinic attractor. The authors gave partial results in the case of a product of two planar homoclinic attractors (Theorem 6 of Ashwin and Field [**12**]). In paper 6, we give general results for the product of independent planar homoclinic and heteroclinic attractors and show that the likely

limit set is always the unique one dimensional heteroclinic network which covers the heteroclinic attractors in the factors. We also consider bifurcation where we break homoclinic connections but preserve the product structure.

I declare that to the best of my knowledge and unless where otherwise stated, all the work presented in this thesis is original. Articles 1 and 2 have been published and paper 6 is accepted for publication. In each article, where there are co-authors, they are mentioned explicitly. I hope the reader will use the margin of this thesis as Pierre de Fermat did with *Diophantus' Arithmetica*.

I have been supported by the grant SFRH/BD/28936/2006 of Fundação para a Ciência e Tecnologia and by Centro de Matemática da Universidade do Porto, which had financial support from Fundação para a Ciência e a Tecnologia, Portugal, through the programs POCTI and POSI with European Union and national funding and from NSF Grant DMS-0806321 (USA).

Article 1 – Switching near a Network of Rotating Nodes

Published in Dynamical Systems: an International Journal, Vol. 25, Issue 1, pages 75–95, 2010

SWITCHING NEAR A NETWORK OF ROTATING NODES

MANUELA A.D. AGUIAR, ISABEL S. LABOURIAU, AND ALEXANDRE A.P. RODRIGUES

ABSTRACT. We study the dynamics of a $\mathbf{Z}_2 \oplus \mathbf{Z}_2$-equivariant vector field in the neighbourhood of a heteroclinic network with a periodic trajectory and symmetric equilibria. We assume that around each equilibrium the linearisation of the vector field has non-real eigenvalues. Trajectories starting near each node of the network turn around in space either following the periodic trajectory or due to the complex eigenvalues near the equilibria. Thus, a network with rotating nodes. The rotations combine with transverse intersections of two-dimensional invariant manifolds to create switching near the network: close to the network there are trajectories that visit neighbourhoods of the saddles following all the heteroclinic connections of the network in any given order. Our results are motivated by an example where switching was observed numerically, by forced symmetry breaking of an asymptotically stable network with $\mathbf{O}(2)$ symmetry.

1. INTRODUCTION

Heteroclinic connections and networks are a common feature of symmetric differential equations, and persist under perturbations that preserve the symmetry. Start with an asymptotically stable network with rotational symmetry. A perturbation that breaks part of the symmetry splits a two-dimensional connection into a pair of one-dimensional ones. The new network is no longer asymptotically stable, nearby trajectories follow the network around in a complex way that we call switching.

By a heteroclinic network we mean a connected flow-invariant set that is the union of heteroclinic cycles. In the present case it is the orbit under the symmetry group $\mathbf{Z}_2 \oplus \mathbf{Z}_2$ of a heteroclinic cycle. These networks are often called heteroclinic cycles in the literature. Heteroclinic cycles and networks are known to occur persistently in the settings of symmetry [8], [16], coupled cell systems (with and without symmetry) [6], [2] and population dynamics [12], [13], [11], [7]. They are induced by the existence of flow invariant subpaces that correspond, respectively, to fixed point subspaces, synchrony subspaces and coordinate axes and hyperplanes.

It is worthwhile to describe general properties that entail switching, so the results may be applied to examples in other contexts. We study the dynamics near a network where all cycles have a common node that is a closed trajectory. We prove that there are trajectories near the network that follow its cycles in any desired order. Trajectories that go near the periodic orbit may switch to any heteroclinic cycle, return and switch again.

There exist in the literature several numerical reports on complicated dynamics near heteroclinic networks of equilibria and of equilibria and periodic trajectories, that include random visits to the nodes of the network in any possible order [10], [8], [5], [23].

This type of behaviour is not possible around asymptotically stable heteroclinic networks whose connections are contained in invariant subspaces. Each cycle in the network cannot be

2000 *Mathematics Subject Classification.* Primary: 37G30; Secondary: 37C10, 34C37, 37C29, 34C28, 37C80.

Key words and phrases. heteroclinic network, switching, vector fields, symmetry breaking, shadowing.

The research of all authors at Centro de Matemática da Universidade do Porto (CMUP) had financial support from Fundação para a Ciência e a Tecnologia (FCT), Portugal, through the programs POCTI and POSI with European Union and national funding. A.A.P. Rodrigues was supported by the grant SFRH/BD/28936/2006 of FCT.

asymptotically stable but it may have strong attractivity properties [19], [24] so that each nearby trajectory outside the invariant subspaces will tend to one of the cycles in the network.

Different forms of switching have been described in several contexts. Networks where all the nodes are equilibria, have been studied by Postlethwaite and Dawes [21] who found trajectories that follow three cycles in a network sequentially, both regularly and irregularly; by Kirk and Silber [15] near a network with two cycles who found nearby trajectories that switch in one direction. Persistent random switching is found by Guckenheimer and Worfolk [10] and Aguiar *et al* [4]; noise induced switching in Armbruster *et al* [5].

A problem similar to ours, where a network involves equilibria and a periodic trajectory, appears in the heteroclinic model of the geodynamo derived in Melbourne et al [20]. Starting with a model with $\mathbf{Z}_2 \oplus \mathbf{Z}_2 \oplus \mathbf{SO}(2)$ symmetry, they perturb the model so the only remaining symmetry is $-Id$. For the perturbed model they establish switching numerically in terms of reversals and excursions.

This has motivated Kirk and Rucklidge [14] to ask whether switching would be observed when all the symmetries are broken. First they analyse partially broken symmetries in two different ways: when only the $\mathbf{SO}(2)$ symmetry remains they find a weak form of switching, where trajectories starting near one equilibrium may visit the neighbourhood of another but not return to the first one; for the $\mathbf{Z}_2 \oplus \mathbf{Z}_2$-symmetric case they find attracting periodic trajectories and no switching. Then they argue that when all symmetries are broken and the network is destroyed, switching will not take place arbitrarily close to $\mathbf{Z}_2 \oplus \mathbf{Z}_2$-symmetric problems because of barriers formed by invariant manifolds. They describe a scenario where switching may arise, if the symmetry-breaking terms are larger than a threshold value. They propose a mechanism for switching arising from the right combination of homoclinic tangencies between the stable and unstable manifolds of a periodic orbit and specific heteroclinic tangencies between stable and unstable manifolds of the equilibria.

Here we analyse equations with a symmetry group $\mathbf{Z}_2 \oplus \mathbf{Z}_2$, a subgroup of that considered by Melbourne et al [20] but not acting in the same way as in Kirk and Rucklidge [14]: each $\mathbf{Z}_2$ in our setting contains a rotation by π that fixes a plane. A discussion of how our results compare with those of [14] and [20] appears at the end of this paper in section 9.

Under generic hypotheses for this symmetry, we prove a strong form of switching: the existence of trajectories that visit neighbourhoods of any sequence of nodes of the network in any order that is compatible with the network connections.

The conditions we need for switching are stated in section 3 preceded by definitions and preliminary results in section 2.

In section 4 we present an example of a $\mathbf{Z}_2 \oplus \mathbf{Z}_2$-equivariant family of ordinary differential equations having a network of rotating nodes and some simulations (see figures 3 and 4). When one of the parameters is set to zero, the equations are $\mathbf{Z}_2 \oplus \mathbf{Z}_2 \oplus \mathbf{SO}(2)$-symmetric and the network is asymptotically stable. Switching occurs for all small non-zero values of this symmetry-breaking parameter.

We linearise the flow around the invariant saddles in section 5, obtaining isolating blocks around each node of the network. This section is mostly concerned with introducing the notation for the proof of switching that occupies the rest of the paper.

The goal of this paper is to prove switching in the neighbourhood of a heteroclinic network that consists of four symmetric copies of a heteroclinic cycle

$$\mathbf{C} \to \mathbf{v} \to \mathbf{w} \to \mathbf{C}$$

where $\mathbf{C}$ is a closed trajectory invariant under the symmetries and $\mathbf{v}$ and $\mathbf{w}$ are equilibria. The connection $\mathbf{v} \to \mathbf{w}$ is one-dimensional and takes place inside a fixed-point subspace, the other connections are transverse intersections of 2-dimensional invariant manifolds. The trajectory $\mathbf{C}$ has real Floquet multipliers and 2-dimensional stable and unstable manifolds; the linearisation

of the flow near $\mathbf{v}$ has a pair of complex eigenvalues with negative real part and one real positive eigenvalue; the linearisation of the flow near $\mathbf{w}$ has one real negative eigenvalue and a pair of complex eigenvalues with positive real part (see figures 1 and 2).

In section 6 we obtain a geometrical description of the way the flow transforms a curve of initial conditions lying across the stable manifold of each node. The curve is wrapped around the isolating block of the next node, accumulating on its unstable manifold and in particular on the next connection. Thus, points on a line across the stable manifold of $\mathbf{v}$ will be mapped into a helix accumulating on the unstable manifold of $\mathbf{w}$ that will cross the transverse stable manifold of $\mathbf{C}$ infinitely many times. Similarly, points on a line across the stable manifold of $\mathbf{C}$ will be mapped into a helix accumulating on its unstable manifold and thus will cross the transverse stable manifold of $\mathbf{v}$ infinitely many times.

The geometrical setting is explored in section 7 to obtain intervals on the curve of initial conditions that are mapped by the flow into curves near the next node in a position similar to the first one. This allows us to establish the recurrence needed for switching in section 8:

for any sequence of nodes like

$$+\mathbf{v} \to -\mathbf{w} \to \mathbf{C} \to -\mathbf{v} \to -\mathbf{w} \to \mathbf{C} \to +\mathbf{v} \to +\mathbf{w} \to \mathbf{C} \to +\mathbf{v} \to \cdots$$

we find trajectories that visits neighbourhoods of these nodes in the same sequence.

We end the paper with a discussion (section 9) of the results obtained and of related results in the literature.

2. Preliminaries

Let f be a smooth vector field on $\mathbf{R}^n$ with flow given by the unique solution $x(t) = \varphi(t, x_0) \in \mathbf{R}^n$ of

$$\dot{x} = f(x) \qquad x(0) = x_0. \tag{1}$$

If A is a compact invariant set for the flow of f, we say, following Field [8], that A is an *invariant saddle* if

$$A \subseteq \overline{W^s(A)\backslash A} \quad \text{and} \quad A \subseteq \overline{W^u(A)\backslash A},$$

where $\overline{A}$ is the closure of A. In this paper all the saddles are hyperbolic.

Given two invariant saddles A and B, an m-dimensional *heteroclinic connection* from A to B, denoted $[A \to B]$, is an m-dimensional connected flow-invariant manifold contained in $W^u(A) \cap W^s(B)$. There may be more than one connection from A to B.

Let $\mathcal{S} = \{A_j : j \in \{1, \ldots, k\}\}$ be a finite ordered set of mutually disjoint invariant saddles. Following Field [8], we say that there is a *heteroclinic cycle* associated to $\mathcal{S}$ if

$$\forall j \in \{1, \ldots, k\}, W^u(A_j) \cap W^s(A_{j+1}) \neq \emptyset \pmod{k}.$$

We refer to the saddles defining the heteroclinic cycle as *nodes*.

A *heteroclinic network* is a finite connected union of heteroclinic cycles.

Let Γ be a compact Lie group acting linearly on $\mathbf{R}^n$. The vector field f is $\Gamma-$equivariant if for all $\gamma \in \Gamma$ and $x \in \mathbf{R}^n$, we have $f(\gamma x) = \gamma f(x)$. In this case $\gamma \in \Gamma$ is said to be a symmetry of f. We refer the reader to Golubitsky, Stewart and Schaeffer [9] for more information on differential equations with symmetry.

The Γ-*orbit* of $x_0 \in \mathbf{R}^n$ is the set $\Gamma(x_0) = \{\gamma x_0, \gamma \in \Gamma\}$ that is invariant under the flow of Γ-equivariant vector fields f. In particular, if x_0 is an equilibrium of (1), so are the elements in its Γ-orbit.

The *isotropy subgroup* of $x_0 \in \mathbf{R}^n$ is $\Gamma_{x_0} = \{\gamma \in \Gamma, \quad \gamma x_0 = x_0\}$. For an isotropy subgroup Σ of Γ, its *fixed-point subspace* is

$$Fix(\Sigma) = \{x \in \mathbf{R}^n : \forall \gamma \in \Sigma, \gamma x = x\}.$$

Fixed-point subspaces are the reason for the robustness of heteroclinic cycles and networks in symmetric dynamics: if f is Γ-equivariant then $Fix(\Sigma)$ is flow-invariant, thus connections occurring inside these spaces persist under perturbations that preserve the symmetry.

For a heteroclinic network Σ with node set $\mathcal{A}$, a *path of order k*, on Σ is a finite sequence $s^k = (c_j)_{j\in\{1,\dots,k\}}$ of connections $c_j = [A_j \to B_j]$ in Σ such that $A_j, B_j \in \mathcal{A}$ and $B_j = A_{j+1}$ *i.e.* $c_j = [A_j \to A_{j+1}]$. For an infinite path, take $j \in \mathbf{N}$.

Let N_Σ be a neighbourhood of the network Σ and let U_A be a neighbourhood of each node A in Σ.

For each heteroclinic connection in Σ, consider a point p on it and a small neighbourhood V of p. We are assuming that the neighbourhoods of the nodes are pairwise disjoint, as well for those of points in connections.

Given neighbourhoods as above, the point q, or its trajectory $\varphi(t)$, *follows* the finite path $s^k = (c_j)_{j\in\{1,\dots,k\}}$ of order k, if there exist two monotonically increasing sequences of times $(t_i)_{i\in\{1,\dots,k+1\}}$ and $(z_i)_{i\in\{1,\dots,k\}}$ such that for all $i \in \{1,\dots,k\}$, we have $t_i < z_i < t_{i+1}$ and:

(1) $\varphi(t) \subset N_\Sigma$ for all $t \in (t_1, t_{k+1})$;
(2) $\varphi(t_i) \in U_{A_i}$ and $\varphi(z_i) \in V_i$ and
(3) for all $t \in (z_i, z_{i+1})$, $\varphi(t)$ does not visit the neighbourhood of any other node except that of A_{i+1}.

There is *finite switching* near Σ if for each finite path there is a trajectory that follows it. Analogously, we define *infinite* switching near Σ by requiring that each infinite path is followed by a trajectory.

An infinite path on Σ may also be seen as a pseudo-orbit of $\dot{x} = f(x)$, with infinitely many discontinuities. Switching near Σ means that these infinite pseudo-orbits can be shadowed.

3. A network of rotating nodes

Our object of study is the dynamics around a special type of heteroclinic network (see figure 2) for which we give a rigorous description here. The network lies in a topological three-sphere and one of its nodes is a closed trajectory with real Floquet multipliers and 2-dimensional stable and unstable manifolds. Near this node, the flow rotates following the closed trajectory. The other nodes are equilibria with a pair of non-real eigenvalues. Thus the local dynamics rotates around each node.

Specifically, we study a smooth vector field f on $\mathbf{R}^4$ with the following properties:

(P1) The vector field f is equivariant under $\Gamma \cong \mathbf{Z}_2 \oplus \mathbf{Z}_2$ acting linearly on $\mathbf{R}^4$ with generators γ_1 and γ_2 and with two transverse two-dimensional fixed-point subspaces. In particular, the origin is an equilibrium.

(P2) There is a three-dimensional flow-invariant manifold $\mathbf{S}^3$ diffeomorphic to a sphere that attracts all the trajectories except the origin. For simplicity, we assume this manifold to be the unit sphere.

By (P1–P2) there are two flow-invariant circles

$$\mathbf{C}_1 = \mathbf{S}^3 \cap Fix(\mathbf{Z}_2(\gamma_1)) \quad \text{and} \quad \mathbf{C} = \mathbf{S}^3 \cap Fix(\mathbf{Z}_2(\gamma_2)).$$

(P3) On $\mathbf{C}_1$ there are exactly four equilibria that will be denoted by $+\mathbf{v}$, $+\mathbf{w}$, $-\mathbf{v} = \gamma_2 \cdot \mathbf{v}$, $-\mathbf{w} = \gamma_2 \cdot \mathbf{w}$. Moreover, the eigenvalues of df restricted to $T\mathbf{S}^3$ are:

- $-C_v \pm i$ and E_v with $C_v \neq E_v > 0$, at $\pm\mathbf{v}$;
- $E_w \pm i$ and $-C_w$ with $C_w \neq E_w > 0$, at $\pm\mathbf{w}$.

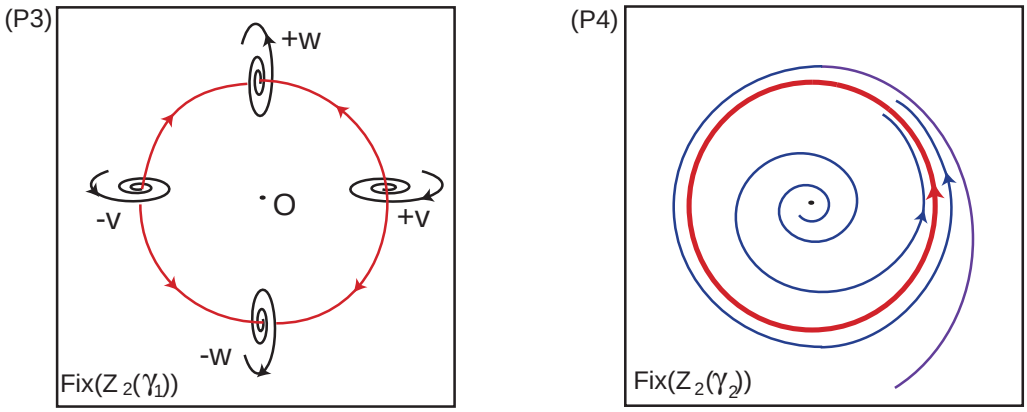

FIGURE 1. Dynamics near a heteroclinic network of rotating nodes. Left: dynamics around the plane $Fix(\mathbf{Z}_2(\gamma_1))$ illustrating property (P3); Right: dynamics in the plane $Fix(\mathbf{Z}_2(\gamma_2))$ illustrating property (P4).

In $Fix(\mathbf{Z}_2(\gamma_1))$ the equilibria $\pm\mathbf{v}$ are saddles and $\pm\mathbf{w}$ are sinks with connections in $\mathbf{C}_1$ from $\pm\mathbf{v}$ to $\pm\mathbf{w}$. These connections are persistent under perturbations that preserve the γ_1-symmetry (see figure 1).

(P4) In the invariant plane $Fix(\mathbf{Z}_2(\gamma_2))$ the only equilibrium is the origin and it is an unstable focus.

Thus $\mathbf{C}$ is a closed trajectory and, from (P2), this trajectory is a sink in $Fix(\mathbf{Z}_2(\gamma_2))$ (see figure 1). Since $\mathbf{C}$ is contained in the flow-invariant plane $Fix(\mathbf{Z}_2(\gamma_2))$, its Floquet multipliers are real.

(P5) The periodic trajectory $\mathbf{C}$ is hyperbolic and, in $\mathbf{S}^3$, $\dim W^u(\mathbf{C}) = \dim W^s(\mathbf{C}) = 2$. Moreover, there are connections $[\mathbf{C} \to +\mathbf{v}]$ and $[+\mathbf{w} \to \mathbf{C}]$ satisfying:

$$W^u(\mathbf{C}) \pitchfork W^s(+\mathbf{v}) \quad \text{and} \quad W^u(+\mathbf{w}) \pitchfork W^s(\mathbf{C}).$$

These intersections are one-dimensional and consist of one pair of γ_1-related trajectories.

From the γ_2- symmetry, we obtain a pair of γ_1-related one-dimensional connections in $W^u(\mathbf{C}) \pitchfork W^s(-\mathbf{v})$ and in $W^u(-\mathbf{w}) \pitchfork W^s(\mathbf{C})$. It follows that there is a heteroclinic network Σ involving the saddles $\pm\mathbf{v}$, $\pm\mathbf{w}$ and $\mathbf{C}$ (figure 2). Such a network Σ is what we call a *network of rotating nodes*. This paper shows switching near this network.

The symmetry γ_1 and its flow invariant fixed point subspace ensure the persistence of the connections $[\pm\mathbf{v} \to \pm\mathbf{w}]$. The other symmetry γ_2 is not essential for the existence of a robust network with these properties but it makes them more natural as illustrated by the example in section 4. The same is true for the existence of the invariant 3-sphere. In section 9 we discuss variants of these hypotheses for which switching may be proved in the same way.

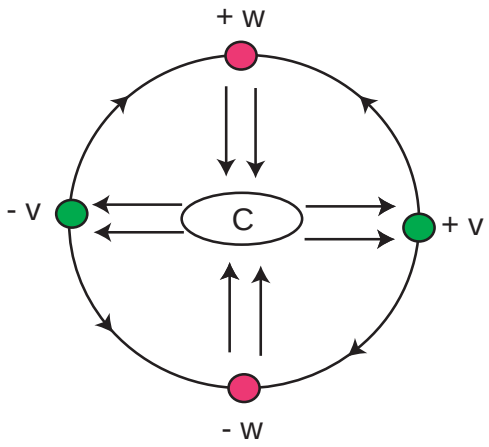

FIGURE 2. Schematic description of a heteroclinic network of rotating nodes satisfying (P1-P5). Each arrow represents a 1-dimensional heteroclinic connection. There is one 1-dimensional heteroclinic connection from each equilibrium $\pm\mathbf{v}$ to each equilibrium $\pm\mathbf{w}$ (P3). There are two 1-dimensional heteroclinic connections involving each equilibrium and the periodic trajectory $\mathbf{C}$ (P5).

4. EXAMPLE

Our study was initially motivated by the following example constructed in Aguiar [1], using the methods of [3]. This is an ordinary differential equation in $\mathbf{R}^4$ given by:

$$\begin{cases} \dot{x}_1 = x_1(\alpha_1 + \alpha_2 r_1^2 + \alpha_3 x_3^2 + \alpha_4 x_4^2 + \alpha_5(x_3^4 - r_1^2 x_4^2)) - x_2 \\ \dot{x}_2 = x_2(\alpha_1 + \alpha_2 r_1^2 + \alpha_3 x_3^2 + \alpha_4 x_4^2 + \alpha_5(x_3^4 - r_1^2 x_4^2)) + x_1 \\ \dot{x}_3 = x_3(\alpha_1 + \alpha_2 x_3^2 + \alpha_3 x_4^2 + \alpha_4 r_1^2 + \alpha_5(x_4^4 - r_1^2 x_3^2)) + \xi h_1(x) \\ \dot{x}_4 = x_4(\alpha_1 + \alpha_2 x_4^2 + \alpha_3 r_1^2 + \alpha_4 x_3^2 + \alpha_5(r_1^4 - x_3^2 x_4^2)) - \xi h_2(x) \end{cases}$$

where $x = (x_1, x_2, x_3, x_4) \in \mathbf{R}^4$, $r_1^2 = x_1^2 + x_2^2$ and

$$h_1(x) = [\alpha_1 + 3\alpha_2(x_1^2 + x_2^2)]x_1x_2x_4 \quad \text{and} \quad h_2(x) = [\alpha_1 + 3\alpha_2(x_1^2 + x_2^2)]x_1x_2x_3.$$

The symmetries of the equation are changes of sign of pairs of coordinates:

$$\gamma_1(x) = (-x_1, -x_2, x_3, x_4) \qquad \gamma_2(x) = (x_1, x_2, -x_3, -x_4).$$

Figures 3 and 4 show a trajectory of this equation. In [1] it is proved that, for parameter values such that

$$\alpha_1 > 0 \qquad \alpha_3 + \alpha_4 = 2\alpha_2 \qquad \alpha_3 < \alpha_2 < \alpha_4 < 0$$
$$\alpha_2(\alpha_3 - \alpha_4) + \alpha_1\alpha_5 > 0$$

and if $\xi \geq 0$ is such that

$$\xi < \frac{-\alpha_2\alpha_3 + \alpha_2\alpha_4 + \alpha_1\alpha_5}{2\alpha_1\alpha_2} \quad \text{and} \quad \xi^2 < \frac{(\alpha_4 - \alpha_3)(2\alpha_1\alpha_5 - \alpha_2\alpha_3 + \alpha_2\alpha_4)}{4\alpha_1^2\alpha_2},$$

then its dynamics satisfies (P1–P4) as we proceed to explain.

For $\xi = 0$ the equation has more symmetry, like the model in Melbourne et al [20]: it is equivariant under the group $\mathbf{Z}_2 \oplus \mathbf{Z}_2 \oplus \mathbf{SO}(2)$, generated by

$$\kappa_\varphi(x) = (x_1\cos(\varphi) - x_2\sin(\varphi), x_1\sin(\varphi) + x_2\cos(\varphi), x_3, x_4)$$
$$\kappa_2(x) = (x_1, x_2, -x_3, x_4) \qquad \kappa_3(x) = (x_1, x_2, x_3, -x_4).$$

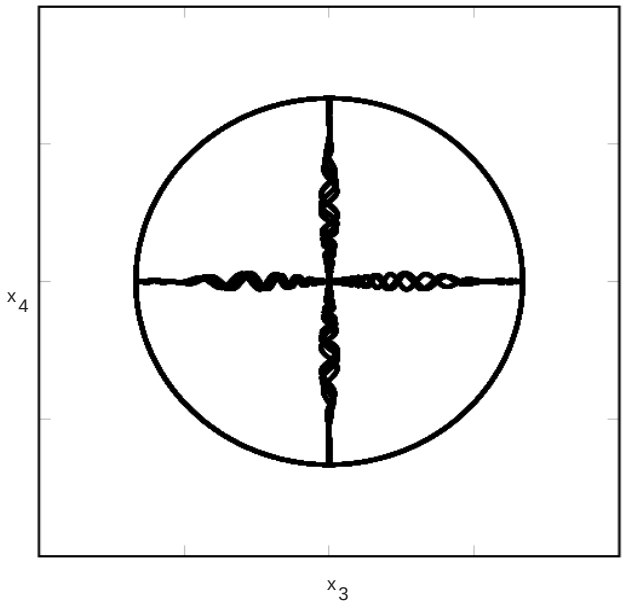

FIGURE 3. Switching trajectory on the example in section 4: projection into the (x_3, x_4)-plane of the trajectory with initial condition $(0.001, 0.001, 0.001, 1)$, with $\alpha_1 = 0.33333333$, $\alpha_2 = -0.33333333$, $\alpha_3 = -0.5$, $\alpha_4 = -0.16666667$, $\alpha_5 = -0.05$ and $\xi = -1$.

When $\xi = 0$, the three-dimensional sphere $\mathbf{S}^3_r$ of radius $r = \sqrt{\frac{-\alpha_1}{\alpha_2}}$ is flow invariant and globally attracting. The equilibria $\pm\mathbf{v}$ (resp. $\pm\mathbf{w}$) lie at the intersection of $\mathbf{S}^3_r$ with the x_3-axis (resp. x_4-axis) fixed by the subgroup generated by κ_φ and κ_3 (resp. κ_φ and κ_2). The closed trajectory $\mathbf{C}$ is the intersection of $\mathbf{S}^3_r$ with the plane fixed by the subgroup generated by κ_2 and κ_3. A direct computation of the eigenvalues and eigenvectors shows that the closed trajectory and the equilibria form a network where the two-dimensional unstable (resp. stable) manifold of $\mathbf{C}$ coincides with the two-dimensional stable (resp. unstable) manifold of $\pm\mathbf{v}$ (resp. $\pm\mathbf{w}$). Since all the heteroclinic connections are contained in fixed point subspaces, there is no swicthing. Moreover, it can be shown (see [1]) that the network is asymptotically stable by the criteria of Krupa and Melbourne [17], [18].

For $\xi > 0$ the $\mathbf{SO}(2)$ symmetry is broken and so are the two-dimensional connections. The only symmetries remaining are $\gamma_1 = \kappa_\pi$ and $\gamma_2 = \kappa_2\kappa_3$. The symmetry-breaking term $(0, 0, h_1(x), h_2(x))$ is tangent to the invariant sphere so it is still flow invariant and properties (P1) and (P2) hold. The perturbation mantains the flow-invariance of the line that is fixed by κ_π and κ_2 (resp. κ_π and κ_3), the equilibria and the periodic trajectory are preserved together with their stability, and properties (P3-P4) hold. Using Melnikov's Method, Aguiar [1] proved that the two-dimensional manifolds of the periodic trajectory and of the saddle-foci intersect transversely. Hence property (P5) holds. It will follow from Theorem 7 that there is switching near this network as suggested by the trajectories like that of figures 3 and 4.

5. Local Dynamics near the saddles

Here and in the next two sections, we define the setup for the proof of swicthing near the network. This section contains mostly notation and coordinates used in the rest of the paper.

We restrict our study to $\mathbf{S}^3$ since this is a compact and flow-invariant manifold that captures all the dynamics.

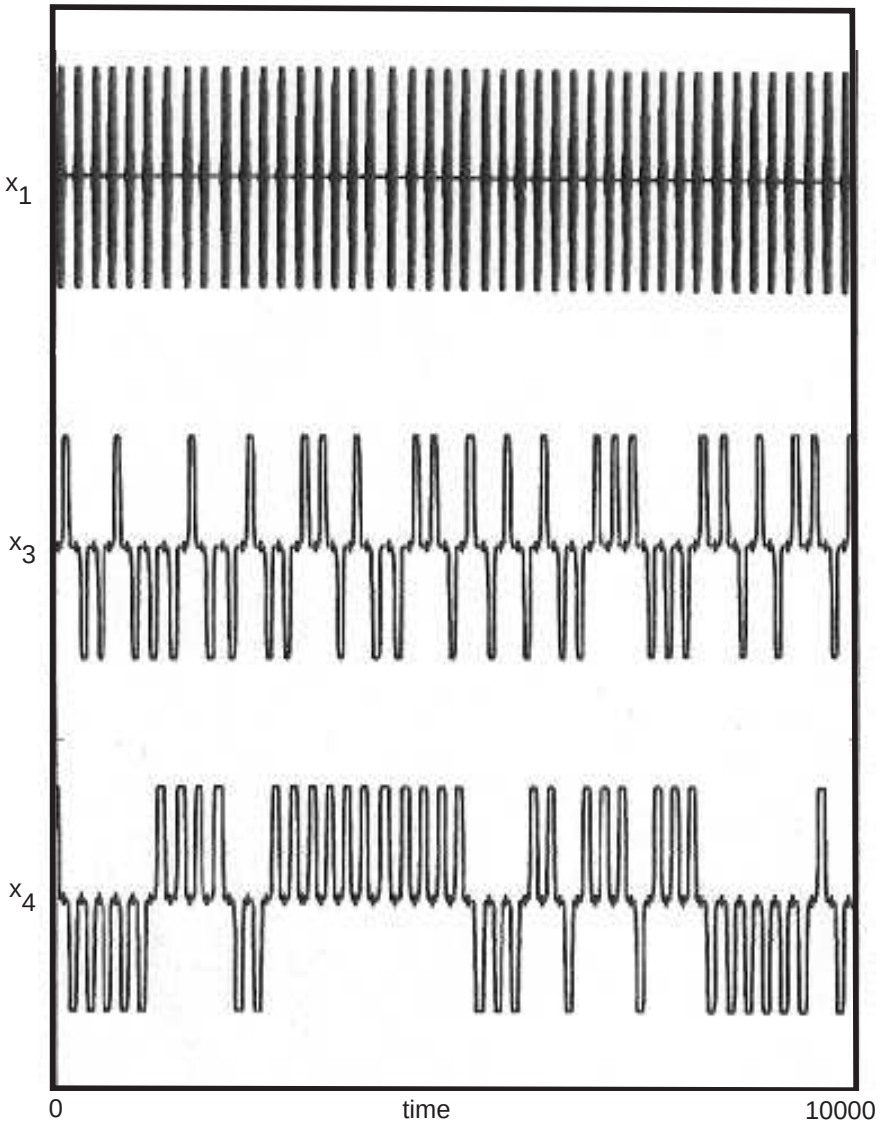

FIGURE 4. Switching trajectory on the example in section 4: time series for x_1, x_3 and x_4 for a trajectory with initial condition $(0.001, 0.001, 0.001, 1)$, with $\alpha_1 = 0.33333333$, $\alpha_2 = -0.33333333$, $\alpha_3 = -0.5$, $\alpha_4 = -0.16666667$, $\alpha_5 = -0.05$ (same as figure 3). The variable x_1 shows visits to the limit cycle, x_3 shows alternate visits to $\pm\mathbf{v}$ and x_4 shows visits to $\pm\mathbf{w}$.

When we refer to the stable/unstable manifold of an invariant saddle, we mean the **local** stable/unstable manifold of that saddle.

We use Samovol's theorem to linearise the flow around each saddle — equilibrium or closed trajectory. We then introduce local cylindrical coordinates and define a neighbourhood with boundary transverse to the linearised flow. For each saddle, we obtain the expression of the local map that sends points in the boundary where the flow goes in, into points in the boundary where it goes out. These expressions will be used in the sequel to obtain a geometrical description of the discretised flow.

5.1. **Coordinates near equilibria.** Let $\mathbf{v}$ and $\mathbf{w}$ stand for any of the two symmetry-related equilibria $\pm\mathbf{v}$ and $\pm\mathbf{w}$, respectively. By Samovol's theorem [22] f may be linearised around them,

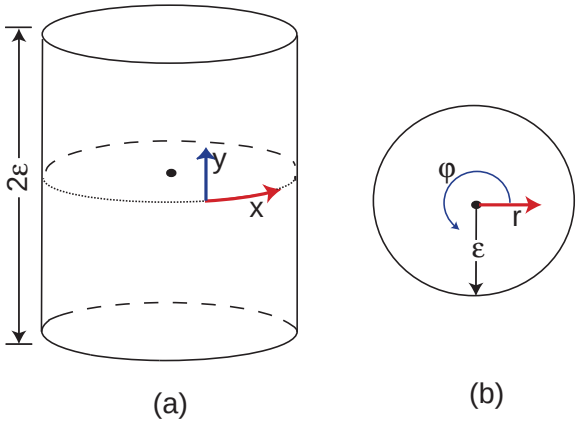

FIGURE 5. Coordinates on the boundaries of the neighbourhood of **v** and **w**: (a) cylinder wall (b) top and bottom.

since nonresonance is automatic here. In cylindrical coordinates (ρ, θ, z) the linearisations take the forms:

$$(2) \qquad \begin{cases} \dot\rho = -C_v\rho \\ \dot\theta = 1 \\ \dot z = E_v z \end{cases} \qquad \begin{cases} \dot\rho = E_w\rho \\ \dot\theta = 1 \\ \dot z = -C_w z. \end{cases}$$

We consider cylindrical neighbourhoods of **v** and **w** in $\mathbf{S}^3$ of radius $\varepsilon > 0$ and height 2ε. Their boundaries consist of three components (see figure 5):

- The cylinder wall parametrized by $x \in \mathbf{R} \pmod{\mathbf{2}\pi}$ and $|y| \le \varepsilon$ with the usual cover $(x, y) \mapsto (\varepsilon, x, y) = (\rho, \theta, z)$.
- Two disks, the top and the bottom of the cylinder. We take polar coverings of these disks: $(r, \varphi) \mapsto (r, \varphi, j\varepsilon) = (\rho, \theta, z)$ where $j \in \{-, +\}$, $0 \le r \le \varepsilon$ and $\varphi \in \mathbf{R} \pmod{\mathbf{2}\pi}$.

We use x for the angular coordinate on the cylinder wall so as to avoid confusion with the angular coordinate on the disks when dealing with the local maps.

Note that the two flows defined by (2) have symmetry $\mathbf{Z}_2 \oplus \mathbf{SO}(2)$ given by $z \mapsto -z$ and rotation around the z axis. This is an artifact of the linearisation and has nothing to do with the original symmetries. It will be used implicitly in the next sections.

5.2. **Local dynamics near v.** The cylinder wall is denoted H_v^{in}. Trajectories starting at interior points of H_v^{in} go inside the cylinder in positive time and $H_v^{in} \cap W^s(\mathbf{v})$ is parametrized by $y = 0$. The set of points in H_v^{in} with positive (resp. negative) second coordinate is denoted $H_v^{in,+}$ (resp. $H_v^{in,-}$).

The top and the bottom of the cylinder are denoted $H_v^{out,+}$ and $H_v^{out,-}$, **r**espectively. Trajectories starting at interior points of **e**ither $H_v^{out,+}$ or $H_v^{out,-}$ go inside the cylinder in negative time (**s**ee figure 6).

After linearisation $W^u(\mathbf{v})$ is the z-axis, intersecting $H_v^{out,+}$ at the origin of coordinates of $H_v^{out,+}$. Trajectories starting at $H_v^{in,j}$, $j \in \{+, -\}$ leave the cylindrical neighbourhood at $H_v^{out,j}$. The orientation of the z-axis may be chosen to have $[\mathbf{v} \to j\mathbf{w}]$ meeting $H_v^{out,j}$.

The local map near **v**, $\phi_v : H_v^{in,+} \to H_v^{out,+}$ is given by

$$(3) \qquad \phi_v(x, y) = \left(K_v y^{\delta_v}, -\tfrac{1}{E_v}\ln y + x + \tfrac{1}{E_v}\ln(\varepsilon)\right) = (r, \phi) \ ,$$

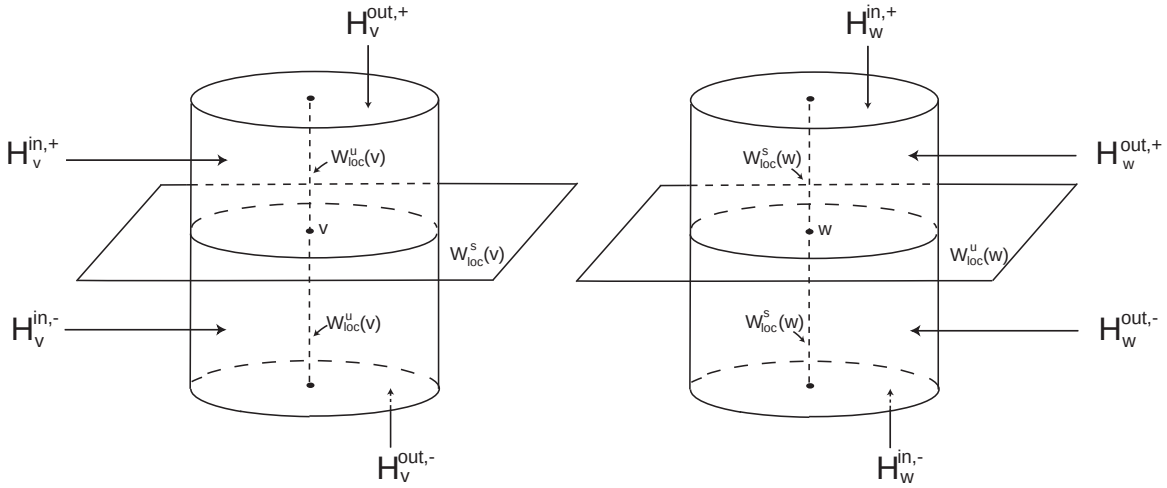

FIGURE 6. Neighbourhoods of the saddle-foci. *Left*: once the flow enters the cylinder transversely across the wall $H_v^{in}\backslash W^s_{loc}(\mathbf{v})$ it leaves it transversely across the cylinder top $H_v^{out,+}$ and bottom $H_v^{out,-}$. *Right*: the flow enters the cylinder transversely across top $H_w^{in,+}\backslash W^s_{loc}(\mathbf{w})$ and bottom $H_w^{in,-}\backslash W^s_{loc}(\mathbf{w})$ and leaves it transversely across the wall H_w^{out}. Inside the two cylinders the vector field is linear.

where

$$\delta_v = \frac{C_v}{E_v} > 0, \quad K_v = \varepsilon^{1-\delta_v} > 0 \quad \text{and } \frac{1}{E_v} > 0.$$

The expression for the local map from $H_v^{in,-}$ to $H_v^{out,-}$ is the same.

5.3. **Local dynamics near w.** After linearisation, $W^s(\mathbf{w})$ is the z-axis, intersecting the top and bottom of the cylinder at the origin of the coordinates. We denote by $H_w^{in,j}$, $j \in \{-,+\}$, the component that $[j\mathbf{v} \to \mathbf{w}] \cap H_w^{in,j} \neq \emptyset$. Trajectories starting at interior points of $H_w^{in,\pm}$ go inside the cylinder in positive time (see figure 6).

Trajectories starting at interior points of the cylinder wall H_w^{out} go inside the cylinder in negative time. The set of points in H_w^{out} whose second coordinate is positive (resp. negative) is denoted $H_w^{out,+}$ (resp. $H_w^{out,-}$) and $H_w^{out} \cap W^u(\mathbf{w})$ is parametrized by $y = 0$. The orientation of the z-axis may be chosen to have trajectories that start at $H_w^{in,j}\backslash W^s(\mathbf{w})$, $j \in \{+,-\}$ leaving the cylindrical neighbourhood at $H_w^{out,j}$.

The local map near $\mathbf{w}$, $\phi_w : H_w^{in,+}\backslash W^s(\mathbf{w}) \to H_w^{out,+}$ is

$$\phi_w(r,\varphi) = \left(\tfrac{1}{E_w}\ln(\varepsilon) - \tfrac{1}{E_w}\ln r + \varphi, K_w r^{\delta_w}\right) = (x,y) \ ,$$

where

$$\delta_w = \frac{C_w}{E_w} > 0, \quad K_w = \varepsilon^{1-\delta_w} > 0 \quad \text{and} \quad \frac{1}{E_w} > 0.$$

The same expression holds for the local map from $H_w^{in,-}\backslash W^s(\mathbf{w})$ to $H_w^{out,-}$.

5.4. **Local dynamics near the closed trajectory C.** Consider a local cross section S to the flow at $p \in \mathbf{C}$. The Poincaré first return map defined on S may be linearised around the hyperbolic fixed point p using Samovol's Theorem. Suspending the linear map yields, in cylindrical coordinates, the differential equations:

$$\begin{cases} \dot{\rho} = -C_C(\rho - 1) \\ \dot{\theta} = 1 \\ \dot{z} = E_C z \end{cases} \tag{4}$$

that are locally orbitally equivalent to the original flow. In these coordinates, $\mathbf{C}$ corresponds to the circle $\rho = 1$ **a**nd $z = 0$, $W^s(\mathbf{C})$ is the plane $z = 0$ and $W^u(\mathbf{C})$ is the cylinder $\rho = 1$.

We work with a hollow three-dimensional cylindrical neighbourhood of $\mathbf{C}$ with boundary $H_C^{in} \cup H_C^{out}$, where trajectories starting in H_C^{in} (resp. H_C^{out}) go into the neighbourhood in positive (resp. negative) small time. In what follows we establish some notation for components of the boundary (see figure 7).

The components of H_C^{in} are the two cylinder walls, $H_{C,+}^{in}$ and $H_{C,-}^{in}$ locally separated by $W^u(\mathbf{C})$ and parametrized by the covering map:

$$(x, y) \mapsto (1 \pm \varepsilon, x, y) = (\rho, \theta, z),$$

where $x \in \mathbf{R} \pmod{2\pi}$, $|y| < \varepsilon$. We denote by $H_{C,+}^{in}$ the component with $\rho = 1 + \varepsilon$.

In these coordinates, $H_C^{in} \cap W^s(\mathbf{C})$ is the union of the two circles $y = 0$ in the two components. It divides $H_{C,+}^{in}$ in two parts, $H_{C,+}^{in,+}$ and $H_{C,+}^{in,-}$, parametrized, respectively, by positive and negative y, with a similar convention for $H_{C,-}^{in,+}$ and $H_{C,-}^{in,-}$.

The components $H_C^{out,+}$ and $H_C^{out,-}$ of H_C^{out} are two anuli, locally separated by $W^s(\mathbf{C})$ and parametrized by the covering:

$$(r, \varphi) \mapsto (r, \varphi, \pm\varepsilon) = (\rho, \theta, z),$$

for $1 - \varepsilon < r < 1 + \varepsilon$ and $\varphi \in \mathbf{R} \pmod{2\pi}$ and where $H_C^{out,+}$ is the component corresponding to the $+$ sign and $H_C^{out} \cap W^u(\mathbf{C})$ is the union of two circles parametrized by $r = 1$.

Denote by $H_{C,+}^{out,k}$ (resp. $H_{C,-}^{out,k}$), $k \in \{+, -\}$ the set parametrized by $1 < r < 1 + \varepsilon$ (resp. $1 - \varepsilon < r < 1$) in $H_C^{out,k}$.

In these coordinates the local map $\phi_C : H_{C,j}^{in,k} \to H_{C,j}^{out,k}$, $j, k \in \{+, -\}$, is given by

$$\phi_C(x, y) = \left(jK_c y^{\delta_c} + 1, \frac{1}{E_c} \ln(\varepsilon) - \frac{1}{E_c} \ln y + x \right) = (r, \varphi),$$

where

$$\delta_c = \frac{C_c}{E_c} > 0 \quad K_c = \varepsilon^{1-\delta_C} > 0 \text{ and } \frac{1}{E_c} > 0.$$

6. Geometry near the saddles

The coordinates and notation of section 5 may now be used to analyse the geometry of the local dynamics near each saddle.

The manifold $W^s(\mathbf{v})$ separates the cylindrical neighbourhood of $\mathbf{v}$ into an upper and a lower component, mapped into neighbourhoods of $+\mathbf{w}$ and $-\mathbf{w}$, respectively.

We show here that initial conditions lying on a segment on the upper part of the cylindrical wall around $\mathbf{v}$ and ending at $W^s(\mathbf{v})$ are mapped into points on a spiral on the top of the cylinder H_v^{out} where the flow goes out (figure 8).

Initial conditions on a spiral on the top of cylindrical neighbourhood of $\mathbf{w}$ are then shown to be mapped into points on a helix around the cylinder accumulating on $W^u(\mathbf{w})$ (figure 8). Since $W^s(\mathbf{C})$ is transverse to $W^u(\mathbf{w})$, then the helix on $H_w^{out,+}$ is mapped across $W^s(\mathbf{C})$ on

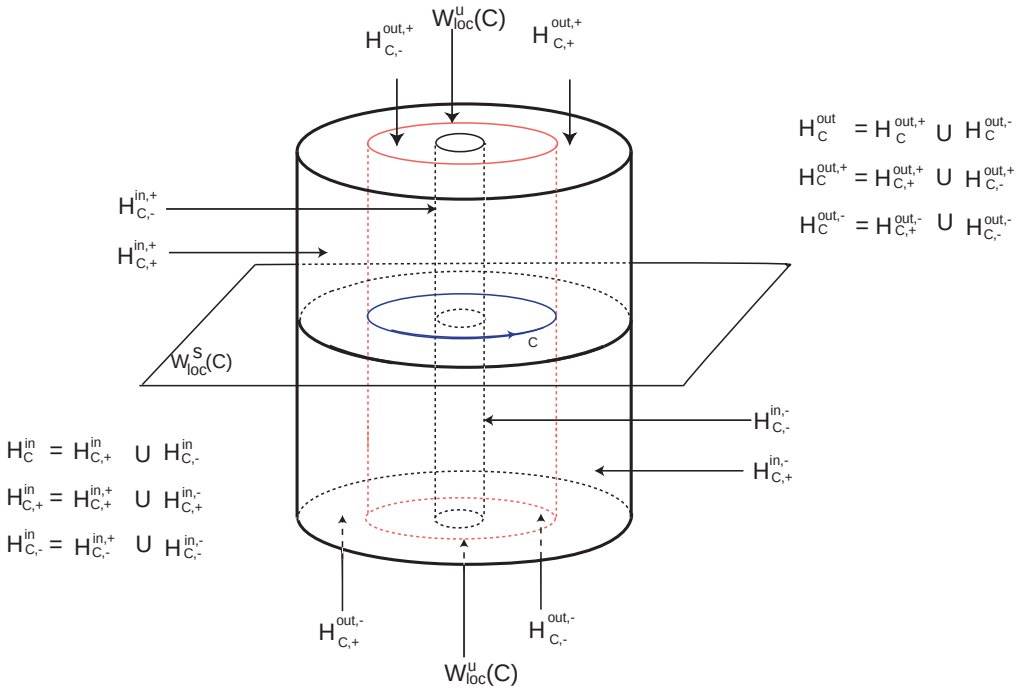

FIGURE 7. Neighbourhood of the closed trajectory **C**. The flow enters the hollow cylinder transversely across cylinder walls $H^{in}_{C,\pm}$ and leaves it transversely across top $H^{out}_{C,+}$ and bottom $H^{out}_{C,-}$.

H^{in}_C infinitely many times. This will be used in section 7 to obtain, in any segment on $H^{in,+}_v$, infinitely many intervals that are mapped into segments on H^{in}_C ending at $W^s(\mathbf{C})$.

Then the image of a segment ending at $W^s(\mathbf{C})$ on one of the walls of H^{in}_C is shown to be mapped into a curve accumulating on $W^u(\mathbf{C}) \cap H^{out}_C$ (see figure 9). This curve meets $W^s(\mathbf{v})$ infinitely many times by transversality and it is thus mapped across $W^s(\mathbf{v})$ on H^{in}_v infinitely many times. Again, we will use this in section 7 to obtain infinitely many intervals that are mapped into segments on H^{in}_v ending at $W^s(\mathbf{v})$.

This structure of segments containing intervals that are successively mapped into segments will allow us to establish a recurrence in section 8 and to construct nested sequences of intervals containing the initial conditions for switching.

Definition 1. *A* segment β on H^{in}_v *(resp.:* H^{in}_C*) is a smooth regular parametrized curve* $\beta : [0,1] \to H^{in}_p$ *(resp.:* $\beta : [0,1] \to H^{in}_C$*) , that meets* $W^s(\mathbf{v})$ *(resp.* $W^s(\mathbf{C})$*) transverselly at the point* $\beta(1)$ *only and such that, writing* $\beta(s) = (x(s), y(s))$*, both* x *and* y *are monotonic functions of* s*.*

The coordinates (x, y) may be chosen so as to make the angular coordinate x an increasing or decreasing function of s as convenient.

Definition 2. *Let* U *be an open set in a plane in* $\mathbf{R}^n$ *and* $p \in U$*. A* spiral on U around p *is a curve* $\alpha : [0,1) \to U$ *satisfying* $\lim_{s\to 1^-} \alpha(s) = p$ *and such that, if* $\alpha(s) = (\alpha_1(s), \alpha_2(s))$ *are its expressions in polar coordinates* (ρ, θ) *around* p*, then* α_1 *and* α_2 *are monotonic, with*

$$\lim_{s\to 1^-} |\alpha_2(s)| = +\infty.$$

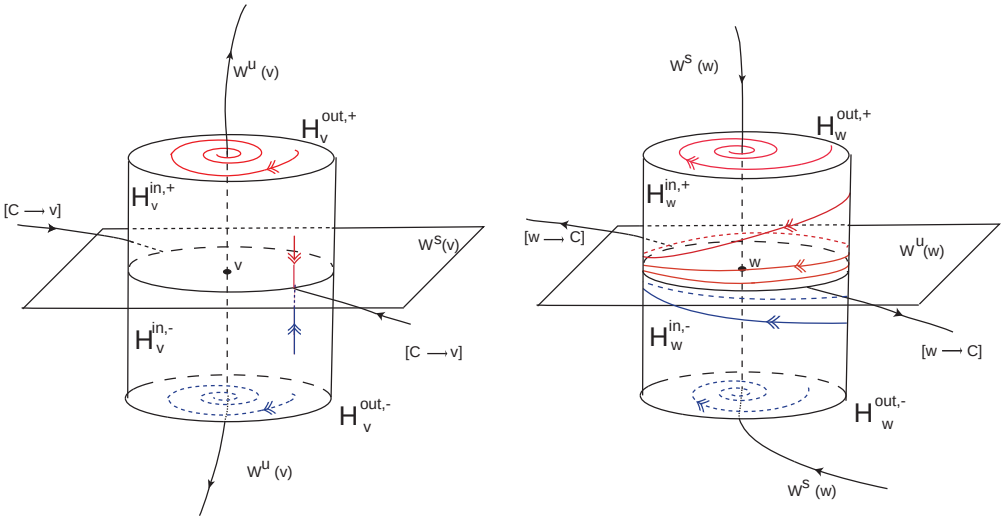

FIGURE 8. Local dynamics near the saddle-foci. *Left*: near **v**, any segment on the cylinder wall is mapped into a spiral on the top or bottom of the cylinder. *Right*: a spiral on the top or bottom of the cylinder near **w** is mapped into a helix on the cylinder wall accumulating on $W^u(\mathbf{w})$. The double arrows on the segment, spiral and helix indicate correspondence of orientation and not the flow.

It follows that α_1 is a decreasing function of s.

Proposition 1. *A segment β on $H_v^{in,+}$ (resp. $H_v^{in,-}$) is mapped by ϕ_v into a spiral on $H_v^{out,+}$ (resp. $H_v^{out,-}$) around $W^u(\mathbf{v})$.*

Proof. Write $\beta(s) = (x(s), y(s))$ on $H_v^{in,+}$ with $y(s) \geq 0$ monotonically decreasing and choose a parametrization of $H_v^{in,+}$ such that $x(s)$ is monotonically increasing. Then, writing $\phi_v(\beta(s)) = (r(s), \theta(s))$, it follows from the expression of ϕ_v in

section 5.2 that $r(s)$ is monotonically decreasing while $\theta(s)$ is monotonically increasing. From $\lim_{s\to 1^-} y(s) = 0$ and $\lim_{s\to 1^-} x(s) = x(1)$ the required limits $\lim_{s\to 1^-} r(s) = 0$ and $\lim_{s\to 1^-} \theta(s) = +\infty$ follow. □

Definition 3. *Let $a, b \in \mathbf{R}$ such that $a < b$ and let H be a surface parametrized by a cover $(\theta, h) \in \mathbf{R} \times [a, b]$ where θ is periodic. A* helix on H accumulating on the circle $h = h_0$ *is a curve $\gamma : [0, 1) \to H$ such that its coordinates $(\theta(s), h(s))$ are monotonic functions of s with*

$$\lim_{s\to 1^-} h(s) = h_0 \qquad \text{and} \qquad \lim_{s\to 1^-} |\theta(s)| = +\infty.$$

Proposition 2. *A spiral on $H_w^{in,+}$ (resp. $H_w^{in,-}$) around $W^s(\mathbf{w})$ is mapped by ϕ_w into a helix on $H_w^{out,+}$ (resp. $H_w^{out,-}$) accumulating on the circle $H_w^{out} \cap W^u(\mathbf{w})$.*

Proof. Parametrize $H_w^{in,+}$ so that a spiral $\sigma(s) = (r(s), \theta(s))$ around $W^s(\mathbf{w})$ has $\theta(s)$ increasing with s.

The expression of ϕ_w of section 5.3 ensures that in $\phi_w(\sigma(s)) = (x(s), y(s))$ we have y decreasing with s and x increasing with s. The limits in the definiton of helix follow from the form of ϕ_w and from $\lim_{s\to 1^-} r(s) = 0$ and $\lim_{s\to 1^-} \theta(s) = +\infty$. □

Proposition 3. *A segment β on $H_{C,+}^{in,+}$ is mapped by ϕ_C into a helix on $H_{C,+}^{out,+}$ accumulating on the circle $W^u(\mathbf{C}) \cap H_C^{out,+}$.*

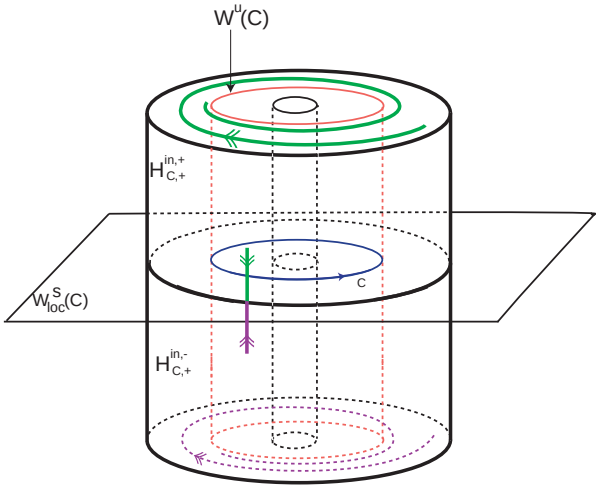

FIGURE 9. Local dynamics near the closed trajectory **C**. A segment on the wall ending at $W^s(\mathbf{C})$ is mapped into a curve accumulating on $W^u(\mathbf{C}) \cap H_C^{out}$.

The proof, as in Propositions 1 and 2, consists of using the expression of ϕ_C of section 5.4 after a suitable choice of orientation in $H_{C,+}^{in,+}$.

Using the symmetries of the linearised flow, it follows that Proposition 3 also holds for a segment β on $H_{C-}^{in,+}$ and for $H_{C-}^{out,+}$, as well as for a segment β on $H_{C+}^{in,-}$ and for $H_{C+}^{out,-}$ and for β on $H_{C-}^{in,-}$ and for $H_{C-}^{out,-}$, considering the circle $W^u(\mathbf{C}) \cap H_C^{out,-}$ (see figure 9).

7. First return to **v**

Let p and q be two nodes of Σ such that there is a connection $[p \to q]$. The transition map $\Psi_{p,q}$ from H_p^{out} to H_q^{in} follows the trajectory $[p \to q]$ in flow-box fashion. In this section we use this information to put together the local behaviour of trajectories that start near $\pm\mathbf{v}$.

To simplify the reading, we omit the $-$ and $+$ signs. Let $P \in H_w^{out}$ be one of the points where $[\mathbf{w} \to \mathbf{C}]$ meets H_w^{out}. For small $a, b > 0$, the rectangle $\left[-\frac{a}{2}, \frac{a}{2}\right] \times \left[-\frac{b}{2}, \frac{b}{2}\right]$ is mapped diffeomorphically into H_w^{out} by the parametrization that maps the origin to P (figure 10). Its image, that we denote by R_w, will be called a *rectangle in* H_w^{out} *centered at* P with *height* b.

The *vertical sides* of R_w are the images of the segments $(\pm\frac{a}{2}, y)$ with $y \in \left[-\frac{b}{2}, \frac{b}{2}\right]$. Rectangles in H_C^{out} centered at a given point are defined in the same way; we denote them by R_C.

By Propositions 1 and 2, the map

$$\eta = \phi_w \circ \Psi_{v,w} \circ \phi_v : H_v^{in} \to H_w^{out}$$

maps a segment β on H_v^{in} infinitely many times across any small rectangle in H_w^{out} centered at a point in $W^u(\mathbf{w})$.

An *admissible family of intervals* $\mathcal{I} = \{[a_i, b_i]\}_{i \in \mathbf{N}}$ is one that satisfies

$$0 < a_i < b_i < a_{i+1} < 1 \qquad \text{and} \qquad \lim_{i \to \infty} a_i = 1.$$

Proposition 4. *Let R_w be a rectangle in H_w^{out} centered at one point P of $H_w^{out} \cap [\mathbf{w} \to \mathbf{C}]$. For any segment $\beta : [0,1] \longrightarrow H_v^{in}$ there is an admissible family of intervals $\{[\sigma_i, \rho_i]\}_{i \in \mathbf{N}}$ such that:*

(1) *each closed interval $[\sigma_i, \rho_i]$ satisfies $\eta \circ \beta([\sigma_i, \rho_i]) \subset R_w$;*

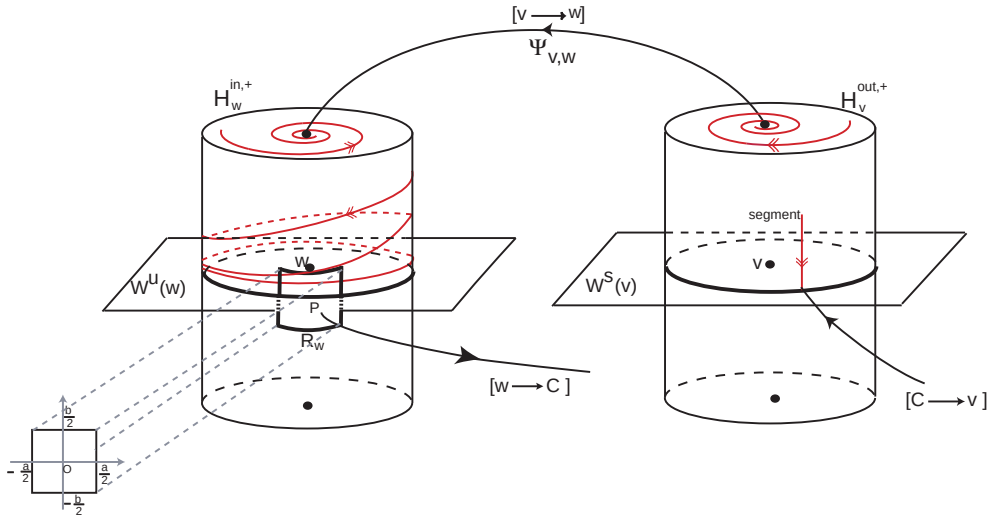

FIGURE 10. Transition from $\mathbf{v}$ to $\mathbf{w}$: a segment on H_v^{in} is mapped into spirals on H_v^{out} around $W^u(\mathbf{v}) \cap H_v^{out}$ and $W^s(\mathbf{w}) \cap H_w^{in}$. The spiral is then mapped into a helix on H_w^{out} accumulating on $W^u(\mathbf{w})$ and crossing infinitely many times a rectangle R_w centered at one of the connections starting at $\mathbf{w}$ (see also figure 11). Double arrows indicate orientation of the segment and not the flow.

(2) *each open interval* (ρ_{i+1}, σ_i) *satisfies* $\eta \circ \beta((\rho_{i+1}, \sigma_i)) \cap R_w = \emptyset$*;*
(3) *the family of curves* $\{\eta \circ \beta([\sigma_i, \rho_i])\}$ *accumulates uniformly on* $W^u(\mathbf{w}) \cap R_w$ *as* $i \to +\infty$.

This also holds for the local map around $\mathbf{C}$*, with* $\mathbf{C}$*,* ϕ_C *and* $\mathbf{C}$ *where we have written* $\mathbf{w}$*,* η *and* $\mathbf{v}$.

Proof. Writing $(x(s), y(s))$ for the coordinates of the helix $\eta \circ \beta(s)$ on the cylinder wall, we have that y decreases with s and that $x(s)$ can be taken as an increasing function of s by choosing compatible orientations in H_v^{in} and H_w^{out} and, if necessary, by restricting the domain of β to a smaller interval $(s_1, 1)$. In particular the helix $\eta \circ \beta$ may be seen as a graph $(x, y(x))$ where $x \in [x(0), +\infty)$ and where y is a decreasing function of x with $\lim_{x\to\infty} y(x) = 0$ (figure 11).

On H_w^{out}, the rectangle R_w is $[n - a/2, n + a/2] \times [-b/2, b/2]$ with $n \in \mathbf{N}$. Let σ_0 be the smallest value of $s \in (s_1, 1)$ such that $(x(s), y(s))$ lies on the left vertical side of R_w, with $y(\sigma_0) < \frac{b}{2}$ as in figure 11. Then $y(s) < \frac{b}{2}$ for all $s \in [\sigma_0, 1)$.

The sequences defining the family of intervals are obtained from points where the helix meets successive copies of the vertical sides of R_w with $x(\sigma_i) = n_0 + i - a/2$ and $x(\rho_i) = n_0 + i + a/2$. The proof for ϕ_C is similar. □

Proposition 5. *Given a segment* $\beta : [0, 1] \longrightarrow H_v^{in}$*, a rectangle* R_w *of sufficiently small height and the family of intervals* $\{[\sigma_i, \rho_i]\}_{i\in\mathbf{N}}$ *of Proposition 4. Then for sufficiently large* i *there are* τ_i *with* $\sigma_i < \tau_i < \rho_i$ *such that* $\Psi_{w,C} \circ \eta(\beta(\tau_i)) \in W^s(\mathbf{C})$ *and* $\Psi_{w,C} \circ \eta \circ \beta$ *maps each one of the intervals* $[\sigma_i, \tau_i]$ *and* $[\tau_i, \rho_i]$ *into a segment on one of the sets* $H_C^{in,+}$ *and* $H_C^{in,-}$*. This also holds for* $\Psi_{C,v} \circ \phi_C : H_C^{in} \longrightarrow H_v^{in,\pm}$ *with the appropriate changes.*

Proof. Since $W^s(\mathbf{C}) \cap H_w^{out}$ meets $W^u(\mathbf{w}) \cap H_w^{out}$ transversally (property (P5)) then if the height of R_w is small, $W^s(\mathbf{C})$ does not meet its vertical sides. Each one of the images $\eta \circ \beta([\sigma_i, \rho_i])$ meets $W^s(\mathbf{C}) \cap H_w^{out}$ transversely at a single point $\eta \circ \beta(\tau_i)$, since they accumulate uniformly on $W^u(\mathbf{w}) \cap R_w$ as $i \to +\infty$. The monotonicity of the coordinates of $\eta \circ \beta$ will be preserved by $\Psi_{w,C}$

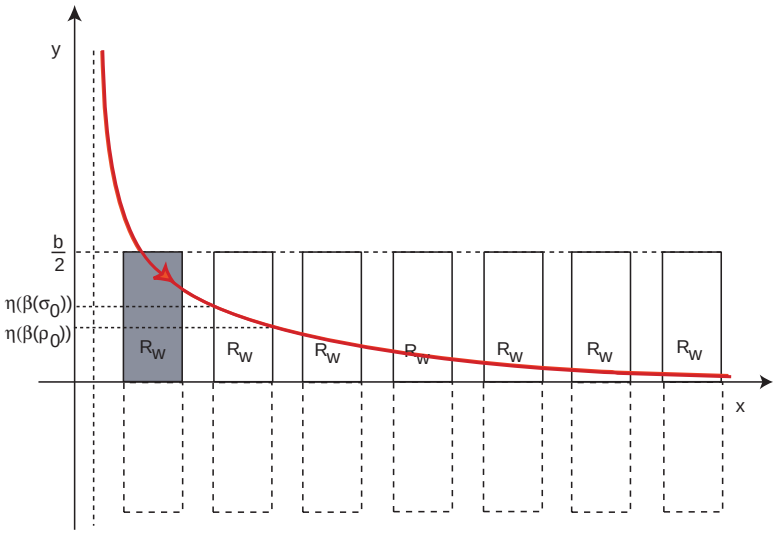

FIGURE 11. A helix on a periodic cover of the cylinder wall H_w^{out}. After it meets the first (shaded) copy of the rectangle, the helix will intersect the rectangle at intervals whose image accumulates on the curve $W^u(\mathbf{w})$, represented here by the x-axis.

close to $W^u(\mathbf{w})$. Each component of $\eta \circ \beta([\sigma_i, \rho_i]) \setminus \{\eta \circ \beta(\tau_i)\}$ will be mapped into a segment, one into each connected component of $H_C^{in,j} \setminus W^s(\mathbf{C})$. The proof for $\Psi_{C,v} \circ \phi_C$ is analogous. □

8. Switching near the Heteroclinic Network

In this section, we put together the information about the first return map to H_v^{in}. In sections 6 and 7 we have found that a segment ending at the stable manifold of one node contains intervals that are mapped into segments ending at the stable manifold of the next node. Starting with a segment on H_v^{in}, here this is used recursively to obtain sequences of nested intervals containing initial conditions that follow sequences of heteroclinic connections.

We say that the path $s^k = (c_j)_{j\in\{1,\dots,k\}}$ of order k on the network Σ is *inside* the path $t^{k+l} = (d_j)_{j\in\{1,\dots,k+l\}}$ of order $k+l$ (denoted $s^k \prec t^{k+l}$) if $c_j = d_j$ for all $j \in \{1,\dots,k\}$.

The family of closed intervals $\mathcal{I} = \{I_i\}_{i\in\mathbf{N}}$ is *inside* the family $\tilde{\mathcal{I}} = \{\tilde{I}_i\}_{i\in\mathbf{N}}$ ($\mathcal{I} < \tilde{\mathcal{I}}$) if, for all $i \in \mathbf{N}$, $I_i \subset \tilde{I}_i$. If $\tilde{\mathcal{I}}$ is admissible in the sense of section 7 and $\mathcal{I} < \tilde{\mathcal{I}}$ then $\mathcal{I}$ is also admissible, provided none of its intervals consists of a point.

Theorem 6. *There is finite switching near the network Σ defined by a vector field satisfying (P1–P5).*

Proof. Given a path, we want to find trajectories that follow it into the neighbourhoods of section 5 going through small disks in H_v^{out} around $W^u(\pm\mathbf{v})$ and through rectangles in H_w^{out} and H_C^{out} centered at the connections. Without loss of generality we only consider paths $s^k = (c_j)_{j\in\{1,\dots,k\}}$ starting with $c_1 = [\pm\mathbf{v} \to \pm\mathbf{w}]$.

Take a segment β on $H_v^{in,\pm}$ of points that follow the first connection c_1. We will construct admissible families of intervals $\mathcal{I}(c_1,\dots,c_n) = \{I_i\}_{i\in\mathbf{N}}$ recursively, such that points in $\beta(I_i)$ follow $(c_1,\dots,c_n)$ and the image of $\beta(I_i)$ by the transition maps is a segment. We will show that $s^k \prec s^{k+l}$ implies $\mathcal{I}(s^k) > \mathcal{I}(s^{k+l})$ and thus the process will be recursive.

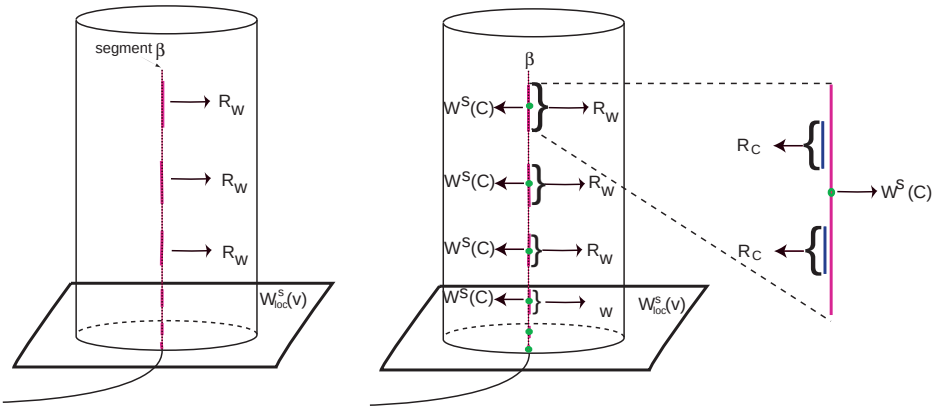

FIGURE 12. On a segment β on H_v^{in}, there are infinitely many small segments that are mapped by η into R_w, each one containing a point mapped into $W^s_{loc}(\mathbf{C})$. The small segments contain smaller ones that are mapped into R_C and this may be continued, forming a nested sequence.

By Propositions 4 and 5, there is an admissible family of intervals $\mathcal{I}(c_1, c_2) = \{I_i\}_{i\in\mathbf{N}}$ such that $\beta(I_i)$ is mapped by $\Psi_{w,C} \circ \phi_w \circ \Psi_{v,w} \circ \phi_v$ into a segment on $H_C^{in,\pm}$ with the choice of sign appropriate for the next connection c_3. Applying the second part of Propositions 4 and 5 to this segment, we obtain an admissible family of intervals $\mathcal{I}(c_1, c_2, c_3) < \mathcal{I}(c_1, c_2)$ corresponding to points that follow (c_1, c_2, c_3) and to intervals that are mapped into a segment on $H_v^{in,\pm}$ with the choice of sign appropriate for following the connection c_4.

In Proposition 5 we assume the height of the rectangle R_w is small and we reduce it if necessary. This is done to ensure that inside R_w the stable manifold $W^s(\mathbf{C})$ is the graph of a function and thus a helix only meets it once at each turn. However, as soon as the choice of height is made it may be kept throughout the proof and thus the construction of $\mathcal{I}(s^k)$ is recursive, proving finite switching near Σ. □

Theorem 7. *There is infinite switching near the network Σ defined by a vector field satisfying (P1–P5).*

Proof. Fix an infinite path $s^\infty = (c_j)_{j\in\mathbf{N}}$ on Σ. For each $k \in \mathbf{N}$ define the finite path s^k of order k by $s^k = (c_j)_{j\in\{1,\dots,k\}}$, with $s^k \prec s^{k+1}$. From the proof of Theorem 6, for each k we have an admissible family of intervals $\mathcal{I}(s^k) = \{J_{ki}\}_{i\in\mathbf{N}}$ such that $\mathcal{I}(s^k) > \mathcal{I}(s^{k+1})$ and all the points in $\beta(J_{ki})$ follow s^k.

Since we have $\mathcal{I}(s^k) > \mathcal{I}(s^{k+1})$ then $\Lambda = \bigcap_{k=1}^\infty \mathcal{I}(s^k)$ is non-empty because each set $\Lambda_i = \bigcap_{k=1}^\infty J_{ki}$ is non empty. From the definition of admissible family of intervals, if we take $a_i \in \Lambda_i$ then $\lim_{i\to\infty} a_i = 1$. From the construction we have that $\beta(a_i)$ follows s^∞. Thus, we have obtained a sequence of points $\beta(a_i)$ that accumulate on Σ as $i \to \infty$ and that follow the infinite path. □

9. Final remarks and discussion

9.1. **Generalisation.** Not all assumptions of Section 3 are essential to prove switching, although some of them simplify the calculations. For instance, the eigenvalues at $\pm\mathbf{v}$ and $\pm\mathbf{w}$ may have any imaginary part, not necessarily 1 as in (P3). The proof also works if at one of the pairs of nodes $\pm\mathbf{v}$ or $\pm\mathbf{w}$ the eigenvalues of df are real, as long as the eigenvalues at the other pair of nodes are not real — it is enough to have one pair of rotating equilibria. Any finite number of

1-dimensional connections $[\mathbf{w} \to \mathbf{C}]$ and $[\mathbf{C} \to \mathbf{v}]$ could have been used instead of two for each equilibrium.

The existence of swicthing near a network may be easily generalised to a heteroclinic network involving any number of rotating nodes such that each heteroclinic connection involving a periodic trajectory is transverse and there are no consecutive non-transverse heteroclinic connections on the network.

It is not essential to have $(\mathbf{Z}_2 \oplus \mathbf{Z}_2)$-equivariance. The symmetry γ_2 is used here to obtain the closed trajectory $\mathbf{C}$ and the role of γ_1 is to guarantee that the one-dimensional connections $[\mathbf{v} \to \mathbf{w}]$ are robust. Symmetries make the existence of the network natural and ensure persistence. Switching will hold for any network without symmetry having the nodes and connections prescribed here, as long as the remaining assumptions are satisfied.

Estimates for the transition maps may be refined as in Aguiar *et al.* [4] to show that near this network there is a suspended horseshoe with transition map described as a full shift over a countable set of symbols. The suspended horseshoe has the same shape as the network. Thus, when the symmetry of the example in section 4 is partly broken we have instant chaos. In particular it can be shown that there are periodic orbits that follow any finite path in the network, but this uses techniques beyond the scope of this paper.

Finite switching is present even when all the local maps are expanding, as in the case $C_v < E_v$, $C_w < E_w$, $C_C < E_C$. This is due to the rotation around the nodes and is markedly different from the situation where all eigenvalues are real. In the example of section 4 this corresponds to parameter values where the $\mathbf{O}(2)$-symmetric network is a repeller.

A path on the network can also be shadowed by trajectories in $W^u(\mathbf{C})$ (see figure 12) because the local unstable manifold of $\mathbf{C}$ meets H_v^{in} at a segment by the transversality assumption (P5). It also follows that there are infinitely many homoclinic connections involving the periodic trajectory $\mathbf{C}$, although there are no homoclinic trajectories involving the equilibria. The geometry of $W^u(\mathbf{C})$ gets extremely complicated as we move away from $\mathbf{C}$, since it will accumulate on the whole network, having $\mathbf{v}$, $\mathbf{w}$ and $\mathbf{C}$ as limit points. A complete description of the nonwandering set for this type of flows is in preparation.

9.2. **Discussion.** Generic breaking of the γ_1-symmetry destroys the network, as in [14] and [20], by breaking the connections $[\mathbf{v} \to \mathbf{w}]$. If the remaining assumptions are still satisfied, a weaker form of switching will hold: for small symmetry-breaking terms, it may still be possible to find trajectories that visit neighbourhoods of finite sequences of nodes. This is because the spirals on top of the cylinder around $\mathbf{w}$ of figure 8 will be off-centered and will turn a finite number of times around $W^s(\mathbf{w})$. From this we may obtain points whose trajectories follow short finite paths on the network. As $W^u(\mathbf{v})$ gets closer to $W^s(\mathbf{w})$ (as the system moves closer to symmetry) the paths that can be shadowed get longer.

This is in contrast to the findings of Kirk and Rucklidge [14], who claim that there can be no switching in generic systems close to the symmetric case, so a comparison of the settings and results of the two papers is in order at this point. The first caveat is that the $\mathbf{Z}_2 \oplus \mathbf{Z}_2$ representations are different: in our case $Fix(\mathbf{Z}_2 \oplus \mathbf{Z}_2) = \{0\}$, and there are two transverse 2-dimensional fixed-point subspaces for the isotropy subgroups, whereas in [14], $Fix(\mathbf{Z}_2 \oplus \mathbf{Z}_2)$ is a plane with two 1-dimensional fixed-point subspaces for the isotropy subgroups. In their setting, our symmetries correspond to the group generated by a rotation of π in $\mathbf{SO}(2)$ and by the product of their $\mathbf{Z}_2 \oplus \mathbf{Z}_2$ generators. Both representations occur in the larger group $\mathbf{Z}_2 \oplus \mathbf{Z}_2 \oplus \mathbf{SO}(2)$ used in [20]. Moreover, we are assuming the existence of an invariant 3-sphere (a natural assumption in the symmetric context, see [8]) and it is not evident that in their context such a sphere will exist.

However, the difference in the results of [14] and ours indicates that vector fields with $\mathbf{Z}_2 \oplus \mathbf{Z}_2 \oplus \mathbf{SO}(2)$ symmetry have codimension higher than 3 in the universe of general vector fields. This will mean that in general systems close to symmetry what will be observed may depend

on the way symmetries are broken and that a lot more needs to be done before switching is well understood.

References

[1] M. Aguiar, *Vector Fields with heteroclinic networks,* PhD Thesis, Departamento de Matemática Aplicada, Faculdade de Ciências da Universidade do Porto, 2003

[2] M. Aguiar, P. Ashwin, A. Dias and M. Field, *Robust heteroclinic cycles in coupled cell systems: Identical cells with asymmetric inputs*, Journal of Nonlinear Science, No. 21, Issue 2, 271–323, 2011

[3] M. Aguiar, S. B. Castro and I. S. Labouriau, *Simple Vector Fields with Complex Behaviour,* Int. Jour. of Bifurcation and Chaos, Vol. 16, No.2, 369–381, 2006

[4] M. Aguiar, S. B. Castro and I. S. Labouriau, *Dynamics near a heteroclinic network,* Nonlinearity 18, 391–414, 2005

[5] D. Armbruster, E. Stone and V. Kirk, *Noisy heteroclinic networks,* Chaos, Vol. 13, No.1, 71–79, 2003

[6] P. Ashwin and M. Field, *Heteroclinic Networks in Coupled Cell Systems* Arch. Rational Mech. Anal., Vol. 148, 107–143, 1999

[7] W. Brannath, *Heteroclinic networks on the tetrahedron*, Nonlinearity, Vol. 7, 1367–1384, 1994

[8] M. Field, *Lectures on bifurcations, dynamics and symmetry*, Pitman Research Notes in Mathematics Series, Vol. 356, Longman, 1996

[9] M. I. Golubitsky, I. Stewart, and D. G. Schaeffer, *Singularities and Groups in Bifurcation Theory* , Vol. II, Springer, 2000

[10] J. Guckenheimer and P. Worfolk, *Instant Chaos*, Nonlinearity, Vol. 5, 1211–1222, 1992

[11] J. Hofbauer, *Heteroclinic Cycles in Ecological Differential Equations*, Tatra Mountains Math. Publ., Vol. 4, 105–116, 1994

[12] J. Hofbauer, *Heteroclinic Cycles on the simplex*, Proc. Int. Conf. Nonlinear Oscillations, Janos Bolyai Math. Soc. Budapest, 1987

[13] J. Hofbauer and K. Sigmund, *The Theory of Evolution and Dynamical Systems*, Cambridge University Press, Cambridge, 1988

[14] V. Kirk and A. M. Rucklidge *The effect of symmetry breaking on the dynamics near a structurally stable heteroclinic cycle between equilibria and a periodic orbit,* Dynamical Systems: An International Journal, 23, 42–74, 2008

[15] V. Kirk and M. Silber, *A competition between heteroclinic cycles*, Nonlinearity, Vol. 7, 1605–1621, 1994

[16] M. Krupa, *Robust Heteroclinic Cycles*, J. Nonlinear Sci., 7, 129–176, 1997

[17] M. Krupa and I. Melbourne, *Asymptotic Stability of Heteroclinic Cycles in Systems with Symmetry,* Ergodic Theory and Dynam. Sys., Vol. 15, 121–147, 1995

[18] M. Krupa and I. Melbourne, *Asymptotic Stability of Heteroclinic Cycles in Systems with Symmetry, II,* Proc. Roy. Soc. Edinburgh, 134A, 1177–1197, 2004

[19] I. Melbourne, *An example of a non-asymptotically stable attractor* Nonlinearity, Vol. 4, 835–844, 1991

[20] I. Melbourne, M. R. E. Proctor and A. M. Rucklidge, *A heteroclinic model of geodynamo reversals and excursions* Dynamo and Dynamics, a Mathematical Challenge (eds. P. Chossat, D. Armbruster and I. Oprea, Kluwer: Dordrecht, 363–370, 2001

[21] C. M. Postlethwaite and J. H. P. Dawes, *Regular and irregular cycling near a heteroclinic network* Nonlinearity, Vol. 18, 1477–1509, 2005

[22] V. S. Samovol, *Linearization of a system of differential equations in the neighbourhood of a singular point,* Sov. Math. Dokl, Vol. 13, 1255–1959, 1972

[23] Y. Sato, E. Akiyama and J. P. Crutchfield, *Stability and diversity in collective adaptation*, Physica D, Vol. 210, 21–57, 2005

[24] T. Ura, *On the flow outside a closed invariant set: stability, relative stability and saddle sets,* Contributions to Differential Equations, vol. III, No. 3, 249–94, 1964

(M.A.D.Aguiar) Centro de Matemática da Universidade do Porto, and Faculdade de Economia da Universidade do Porto, Rua Dr. Roberto Frias, 4200-464 Porto, Portugal

E-mail address: maguiar@fep.up.pt

(I.S. Labouriau and A.A.P. Rodrigues) Centro de Matemática da Universidade do Porto, and Faculdade de Ciências da Universidade do Porto, Rua do Campo Alegre 687, 4169–007 Porto, Portugal

E-mail address, I.S.Labouriau: islabour@fc.up.pt

E-mail address, A.A.P.Rodrigues: alexandre.rodrigues@fc.up.pt

Article 2 – Chaotic Double Cycling

Published in Dynamical Systems: an International Journal, Vol. 26, Issue 2, pages 199–233, 2011

CHAOTIC DOUBLE CYCLING

ALEXANDRE A.P. RODRIGUES, ISABEL S. LABOURIAU, AND MANUELA A.D. AGUIAR

Abstract. We study the dynamics of a generic vector field in the neighbourhood of a heteroclinic cycle of non-trivial periodic solutions whose invariant manifolds meet transversely. The main result is the existence of chaotic double cycling: there are trajectories that follow the cycle making any prescribed number of turns near the periodic solutions, for any given bi-infinite sequence of turns. Using symbolic dynamics, arbitrarily close the cycle, we find a robust and transitive set of initial conditions whose trajectories follow the cycle for all time and that is conjugate to a Markov shift over a finite alphabet. This conjugacy allows us to prove the existence of infinitely many heteroclinic and homoclinic subsidiary connections, which give rise to a heteroclinic network with infinitely many cycles and chaotic dynamics near them, exhibiting themselves switching and cycling. We construct an example of a vector field with $\mathbf{Z}_3$ symmetry in a 5-dimensional sphere with a heteroclinic cycle having this property.

1. Introduction

A particularly important subject in the theory of nonlinear dynamical systems is the study of the behaviour near homoclinic and heteroclinic cycles. A review of homoclinic and heteroclinic theory for autonomous vector fields is given in Homburg *et al* [16]. Symmetry is a natural setting for persistent heteroclinic cycles. In this context, Krupa *et al* [21] give a sufficient condition (also necessary when some additional conditions are satisfied) for a heteroclinic cycle to be asymptotically stable: trajectories near the heteroclinic cycle will follow and approach it infinitely.

Associated to asymptotically stable heteroclinic cycles we observe intermittency: trajectories near it take some time near each node and spend more and more time near the nodes on each subsequent return. For a given trajectory approaching the cycle, the duration of visits is a geometrically increasing sequence of times. A natural question arises: is it possible to control the time on each visit to a neighbourhood of the nodes of the cycle?

If the cycle is asymptotically stable, the answer has been given by Melbourne [22]. If the invariant manifolds of the nodes meet transversely, the cycle is not asymptotically stable, the system is chaotic and there are few results concerning the dynamic behaviour in the neighbourhood of the cycle. In this paper, we provide an affirmative answer to the question in the context of non-asymptotically stable heteroclinic cycles between non-trivial periodic solutions, by counting the number of times a trajectory turns around each node.

Given a set of neighbourhoods of the nodes and any prescribed number of turns inside each of the neighbourhoods, we prove the existence of trajectories that follow the cycle making the prescribed turns as it travels alongside the cycle. The number of turns may be chosen as an arbitrary bi-infinite sequence of numbers. This is not a temporal transient phenomenon; it is a robust behaviour that we call chaotic double cycling.

2000 *Mathematics Subject Classification.* Primary: 37C29; Secondary: 34E10, 34C28, 37C27, 37C20.

Key words and phrases. vector fields, heteroclinic cycle and networks, bi-infinite cycling, symbolic dynamics, horseshoe in time.

The research of all authors at Centro de Matemática da Universidade do Porto (CMUP) had financial support from Fundação para a Ciência e a Tecnologia (FCT), Portugal, through the programs POCTI and POSI with European Union and national funding. A.A.P. Rodrigues was supported by the grant SFRH/BD/28936/2006 of FCT.

In the Hamiltonian setting this has been studied in the context of the two and three-body problems by Moeckel [23] and by Koon *et al* [19]. Both papers prove the existence of homoclinic and heteroclinic cycles between two periodic solutions which have the same energy for a Hamiltonian vector field and adress some other dynamical properties like switching and chaotic changes of configuration. However, the restriction of a Hamiltonian system to an energy level does not define a generic differential equation — for instance, its flow preserves volume and the dynamical issues addressed are different from ours. In particular they do not discuss cycling, which is the main point of this article.

We show cycling with chaotic behaviour, even though the nodes in the heteroclinic cycles we consider are not chaotic sets. This differs from the situation studied in Dellnitz *et al* [9], where cycling chaos is proved for heteroclinic cycles whose nodes are chaotic attractors. For robust cycling between chaotic sets, see also Ashwin *et al* [8].

Framework of the paper. We study the dynamics near a cycle of periodic solutions, first in a 3-dimensional manifold, then in any dimension. We ask for transverse intersection of the invariant manifolds of all successive nodes. This is possible only because the heteroclinic cycle contains periodic trajectories and not equilibria.

After some preliminary definitions in section 2, the proof in 3 dimensions occupies sections (3-5): notation and definitions in section 3; results that prepare the proof in section 4.

The main point of the proof given in section 5 is to find a set Λ of initial conditions whose trajectories remain near the cycle for all time and whose behaviour may be coded using symbolic dynamics. However, our coding is not only related to the space orbit of the associated trajectory, but also to the number of times that the trajectory cycles around each node, like a horseshoe in time.

The coding by a finite set of symbols allows us to obtain further results on the dynamics, presented in section 6. In particular we prove the existence of infinitely many subsidiary homoclinic and heteroclinic connections near the original cycle. Each new cycle may exhibit persistent cycling, giving rise to a very complicated heteroclinic network. This leads to horseshoe dynamics (in space) conjugated to a Markov shift near any cycle in the network, including the original one. The use of symbolic dynamics allows us to conclude other properties of the invariant set, such as topological mixing and the existence of a Gibbs measure (under the restrictions presented by Sarig [24]).

The extension of our results to higher dimensions is proved in section 7, where we use the center manifold theorem for heteroclinic cycles studied by Shaskov *et al* [25] (in the context of homoclinic orbits) and Shilnikov *et al* [27]. Under some generic hypothesis, we reduce the study of the dynamics near a heteroclinic cycle in an n-dimensional manifold, to a 3-dimensional flow-invariant centre manifold containing the cycle. We end by presenting the construction of an example of a system of differential equations with $\mathbf{Z}_3$ symmetry in a 5-dimensional globally attracting sphere in $\mathbf{R}^6$, whose flow has a heteroclinic cycle between three periodic solutions. We show numerical evidence that the invariant manifolds meet transversely and that thus the example satisfies the conditions of the result and chaotic cycling holds. This last property is illustrated by numerical plots of solutions to the equations.

2. Preliminaries

Let M be a smooth n-dimensional manifold and let $f : M \to TM$ be a smooth vector field defined on M. Denote by $\phi(t, p)$ the unique solution $x(t)$ of the initial value problem:

$$\dot{x} = f(x), \quad x(0) = p. \tag{1}$$

In this paper we consider non-trivial periodic solutions of (1) that are hyperbolic and that have at least one Floquet multiplier with absolute value greater than 1 and at least one Floquet multiplier with absolute value less than 1. We call these *periodic solutions of saddle type.*

Given two periodic solutions c_i and c_j of (1) of saddle type, a heteroclinic connection from c_i to c_j is a trajectory contained in $W^u(c_i) \cap W^s(c_j)$ that will be denoted $[c_i \to c_j]$.

Let $\mathcal{S} = \{c_j : j \in \{1, \dots, k\}\}$ be a finite ordered set of periodic solutions of saddle type of (1) such that

$$\forall j \in \{1, \dots, k\} \quad W^u(c_j) \cap W^s(c_{j+1}) \neq \emptyset \pmod{k}.$$

A *heteroclinic cycle* Σ associated to $\mathcal{S}$ is the union of the saddles in $\mathcal{S}$ with a heteroclinic connection $[c_j \to c_{j+1}] \pmod{k}$, for each $j \in \{1, \dots, k\}$. If $k = 1$, the heteroclinic cycle is called *homoclinic* cycle. We denote by $\Sigma = \langle c_1, \dots, c_k \rangle$ a heteroclinic cycle associated to $\{c_j : j \in \{1, \dots, k\}\}$ and we refer to the saddles defining the heteroclinic cycle as *nodes.* A *heteroclinic network* is a connected set that is the union of heteroclinic cycles.

Given a heteroclinic cycle of periodic solutions Σ with nodes c_j, $j = 1, \dots, k$, let V_Σ be a compact neighbourhood of Σ and let V_j be pairwise disjoint compact neighbourhoods of the nodes $c_j \in \mathcal{S}$, such that each boundary ∂V_j is a finite union of smooth manifolds with boundary, that are transverse to the vector field everywhere, except for their boundary. Then each V_i is called an *isolating block for* c_i and $\mathcal{V} = \{V_i\}_{i \in \{1,\dots,k\}}$ is called a *system of isolating blocks for* Σ.

For each $V_j \in \mathcal{V}$, consider a codimension 1 submanifold with boundary $\Pi_j \subset V_j$ of M, such that:

- the flow is transverse to Π_j;
- Π_j intersects ∂V_j transversely;
- $\Pi_j \cap c_j$ has only one element.

We call Π_j a *counting section.* Any set of k counting sections, one inside each isolating block, is called a *system of counting sections associated to* $\mathcal{V}$.

We are interested in trajectories that go inside a neighbourhood V_j in positive time and hit the counting section Π_j a finite number of times (which can be zero) until they leave the neighbourhood. Every time the trajectory makes a turn inside V_j it hits the counting section (see figure 1 (a)). Hence, it is natural to have the following definition where $int(A)$ is the interior of $A \subset M$:

Definition 1. *Let c_j be a periodic trajectory of saddle type, with V_j an isolating block for c_j and Π_j a counting section. Let $q \in \partial V_j$ be a point such that the following properties hold:*

- $\exists \tau > 0, \forall t \in (0, \tau), \phi(t, q) \in int(V_j)$
- $\phi(\tau, q) \in \partial V_j$.

The trajectory of q turns n times around c_j in V_j, relatively to Π_j *if*

$$\#\left(\{\phi(t, q), t \in [0, \tau]\} \cap \Pi_j\right) = n \geq 0 \ .$$

Definition 2. *A heteroclinic cycle $\Sigma = \langle c_1, \dots, c_k \rangle$ of periodic trajectories has* cycling *if there exist:*

- *V_Σ a neighbourhood of Σ;*
- *$\mathcal{V} = \{V_j\}_{j \in \{1,\dots,k\}}$ a system of isolating blocks;*
- *$\{\Pi_j\}_{j \in \{1,\dots,k\}}$ a system of counting sections;*

such that given an index set I to be specified below, for any sequence of nonnegative integers $(z_i)_{i \in I}$, there exists a point q and there are times $(t_i^{in})_{i \in I}$ and $(t_i^{out})_{i \in I}$ satisfying $t_i^{in} < t_i^{out} < t_{i+1}^{in}$ such that, for each $i \in I$, if $i \equiv j \pmod{k}$:

- *$\phi(t, q) \in V_\Sigma$ for $t \in [t_i^{in}, t_i^{out}]$ and for $t \in [t_i^{out}, t_{i+1}^{in}]$;*
- *for all $t \in (t_i^{in}, t_i^{out})$, the trajectory $\phi(t, q)$ lies in $int(V_j)$;*

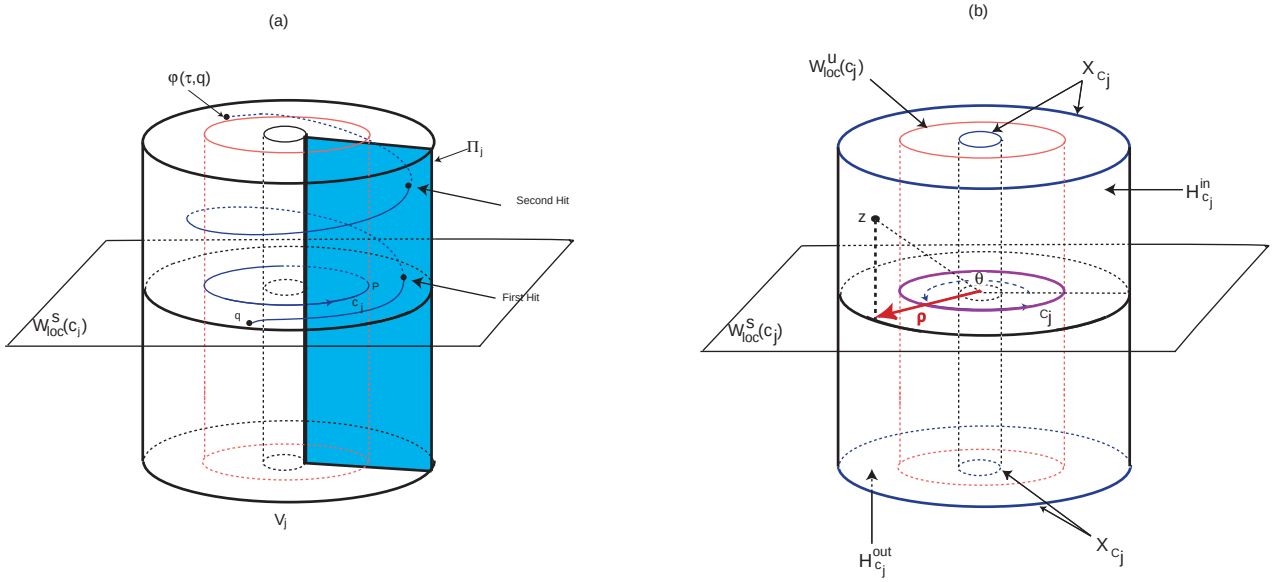

FIGURE 1. (a): Example of a trajectory turning twice around a periodic trajectory c_j, in V_j with respect to Π_j. (b): General cylindrical coordinates on the neighbourhood V_j of c_j and isolating blocks. The set $H^{in}_{c_j}$ is formed by two cylinder walls, the set $H^{out}_{c_j}$ corresponds to the top and bottom anuli and $X_{c_j} = \overline{H^{in}_{c_j}} \cap \overline{H^{out}_{c_j}}$ consists of four circles.

- *for* $t \in [t_i^{in}, t_i^{out}]$, *the trajectory* $\phi(t,q)$ *turns* z_i *times around* c_j, *in* V_j, *with respect to* Π_j;
- *for* $t \in (t_i^{out}, t_{i+1}^{in})$, $\phi(t,q)$ *does not visit the isolating block for any node in* Σ.

When the property above holds for a finite index set $I = \{1, \ldots, m\}$, *then* Σ *has* finite cycling of order m. *When it holds for* $I = \mathbf{Z}$ *then* Σ *has* bi-infinite cycling *(also called* chaotic double cycling *for reasons that will be apparent in the sequel).*

We refer to the difference $t_j^{out} - t_j^{in}$ as the *time of flight* of the first visit of the trajectory $\phi(t,q)$ to V_j.

For a heteroclinic network Σ^* with node set $\mathcal{A} = \{c_j\}_{j=1,\ldots,k}$, a *path on* Σ^* is an infinite sequence (s_l) of connections $s_l = [x_l \to y_l]$ in Σ^* such that x_l , $y_l \in \mathcal{A}$ and $y_l = x_{l+1}$, thus forming a connected graph. For each heteroclinic connection in a network Σ^* , consider a point p on it and a small neighbourhood V of p, so that these neighbourhoods are pairwise disjoint. Given a system of isolating blocks for the nodes of Σ^*, if a trajectory $\phi(t)$ visits all these neighbourhoods in the same sequence as the path (s_l) we say it *follows the path* (s_l).

There is *switching near* Σ^* if for each system of neighbourhoods as above and for each path on Σ^* there is a trajectory that follows it. See Aguiar *et al* [4, 6] for a detailed discussion of these concepts.

3. Local dynamics and transition maps

In this section, we obtain a system of isolating blocks for a cycle $\Sigma = \langle c_1, \ldots, c_k \rangle$ of periodic trajectories in a 3-dimensional manifold. We also establish the notation for the proof of our main results in 3 dimensions.

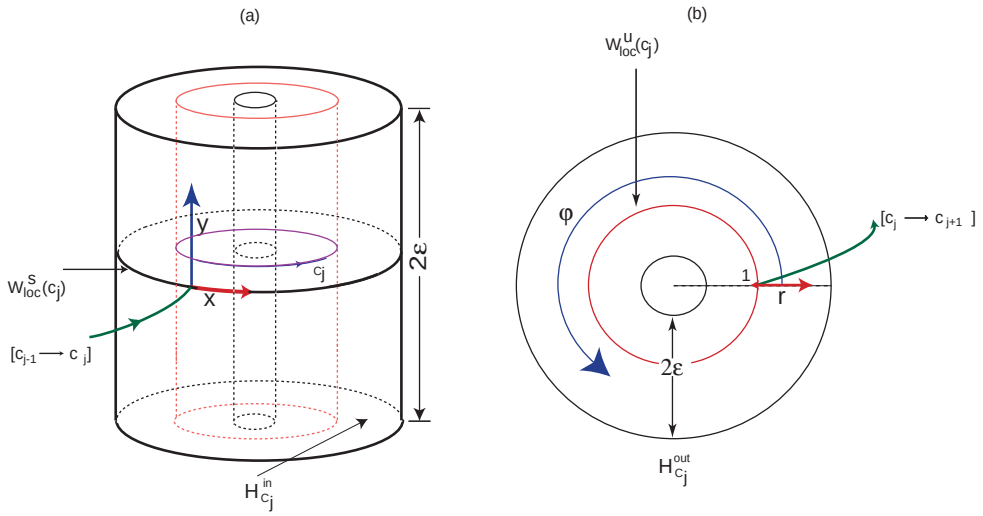

FIGURE 2. Isolating block for the closed trajectory c_j. (a): coordinates on the walls of the hollow cylinder (cross section *in*); (b): coordinates on the top and bottom of the hollow cylinder (cross section *out*). The flow enters the hollow cylinder transversely across the cylinder walls $H^{in}_{c_j}$ and leaves it transversely across the top and bottom $H^{out}_{c_j}$.

3.1. **Suspension.** Consider a local cross-section Π_j at a point p_j in c_j, for $j \in \{1, \dots, k\}$. Since c_j is hyperbolic, by a result of Hartman [14], there is a neighbourhood V_j^* of p_j in Π_j where the first return map π_j is C^1 conjugate to its linear part. The eigenvalues of $d\pi_j$ are e^{E_j} and e^{-C_j}, where $E_j > 0$ and $C_j > 0$.

Suspending the linear map gives rise, in cylindrical coordinates (ρ, θ, z) around c_j (see figure 1 (b)), to the system of differential equations:

$$\left\{ \begin{array}{l} \dot{\rho} = -C_j(\rho - 1) \\ \dot{\theta} = 1 \\ \dot{z} = E_j z \end{array} \right. \tag{2}$$

which is equivalent to the original flow near c_j, although the suspension does not preserve the return time of the original trajectories. In these coordinates, the periodic trajectory c_j is the circle defined by $\rho = 1$ and $z = 0$, its local stable manifold, $W^s_{loc}(c_j)$, is the plane $z = 0$ and $W^u_{loc}(c_j)$ is the surface defined by $\rho = 1$.

3.2. **Isolating blocks for c_j.** We will work with a hollow three-dimensional cylindrical neighbourhood $V_j(\varepsilon)$ of c_j contained in the suspension of V_j^*

$$V_j(\varepsilon) = \{(\rho, \theta, z) : \quad 1 - \varepsilon \leq \rho \leq 1 + \varepsilon, \quad -\varepsilon \leq z \leq \varepsilon \quad \text{and} \quad \theta \in \mathbf{R} \pmod{2\pi}\} \ .$$

When there is no ambiguity, we write V_j instead of $V_j(\varepsilon)$. Its boundary (see figure 1 (b)) is a disjoint union

$$\partial V_j = H^{in}_{c_j} \cup H^{out}_{c_j} \cup X_{c_j}$$

such that :

- $H^{in}_{c_j}$ is the union of the walls, $\rho = 1 \pm \varepsilon$, of the cylinder, locally separated by $W^u(c_j)$. Trajectories starting at $H^{in}_{c_j}$ go inside the cylinder V_j in small positive time.

- $H^{out}_{c_j}$ is the union of two anuli, the top and the bottom, $z = \pm\varepsilon$ of the cylinder, locally separated by $W^s(c_j)$. Trajectories starting at $H^{out}_{c_j}$ go inside the cylinder V_j in small negative time.
- The vector field is transverse to ∂V_j at all points except at the four circles $X_{c_j} = \overline{H^{in}_{c_j}} \cap \overline{H^{out}_{c_j}}$.

The two cylinder walls, $H^{in}_{c_j}$ are parametrised by the covering maps:

$$(\theta_0, z_0) \mapsto (1 \pm \varepsilon, \theta_0, z_0) = (\rho, \theta, z),$$

where $\theta_0 \in \mathbf{R} \pmod{2\pi}$, $|z_0| < \varepsilon$ (see figure 2 (a)). In these coordinates, $H^{in}_{c_j} \cap W^s(c_j)$ is the union of the two circles $z_0 = 0$. The two anuli $H^{out}_{c_j}$ are parametrised by the coverings:

$$(\varphi, r) \mapsto (r, \varphi, \pm\varepsilon) = (\rho, \theta, z),$$

for $1 - \varepsilon < r < 1 + \varepsilon$ and $\varphi \in \mathbf{R} \pmod{2\pi}$ and where $H^{out}_{c_j} \cap W^u(c_j)$ is the union of the two circles $r = 1$ (see figure 2 (b)). In these coordinates $X_{c_j} = \overline{H^{in}_{c_j}} \cap \overline{H^{out}_{c_j}}$ is the union of the four circles defined by $\rho = 1 \pm \varepsilon$ and $z = \pm\varepsilon$.

3.3. **Local map near c_j.** For each $j \in \{1, \dots, k\}$, in the above coordinates, there are local maps ϕ_{c_j} from a connected component of $H^{in}_{c_j}$ into a connected component of $H^{out}_{c_j}$, given by:

$$\phi_{c_j}(\theta_0, z_0) = \left(\theta_0 - \frac{1}{E_j} \ln\left(\frac{z_0}{\varepsilon}\right), 1 \pm \varepsilon \left(\frac{z_0}{\varepsilon}\right)^{\delta_j}\right) = (\varphi, r) \qquad \text{where} \quad \delta_j = \frac{C_j}{E_j} > 0 \ . \tag{3}$$

The signs $\pm$ depend on the component of $H^{in}_{c_j}$ we started at, $+$ for trajectories starting with $\rho > 1$ and $-$ for $\rho < 1$. From now on we use as counting section the rectangle, denoted by Π_j

$$\Pi_j = \{(\rho, \theta, z) : \quad \theta = 0, \quad 1 \le \rho \le 1 + \varepsilon \quad \text{and} \quad 0 \le z \le \varepsilon\} \ .$$

We denote by S^j its intersection with $H^{out}_{c_j}$ (see figure 3 (a)). Without loss of generality we assume each connection $[c_j \to c_{j+1}]$ meets $H^{out}_{c_j}$ far from the counting section Π_j.

3.4. **Transition maps from c_j to c_{j+1}.** Using the parametrisations above, let $(A, 1) = (\varphi, r)$ be the coordinates of the point in $[c_j \to c_{j+1}] \cap H^{out}_{c_j}$ and let $(B, 0) = (\theta_0, z_0)$ be the coordinates of $[c_j \to c_{j+1}] \cap H^{in}_{c_{j+1}}$, with $c_{k+1} = c_1$. A flow-box around a piece of $[c_j \to c_{j+1}]$ containing these two points meets $H^{out}_{c_j}$ and $H^{in}_{c_{j+1}}$ at neighbourhoods of $(A, 1)$ in $H^{out}_{c_j}$ and of $(B, 0)$ in $H^{in}_{c_{j+1}}$. A transition map $\Psi_{j \to j+1}$ is well defined in these neighbourhoods and C^1 close to a non trivial rotation (without loss of generality, for computations, we will use the rotation of $\frac{\pi}{2}$) (see figure 4).

The size of these neighbourhoods depend on the size, ε, of V_j and V_{j+1}; for smaller values of ε, if we extend the flow-box the neighbourhood becomes larger due to the expanding Floquet exponent at each node as in figure 3 (b). Since $W^u(c_j)$ and $W^s(c_{j+1})$ meet transversely, we may take a sufficiently small ε for the neighbourhood V_j so the part of $W^u_{loc}(c_j)$ that lies inside the neighbourhood is mapped by $\Psi_{j \to j+1}$ across the height of $H^{in}_{c_{j+1}}$ as in figure 4. Thus it is possible to define a region $\mathcal{R}^{in,j+1}$ parametrised by a rectangle in $H^{in}_{c_{j+1}}$ around $(B, 0)$, contained in the image of $\Psi_{j \to j+1}$ and such that two opposite sides of $\mathcal{R}^{in,j+1}$ are contained in $X_{c_{j+1}}$. Moreover, $\mathcal{R}^{in,j+1}$ will contain the image of a piece of $\Psi_{j \to j+1}\left(W^u_{loc}(c_j)\right)$ joining two components of X_{c_j} (see figure 4). We will call $\mathcal{R}^{in,j+1}$ *a rectangle in* $H^{in}_{c_{j+1}}$. Note that once this holds for V_j, the same is true for all hollow cylinder neighbourhoods of c_j with smaller size ε. Thus, we may also have a piece of $W^s_{loc}(c_{j+1})$ mapped by $\Psi^{-1}_{j \to j+1}$ across the width of $H^{out}_{c_j}$ and meeting X_{c_j} at two points, reducing ε if necessary.

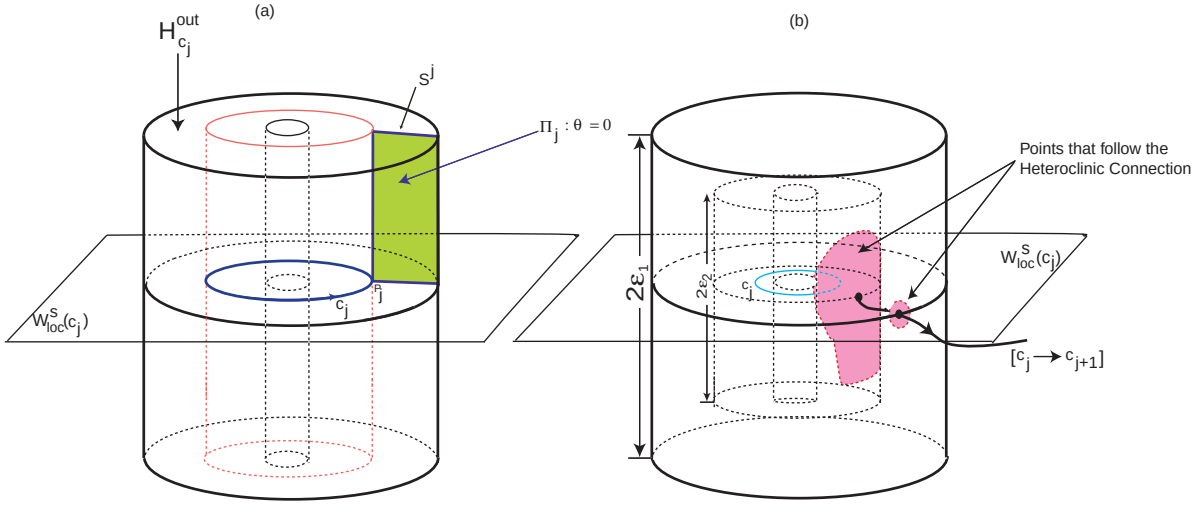

FIGURE 3. (a): The counting section Π_j at c_j is represented by the shaded rectangle and the segment S^j is $\Pi_j \cap H^{out}_{c_j}$; (b) Subsets where a flow-box around the connection $[c_j \to c_{j+1}]$ meets the boundary of cylindrical neighbourhoods $V_j(\varepsilon_2) \subset V_j(\varepsilon_1)$ of c_j. If $\varepsilon_1 > \varepsilon_2 > 0$ the intersection is a larger set, due to the expanding Floquet exponent at each node.

It will also be convenient to assume that, for each j, $\mathcal{R}^{in,j}$ does not intersect S^j, the boundary of the section where turns are counted. This may be achieved by changing the position of the sections if necessary. For sections 4 and 5, we are always considering the system of isolating blocks $\mathcal{V} = \{V_j\}_j$ defined in this section and satisfying these properties.

4. Geometry near the nodes

The notation and constructions of section 3 may now be used to study the geometry associated to the local dynamics around each node of the heteroclinic cycle Σ.

Definition 3. *A* segment β on $H^{in}_{c_j}$ *is a smooth regular parametrized curve* $\beta : [0,1] \to H^{in}_{c_j}$, *that meets* $W^s_{loc}(c_j)$ *transversely at the point* $\beta(1)$ *only and such that, writing* $\beta(s) = (x(s), y(s))$, *both* x *and* y *are monotonic functions of* s. *A restriction of any segment to an interval not containing 1, will be called a* piece of segment.

Definition 4. *Let* $a, b \in \mathbf{R}$ *such that* $a < b$ *and let* H *be a surface parametrized by a covering* $(\theta, h) \in \mathbf{R} \times [a, b]$ *where* θ *is periodic. A* helix on H accumulating on the circle $h = h_0$ *is a curve* $\gamma : [0,1) \to H$ *such that its coordinates* $(\theta(s), h(s))$ *are monotonic functions of* s *with*

$$\lim_{s \to 1^-} h(s) = h_0 \qquad \textit{and} \qquad \lim_{s \to 1^-} |\theta(s)| = +\infty.$$

Lemma 1. *The image of a segment in* $H^{in}_{c_j}$ *by* ϕ_{c_j} *is a helix accumulating on* $W^u_{loc}(c_j) \cap H^{out}_{c_j}$. *Similarly* $\phi^{-1}_{c_j}$ *maps a segment in* $H^{out}_{c_j}$ *into a helix accumulating on* $W^s_{loc}(c_j) \cap H^{in}_{c_j}$ *(see figure 5).*

Proof. The proof is a direct calculation using the expresssion (3) for ϕ_{c_j} and

$$\phi^{-1}_{c_j}(0, r) = \left(-\frac{\ln(\varepsilon)}{\varepsilon E_j} \left[\frac{\varepsilon}{1-r} \right]^{\frac{1}{\delta_j}} ; \varepsilon \left[\frac{1-r}{\varepsilon} \right]^{\frac{1}{\delta_j}} \right) \qquad r \in (1-\varepsilon, 1)$$

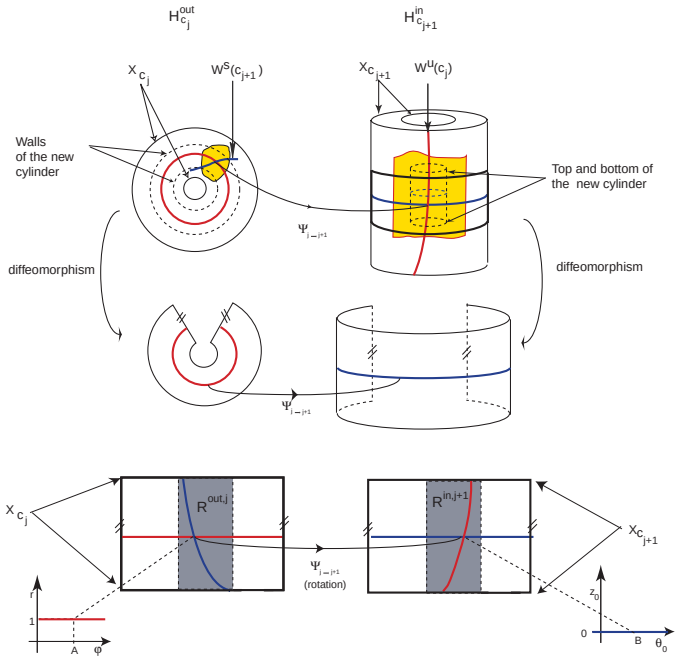

FIGURE 4. The transition map, defined near the connection $[c_j \to c_{j+1}]$, maps the invariant manifold $W^u(c_j)$ across $H^{in}_{c_{j+1}}$, if V_j and V_{j+1} are sufficiently small. By taking a smaller cylinder we obtain a rectangle $\mathcal{R}^{out,j}$ centered at $H^{out}_{c_j} \cap [c_j \to c_{j+1}]$ such that two opposite sides lie in X_{c_j} and $\Psi_{j\to j+1}(\mathcal{R}^{out,j}) \cap H^{in}_{c_{j+1}}$ is a rectangle with the same property in $H^{in}_{c_{j+1}}$.

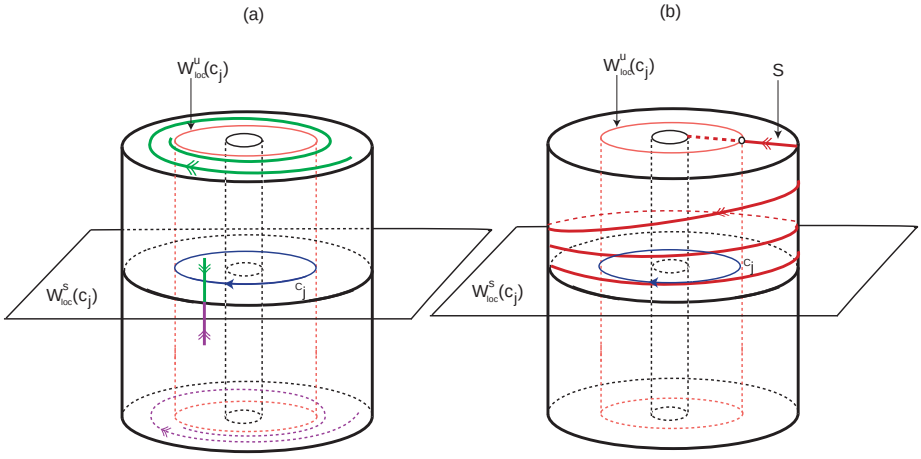

FIGURE 5. Local dynamics in the neighbourhood of the periodic solution c_j (see lemma 1). Left: any segment in $H^{in}_{c_j}$ is mapped into a helix in $H^{out}_{c_j}$ accumulating on $W^u_{loc}(c_j) \cap H^{out}_{c_j}$. Right: the image of any segment in $H^{out}_{c_j}$, by $\phi^{-1}_{c_j}$, a helix accumulating on $W^s_{loc}(c_j) \cap H^{in}_{c_j}$. The double arrow on the lines represents the orientation and not the flow.

defined into the component of $H^{in}_{c_j}$ with $\rho = 1 - \varepsilon$. For $r \in (1, 1+\varepsilon)$ a similar expression holds. A similar proof may be found in Aguiar *et al* [6] (section 6, proposition 3). □

From the same calculations it follows that for a point $q \in H^{in}_{c_j} \backslash W^s_{loc}(c_j))$ the closer it is to $W^s_{loc}(c_j))$ the larger will be the number of loops inside V_j of its trajectory (see figure 7). We also get:

Corollary 2. *The inverse image $\phi^{-1}_{c_j}(S^j \backslash W^u_{loc}(c_j))$ has two connected components lying on $H^{in}_{c_j}$ and each component is a helix accumulating on $W^s_{loc}(c_j) \cap H^{in}_{c_j}$.*

The next step is to compute the number of loops of a trajectory inside V_j. This is done using the linearised equations (2) and noting that the trajectory of $q = (\theta_0, z_0) \in H^{in}_{c_j} \backslash W^s_{loc}(c_j))$ arrives at $H^{out}_{c_j}$ at time

$$\tau = \frac{1}{E_j} \ln \left(\frac{\varepsilon}{z_0} \right).$$

Denoting by $[a]$ the greatest integer less than or equal to a, we have:

Proposition 3. *The number of turns made by the trajectory of a point $q = (\theta_0, z_0) \in H^{in}_{c_j} \backslash W^s_{loc}(c_j)$ inside V_j with respect to Π_j is given by:*

$$\left[\left| \left(\frac{1}{E_j} \ln \left(\frac{\varepsilon}{z_0} \right) + \theta_0 \right) / 2\pi \right| \right].$$

The calculations used for proposition 3 yield:

Corollary 4. *If β is a piece of segment meeting transversely $\phi^{-1}_{c_j}(S^j \backslash W^u(c_j))$ only at the end points, then $\phi_{c_j}(\beta)$ is a piece of helix on the annulus $H^{out}_{c_j}$ meeting S^j only at its end points.*

From corollary 4, it follows that:

Corollary 5. *If β is a piece of segment meeting $\phi^{-1}_{c_j}(S^j \backslash W^u(c_j))$ transversely whith end points lying in $\phi^{-1}_{c_j}(S^j)$, then $\phi_{c_j}(\beta)$ is a piece of helix turning $m-1$ times around $W^u(c_j) \cap H^{out}_{c_j}$ relatively to S^j on the annulus $H^{out}_{c_j}$, where m is the number of elements of the set $\phi^{-1}_{c_j}(S^j) \cap \beta$.*

5. Chaotic double cycling in 3-dimensions

In this section we put together all the information about the local maps to prove:

Theorem 6. *Let $\Sigma = \langle c_1, \ldots, c_k \rangle$ be a heteroclinic cycle of hyperbolic periodic trajectories in a 3-dimensional manifold such that the invariant manifolds of consecutive nodes of Σ meet transversely. Then:*

a) *in every neighbourhood of Σ there is a suspension of an invariant Cantor set of trajectories that follow Σ in positive and negative time;*
b) *Σ has bi-infinite cycling.*

The proof of theorem 6 uses symbolic dynamics and occupies all of this section. We define a discretisation of the flow and then the result follows from standard methods in symbolic dynamics, see for instance Alekseev [3], Kitchens [18] and Wiggins [28, 29]. The only delicate point is the construction of the non-wandering set of statement a) where the discretised flow may be indefinitely iterated. In 5.2 and 5.3 we construct the intersection of the non-wandering set with $H^{in}_{c_j}$ and $H^{out}_{c_j}$, using similar methods to the pioneering work of Shilnikov [26], and then we move it to the counting sections Π_j. This is the part of the proof for which we have to modify the methods of Wiggins [29], the rest follows from the same arguments given in that source. Then in section 6 we look at extensions and consequences, both of theorem 6 and of the method used for the proof. We start with some terminology.

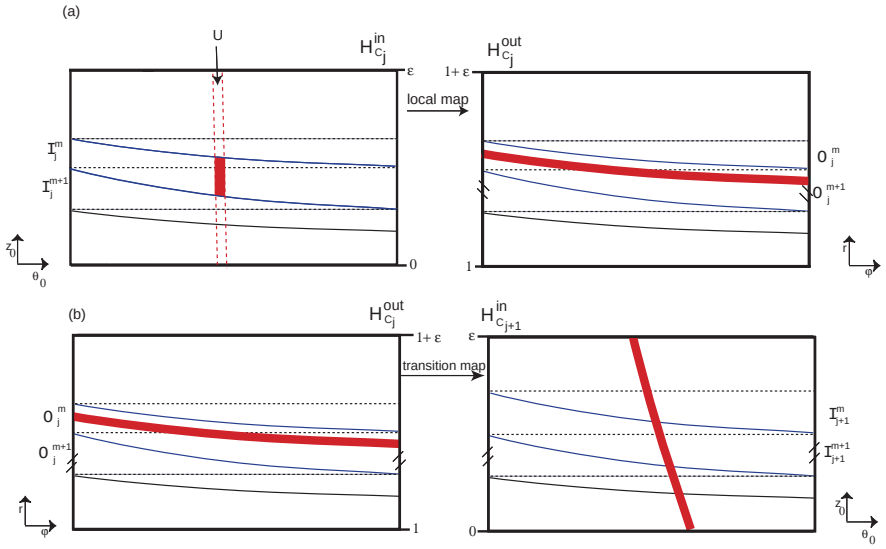

FIGURE 6. (a): If a strip in the cylinder $H^{in}_{c_j}$ has its horizontal boundaries in $\phi^{-1}_{c_j}(S^j)$ then its image by ϕ_{c_j} makes a complete turn in the annulus $W^u_{loc}(c_j) \cap H^{out}_{c_j}$ (corollary 7). (b): The image by $\Psi_{j\to j+1}$ of a horizontal strip in $H^{out}_{c_j}$ is a vertical strip in $H^{in}_{c_{j+1}}$.

5.1. **Strips.** Given a region $\mathcal{R}$ in $H^{in}_{c_j}$ or in $H^{out}_{c_j}$ parametrized by a rectangle $R = [w_1, w_2] \times [z_1, z_2]$, a *horizontal strip* in $\mathcal{R}$ will be parametrized by:

$$\mathcal{H} = \{(x, y) : x \in [w_1, w_2], y \in [u_1(x), u_2(x)]\},$$

where

$$u_1, u_2 : [w_1, w_2] \to [z_1, z_2]$$

are Lipschitz functions such that $u_1(x) < u_2(x)$.

The *horizontal boundaries* of the strip are the lines parametrized by the graphs of the u_i, the *vertical boundaries* are the lines $\{w_i\} \times [u_1(w_i), u_2(w_i)]$ and its *heigth* is

$$h = \max_{x\in[w_1,w_2]} (u_2(x) - u_1(x)) .$$

When both $u_1(x)$ and $u_2(x)$ are constant functions we call $\mathcal{H}$ a *horizontal rectangle across* $\mathcal{R}$.

A *vertical strip across* $\mathcal{R}$, its *width* and a *vertical rectangle* have similar definitions, with the roles of x and y reversed. A *strip* in $H^{in}_{c_j}$ is the intersection of a vertical strip and a horizontal strip. From corollary 4, it follows:

Corollary 7. *If $\mathcal{S}$ is a strip in $H^{in}_{c_j}$ such that:*

- *the horizontal boundaries of $\mathcal{S}$ lie in $\phi^{-1}_{c_j}(S^j)$*
- *$int(\mathcal{S}) \cap \phi^{-1}_{c_j}(S^j) = \emptyset$,*

then ϕ_{c_j} maps $\mathcal{S}$ into a horizontal strip in $H^{out}_{c_j}$ having two intervals in S^j as vertical boundaries and whose horizontal boundaries consist of two arcs of helices, each one starting and ending at S^j, that make a complete turn around $W^u_{loc}(c_j) \cap H^{out}_{c_j}$ (see figure 6 (a)).

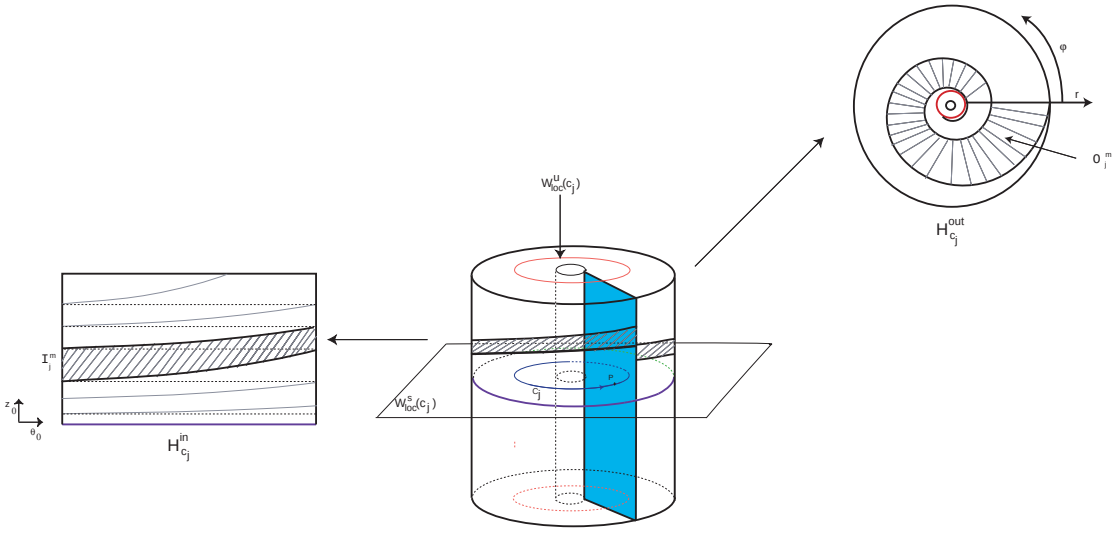

FIGURE 7. Partitions of $H^{in}_{c_j}$ and $H^{out}_{c_j}$ corresponding to trajectories that make any integer number of turns in V_j. For a point $q \in H^{in}_{c_j} \backslash W^s_{loc}(c_j))$ the closer it is to $W^s_{loc}(c_j))$ the larger will be the number of loops inside V_j of its trajectory.

5.2. **Partitions.** For the proof of theorem 6, consider a small neighbourhood of Σ, with a system of isolating blocks $\mathcal{V} = \{V_j\}_{j\in\{1,\dots,k\}}$ and counting sections $\{\Pi_j\}_{j\in\{1,\dots,k\}}$ associated to $\mathcal{V}$ as defined in section 3. We restrict our attention to the rectangles, constructed in 3.4, where the transition maps are well defined and to the $z \geq 0$ and $\rho \geq 1$ components of $H^{in}_{c_j}$ and $H^{out}_{c_j}$, that we continue to represent by the same symbols.

The set $\overline{H^{in}_{c_j}} \backslash W^s_{loc}(c_j)$ is partitioned into subsets $\mathcal{I}^m_j$ of points whose trajectory hits m times the counting section Π_j without leaving V_j (figure 7). A partition of $\overline{H^{out}_{c_j}} \backslash W^u_{loc}(c_j)$ into sets $\mathcal{O}^m_j$, $m \in \mathbf{N}$, is defined in a similar way.

For $m \in \mathbf{N}$ the closure $\overline{\mathcal{I}^m_j}$ is a horizontal strip in $H^{in}_{c_j}$ and it also intersects in a horizontal strip the rectangle $\mathcal{R}^{in,j}$ where the transition map $\Psi_{j-1\to j}$ is well defined. The elements $\mathcal{I}^m_j$ of the partition are connected sets with vertical boundary consisting of two pieces of $\partial\Pi_j$ and horizontal boundary consisting of two arcs of $\phi^{-1}_{c_j}(S^j \backslash W^u_{loc}(c_j)) = \phi^{-1}_{c_j}([\partial\Pi_j \cap H^{out}_{c_j}] \backslash W^u_{loc}(c_j))$ (figures 6 (a) and 7).

Let U be a vertical strip across $\mathcal{R}^{in,j}$. The following properties follow from the results of sections 3 and 4 and from corollary 7:

(1) By corollary 7 , for $m \in \mathbf{N}$ the set $\widehat{U} = \phi_{c_j}\left(U \cap \overline{\mathcal{I}^m_j}\right)$ is a horizontal strip across the width of $H^{out}_{c_j}$ (figure 6 (a)) and thus $\widehat{U} \cap \mathcal{R}^{out,j}$ is a horizontal strip;
(2) If the vertical boundaries of U are the graphs of smooth monotonically decreasing functions, then the horizontal boundaries of $\widehat{U} \cap \mathcal{R}^{out,j}$ are the graphs of smooth monotonically decreasing functions;
(3) The set $\widetilde{U} = \Psi_{j\to j+1}\left(\widehat{U} \cap \mathcal{R}^{out,j}\right)$ is a vertical strip across $\mathcal{R}^{in,j+1} \subset H^{in}_{c_{j+1}}$ (figure 6 (b)).

Going backwards in time we get dual results, for U a horizontal strip across $\mathcal{R}^{in,j}$:

(4) The set $\Psi^{-1}_{(j-1)\to j}(U)$ is a vertical strip across $\mathcal{R}^{out,j-1} \subset H^{out}_{c_{j-1}}$.

We get dual results, for W a vertical strip across $\mathcal{R}^{out,j-1}$:

(5) For $m \in \mathbf{N}$, the set $\widehat{W} = W \cap \overline{\mathcal{O}_{j-1}^m}$ is a strip in $H_{c_{j-1}}^{out}$ with horizontal boundaries contained in $S'^{,j} = \phi_{c_{j-1}}(\Pi_{j-1} \cap H_{c_{j-1}}^{in})$;
(6) The set $\phi_{c_{j-1}}^{-1}\left(\widehat{W}\right)$ is a horizontal strip across $\mathcal{R}^{in,j-1} \subset H_{c_{j-1}}^{in}$ (by the dual of corollary 7);
(7) If the vertical boundaries of W are the graphs of smooth monotonically increasing functions, then the horizontal boundaries of $\phi_{c_{j-1}}^{-1}\left(\widehat{W}\right) \cap \mathcal{R}^{in,j-1}$ are the graphs of smooth monotonically increasing functions;
(8) The set $\widetilde{W} = \Psi_{(j-2)\to(j-1)}^{-1}\left(\phi_{c_{j-1}}^{-1}\left(\widehat{W}\right) \cap \mathcal{R}^{in,j-1}\right)$ is a vertical strip across $\mathcal{R}^{out,j-2}$.

5.3. **Coding.** We start by the description of the set of points whose trajectory makes a prescribed number of turns around each node in Σ, the phenomenon that we call cycling. From now on we assume the indexing over the k symbols for the nodes is always done (mod k).

Since we are assuming that the invariant manifolds $W^u(c_j)$ and $W^s(c_{j+1})$ meet transversely, then $W_{loc}^s(c_{j+1}) \cap H_{c_j}^{out}$ is the graph of a smooth function $(\varphi(r), r)$. From transversality it follows that the function $\varphi(r)$ is monotonic near $r = 1$ for $r - 1 > 0$ small. In what follows, for the sake of definiteness, we will assume that this function is either decreasing or constant. If it is an increasing function the main result still holds, but either we would have to change the choice of parametrisation or we would have to adapt the intermediate statements. Similarly, without loss of generality, the curve $(\theta_0(z_0), z_0)$ representing $W_{loc}^u(c_j) \cap H_{c_{j+1}}^{in}$ is assumed to be the graph of a monotonically decreasing function for $z_0 > 0$ near $z_0 = 0$.

Given a natural number m and a subset U of $\mathcal{R}^{in,j}$ consider the set $P_j(m, U)$ given by:

$$P_j(m, U) = \Psi_{j\to(j+1)}\left(\phi_{c_j}\left(U \cap \overline{\mathcal{I}_j^m}\right) \cap \mathcal{R}^{out,j}\right) \subset \mathcal{R}^{in,j+1} \subset H_{c_{j+1}}^{in} .$$

From properties (1) - (3) and a direct calculation, it follows that if U is a vertical strip across $\mathcal{R}^{in,j}$ then:

(9) The set $P_j(m, U)$ is a vertical strip across $\mathcal{R}^{in,j+1}$;
(10) If the vertical boundaries of U are the graphs of smooth monotonically decreasing functions then the vertical boundaries of $P_j(m, U)$ are the graphs of smooth monotonically decreasing functions;
(11) If moreover the width of U is d then the width of $P_j(m, U)$ is at most $\mu_m d$ for $\mu_m = \varepsilon C_j e^{-2\pi C_j(m-1)}$. Note that $\mu_m < 1$ for all $m > 0$ if $\varepsilon < 1/C_j$ (see lemma 17 in appendix A).

Note that if U is a vertical strip across $\mathcal{R}^{in,j}$, then $P_j(m, U)$ is the image by $\Psi_{j\to(j+1)}$ of a horizontal strip across $H_{c_j}^{out}$ and it is transformed into a vertical strip across $H_{c_{j+1}}^{in}$ intersecting $\mathcal{I}_{j+1}^m$, for all m. Here we are using the property of the neighbourhoods V_j we have constructed in 3.4.

Similarly, to each natural number m and each subset W of $\mathcal{R}^{out,j}$ we associate a subset $Q_j(m, W)$ of $\mathcal{R}^{out,j-1}$ given by

$$Q_j(m, W) = \Psi_{(j-1)\to j}^{-1}\left(\phi_{c_j}^{-1}\left(W \cap \overline{\mathcal{O}_j^m}\right) \cap \mathcal{R}^{in,j}\right) \subset \mathcal{R}^{out,j-1} \subset H_{c_{j-1}}^{out} .$$

If W is a vertical strip across $\mathcal{R}^{out,j}$ then from properties (4) - (8) we get:

(12) The set $Q_j(m, W)$ is a vertical strip across $\mathcal{R}^{out,j-1}$;
(13) If the vertical boundaries of W are the graphs of smooth monotonically decreasing functions then the vertical boundaries of $Q_j(m, W)$ are the graphs of smooth monotonically decreasing functions;
(14) If moreover the width of W is d then the width of $Q_j(m, U)$ is at most $\nu_m d$ for $\nu_m = \varepsilon E_j e^{-2\pi E_j m}$. Note that $\nu_m < 1$ for all $m \geq 0$ if $\varepsilon < 1/E_j$ (see lemma 17 in appendix A).

For $j = 1, \dots, k$, denote by Φ_j the expression

$$\Phi_j = \phi_{c_j} \circ \Psi_{(j-1)\to j} : \mathcal{R}^{out,j-1} \to \mathcal{R}^{out,j} \ .$$

Points q in $\mathcal{R}^{out,j}$ whose forward trajectory follows the cycle from c_j to c_{j+1} and arrive at $\Phi_{j+1}(q) \in \mathcal{R}^{out,j+1}$ lie in the set

$$W_j^1 = \bigcup_{m=1}^{\infty} Q_{j+1}\left(m, \mathcal{R}^{out,j+1}\right) \subset \mathcal{R}^{out,j}$$

which is the disjoint union of vertical strips across $\mathcal{R}^{out,j}$. Points q in $\mathcal{R}^{out,j}$ with forward trajectories that follow the connections $[c_j \to c_{j+1}]$ and $[c_{j+1} \to c_{j+2}]$ to arrive at $\Phi_{j+2} \circ \Phi_{j+1}(q) \in \mathcal{R}^{out,j+2}$ lie in the set

$$W_j^2 = \bigcup_{m=1}^{\infty} Q_{j+1}\left(m, W_{j+1}^1\right) \subset W_j^1 \subset \mathcal{R}^{out,j} \ ,$$

a disjoint union of vertical strips. Similarly points q with forward trajectory that follows the cycle along l connections from c_j to c_{j+l}, arriving at $\Phi_{j+l} \circ \cdots \circ \Phi_{j+1}(q) \in \mathcal{R}^{out,j+l}$ lie in the set $W_j^l \subset \mathcal{R}^{out,j}$ defined recursively by

$$W_j^0 = \mathcal{R}^{out,j} \qquad\qquad W_j^l = \bigcup_{m=1}^{\infty} Q_{j+1}\left(m, W_{j+1}^{l-1}\right) \subset W_j^{l-1} \subset \mathcal{R}^{out,j}$$

a disjoint union of vertical strips across $\mathcal{R}^{out,j}$, the *vertical strips in* W_j^l. We obtain chains of nested strips comprising the sets

$$\cdots \subset W_j^{l+1} \subset W_j^l \subset W_j^{l-1} \subset \cdots \subset W_j^1 \subset W_j^0.$$

The same procedure may be used going backwards in time. For $j = 1, \dots, k$, let

$$U_j^0 = \mathcal{R}^{in,j} \qquad\qquad U_j^l = \bigcup_{m=1}^{\infty} P_{j-1}\left(m, U_{j-1}^{l-1}\right) \subset U_j^{l-1} \subset \mathcal{R}^{in,j} \ ,$$

where each U_j^l is a disjoint union of vertical strips across $\mathcal{R}^{in,j}$, the *vertical strips in* U_j^l. A point $q \in U_j^1$ lies in the forward trajectory of $p = \phi_{c_{j-1}}^{-1} \circ \Psi_{(j-1)\to j}^{-1}(q)$ that follows the connection $[c_{j-1} \to c_j]$ from $p \in \mathcal{R}^{in,j-1}$ to $q \in \mathcal{R}^{in,j}$. Let $\widetilde{\Phi}_j^{-1}$ be given by $\widetilde{\Phi}_j^{-1} = \phi_{c_j}^{-1} \circ \Psi_{j\to(j+1)}^{-1}$. Then the trajectory of a point $q \in U_j^l$, starting at

$$p = \widetilde{\Phi}_{j-l}^{-1} \circ \cdots \circ \widetilde{\Phi}_{j-1}^{-1}(q) \in \mathcal{R}^{in,j-l}$$

follows the l connections from c_{j-l} to c_j until it reaches q in $\mathcal{R}^{in,j}$.

The following properties of the sets U_j^l and W_j^l follow from direct calculations and from the properties (1)–(8) of section 5.2:

(15) Each one of the vertical strips in W_j^l and in U_j^l, respectively, except for its horizontal boundaries is contained in the interior of a vertical strip, respectively in W_j^{l-1} and in U_j^{l-1};
(16) The vertical boundaries of the strips in W_j^l and U_j^l are the graphs of smooth monotonically decreasing functions;
(17) The first hit map Φ_{j+1} sends W_j^l onto W_{j+1}^{l-1} contracting the width of strips by $\nu < 1$, by construction;
(18) The last hit map $\widetilde{\Phi}_j^{-1}$ sends U_{j+1}^l onto U_j^{l-1} contracting the width of strips by $\mu < 1$, by construction;

(19) The sets

$$\Lambda_j^{out} = \bigcap_{l=1}^{\infty} W_j^l \subset \mathcal{R}^{out,j} \qquad \text{and} \qquad \Lambda_j^{in} = \bigcap_{l=1}^{\infty} U_j^l \subset \mathcal{R}^{in,j}$$

are the disjoint union of graphs of smooth monotonically decreasing functions, the *curves in* Λ_j^{out} and Λ_j^{in}, respectively.

The trajectory of each point in one of the curves in Λ_j^{out} follows the cycle Σ for positive time t making the same number of turns around each node. The same holds in negative time t for the curves in Λ_j^{in}.

Each one of the sets Λ_j^{out} and Λ_j^{in} meets each horizontal line in $\mathcal{R}^{out,j}$ and $\mathcal{R}^{in,j}$, respectively, in an uncountable set of points. This intersection is not a Cantor set because it is not closed, since

$$\bigcup_{m=0}^{\infty} \overline{\mathcal{O}}_j^m = \overline{H_{c_j}^{out}} \backslash W_{loc}^u(c_j)$$

is not a closed set and for each l the strips in W_j^l accumulate on the vertical axis $W_{loc}^u(c_j) \cap \overline{H_{c_j}^{out}}$ but $W_{loc}^u(c_j) \cap W_j^l = \emptyset$, with a similar statement for U_j^l.

(20) The set $\Psi_{(j-1)\to j}\left(\Lambda_{j-1}^{out}\right) \subset \mathcal{R}^{in,j}$ is the disjoint union of horizontal curves that are the graphs of smooth monotonic functions. Therefore, each vertical curve in Λ_j^{in} meets each horizontal curve in $\Psi_{(j-1)\to j}\left(\Lambda_{j-1}^{out}\right)$ at exactly one point.

Let

$$\Lambda_j = \Lambda_j^{in} \cap \Psi_{(j-1)\to j}\left(\Lambda_{j-1}^{out}\right) \subset \mathcal{R}^{in,j} \qquad\qquad \Lambda_{\mathbf{N}} = \bigcup_{j=1}^{k} \Lambda_j$$

and let $F : \Lambda_{\mathbf{N}} \longrightarrow \Lambda_{\mathbf{N}}$ be given by $F(p) = \Psi_{j\to j+1} \circ \phi_{c_j}(p)$ for $p \in \mathcal{R}^{in,j}$. Then F may be indefinitely iterated in $\Lambda_{\mathbf{N}}$. In order to complete the proof of Theorem 6, we will transfer the geometrical information to the counting sections Π_i and use symbolic dynamics.

The geometrical behaviour of the first return to Π_j is a lot more complicated than in $H_{c_j}^{in}$ but this technique will provide additional dynamical information that will be discussed in the next section. Each counting section Π_j has been identified with the rectangle $(\rho, z) \in [1, 1+\varepsilon] \times [0, \varepsilon]$ (see figures 3 (a) and 8 (a)). Then for each Π_j we consider a partition into horizontal rectangles (figure 8 (b)):

$$\mathcal{F}_j^m = [1, 1+\varepsilon] \times \left(\varepsilon(e^{-2\pi E_j})^{m+1} \ , \ \varepsilon(e^{-2\pi E_j})^m\right] \qquad m = 0, 1, \ldots$$

and

$$\mathcal{F}_j^{\infty} = [1, 1+\varepsilon] \times \{0\} = W^s(c_j) \cap \Pi_j$$

as well as a partition into vertical rectangles

$$\mathcal{G}_j^m = \left(1 + \varepsilon(e^{-2\pi C_j})^{m+1} \ , \ 1 + \varepsilon(e^{-2\pi C_j})^m\right] \times [0, \varepsilon] \qquad m = 0, 1, \ldots$$

and

$$\mathcal{G}_j^{\infty} = \{1\} \times [0, \varepsilon] = W^u(c_j) \cap \Pi_j \ .$$

Trajectories starting in $\Pi_j \backslash \mathcal{F}_j^0$ return to Π_j without leaving V_j, so there are well defined first hit maps $h_j : \Pi_j \backslash \mathcal{F}_j^0 \longrightarrow \Pi_j$ that send each rectangle $\mathcal{F}_j^m$, $m \geq 1$ onto

$$h_j\left(\mathcal{F}_j^m\right) = \mathcal{F}_j^{m-1} \backslash \mathcal{G}_j^0.$$

Their inverses h_j^{-1} are well defined in $\Pi_j \backslash \mathcal{G}_j^0$ and send each rectangle $\mathcal{G}_j^m$, $m \geq 1$ onto

$$h_j^{-1}\left(\mathcal{G}_j^m\right) = \mathcal{G}_j^{m-1} \backslash \mathcal{F}_j^0 \ .$$

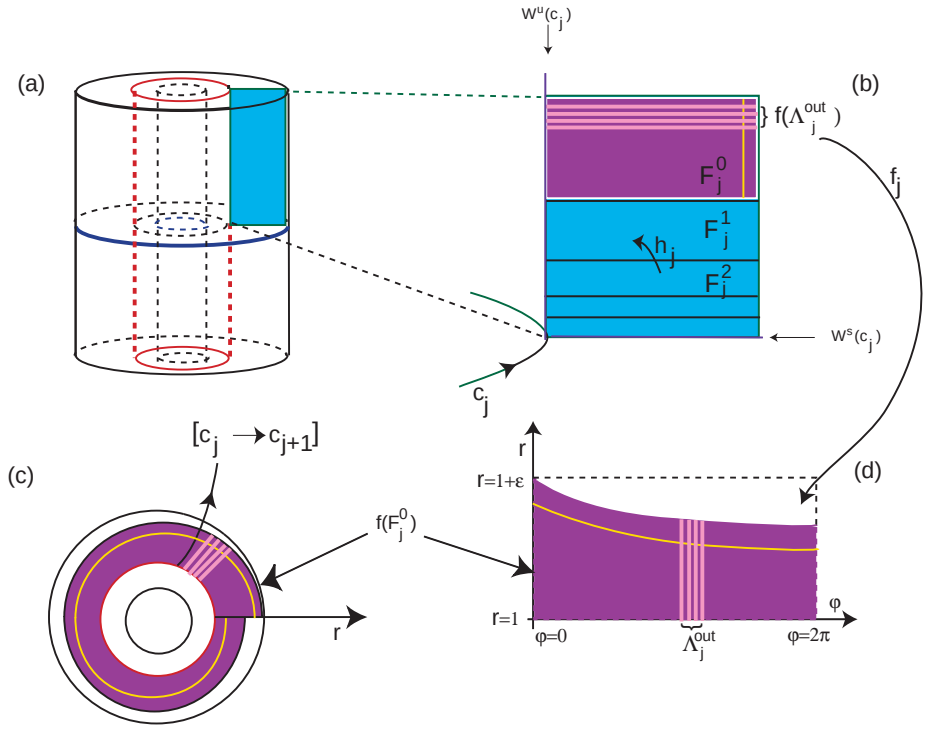

FIGURE 8. (a): The shaded rectangle represents the counting section Π_j at c_j. (b): The section Π_j may be partioned into horizontal strips $\mathcal{F}_j^m$ ($m \in \mathbf{N}_0$). For $m \geq 1$, the forward trajectory of a point in $\mathcal{F}_j^m$ first hits Π_j at $\mathcal{F}_j^{m-1}$ and then at $\mathcal{F}_j^{m-2}$ and so on, until it reaches in $\mathcal{F}_j^0$. The images of these points are governed by the map h_j. (c): The forward trajectory of a point in $\mathcal{F}_j^0$ goes to H_j^{out} without crossing Π_j. The shaded regions in (c) and (d) correspond to $h_j(\mathcal{F}_j^0)$. In (b), it is possible to see the representation of the Cantor set $f_j^{-1}(\Lambda_j^{out})$ as a disjoint union of horizontal strips across $\mathcal{F}_j^0$. A similar statement holds for $g_j(\Lambda_j^{in})$ replacing horizontal strips across $\mathcal{F}_j^0$ by vertical strips across $\mathcal{G}_j^0$.

Trajectories $\phi(t,q)$ starting at $q \in \mathcal{F}_j^0$ go out of V_j for positive t through H_j^{out} without crossing Π_j, so there are well defined first hit maps $f_j : \mathcal{F}_j^0 \longrightarrow H_j^{out}$. Then, by (19) above, the set $M_j^0 = f_j^{-1}\left(\Lambda_j^{out}\right)$ is the disjoint union of horizontal curves across $\mathcal{F}_j^0$ that are the graphs of smooth monotonic functions.

Similarly, trajectories $\phi(t,q)$ of points $q \in \mathcal{G}_j^0$ come from outside V_j through H_j^{in} without crossing Π_j for negative t, so there are well defined last hit maps $g_j^{-1} : \mathcal{G}_j^0 \longrightarrow H_j^{in}$ and $L_j^0 = g_j\left(\Lambda_j^{in}\right)$ is the disjoint union vertical curves across $\mathcal{G}_j^0$ that are the graphs of smooth monotonic functions.

The maps h_j may now be used to obtain the first return to Π_j of trajectories of points in L_j^0 that do not go out of V_j without returning to Π_j. This is given by the set $L_j^1 = h_j\left(g_j\left(\Lambda_j^{in}\right) \setminus \mathcal{F}_j^0\right)$, a disjoint union vertical curves across $\mathcal{G}_j^1$. Iterating the process we get $L_j^m = h_j\left(L_j^{m-1} \setminus \mathcal{F}_j^{m-1}\right)$, a

disjoint union vertical curves across $\mathcal{G}_j^m$. Similarly, define $M_j^m = h_j^{-1}\left(M_j^{m-1} \backslash \mathcal{G}_j^{m-1}\right)$, a disjoint union of horizontal curves across $\mathcal{F}_j^m$.

The Cantor set

$$\Lambda = \bigcup_{j=1}^{k} \left(\mathcal{F}_j^\infty \cup \bigcup_{m=0}^{\infty} M_j^m \right) \cap \left(\mathcal{G}_j^\infty \cup \bigcup_{m=0}^{\infty} L_j^m \right) \subset \bigcup_{j=1}^{k} \Pi_j$$

consists of points whose trajectories return to $\bigcup_{j=1}^k \Pi_j$ infinitely many times in the future and in the past. This proves statement a) of theorem 6.

The first return of $p \in \Lambda$ to $\bigcup_{j=1}^k \Pi_j$ is given by the map $G : \Lambda \longrightarrow \Lambda$

$$G(p) = \begin{cases} h_j(p) & \text{for } p \in \Pi_j \backslash \mathcal{F}_j^0 \\ g_{j+1} \circ \Psi_{j\to(j+1)} \circ f_j(p) & \text{for } p \in \mathcal{F}_j^0 \end{cases}$$

and G may be indefinitely iterated in Λ. The expression for $G(p)$ is a well defined map in all of $\Pi_j \backslash \mathcal{F}_j^0$ and also in a vertical strip in $\mathcal{F}_j^0$, but it has a discontinuity at the common boundary of $\mathcal{F}_j^0$ and $\mathcal{F}_j^1$, if we use the induced topology in $\bigcup_j \Pi_j$.

Let $\Omega_T \subset \{1, \ldots, k\}^{\mathbf{Z}}$ be the subspace of bi-infinite sequences of k symbols with transition matrix $T = (T_{ij})$ where $T_{ij} = 1$ if either $j = i$ or $j = i + 1 \pmod k$, $T_{ij} = 0$ otherwise and let σ be the shift operator on Ω_T. Given $p \in \Lambda$ and $i \in \mathbf{Z}$ let $s_i(p) = j$ if $G^i(p) \in \Pi_j$. This is a bijection from Λ onto Ω_T, by construction. The standard treatment of Wiggins [29] can now be used to yield:

Theorem 8. *The dynamical system (Λ, G) is topologically conjugate to (Ω_T, σ).*

A sequence $(z_i)_{i\in\mathbf{Z}} \in \Omega_T$ gives us information about the number of turns around consecutive nodes of Σ of trajectories that remain close the cycle in forward and backward time. For example, if $k = 3$, the sequence

$$\ldots 2233112233.1123333112233112233 \ldots$$

corresponds to a trajectory turning twice around c_1, once around c_2, four times around c_3, twice around c_1 and so on. Each repetition of the symbol j corresponds to a new turn around c_j. Thus Theorem 6 follows from Theorem 8. This is why we call the dynamics a *horseshoe in time*: the number of turns in a neighbourhood of each closed orbit in the cycle, and consequently the time spent near each closed orbit, is coded like a horseshoe. Other interesting dynamical features are discussed in the next section.

6. Extensions and discussion of results

In this section we describe further consequences of the methods of Section 5 for the dynamics around the heteroclinic cycle Σ. The results are not the main goal of the paper, so the presentation is less detailed. From the results used to prove Theorem 8 it follows:

Corollary 9. *Let $\Sigma = \langle c_1, \ldots, c_k \rangle$ be a heteroclinic cycle of hyperbolic periodic trajectories in a 3-dimensional manifold embedded in $\mathbf{R}^n$ such that the invariant manifolds of consecutive nodes of Σ meet transversely. Then there exists a set with positive Lebesgue measure exhibiting finite cycling of any order and the finite cycling near Σ may be realised by periodic trajectories.*

Proof. Arbitrarily close to the cycle it is possible to define the set $\Lambda_{\mathbf{N}}$ as in (20). This set is constructed as an infinite intersection of nested strips U_j^l and $\Psi_{(j-1)\to j}\left(W_j^l\right)$. Each finite intersection of strips has positive measure in $\mathcal{R}^{in,j}$. Then for any m, points in the set

$$\bigcup_{j=1}^{k} \left(\bigcap_{l=1}^{m} U_j^l \cap \Psi_{(j-1)\to j}\left(W_j^l\right) \right)$$

exhibit cycling of finite order m. Saturating this set by the flow we obtain a set of positive Lebesgue measure in the manifold.

Pick a finite sequence $\omega = z_1 \cdots z_m$ with $z_j \in \mathbf{N}$ and, without loss of generality, suppose its length is an integer multiple of k, *ie*, $m = nk$, $n \in \mathbf{N}$. For each j, form the sequence s_j by repeating z_j times the symbol $i \in \{1, \ldots, k\}$, $i \equiv j \pmod k$. Concatenate the s_j to form a finite sequence and then concatenate this sequence infinitely many times to form the sequence s. Then $s \in \Omega_T$ is a periodic sequence of period $p = \sum_{j=1}^{m} z_j$, a fixed point of σ^p. The point in Λ that corresponds to s has a periodic trajectory that exhibits finite cycling associated to the sequence ω. □

From theorem 8 we also get:

Corollary 10. *For the dynamical system (Λ, G) defined in subsection 5.3 we have:*

(i) *the topological entropy of (Λ, G) is $\log 2$;*
(ii) *the topological entropy of the associated suspended flow ϕ^t is positive;*
(iii) *(Λ, G) is topologically mixing, in particular (Λ, G) is topologically transitive and the set of periodic points of (Λ, G) is dense in Λ.*

Proof. (i) The topological entropy is invariant under conjugacy, thus by theorem 8 it is enough to show that (Ω_T, σ) has topological entropy $\log 2$.

The graph associated to T is strongly connected (it is possible to get from any vertex to any other by traversing a sequence of edges), therefore the matrix T is irreducible. Moreover, for each $j \in \{1, \ldots, k\}$, the entries of any row of T^{k-1} correspond to permutations of the k elements of the line k of Pascal's triangle, thus it follows that T is aperiodic.

Since T is irreducible and aperiodic, by the Perron-Frobenius theorem, its topological entropy h_{top} satisfies $h_{top} = \log(\lambda)$ where λ is the spectral radius of T (see Katok *et al* [17] and Kitchens [18] for details). Developing $\det(T - \lambda I)$ along the k-th row, we have

$$P(\lambda) = \det(T - \lambda I) = (-1)^{k+1} + (1 - \lambda)(1 - \lambda)^{k-1} = (-1)^{k+1} + (1 - \lambda)^k.$$

Hence $P(2) = 0$ and 2 is the real number with largest absolute value satisfying $P(\lambda) = 0$. Thus, $h_{top} = \log(2)$.

(ii) It is well known that the topological entropy of a flow $\phi^t \equiv \phi(t, .)$ is given by the topological entropy of the time 1 difeomorphism ϕ^1 (see proposition 3.1.8 of Katok *et al* [17]). More generally, for a measure space A, if $R : A \to A$ is a map for which μ is a R-invariant probability measure, Abramov [1] showed that the measure theoretic entropy, h_μ, with respect to μ, is related to the measure theoretic entropy of the associated suspended flow ϕ^t by the formula $h_\mu(R) = \overline{\tau} h_{\mu \times Leb_1}(\phi^t)$ where:

- Leb_1 denotes the one-dimensional Lebesgue measure;
- $\tau(x) \geq 0$ is the return time of the unique solution whose initial condition is x;
- $\overline{\tau}$ is the mean return time to A with respect to μ, *ie*, $\overline{\tau} = \int_A \tau(x) d\mu$.

In particular, combining statement (i) with the variational principle, it follows that:

$$\log 2 = h_{top}(G|_\Lambda) \leq h_{top}(G) = \sup_\mu h_\mu(G) = \sup_\mu h_{\mu \times Leb_1}(\phi^t)\overline{\tau},$$

where μ runs over the set of G-invariant probability measures defined in Λ. Since in our context, the nodes of the heteroclinic cycle are periodic solutions, then the ceiling function τ is bounded above and below, and so is $\overline{\tau}$. This implies immediately that

$$h_{top}(\phi^t) = \sup_\mu h_{\mu \times Leb_1}(\phi^t) > 0.$$

(iii) By Katok & Hasselblatt (proposition 1.9.9 of Katok *et al* [17]), since the matrix T is aperiodic, the dynamical system (Ω_T, σ) is topologically mixing and its periodic orbits are dense in Ω_T. The result follows by conjugacy. □

Roughly speaking, the topological entropy is a single positive number that represents the exponential growth rate of the total number of orbit segments distinguishable with arbitrarily fine but finite precision and it describes the exponential complexity of the orbit structure. Corollary 10 shows that if a cycle Σ whose nodes are periodic trajectories has more than two nodes, then the topological dynamics of (Λ, G) is of the same type for all $k > 1$, *ie* increasing the number of periodic nodes does not increase the number of statistically observable orbits near the cycle. Positive topological entropy of the flow implies the existence of infinitely many distinct knot types.

Theorem 8, together with the geometrical information of section 4, provides information on additional heteroclinic connections, as follows:

Proposition 11. *Let $\Sigma = \langle c_1, \ldots, c_k \rangle$ be a heteroclinic cycle of hyperbolic periodic trajectories in a 3-dimensional manifold such that the invariant manifolds of consecutive nodes of Σ meet transversely. Then:*

(1) *The trajectories $c_1, \ldots, c_k$ are the nodes of a heteroclinic network with all-to-all coupling, including homoclinic connections. Each pair of nodes is connected by a countable infinite set of trajectories.*
(2) *At each heteroclinic connection the invariant manifolds of consecutive nodes meet transversely. Two different heteroclinic connections between the same pair of nodes are distinguished by the number of loops they make around the nodes in the cycle.*
(3) *Points lying in heteroclinic connections are dense in Λ.*
(4) *Σ is not asymptotically stable.*

Proof. (1) In our coding, a sequence $(z_i)_{i\in\mathbf{Z}} \in \Omega_T$ with z_i constant and equal to j for all $i > p$ corresponds to a point in the stable manifold of c_j and a sequence that is constant and equal to j for $i < p$ corresponds to a point in the unstable manifold of c_j. Thus, a sequence $(z_i)_i$ such that there exists $t_q < t_p \in \mathbf{Z}$ for which $\forall i < t_q, z_i = q$ and $\forall i > t_p, z_i = p$ codes a heteroclinic connection $[c_q \to c_p]$. Each central block from z_{t_q+1} to z_{t_p-1} corresponds to a different heteroclinic connection and the central block determines the number of turns around the nodes.

Note that the constant sequence $(z_i)_i$ such that $\forall i \in \mathbf{Z}, z_i = p$ corresponds to the node c_p of Σ, since any invariant saddle is contained in its stable and unstable manifolds.

(2) For $k = 1$ the result is trivial. For $k \geq 2$, consider $m \in \{1, \ldots, k\}$. Since the invariant manifolds of consecutive nodes in Σ intersect transversely, then locally $W^u(c_m) \cap H^{in}_{c_{m+1}}$ is a segment (in the terminology of section 4) near each intersection point. Its image by $\phi_{c_{m+1}}$ is a helix on $H^{out}_{c_{j+1}}$ accumulating on $W^u(c_{m+1})$. By transversality, there are infinitely many *arcs* of this helix, whose end points lie in $W^s(c_{m+2})$, which are mapped by $\Psi_{m+1\to m+2}$ into segments on $H^{in}_{c_{m+2}}$. Each one of these segments is mapped into a helix on $H^{out}_{c_{m+2}}$ accumulating on $W^u(c_{m+2})$. This curve cuts $W^s(c_{m+3})$ transversely infinitely many times. It is possible to repeat the argument until, for any $n \in \{1, \ldots, k\}$, the helix meets $W^s(c_n)$ infinitely many times. This helix corresponds to points of $W^u(c_m)$, hence, there exist infinitely many heteroclinic connections from c_m to c_n. It is possible to choose the heteroclinic connection from c_m to c_n turning around the nodes c_{m+1}, ..., c_{n-1} any sequence of nonnegative numbers.

(3) Pick $p \in \Lambda$ and let U be an open set such that $p \in U$. The image of U under the conjugacy ϑ is an open set corresponding to a set of sequences with the same central block X. Concatenating with a left infinite sequence of the type $\overleftarrow{a} = \ldots aaa$ and with a right infinite sequence of the type $\overrightarrow{b} = bbb\ldots$, the element $\overleftarrow{a}\, X\, \overrightarrow{b}$ belongs to $\vartheta(U)$ and corresponds to a heteroclinic connection from the saddle $\vartheta^{-1}(\ldots aaa\ldots)$ to the saddle

$\vartheta^{-1}(\dots bbb\dots)$. The results follows imediately by conjugacy. It is worth noting that this holds for any choice of heteroclinic connection.

(4) Trajectories starting close to an asymptotically stable heteroclinic cycle spend more and more time near each node on each visit. If Σ were asymptotically stable, then the times spent by a trajectory inside each of the neighbourhoods V_j would be a monotonically increasing sequence. This contradicts cycling because it is possible to find trajectories associated to any possible sequence of symbols.

□

Theorem 8 may also be used to obtain a description of the behaviour of trajectories near the network of proposition 11.

Corollary 12. *Let $\Sigma = \langle c_1, \dots, c_k \rangle$ be a heteroclinic cycle of hyperbolic periodic trajectories in a 3-dimensional manifold such that the invariant manifolds of consecutive nodes of Σ meet transversely. Let Σ^* be a subnetwork of the network of proposition 11 such that Σ^* has finitely many hetero/homoclinic connections. Then there is switching near Σ^*. Moreover, we may prescribe the number of turns around each node for the trajectory that follows any sequence of connections. The combination of following a particular path and a given number of turns is realised by a unique trajectory.*

Thus, near the cycle Σ, there is a dense set corresponding to the transverse intersection of the invariant manifolds of different nodes, giving rise to a robust and transitive set with very rich persistent properties. The result is even more interesting due to the fact that the map F above defined is uniformly hyperbolic in the intersection of $\Lambda_{\mathbf{N}}$ with any compact subset of $\mathcal{R}^{in,j}$, where it admits an invariant dominated splitting, see Araújo and Pacífico [7]. The map G is uniformly hyperbolic at the points where it is defined and continuous.

7. Cycling in higher dimensions

The results of the previous sections can be extended to higher dimensions using the centre manifold techniques of Homburg [15], Shaskov *el al* [25] and Shilnikov *et al* [27].

Consider a heteroclinic cycle Σ in $\mathbf{R}^n$ whose nodes are hyperbolic periodic solutions c_j, $j = 1, \cdots, k$ of $\dot{x} = f(x)$ with (possibly multiple) Floquet exponents $\lambda_i^j, 0, \gamma_l^j$, $i = 1, \dots, s$, $l = 1, \dots, u$, with $n = u + s + 1$, satisfying

$$\mathrm{Re}(\lambda_s^j) < \ldots < \mathrm{Re}(\lambda_2^j) < \mathrm{Re}(\lambda_1^j) < 0 < \mathrm{Re}(\gamma_1^j) < \mathrm{Re}(\gamma_2^j) < \ldots < \mathrm{Re}(\gamma_u^j) \ .$$

Suppose the leading Floquet exponents λ_1^j and γ_1^j are both real and simple. Under these conditions, the results of Shilnikov *et al* [27] imply that generically there exists a smooth 3-dimensional flow-invariant centre manifold $W^c(\Sigma)$ that contains Σ.

We discuss briefly the genericity conditions and the properties of this manifold.

At each point p of c_j denote by E^{ss}, E^c and E^{uu} the subspaces associated to the Floquet exponents $\{\lambda_s^j, \dots, \lambda_2^j\}$, $\{\lambda_1^j, 0, \gamma_1^j\}$ and $\{\gamma_2^j, \dots, \gamma_u^j\}$, respectively. Besides the s-dimensional stable and u-dimensional unstable manifolds of c_j, there exists a centre unstable manifold $W^{cu}(c_j)$ that is tangent, at each point p of c_j, to the subspace $E^c \oplus E^{uu}$ and a centre stable manifold $W^{cs}(c_j)$ tangent to $E^{ss} \oplus E^c$. It is clear that $[c_j \to c_{j+1}] \subset W^{cu}(c_j) \cap W^{cs}(c_{j+1})$.

Shilnikov *et al* [27] proved that along $W^{cu}(c_j)$, there exists a u-dimensional strong unstable foliation $\mathcal{F}^{uu}$ whose leaves at $p \in c_j$ include $W^{uu}(p)$. Similarly, along $W^{cs}(c_j)$ there exists an s-dimensional strong stable foliation $\mathcal{F}^{ss}$ containing $W^{ss}(p)$ as a leaf at p. Both foliations are at least of class C^1.

The genericity condition for existence of the centre manifold $W^c(\Sigma)$ is that at each point p of each heteroclinic connection, the centre unstable manifold $W^{cu}(c_j)$ is transverse to a leaf of $\mathcal{F}^{ss}$ and $W^{cs}(c_{j+1})$ is transverse to a leaf of $\mathcal{F}^{uu}$. This condition avoids degenerate cases like

the orbit flip, inclination flip, bellows and the homoclinic butterfly (see Homburg *et al* [16] for details).

On the centre manifold $W^c(\Sigma)$ the results of the preceding sections hold, so from Theorems 6, 8 and the results of Section 6 we get:

Theorem 13. *Let $\Sigma = \langle c_1, \ldots, c_k \rangle$ be a heteroclinic cycle of hyperbolic non trivial periodic trajectories in a manifold of dimension $n \geq 3$ such that all c_j have the same number of Floquet exponents with negative real parts and the leading Floquet exponents are real and simple. If the invariant manifolds of consecutive nodes meet transversely, then, generically:*

1. *Σ is contained in a smooth, flow-invariant, 3-dimensional center manifold $W^c(\Sigma)$;*
2. *Σ has finite and bi-infinite cycling;*
3. *there is a Cantor set Λ contained in $W^c(\Sigma)$ such that the first return map on Λ is conjugated to a subshift of finite type on k symbols;*
4. *Σ is not asymptotically stable neither in forward nor in backward time;*
5. *for each $j \in \{1, \ldots, k\}$, there exist infinitely many homoclinic trajectories associated to c_j;*
6. *if $k \geq 2$, for each $m, n \in \{1, \ldots, k\}$, there exist infinitely many heteroclinic trajectories from c_m to c_n;*
7. *for each $l \in \{2, \ldots, k\}$ and each permutation $\sigma \in S_k$ of k elements there exists a heteroclinic network of periodic trajectories*

$$\Sigma^{l\sigma} = \left\langle c_{\sigma(1)}, \ldots, c_{\sigma(l)} \right\rangle .$$

whose invariant manifolds of consecutive nodes meet transversely.

8. Construction of a heteroclinic cycle between three periodic trajectories in a five dimensional sphere

In this section we construct a vector field in $\mathbf{R}^6$ for which our results may be applied. Restricted to a five dimensional invariant sphere it has a heteroclinic cycle between periodic trajectories and the invariant manifolds of two consecutive periodic trajectories intersect transversely. Thus, by the results above, the dynamics near the heteroclinic cycle exibits chaotic cycling and all the associated dynamics.

The construction of the example relies on the technique presented in Aguiar *et al* [5] which consists essentially in three steps. In Aguiar *et al* [5], the authors start with a vector field on $\mathbf{R}^3$ with an attracting flow-invariant two-sphere containing a heteroclinic network. The heteroclinic network involves equilibria and one-dimensional heteroclinic connections that correspond to the intersection of fixed-point subspaces with the invariant sphere. The vector field needs to be at least $\mathbf{Z}_2$-equivariant. Due to the $\mathbf{Z}_2$-equivariance the vector field can be lifted by a rotation to a vector field on $\mathbf{R}^4$ with an attracting flow-invariant three-sphere. This forces some of the one-dimensional heteroclinic connections to become two-dimensional heteroclinic connections. The resulting vector field is $\mathbf{SO}(2)$-equivariant. Finally, they perturb the vector field in a way that destroys the $\mathbf{SO}(2)$-equivariance and such that the three-sphere remains invariant and globally attracting and some of the nontransverse two-dimensional heteroclinic connections perturb to transverse connections. Here we extend this procedure to three rotations.

This may be related to the construction in Melbourne [22] that starts with a $(\mathbf{Z}_2 \oplus \mathbf{Z}_2 \oplus \mathbf{Z}_2)$-equivariant system of differential equations in $\mathbf{R}^3$ whose flow has an asymptotically stable heteroclinic network between six equilibria. Using this system as an amplitude equation and adding three phase equations, the system lifts to a flow in $\mathbf{R}^6$ that has now an asymptotically stable heteroclinic cycle between three periodic solutions with three-torus $\mathbf{T}^3$ symmetry. Each saddle of the cycle is what Krupa [20] calls a *relative equilibrium*. Adding a symmetry breaking term to the amplitude system breaks all the connections, the cycle disappears in the corresponding

system in $\mathbf{R}^6$, but any trajectory near the *ghost* of the cycle will reconstruct its shape. Melbourne estimated the quasi-period of trajectories near each periodic solution. In our approach, instead of perturbing the amplitude equations, we perturb the lifted vector field in $\mathbf{R}^6$ in such way that the heteroclinic cycle does not disappear and the invariant manifolds of consecutive nodes meet transversely. We use the terminology of Aguiar *et al* [5], for results on dynamics. For symmetry, we refer the reader to Field [10] or Golubitsky *et al* [11].

8.1. **Lifting a vector field.** In Aguiar *et al* [5], it is proven how some properties of a $\mathbf{Z}_2$-equivariant vector field in $\mathbf{R}^3$ lift by a rotation to properties of the resulting vector field in $\mathbf{R}^4$. Those results generalize trivially to the lift by a rotation of a $\mathbf{Z}_2$-equivariant vector field on $\mathbf{R}^n$ to a vector field on $\mathbf{R}^{n+1}$. More concretely, let $\mathbf{X}_n$ be a $\mathbf{Z}_2$-equivariant vector field on $\mathbf{R}^n$. Without loss of generality, we can assume that $\mathbf{X}_n$ is equivariant by the action

$$k_n(x_1,\dots,x_{n-1},\omega) = (x_1,\dots,x_{n-1},-\omega).$$

The vector field $\mathbf{X}_{n+1}$ on $\mathbf{R}^{n+1}$ is obtained by adding the auxiliary equation $\dot{\varphi}_n = 1$ and interpreting the coordinates (ω,φ_n) as polar coordinates. In rectangular coordinates $(x_1,\dots,x_{n+1})$ on $\mathbf{R}^{n+1}$, it corresponds to $x_n = \omega\cos\varphi_n$ and $x_{n+1} = \omega\sin\varphi_n$. The resulting vector field $\mathbf{X}_{n+1}$ on $\mathbf{R}^{n+1}$ is $\mathbf{SO}(2)$-equivariant.

As in Aguiar *et al* [5], for $\Sigma\subset\mathbf{R}^n$ let $\mathcal{L}(\Sigma)\subset\mathbf{R}^{n+1}$ be the *lift by rotation* of Σ, the set of points $(x_1,\dots,x_{n+1})$ such that either $(x_1,\dots,\omega)$ or $(x_1,\dots,-\omega)$ lies in Σ, whith $|\omega| = ||(x_n,x_{n+1})||$. Consider the inclusion map $i_n:\mathbf{R}^n\to\mathbf{R}^{n+1}$, with

$$i_n(x_1,\dots,\omega) = (x_1,\dots,x_{n-1},\omega,0).$$

Extending the definition of heteroclinic connection between two invariant periodic solutions c_i and c_j as an m-dimensional connected flow-invariant manifold contained in $W^u(c_i)\cap W^s(c_j)$, the results in section 3 of Aguiar *et al* [5] generalize to:

Proposition 14. *Let $\mathbf{X}_n$ be a $\mathbf{Z}_2(k_n)$-equivariant vector field in $\mathbf{R}^n$ and $\mathbf{X}_{n+1}$ its lift to $\mathbf{R}^{n+1}$ by rotation.*

(a) *If $\Sigma\subset\mathbf{R}^n$ is invariant by the flow of $\mathbf{X}_n$, the $\mathcal{L}(\Sigma)$ is invariant by the flow of $\mathbf{X}_{n+1}$. In particular, if p is an equilibrium of $\mathbf{X}_n$ then $\mathcal{L}(\{p\})$ is a relative equilibrium of $\mathbf{X}_{n+1}$.*

(b) *If r_0 and r_1 are relative equilibria of $\mathbf{X}_n$ and ξ is a k-dimensional connection from r_0 to r_1, then:*
   (1) *If ξ lies in $Fix(\mathbf{Z}_2(k_n))$, then r_0 and r_1 also lie in $Fix(\mathbf{Z}_2(k_n))$ and ξ lifts to a k-dimensional from the relative equilibria $i(r_0) = r_0$ to $i(r_1) = r_1$ of $\mathbf{X}_{n+1}$.*
   (2) *If ξ is not contained in $Fix(\mathbf{Z}_2(k_n))$, then ξ lifts to a $(k+1)$-dimensional connection from the relative equilibria $\mathcal{L}(r_0)$ to $\mathcal{L}(r_1)$ of $\mathbf{X}_{n+1}$.*

(c) *If Σ is a compact $\mathbf{X}_n$-invariant asymptotically stable set then $\mathcal{L}(\Sigma)$ is a compact $\mathbf{X}_{n+1}$-invariant asymptotically stable set.*

(d) *If $\mathbf{S}^{n-1}_r$ is an $\mathbf{X}_n$-invariant globally attracting sphere then $\mathcal{L}(\mathbf{S}^{n-1}_r) = \mathbf{S}^n_r$ is an $\mathbf{X}_{n+1}$-invariant globally attracting sphere.*

(e) *If p is an hyperbolic equilibrium of $\mathbf{X}_n$ then $\mathcal{L}(\{p\})$ is also hyperbolic.*

(f) *The $\mathbf{SO}(2)$-orbit of any $\mathbf{X}_{n+1}$-invariant set is always the lift of an $\mathbf{X}_n$-invariant set. In particular, any $\mathbf{SO}(2)$-relative equilibrium of $\mathbf{X}_{n+1}$ is the lift of an equilibrium of $\mathbf{X}_n$.*

Moreover, it may be proved that if $\Sigma\subset\mathbf{R}^n$ is a compact flow-invariant set such that $\Sigma\subset\overline{W^s(\Sigma)\backslash\Sigma}$ and $\Sigma\subset\overline{W^u(\Sigma)\backslash\Sigma}$ then $\mathcal{L}(\Sigma)$ is also a compact flow-invariant set satisfying $\mathcal{L}(\Sigma)\subset\overline{W^s(\mathcal{L}(\Sigma))\backslash\mathcal{L}(\Sigma)}$ and $\mathcal{L}(\Sigma)\subset\overline{W^u(\mathcal{L}(\Sigma))\backslash\mathcal{L}(\Sigma)}$.

8.2. **Construction of the example.** Let $\Gamma\subset O(3)$ be the finite group generated by:

$$d(\rho_0,\rho_1,\rho_2) = (\rho_1,\rho_2,\rho_0),$$
$$q(\rho_0,\rho_1,\rho_2) = (-\rho_0,\rho_1,\rho_2).$$

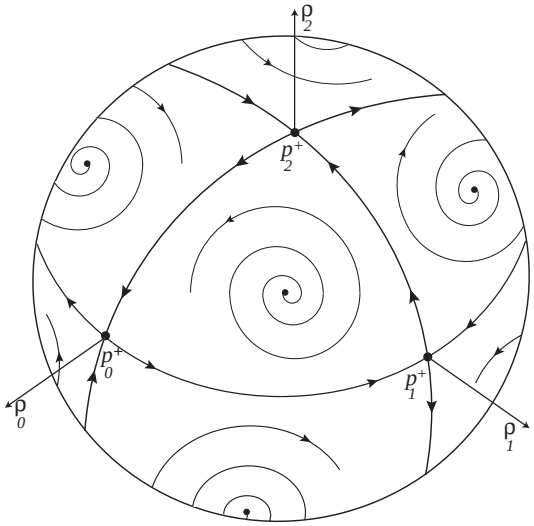

FIGURE 9. Heteroclinic network of the flow of the vector field $\mathbf{X}_3$, restricted to the invariant sphere $\mathbf{S}^2_r$. The intersection of the invariant sphere $\mathbf{S}^2_r$ with the invariant coordinate planes gives rise to three invariant circles. The union of these circles is the heteroclinic network whose existence is proved in theorem 16.

Let $\mathbf{X}_3$ be the fifth-order perturbation, studied in Aguiar [2], of the degree three normal form for the vector fields that are Γ-equivariant (see Guckenheimer *et al* [12], [13]):

$$\begin{array}{rcl} \dot{\rho}_0 &=& \rho_0\left(\lambda+\alpha\rho_0^2+\beta\rho_1^2+\gamma\rho_2^2+\delta(\rho_1^4-\rho_0^2\rho_2^2)\right),\\ \dot{\rho}_1 &=& \rho_1\left(\lambda+\alpha\rho_1^2+\beta\rho_2^2+\gamma\rho_0^2+\delta(\rho_2^4-\rho_0^2\rho_1^2)\right),\\ \dot{\rho}_2 &=& \rho_2\left(\lambda+\alpha\rho_2^2+\beta\rho_0^2+\gamma\rho_1^2+\delta(\rho_0^4-\rho_1^2\rho_2^2)\right). \end{array} \tag{4}$$

Theorem 15. *For $\lambda>0$, $\beta+\gamma=2\alpha$, $\beta<\alpha<\gamma<0$ and $\delta<0$ the flow of the vector field $\mathbf{X}_3$ satisfies (see figure 9):*

(a) *The sphere $\mathbf{S}^2_r$, of radius $r=\sqrt{-\frac{\lambda}{\alpha}}$, is invariant by the flow and globally attracting.*
(b) *The equilibria $p_0^{\pm}=(\pm r,0,0)$, $p_1^{\pm}=(0,\pm r,0)$ and $p_2^{\pm}=(0,0,\pm r)$ are hyperbolic saddles.*
(c) *When restricted to the invariant sphere $\mathbf{S}^2_r$ the invariant manifolds of $p_i^{\pm}, i=0,1,2$ satisfy:*
  (c.1) *$W^u(p_i^{\pm})\cap W^s(p_{i+1}^{\pm})$ (mod 3) is one-dimensional and*
  (c.2) *$\cup_{i=0,1,2}\left[\{p_i^{\pm}\}\cup W^u(p_i^{\pm})\right]=\cup_{i=0,1,2}\left[\{p_i^{\pm}\}\cup W^s(p_i^{\pm})\right]$ is an asymptotically stable heteroclinic network with twelve connections between the saddles $p_i^{\pm}$.*
(d) *Besides $p_i^{\pm}$, $i=0,1,2$ and the origin, which is repelling, there are eight equilibria which are unstable foci on the restriction to $\mathbf{S}^2_r$.*

Proof. See the proof of Theorem 24 in Aguiar *et al* [2]. □

We use the procedure described in Section 2 of [5] to lift the three-dimensional vector field $\mathbf{X}_3$, by three rotations, to a vector field in $\mathbf{R}^6$. More specifically, since the vector field $\mathbf{X}_3$ is equivariant by the action $\mathbf{Z}_2(q)\oplus\mathbf{Z}_2(d^2qd)\oplus\mathbf{Z}_2(dqd^2)$, it has the form

$$\begin{array}{rcl} \dot{\rho}_0 &=& \rho_0 f(\rho_0^2,\rho_1^2,\rho_2^2),\\ \dot{\rho}_1 &=& \rho_1 f(\rho_1^2,\rho_2^2,\rho_0^2),\\ \dot{\rho}_2 &=& \rho_2 f(\rho_2^2,\rho_0^2,\rho_1^2), \end{array}$$

with $f:\mathbf{R}^3\to\mathbf{R}$ such that

$$f(u_1,u_2,u_3)=(\lambda+\alpha u_1+\beta u_2+\gamma u_3+\delta(u_2^2-u_1u_3)). \tag{5}$$

Adding the auxiliary equations $\dot{\varphi} = 1$, $\dot{\psi} = 1$ and $\dot{\sigma} = 1$ and interpreting each pair of coordinates (ρ_0, φ), (ρ_1, ψ) and (ρ_2, σ) as polar coordinates, the vector field $\mathbf{X}_3$ lifts by three rotations to a vector field $\mathbf{X}_6$ on $\mathbf{R}^6$ of the form:

$$\begin{aligned}
\dot{x}_1 &= x_1 f(x_1^2 + x_2^2, x_3^2 + x_4^2, x_5^2 + x_6^2) - x_2,\\
\dot{x}_2 &= x_2 f(x_1^2 + x_2^2, x_3^2 + x_4^2, x_5^2 + x_6^2) + x_1,\\
\dot{x}_3 &= x_3 f(x_3^2 + x_4^2, x_5^2 + x_6^2, x_1^2 + x_2^2) - x_4,\\
\dot{x}_4 &= x_4 f(x_3^2 + x_4^2, x_5^2 + x_6^2, x_1^2 + x_2^2) + x_3,\\
\dot{x}_5 &= x_5 f(x_5^2 + x_6^2, x_1^2 + x_2^2, x_3^2 + x_4^2) - x_6,\\
\dot{x}_6 &= x_6 f(x_5^2 + x_6^2, x_1^2 + x_2^2, x_3^2 + x_4^2) + x_5.
\end{aligned}$$

Theorem 16. *For the parameter values in theorem 15 the flow of the vector field $\mathbf{X}_6$ satisfies*

- (C1) *There is a five-dimensional sphere, $\mathbf{S}_r^5$, that is invariant by the flow and globally attracting.*
- (C2) *On the invariant five-sphere, there is an asymptotically stable heteroclinic cycle Σ with three periodic trajectories, c_i, $i = 0, 1, 2$. The invariant manifolds of the periodic trajectories satisfy, on the invariant sphere, $W^u(c_i) = W^s(c_{i+1})$ (mod 3), corresponding to three-dimensional heteroclinic connections.*
- (C3) *The origin is the only equilibrium and it is repelling.*
- (C4) *In the restriction to the invariant sphere $\mathbf{S}_r^5$, there is a three-dimensional flow-invariant torus that is repelling.*

Proof. The proof relies on the results in proposition 14.

Number the rotations associated to the angular coordinates φ, ψ and σ as rotations 1, 2 and 3, respectively. The lift of the vector field $\mathbf{X}_3$ in $\mathbf{R}^3$ to the vector field $\mathbf{X}_6$ in $\mathbf{R}^6$ by the three rotations corresponds to a sequence of three lifts, by each of the three rotations.

Due to assertion (d) in proposition 14, since the sphere $\mathbf{S}_r^2$ is $\mathbf{X}_3$-invariant and globally attracting, the sphere $\mathbf{S}_r^5 = \mathcal{L}(\mathbf{S}_r^4)$ is $\mathbf{X}_6$-invariant and globally attracting.

Let $\Sigma_1 = \mathbf{Z}_2(q)$, $\Sigma_2 = \mathbf{Z}_2(d^2qd)$ and $\Sigma_3 = \mathbf{Z}_2(dqd^2)$. The fixed-point subspace $Fix(\Sigma_i) = \{(\rho_1, \rho_2, \rho_3) \in \mathbf{R}^3 : \ \rho_i = 0\}$, $i = 1, 2, 3$, is invariant by rotation i.

In the flow of $\mathbf{X}_3$, the equilibria $p_{i-1}^{\pm}$, $i = 1, 2, 3$, lie in $Fix(\Sigma_{i+1}) \cap Fix(\Sigma_{i+2})$ and the heteroclinic trajectories connecting the equilibria $p_{i-1}^{\pm}$ and $p_i^{\pm}$ lie in $Fix(\Sigma_{i+2})$, (*mod* 3). These, together with assertion (b) in proposition 14, prove the existence of the heteroclinic cycle Σ in assertion (C2).

More specifically, the equilibria $p_{i-1}^{\pm}$, $i = 1, 2, 3$, lift by rotation i to a periodic trajectory c_{i-1}, which remains invariant by the other two rotations. The periodic trajectory c_i, $i = 0, 1, 2$ has equations

$$x_{2i+1}^2 + x_{2i+2}^2 = r^2$$

and

$$x_{2i+3} = x_{2i+4} = x_{2i+5} = x_{2i+6} = 0 \qquad (\text{mod } 6).$$

By assertion (f) in proposition 14, the periodic trajectories c_i, $i = 0, 1, 2$, are hyperbolic.

The heteroclinic trajectories connecting equilibria $p_{i-1}^{\pm}$ and $p_i^{\pm}$, $i = 1, 2, 3$, lift by rotation i to a pair of two-dimensional connections from the periodic trajectory c_{i-1} to the equilibria $p_i^{\pm}$. Then by rotation $i+1$, they lift to a three-dimensional connection from the periodic trajectories c_{i-1} to c_i which remains invariant by rotation $i + 2$. The three-dimensional connection of the periodic trajectories c_{i-1} and c_i has equations

$$x_{2i+1}^2 + x_{2i+2}^2 + x_{2i+3}^2 + x_{2i+4}^2 = r^2$$

and

$$x_{2i+5} = x_{2i+6} = 0 \qquad (\text{mod } 6).$$

The asymptotic stability of the heteroclinic network in $\mathbf{S}_r^2$ and assertion (c) in proposition 14 imply the asymptotic stability of the heteroclinic cycle Σ in $\mathbf{S}_r^5$.

Assertion (C4) follows from the existence of the eight unstable foci on $\mathbf{S}_r^2$, that lie outside $Fix(\mathbf{Z}_2(q)) \cup Fix(\mathbf{Z}_2(d^2qd)) \cup Fix(\mathbf{Z}_2(dqd^2))$ and that their coordinates are

$$\left(\pm\sqrt{-\frac{\lambda}{3\alpha}}, \pm\sqrt{-\frac{\lambda}{3\alpha}}, \pm\sqrt{-\frac{\lambda}{3\alpha}}\right).$$

Thus, by rotation 1, they lift to four periodic trajectories, which lift to a pair of two-dimensional tori by rotation 2 and to a three-dimensional torus by rotation 3. Since the equilibria are repelling and due to assertion (e) in proposition 14 the torus is repelling.

By (e) and (f) in proposition 14 and assertions (d) and (e) in theorem 15 we obtain (C3). □

Figure 10 corresponds to the time series of a trajectory in a neighbourhood of the asymptotically stable heteroclinic cycle in the flow of $\mathbf{X}_6$. As in Melbourne [22], the trajectory starts near the periodic trajectory c_2, spending some time nearby and jumps to the next periodic trajectory in the cycle, c_0, staying there for a longer period of time. This kind of motion continues around the heteroclinic cycle before returning to the periodic trajectory c_2. The asymptotic stability of the heteroclinic cycle implies that the sequence of times spent near the nodes is monotonically increasing.

Perturbation and transverse intersection of manifolds - numerical simulation. The vector field $\mathbf{X}_6$ is $\mathbf{Z}_3 \times \mathbf{SO}(2)^3$-equivariant. The three-dimensional heteroclinic connections in Σ correspond to the intersection of the invariant sphere $\mathbf{S}_r^5$ with the fixed-point subspaces of the rotational symmetries. Moreover, on the the invariant sphere $\mathbf{S}_r^5$ they correspond to the nontransverse intersection of the invariant manifolds of the periodic trajectories. We now perturb $\mathbf{X}_6$ keeping $\mathbf{S}_r^5$ invariant while forcing those invariant manifolds to intersect transversely on one-dimensional heteroclinic connections between the periodic trajectories.

The perturbing term we consider is:

$$P(x_1, x_2, x_3, x_4, x_5, x_6) = \begin{pmatrix} x_4x_5x_6 \\ -x_3x_4x_5 \\ x_1x_2x_6 \\ -x_1x_5x_6 \\ x_2x_3x_4 \\ -x_1x_2x_3 \end{pmatrix}$$

and thus the perturbed vector field is $\mathbf{X}_6^p = \mathbf{X}_6 + \varepsilon P$, with ε small. Note that this perturbation is $\mathbf{Z}_3$-equivariant. The perturbation keeps the invariance of the planes defined by

$$x_3 = x_4 = x_5 = x_6 = 0, \quad x_1 = x_2 = x_5 = x_6 = 0$$

and

$$x_1 = x_2 = x_3 = x_4 = 0$$

and is tangent to the invariant sphere; thus the invariant sphere and the three periodic trajectories are invariant by the perturbed flow. However, the perturbation breaks the invariance of the hyperplanes defined by $x_1 = x_2 = 0$, $x_3 = x_4 = 0$ and $x_5 = x_6 = 0$ that contain the heteroclinic connections and so the connections are perturbed.

Although we do not prove analytically that the invariant manifolds of consecutive periodic trajectories intersect transverselly, this will generically be the case. Here, we intend to present some evidences of that, namely chaotic behaviour. High sensibility to initial conditions is emphasized in figures 11, 12 and 13. Figures 11 and 12 show the abrupt x_i-variation of two trajectories having started very close. Figure 12 claims also the existence of chaotic cycling. The simulations

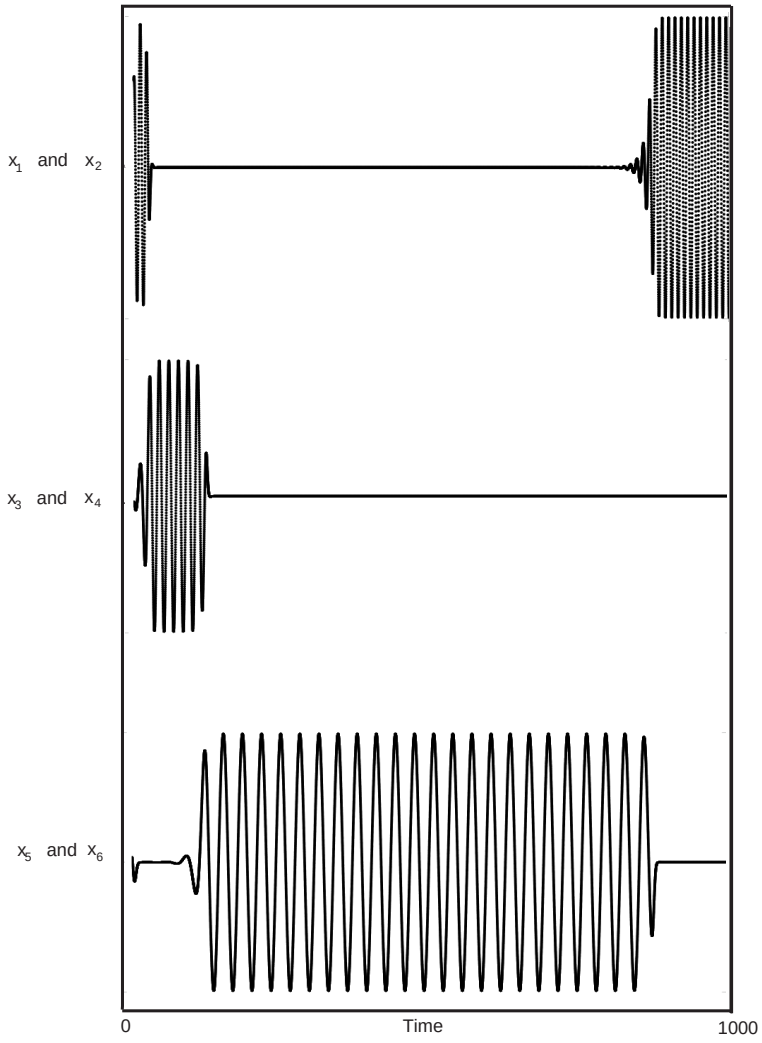

FIGURE 10. Time series corresponding to a solution near the asymptotically stable heteroclinic cycle in the flow of the vector field $\mathbf{X}_6$, with $\lambda = 1$, $\alpha = -0.33333333$, $\beta = -0.5$, $\gamma = -0.16666667$ and $\delta = -0.05$. The initial condition is $(-1.0083, -0.0927, -0.1043, -0.0695, 0.0695, 0.1037)$.

in figures 11 and 12 show evidence of instant chaos near the perturbed heteroclinic cycle due to the explosion of suspended horseshoes and homoclinic classes.

Bifurcating to chaos. As we know from the previous sections, for $\varepsilon \neq 0$, there is a infinite number of heteroclinic and homoclinic connections between any two periodic trajectories and the dynamics near the heteroclinic network is very complex. As we have seen using symbolic dynamics, the set of homo and heteroclinic connections near the perturbed cycle is dense in the set of nonwandering trajectories of the cycle. As $\varepsilon \to 0$, the infinity of connections tend to the two dimensional connections between consecutive periodic trajectories that exist for $\varepsilon = 0$, and the remaining cycle becomes asymptotically stable, attracting all trajectories in a small neighbourhood.

This phenomenon is a consequence of the symmetry breaking and the route to the chaos corresponds to a curious interaction between symmetry breaking, robust switching and chaotic cycling. This dynamical phenomenon is even more interesting because of the emergence of

chaotic cycling (after perturbation) do not depend on the magnitude of the multipliers of the periodic trajectories. It depends only on the geometry of the flow near the cycle. The magnitude of the multipliers is only crucial to study the stability of the unperturbed cycle.

Lyapunov exponents. One of the most efficient tools for the study of chaotic dynamical systems is the computation of the Lyapunov Exponents. Roughly speaking, they measure the stability and instability of trajectories under perturbation. For $\mathbf{X}_6^p$ and $\lambda = 1$, $\alpha = -0.33333333$, $\beta = -0.5$, $\gamma = -0.16666667$ and $\delta = -0.05$, one of the Lyapunov Exponents is $0.00055 > 0$. By Oseledets' Theorem, this means that there exists x and $v \in T_x\mathbf{S}^5$ such that

$$||D_xF^n(v)|| > 1,$$

where F is the first return map near the heteroclinic cycle. Thus, v grows exponentially at a rate $0,00055$ in the future and contract exponentially at the same rate in the past. In our setting, it shows that P corresponds to a unstable perturbation, illustrating that the distant future is practically inaccessible and may only be described in average, in probabilistic and ergodic terms. Since, on a large scale, the evolution resembles a random process, the symbolic dynamics used in section 5.3 will be a very helpful tool to tackle the complete characterization of this network.

Acknowledgements

The authors are grateful to Mário Bessa, D. Turaev and W. S. Koon for helpful comments, to Oksana Koltsova from the Imperial College of London for helpful discussions and to Murilo S. Baptista for the numerical computation of the Lyapunov exponents. The first author thanks to Jeroen Lamb for the hospitality at the Imperial College of London.

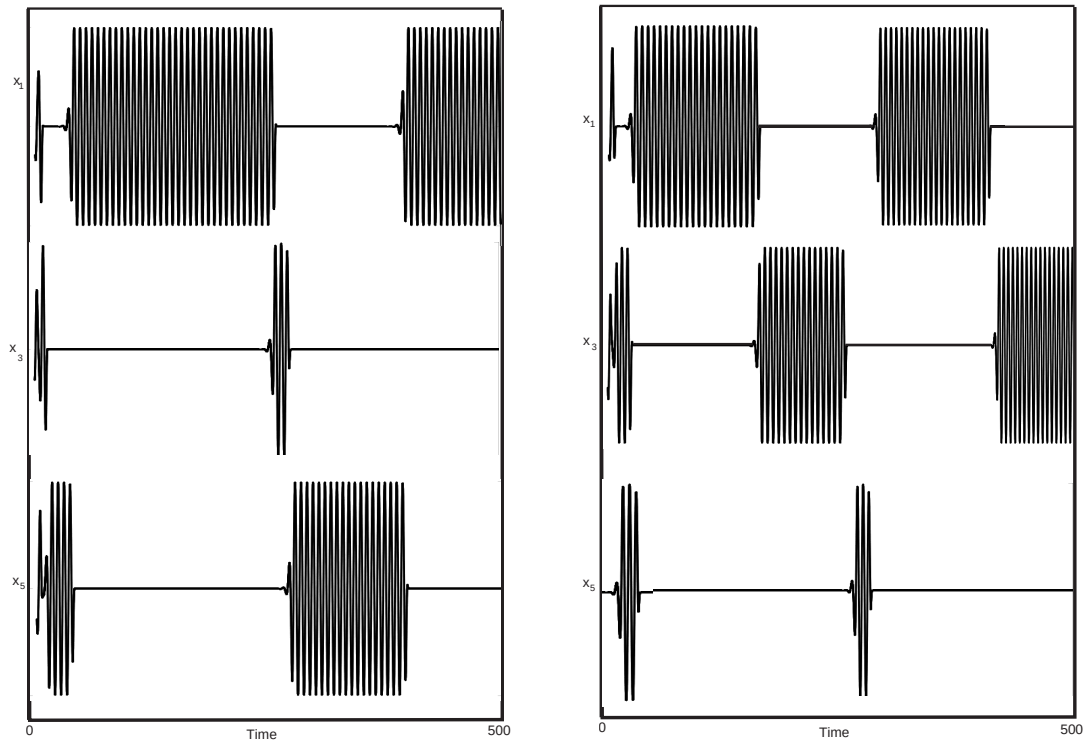

FIGURE 11. Time series for two trajectories with close initial condition for the flow corresponding to the vector field $\mathbf{X}_6 + \varepsilon P$, with $\lambda = 1$, $\alpha = -0.33333333$, $\beta = -0.5$, $\gamma = -0.16666667$, $\delta = -0.05$ and $\varepsilon = 1$ (the same trajectories as in figure 12). Left: the initial condition is $(-1.089, 1.715, -0.5, -0.5, 0.406, -0.5)$; Right: the initial condition is $(-1.090, 1.715, -0.5, -0.5, 0.407, -0.5)$. These time series illustrate the cycling of finite order.

APPENDIX A. ESTIMATES OF CONTRACTION RATES ON STRIPS

Lemma 17. *If U is a vertical strip of width d across $\mathcal{R}^{in,j}$ and $m \geq 1$, then $P_j(m, U)$ is a vertical strip across $\mathcal{R}^{in,j+1}$ of width $D \leq \mu_m d$, where*

$$\mu_m = \varepsilon C_j e^{-2\pi C_j (m-1)}.$$

If W is a vertical strip of width d across $\mathcal{R}^{out,j}$ and $m \geq 1$, then $Q_j(m, W)$ is a vertical strip across $\mathcal{R}^{out,j-1}$ of width $D \leq \nu_m d$, where

$$\nu_m = \varepsilon E_j e^{-2\pi E_j m}.$$

Proof. We only prove the assertion about $P_j(m, U)$ since the proof for $Q_j(m, W)$ is quite similar, with appropriate adaptations. By corollary 7, if U is a vertical strip across $\mathcal{R}^{in,j}$ then $\widehat{U} = \phi_{c_j}(U \cap \overline{\mathcal{I}_j^m})$ is a horizontal strip across $\mathcal{R}^{out,j}$, which is mapped by $\Psi_{j\to j+1}$ into a vertical strip across $\mathcal{R}^{in,j+1}$. For these estimates we make the simplifying assumption that $\Psi_{j\to j+1}$ is a rotation of $\pi/2$ around $(A, 1)$ followed by a translation mapping $(A, 1)$ to $(B, 0)$. Without this assumption the estimates hold with all the μ_m multiplied by a suitable constant. Thus, the width D that we want to estimate is the height of $\widehat{U} = \phi_{c_j}(U \cap \overline{\mathcal{I}_j^m})$. This height is the lenght of a segment connecting two points with the same angular coordinate (see figure 14). Let (φ_1, r_1) and $(\varphi_1, r_1 + D)$ be these points and denote their pre-image under ϕ_{c_j} by (θ_1, z_1) and (θ_2, z_2), respectively, with $\theta_1, \theta_2 \in [0, 2\pi]$.

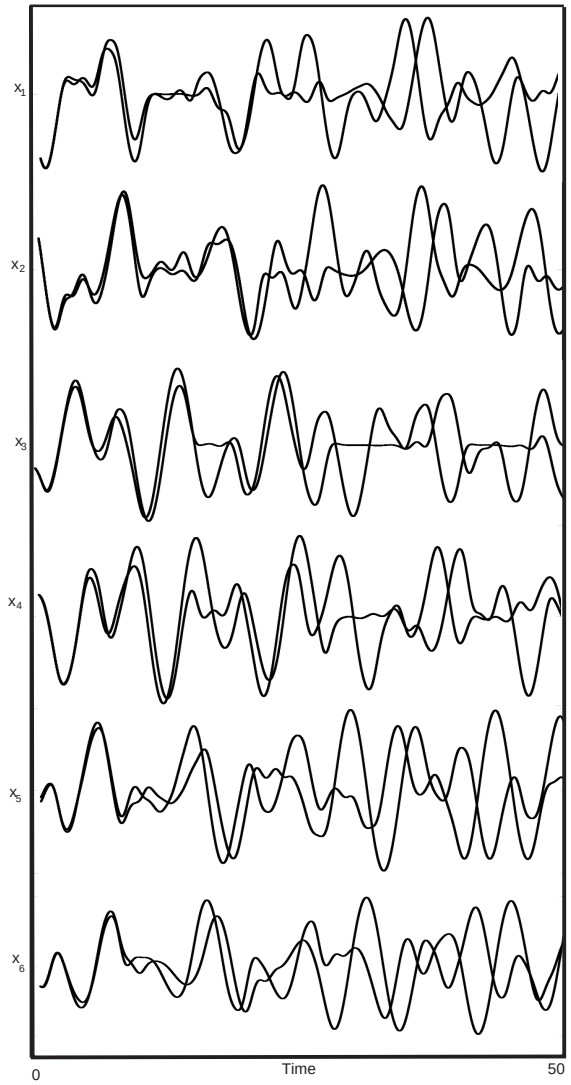

FIGURE 12. Time series for two trajectories with close initial condition for the flow corresponding to the vector field $\mathbf{X}_6 + \varepsilon P$, with $\lambda = 1$, $\alpha = -0.33333333$, $\beta = -0.5$, $\gamma = -0.16666667$, $\delta = -0.05$ and $\varepsilon = 1$ (the same trajectories as in figure 11). For each coordinate, we plot two time series, one with initial condition $(-1.089, 1.715, -0.5, -0.5, 0.406, -0.5)$ and the other with initial condition $(-1.090, 1.715, -0.5, -0.5, 0.407, -0.5)$. Note that the two time series are different, illustrating the *high* sensitivity to initial conditions.

From the expression (3) for ϕ_{c_j} given in section 3, it follows that since the angular coordinates of $\phi_{c_j}(\theta_1, z_1)$ and $\phi_{c_j}(\theta_2, z_2)$ are equal, then:

$$\theta_1 - \frac{1}{E_j} \ln\left(\frac{z_1}{\varepsilon}\right) = \theta_2 - \frac{1}{E_j} \ln\left(\frac{z_2}{\varepsilon}\right)$$

which is equivalent to:

$$z_2 = z_1 e^{E_j(\theta_2 - \theta_1)}.$$

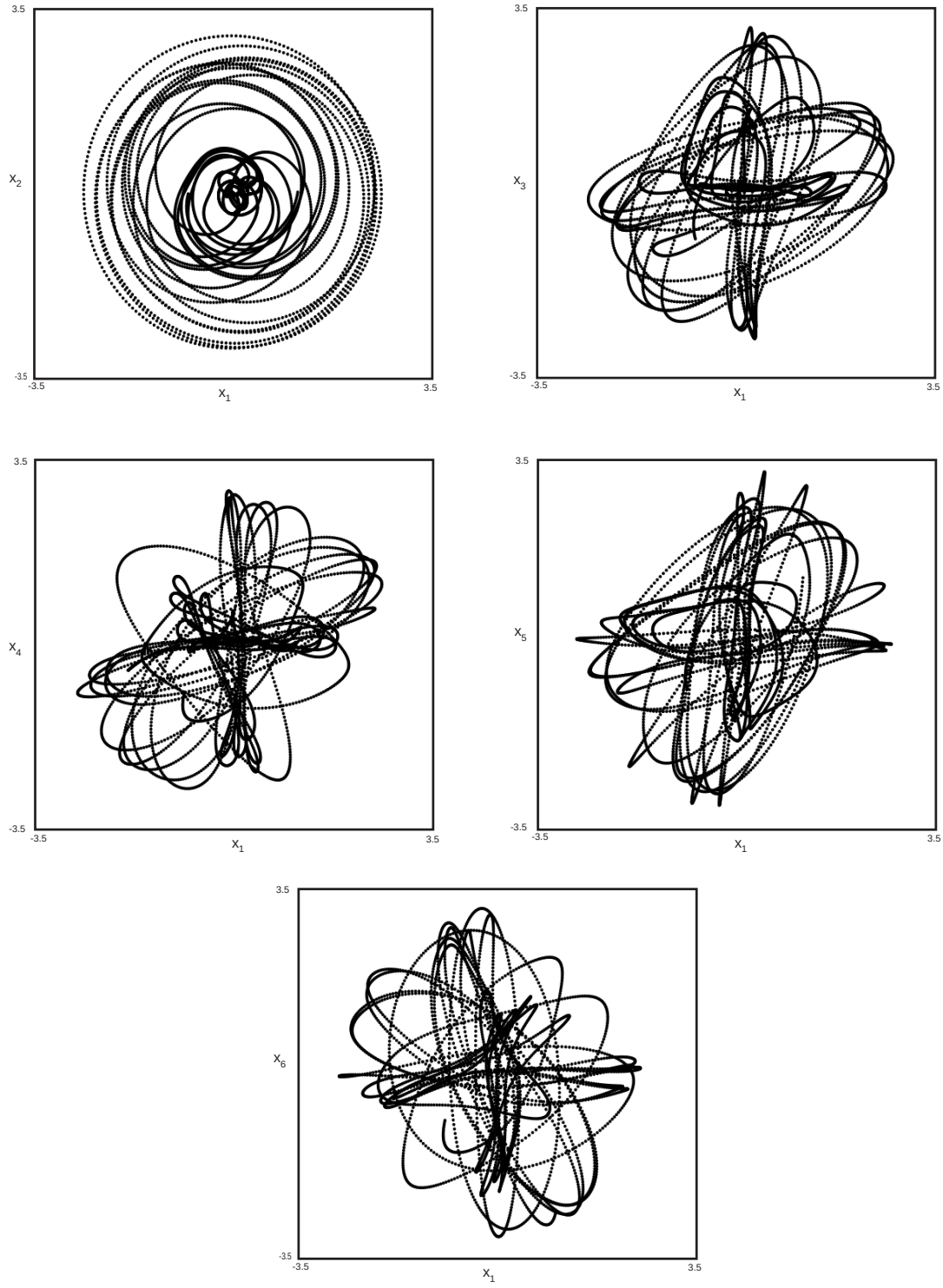

FIGURE 13. Projection in the (x_1, x_2), (x_1, x_3), (x_1, x_4), (x_1, x_5) and (x_1, x_6) planes of the trajectory with initial condition $(-1.089, 1.715, -0.500, -0.500, 0.406, -0.5)$ for the flow corresponding to the vector field $\mathbf{X}_6 + \varepsilon P$, with $\lambda = 1$, $\alpha = -0.33333333$, $\beta = -0.5$, $\gamma = -0.16666667$, $\delta = -0.05$ and $\varepsilon = 1$.

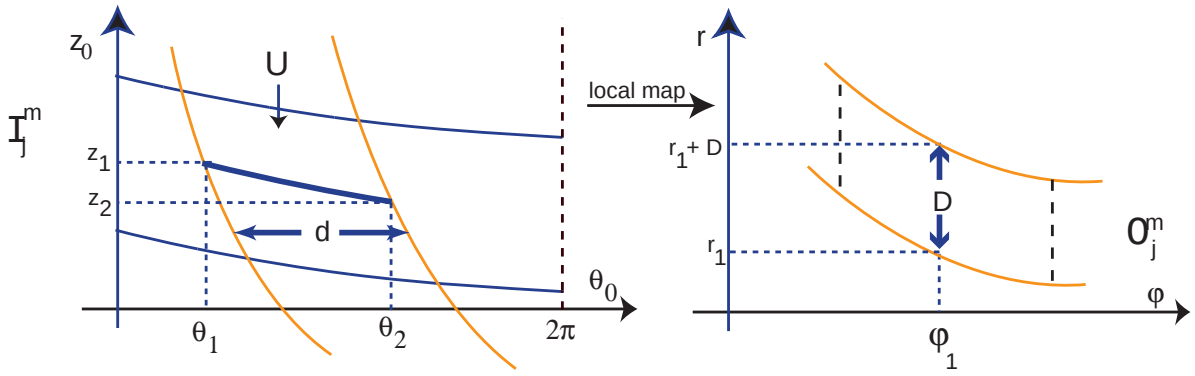

FIGURE 14. By corollary 7, for $m \in \mathbf{N}$ the set $\widehat{U} = \phi_{c_j}\left(U \cap \overline{\mathcal{I}_j^m}\right)$ is a horizontal strip across the width of $H_{c_j}^{out}$ and thus $\widehat{U} \cap \mathcal{R}^{out,j}$ is a horizontal strip.

Since $\phi_{c_j}(\theta_1, z_1)$ and $\phi_{c_j}(\theta_2, z_2)$ lie in the same vertical segment of lenght D, this means that:

$$1 + \varepsilon \left(\frac{z_2}{\varepsilon}\right)^{\frac{C_j}{E_j}} = 1 + \varepsilon \left(\frac{z_1}{\varepsilon}\right)^{\frac{C_j}{E_j}} + D.$$

and therefore

$$\frac{D}{\varepsilon} = \left(\frac{z_1}{\varepsilon}\right)^{\frac{C_j}{E_j}} \left(e^{C_j(\theta_2 - \theta_1)} - 1\right). \tag{6}$$

Since (θ_1, z_1) and (θ_2, z_2) lie inside the strip $\mathcal{I}_j^m$, we have:

$$2\pi m \leq \theta_1 - \frac{1}{E_j} \ln\left(\frac{z_1}{\varepsilon}\right) \leq 2\pi(m+1)$$

and thus it follows that:

$$E_j(-2\pi(m+1) + \theta_1) \leq \ln\left(\frac{z_1}{\varepsilon}\right) \leq E_j(-2\pi m + \theta_1)$$

giving rise to:

$$e^{-2\pi(m+1)E_j} e^{\theta_1 E_j} \leq \frac{z_1}{\varepsilon} \leq e^{-2\pi m E_j} e^{\theta_1 E_j}. \tag{7}$$

From the second inequality of (7), we may conclude that:

$$\frac{z_1}{\varepsilon} \leq e^{-2\pi m E_j} e^{\theta_1 E_j} \leq e^{-2\pi m E_j} e^{2\pi E_j} = e^{-2\pi E_j(m-1)} \tag{8}$$

Substituting (8) into (6), and taking into account that $\theta_2 - \theta_1 \leq d$ (since the width of U is d), we show that

$$\frac{D}{\varepsilon} \leq e^{-2\pi C_j(m-1)} \left(e^{C_j(\theta_2 - \theta_1)} - 1\right) \leq e^{-2\pi C_j(m-1)} \left(C_j d + |o(d^2)|\right)$$

with a positive remainder $|o(d^2)|$ and hence $D \leq \varepsilon C_j d e^{-2\pi C_j(m-1)}$.

□

References

[1] L. Abramov, *On the entropy of a flow* (Russian), Dokl. Akad. Nauk. SSSR 128, 873–875, 1959

[2] M. A. D. Aguiar. Vector fields with heteroclinic networks, *Phd thesis, Departamento de Matemática Aplicada, Faculdade de Ciências da Universidade do Porto*, 2003

[3] V. M. Alekseyev, *Quasirandom Dynamical Systems. I. Quasirandom Diffeomorphisms*, Math. USRR Sbornik, 5, No. 1, 73–128, 1968

[4] M. A. D. Aguiar, S. B. S. D. Castro and I. S. Labouriau, *Dynamics near a heteroclinic network,* Nonlinearity 18, 391–414, 2005

[5] M. A. D. Aguiar, S. B. S. D. Castro and I. S. Labouriau. *Simple Vector Fields with Complex Behavior*, Int. Jour. of Bif. and Chaos, Vol. 16 No. 2, 369–381, 2006

[6] M. A. D. Aguiar, I. S. Labouriau and A. A. P. Rodrigues, *Switching near a heteroclinic network of rotating nodes*, Dynamical Systems: an International Journal, Vol. 25, Issue 1, 75–95, 2010

[7] V. Araújo and M. J. Pacífico, *Three-Dimensional Flows*, Vol 53 of Ergebnisse der Mathematik und ihrer Grenzgebiete, Springer, 2010

[8] P. Ashwin, M. Field, A. M. Rucklidge and R. Sturman, *Phase resetting effects for robust cycles between chaotic sets*, Chaos 13, 973–981, 2003

[9] M. Dellnitz, M. Field, M. Golubitsky, A. Hohmann and J. Ma, *Cycling Chaos*, IEEE Transactions on Circuits and Systems. 1. Fundamental Theory and Applications, Vol. 42, No. 10, 1243–1247, 1995

[10] M. Field, *Lectures on bifurcations, dynamics and symmetry*, Pitman Research Notes in Mathematics Series, Vol. 356, Longman, 1996

[11] M. I. Golubitsky, I. Stewart and D. G. Schaeffer, *Singularities and Groups in Bifurcation Theory* , Vol. II, Springer, 2000

[12] J. Guckenheimer and P. Holmes, *Nonlinear and Bifurcations of Vector Fields*, Applied Mathematical Sciences, No. 42, Springer-Verlag, 1983

[13] J. Guckenheimer and P. Holmes, *Structurally stable heteroclinic cycles,* Math. Proc. Camb. Phil. Soc., No. 103, 189–192, 1988

[14] P. Hartman, *On local homeomorphisms of Euclidean spaces*, Bol. Soc. Math. Mexicana, No. 5, 220–241, 1960

[15] A. J. Homburg, *Global Aspects of Homoclinic Bifurcations in Vector Fields*, Memoirs of the American Mathematical Society, No. 578, Vol. 121, American Mathematical Society, Providence (USA), 1996

[16] A. J. Homburg and B. Sandstede, *Homoclinic and Heteroclinic Bifurcations in Vector Fields*, Handbook of Dynamical Systems, Vol. 3, North Holland, Amsterdam, 379-524, 2010

[17] A. Katok and B. Hasselblatt, *Introduction to the Modern Theory of Dynamical Systems*, Cambridge University Press, 1995

[18] B. P. Kitchens, *Symbolic Dynamics,* Springer, Berlin, Heidelberg, 1998

[19] W. S. Koon, M. Lo, J. Marsden and S. Ross, *Heteroclinic Connections between Periodic Orbits and Resonance Transition in Celestial Mechanics*, Control and Dynamical Systems Seminar (California Institute of Technology), Pasadena, California, 1999

[20] M. Krupa, *Bifurcations of relative equilibria*, SIAM J. Math. Anal., Vol 21, No. 6, 1453–1486, 1990

[21] M. Krupa and I. Melbourne, *Asymptotic Stability of Heteroclinic Cycles in Systems with Symmetry, II,* Proc. Roy. Soc. Edinburgh, No. 134A(6), 1177–1197, 2004

[22] I. Melbourne, *Intermittency as a Codimension-Three Phenomenon*, Journal of Dynamics and Differential Equations, Vol. 1, No. 4, 347–367, 1989

[23] R. Moeckel, *Chaotic Orbits in the Three Body Problem*, in P.H. Rabinowitz, A. Ambrosetti, I. Ekeland and E.J. Zehnder (eds.) *Periodic Solutions of Hamiltonian Systems and Related Topics (Il Ciocco 1986)* NATO ASI Ser. C 209, Reidel, Dordrecht, 203–219, 1987

[24] O. Sarig, *Thermodynamic Formalism for Countable Markov Shifts*, Ergodic Th. Dynam. Sys., No. 19, 1565–1593, 1999

[25] M. Shashkov and D. V. Turaev, *An Existence Theorem of Smooth Nonlocal Center Manifolds for Systems Close to a System with a Homoclinic Loop*, J. Nonlinear Sci., Vol. 9, No. 5, 525–573, 1999

[26] L. P. Shilnikov, *On a Poincaré Birkhoff Problem*, Math. USSR. Sb., Vol. 3, 378–397, 1967

[27] L. P. Shilnikov, A. L. Shilnikov, D. M. Turaev, and L. U. Chua, *Methods of Qualitative Theory in Nonlinear Dynamics*, Part I, World Scientific Publishing Co., 1998

[28] S. Wiggins, *Global Bifurcations and Chaos: Analytical Methods*, Springer, New York, 1988

[29] S. Wiggins, *Introduction in Applied Nonlinear Dynamical Systems and Chaos*, Springer-Verlag, TAM 2, New York, 1990

(I.S. Labouriau and A.A.P. Rodrigues) Centro de Matemática da Universidade do Porto, and Faculdade de Ciências da Universidade do Porto, Rua do Campo Alegre 687, 4169–007 Porto, Portugal
E-mail address, A.A.P.Rodrigues: alexandre.rodrigues@fc.up.pt
E-mail address, I.S.Labouriau: islabour@fc.up.pt

(M.A.D.Aguiar) Centro de Matemática da Universidade do Porto, and Faculdade de Economia da Universidade do Porto, Rua Dr. Roberto Frias, 4200-464 Porto, Portugal
E-mail address: maguiar@fep.up.pt

Appendix 1 – Center Manifolds for Heteroclinic Cycles

We review briefly some results that have been used in section 7 - *Cycling in higher dimensions* of article 2. We use notations and results from Homburg [**35**], Shaskov and Turaev [**68**] and Shilnikov *et al* [**75**] adapted to our purposes.

Let c_j be a hyperbolic invariant saddle, associated to the flow of $\dot{x} = f(x)$. The set of its Floquet exponents, for each $j \in \{1, \ldots, k\}$ is given by

$$\{\lambda_r^j, 0, \gamma_s^j\}_{r\in\{1,\ldots,n_s\}, s\in\{1,\ldots,n_u\}}$$

where

$$\lambda_{n_s}^j < \ldots < \lambda_1^j < 0 < \gamma_1^j < \ldots < \gamma_{n_u}^j,$$

and n_s^j (respectively: n_u^j) is the number (with multiplicities) of eigenvalues whose module is less (respectively: greater) than 1, for the jacobian matrix associated to the first return map π_j. We call the characteristic Floquet exponents $\lambda_1^j < 0$ and $\gamma_1^j > 0$ *leading characteristic Floquet exponents.*

Definition [**35**]**:** *Let $\mathcal{V}$ be an open subset of M. A continuous foliation $\mathcal{F}$ is a disjoint decomposition of $\mathcal{V}$ into k-dimensional embedded submanifolds (the leaves), such that $\mathcal{V}$ is covered by C^0 charts*

$$\phi : \mathcal{D}^k \times \mathcal{D}^{n-k} \to \mathcal{V}$$

and $\phi(\mathcal{D}^k \times \{x\}) \subset \mathcal{F}_x$, where $\mathcal{F}_x$ is the leaf of $\mathcal{F}$ through x.

The foliation is C^k if the map $x \mapsto T_x\mathcal{F}_x$ is C^k.

Hereafter, we follow Shilnikov *et al* [**75**]. Suppose that $\Sigma = \langle c_1, \ldots, c_k\rangle$ is a heteroclinic cycle in an n-dimensional manifold whose nodes are hyperbolic non-trivial periodic trajectories. All heteroclinic connections are one-dimensional.

Trichotomy Condition *There exists a tern $(k_c, m_s, m_u) \in \boldsymbol{N}\times\boldsymbol{N}_0^2$ such that for each node c_j of Σ, there exists $\beta_j^u > 0$ and $-\beta_j^s < 0$, such that:*

- *the real part of k_c characteristic exponents belongs to $(-\beta_j^s, \beta_j^u)$;*
- *exactly m_u characteristic exponents have real part greater than β_j^u and m_s characteristic exponents have real part less than $-\beta_j^s$.*

The characteristic exponents that lie on the interval $(-\beta_j^s, \beta_j^u)$ are called the *center part of the spectrum*. The main restriction of the *Trichotomy Condition* is that the number of characteristic exponents that belong to each part of the spectrum does not depend on the nodes. The real numbers $\beta_j^u > 0$ and $-\beta_j^s < 0$ may be different for different nodes in Σ. In the specific case of a periodic trajectory c_j, we know that 0 is a characteristic exponent.

The Floquet exponents less than $-\beta_j^s$ are called *strong stable characteristic exponents* and the subspace generated by them will be called the *strong stable subspace* (we denote it by E^{ss}). Analogously, the Floquet exponents greater than β_j^u are called *strong unstable characteristic exponents* and the subspace generated by them will be called the *strong unstable subspace* (denoted by E^{uu}). The subspaces E^{ss} and E^{uu} are tangent (at each point of c_j) to the unique manifold containing all trajectories approaching exponentially to c_j in positive and negative times, respectively.

Besides the (n_s+1)-dimensional stable and (n_u+1)-dimensional unstable manifolds of a periodic trajectory c_j, there exists a local (non unique) center unstable manifold $W^{cu}_{loc}(c_j)$ tangent to the subspace $E^c_p \oplus E^{uu}_p$ (at each point p of c_j) and center stable manifold $W^{cs}_{loc}(c_j)$ tangent to the subspace $E^{ss}_p \oplus E^c_p$ (at each point p of c_j). The extension of these manifolds exists and it will be denoted by $W^{cu}(c_j)$ and $W^{cs}(c_j)$ and their dimension is $k + m_u$ and $k + m_s$, respectively. In general, these manifolds are not unique. The manifold $W^{cu}(c_j)$ contains all trajectories which stay near c_j in negative time. The dual property holds for $W^{cs}(c_j)$. It is clear that, for each j, $[c_j \to c_{j+1}] \subset W^{cu}(c_j) \cap W^{cs}(c_{j+1})$.

Along $W^{cu}(c_j)$, there exists a m_u-dimensional strong unstable foliation $\mathcal{F}^{uu}$ where the corresponding leaves of $\mathcal{F}^{uu}$ include $W^{uu}_{loc}(c_j)$ which are tangent to E^{uu}, at each point $p \in c_j$. Similarly, along $W^{cs}(c_j)$ there exists a m_s-dimensional strong stable foliation $\mathcal{F}^{ss}$ where the corresponding leaves include $W^{ss}_{loc}(c_j)$ which are tangent to E^{ss}_p. Here, we are considering both foliations at least C^1.

Now, we state a generic condition about the intersection of leaves through the heteroclinic connections. This condition avoids degenerated cases like the orbit flip, inclination flip, bellows and the homoclinic butterfly (see Homburg *et al* [**38**] for details).

Transversality Condition *At each point p of each heteroclinic connection $[c_j \to c_{j+1}]$:*

- *$W^{cu}(c_j)$ is transverse to a leaf of the strong stable foliation $\mathcal{F}^{ss}$ and*
- *$W^{cs}(c_{j+1})$ is transverse to a leaf of the strong unstable foliation $\mathcal{F}^{uu}$.*

The condition above only makes sense if $\mathcal{F}^{ss}$ corresponds to the strong stable foliation associated to c_{j+1} and $\mathcal{F}^{uu}$ corresponds to the strong unstable foliation associated to c_j. It is worth noting that although the manifolds $W^{cu}(c_j)$ and $W^{cs}(c_j)$ are not unique, the *Transversality Condition* is well defined since the tangent spaces are unique. Now, we state the *Center Manifold for Heteroclinic Cycles*, adapted to our case:

Theorem (Shilnikov *et al* [75]) *If a differential equation has a heteroclinic cycle* $\Sigma = \langle c_1, \ldots, c_k \rangle$ *such that the* trichotomy *and the* transversality *conditions hold, then in a small neighbourhood* V_Σ *of* Σ *there is a smooth* k_c*-dimensional flow-invariant manifold* $W^c(\Sigma)$ *which contains* Σ*, and which is tangent to the center unstable invariant subspace of* c_j *and to the center stable invariant subspace of* c_{j+1} *if and only if any leaf of* $W^{uu}_{loc}(c_j)$ *and* $W^{ss}_{loc}(c_{j+1})$ *intersects* Σ *at not more than one point. Moreover, all trajectories that stay in* V_Σ *for positive and negative times belong to the invariant manifold* $W^c(\Sigma)$*.*

The manifold $W^c(\Sigma)$ in the theorem above is called the *center manifold associated to* Σ. For our purposes, the important statement of the result is that we may restrict the flow to a flow-invariant manifold that contains Σ and has dimension smaller than the initial state space.

Note that in the case $k = 1$ (homoclinic cycle), the center manifold may be either difeomorphic to a cylinder or to a Moebius band (see Homburg and Sandstede [**38**]).

Article 3 – Persistent Switching near the Heteroclinic Model for the Geodynamo Problem

Submitted

Persistent Switching near the Heteroclinic Model for the Geodynamo Problem

Alexandre A. P. Rodrigues[1,2]
[1] Centro de Matemática da Universidade do Porto
Rua do Campo Alegre, 687, 4169-007 Porto, Portugal
[2] Faculdade de Ciências, Universidade do Porto
Rua do Campo Alegre, 687, 4169-007 Porto, Portugal,
Phone (+351) 220 402 248; Fax (+351) 220 402 209
alexandre.rodrigues@fc.up.pt

Abstract

Modelling chaotic and intermittent behaviour, namely the excursions and reversals of geomagnetic field, is a big problem far from being solved. Some scientists believe that structurally stable heteroclinic networks associated to invariant saddles are the mathematical object responsible for the aperiodic reversals. In this paper, invoking the notion of switching near a network of rotating nodes, we present analytical evidences that the mathematical model given by Melbourne, Proctor and Rucklidge [23] is relevant for the study of reversals. We also present numerical plots of solutions of the model, all of them consistent with the behaviour of the geomagnetic field documented by several paleomagnetic studies.

1 Introduction

Roughly speaking, the history of the geomagnetic field can be described as a strong axial dipole (see Figure 1(a)). However, several paleomagnetic studies show that the Earth's magnetic field flips from time to time, with the poles reversing sign. Altough it is known that the mean time between geo-reversals in the past is about 2×10^5 years as documented in Stefani *et al* [31], we cannot predict their occurrence as they have not happened at defined intervals of times. In spite of the ongoing discussion about this issue, several physicists believe in the existence of an internal cause which is responsible for the dynamical behaviour for the geomagnetic field.

The geodynamo model (constructed in the context of magnetohydrodynamics equations) is the only plausible model describing the mechanism by which the Earth generates and maintains a magnetic field, under the action of the velocity field. This velocity is due to the twisting fluid motions within the Earth's core. The geodynamo model has been known for a long time but it still constitutes a difficult problem far from being solved.

Following Krupa [17], aperiodic reversals of the geomagnetic field may be generated by models whose flows involve the existence of heteroclinic cycles and networks between invariant saddles, see also the paper of Chossat and Armbruster [5].

Armbruster *et al* [4] proposed a dynamo model considering convection in a spherical shell without rotation where symmetric heteroclinic cycles appear in the associated flow. Later, in 2003, Chossat and Armbruster [5] gave a rigorous proof of the existence of structurally stable heteroclinic cycles involving dipolar magnetic fields generated by convection in a spherical shell for a non-rotating sphere. Their results have been confirmed numerically. More recently, in Podvigina [24], reversals may be seen as a interaction of two distinct attractors, apparently

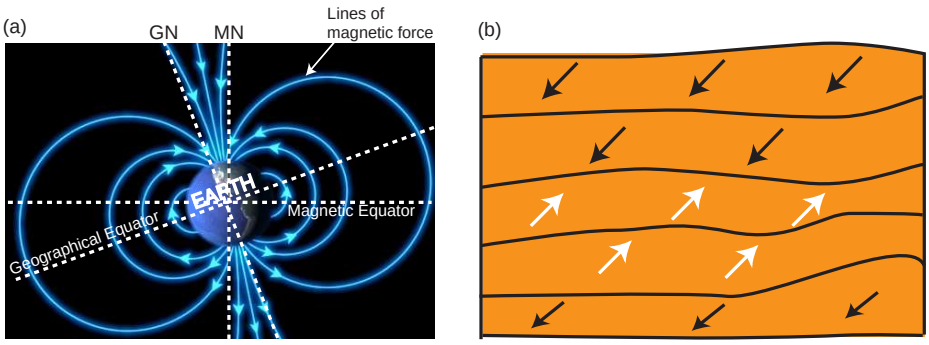

Figure 1: (a): Scheme of the Earth's magnetic field, approximated as a magnetic axial dipole. Note that the locus of points with the same intensity of magnetic field is a closed curve; MN - Magnetic North; GN - Geographical North; (b): Scheme of the lave flow layers; the magnetic alignment preserved after cooling records reversion of the geomagnetic field. Each layer maintains the original magnetic field at its time of cooling. Scientists claimed that the poles have shifted throughout the history.

via heteroclinic connections due to the intersection of stable and unstable manifolds of periodic orbits. The interactions depend on the Reynolds number.

In 2001, Melbourne, Proctor and Rucklidge [23] suggested a model involving a heteroclinic cycle in which the associated geometry resembled the Earth's magnetic field reversals. Using the induction equation and supposing that the flow sustaining the dynamo was equivariant under the continuous Lie group whose action is isomorphic to $\mathbf{SO}(2) \oplus \mathbf{Z}_2 \oplus \mathbf{Z}_2$, they wrote the magnetic field as the coupling of dynamically quadrupolar and dipolar symmetric models (see Gubbins *et al* [10] for details about the symmetric modes). The amplitude of these modes (y_1, y_2, x_3, x_4) can be seen as coordinates of a continuous dynamical system whose flow contains an asymptotically stable heteroclinic network associated to two pairs of saddle-foci and a non trivial closed trajectory with real Floquet multipliers, embedded in a four dimensional spherical shell.

Due to the symmetry, trajectories whose initial condition lies outside the invariant subspaces will approach one of the cycles in the heteroclinic network. The fixed point subspaces work as a barrier and the time spent near consecutive saddles increases geometrically with each visit. The regime of geo-reversals is one of the reasons why the constructed model was unsatisfactory. This fact led the authors in [23] to consider breaking all the symmetries of the velocity field to kick the system away from the invariant saddles and to generate random reversals with a finite mean period.

In the symmetry breaking context, Kirk and Rucklidge [15] analised a type of codimension three bifurcation and concluded that when all the symmetries are broken, the heteroclinic network is destroyed and orbits may switch, *ie*, they may make traversals near more than one of the original cycles, giving a satisfactory model for the numerical evidences of intermittency of the geomagnetic field. This is what the authors call *switching* (note that in their case, the heteroclinic network is broken).

Recently, Aguiar *et al* [3] defined and proved a strong form of *switching* near generic heteroclinic networks of rotating nodes charaterized by the following two properties:

- the invariant saddles of the network are either periodic solutions or saddle foci;

- all connections that take place in 2-dimensional invariant manifolds occur as transverse intersections.

Roughly speaking, switching is characterized by the following property: close to the heteroclinic network there are trajectories that visit neighbourhoods of the saddles following any prescribed admissible set of heteroclinic connections of the network (heteroclinic path). If the set of connections to be followed is finite, we say that the network has finite switching; if it is infinite, we say that the network has persistent switching. More recently, Homburg and Knobloch [14] gave an equivalent definition of forward switching for a heteroclinic network, using the notion of connectivity matrix (which characterizes the admissible sequences) and symbolic dynamics. Basically, the proof of switching is achieved by showing in a section transverse to the flow, the existence of initial conditions of trajectories which visit neighbourhoods of any admissible sequence of nodes of the network. While in [15] it is not evident that switching is not a transient phenomenon, in [3] it is proved that this behaviour is persistent (*ie*, switching holds for any infinite sequence of heteroclinic paths).

The perturbed dynamo model presented in [23] has an invariant plane whose invariance is not broken and it has not been studied rigorously yet. In particular, the considered perturbation does not break the heteroclinic network. The retention of this flow-invariant set has some effects on the switching properties. This is the interesting bridge between the work in [3] and that of [23].

There are several examples in which some authors doing numerics, deduce general properties of networks, namely its stability. However, in some packages of numerical simulations, a trajectory tending to a robust heteroclinic cycle will continue to approach the cycle until the numerical error is greater than the distance between the solution and the invariant subspace. Then, the program assumes that the solutions has been captured. In particular, Postlehwaite [25] found open sets of trajectories approaching a cycle during an extended period of time, before moving to another cycle. This stresses that doing numerics is different from doing an analytical proof. The present paper confirms the suggested behaviour from the simulations in [23]; more precisely we show analytically that the switching behaviour is not only a transient phenomenon.

The main goal of this paper is to enframe the model of Melbourne, Proctor and Rucklidge [23] and its numerics, in the context of Aguiar *et al* [1, 2, 3], and Rodrigues *et al* [27], to conclude analytically that all the properties for infinite switching hold. We show that the amplitude equations of the model in [23] has a heteroclinic network associated to a periodic solution and four equilibria, embedded in an flow-invariant 3-dimensional manifold. Near the heteroclinic network of the perturbed flow, there are trajectories making excursions around the whole network in an irregular way. Besides the interest of this system from the physical point of view, since it is closely related to the magnetohidrodynamic problem (see for instance Podvigina [24]), it is important as an example once it describes very interesting dynamics for a vector field which unfolds from a fully symmetric differential equation.

Framework of the paper

This paper is organized as follows. Section 2 sets up the construction of the heteroclinic model given by Melbourne *et al* [23] as a convection dynamo problem. Using the equivariance of the system under a Lie group Θ, section 3 gives an analytical description of the associated Θ-equivariant Birkhoff normal form of degree 3 and we discuss the geometry of the flow of the corresponding lift. Section 4 contains a proof of switching near the networks which appears near the perturbation of the system constructed in section 3. This phenomenon enables the occurrence of intermittency. Section 5 is a short explanation of the physics underlying the system, in the context of geo-reversals. After the analysis of time series and plots associated to

the model, we include in section 6 a discussion and a conclusion about the results.

2 Construction and Description of the Model

The system in Melbourne *et al* [23] models the evolution of a magnetic field B in the pre-relativistic setting, through the equation (2.1), obtained combining Maxwell's equations and Ohm's Law, and the equation (2.2). The later means that B is a *preserving volume* vector field. Here $R_m = \frac{K}{\eta}$ is the dimensionless magnetic Reynolds number, η gives the magnetic diffusivity and K is a positive real number.

$$\frac{\partial B}{\partial t} = R_m \nabla \times (v \times B) + \nabla^2 B \tag{2.1}$$

$$divB = 0. \tag{2.2}$$

Since (2.1) is linear in B, it is known that solutions of (2.1) with different symmetries are independent (see Gubbins [10]). Based on the idea of McFadden *et al* [21], who proposed that reversals involve an interaction between dipolar and quadrupolar modes, Melbourne *et al* [23] assumed that solutions of (2.1) may be written as a linear combination of the symmetric modes D_e, Q_a, D_a and Q_e (notation of Holme [13]), where:

- D_a is a dipolar solution of (2.1) antisymmetric with respect to the equatorial plane and symmetric with respect to rotations by angle π around the polar axis;
- Q_a is a quadrupolar solution of (2.1) symmetric with respect to the equatorial plane and symmetric with respect to rotations by angle π around the polar axis;
- D_e is a dipolar solution of (2.1) symmetric with respect to the equatorial plane and antisymmetric with respect to rotations by angle π around the polar axis;
- Q_e is a quadrupolar solution of (2.1) antisymmetric with respect to the equatorial plane and antisymmetric with respect to rotations by angle π around the polar axis.

Since equatorial quadrupole solutions Q_e have not been found (see Gubbins [10]), we may write the magnetic field $B(r,t)$, in real coordinates, as follows:

$$B(r,t) = y_1(t)D_e^1(r) + y_2(t)D_e^2(r) + x_2(t)Q_a(r) + x_3(t)D_a(r), \tag{2.3}$$

where $r = (||(y_1, y_2)||, x_2, x_3)$ and $D_e = (D_e^1, D_e^2)$ is an oscillatory mode. Note that the symmetric modes may be seen as vector fields in $\mathbf{R}^3$ where r is a general position in the phase space. We are interested in the geometry of (y_1, y_2, x_2, x_3), the coefficients of the symmetric modes (hereafter called the *amplitude* of the symmetric modes).

3 Truncated Birkhoff Normal Form of Degree 3

We concentrate our attention in the dynamics of the amplitude equations of $B(r,t)$. The model constructed in [23] has the particularity that the velocity of the flow which generates the dynamo action is equivariant under the action of compact Lie group $\Gamma = \mathbf{SO}(2) \oplus \mathbf{Z}_2 \oplus \mathbf{Z}_2$. Previous models, for instance that of Chossat *et al* [6] and Chossat *et al* [7], have been constructed in the context of the spherical Bénard problem, using $\mathbf{O}(3)$ and $\mathbf{SO}(3)$-equivariance. In these models,

the Earth's rotation speed is omitted because it is much less than the velocity of the convection inside the core. In [23], the authors do not assume this restriction. This is why they used the $\mathbf{SO}(2)$-symmetry instead of $\mathbf{SO}(3)$.

In $\mathbf{R}^4$, assuming the usual representation of $\mathbf{SO}(2)$ in the first two coordinates and the usual representation of $\mathbf{Z}_2 \oplus \mathbf{Z}_2$ generated by ζ:

$$\zeta(y_1, y_2, x_2, x_3) = (y_1, y_2, -x_2, -x_3),$$

the truncated Birkhoff normal form of degree 3 in real coordinates, acting as organizing center, is given by:

$$\begin{cases} \dot{y}_1 = y_1(\mu_1 - (y_1^2 + y_2^2) + A_{12}x_2^2 + A_{13}x_3^2) - \omega_1 y_2 \\ \dot{y}_2 = y_2(\mu_1 - (y_1^2 + y_2^2) + A_{12}x_2^2 + A_{13}x_3^2) + \omega_1 y_1 \\ \dot{x}_2 = x_2(\mu_2 + A_{21}(y_1^2 + y_2^2) - x_2^2 + A_{23}x_3^2) \\ \dot{x}_3 = x_3(\mu_3 + A_{31}(y_1^2 + y_2^2) + A_{32}x_2^2 - x_3^2). \end{cases} \tag{3.4}$$

The procedure of reduction to the normal form is rather straightforward involving step by step elimination of the non resonant terms. Following Aguiar *et al* [2] and Rodrigues *et al* [27], the vector field associated to system (3.4) can be seen as the *lifting by rotation* with respect to the pair (x_1, ω_1) of the vector field X_3 where

$$X_3(x_1, x_2, x_3) = \begin{pmatrix} x_1(\mu_1 - x_1^2 + A_{12}x_2^2 + A_{13}x_3^2), \\ x_2(\mu_2 + A_{21}x_1^2 - x_2^2 + A_{23}x_3^2), \\ x_3(\mu_3 + A_{31}x_1^2 + A_{32}x_2^2 - x_3^2) \end{pmatrix}. \tag{3.5}$$

Passing from (3.4) to (3.5) can be understood as a standard technique of phase-amplitude equations: (3.5) corresponds to the amplitude equations. We refer the technique *lifting by rotation* presented in the papers of Aguiar *et al* [2] and Rodrigues *et al* [27], once their results about lifted vector fields will be relevant for our further conclusions.

If follows from straightforward computations that the vector field X_3 is equivariant under the action of the compact Lie group $\Theta = \langle \gamma_1, \gamma_2, \gamma_3 \rangle$ where

$$\gamma_1(x_1, x_2, x_3) = (-x_1, x_2, x_3), \quad \gamma_2(x_1, x_2, x_3) = (x_1, -x_2, x_3) \quad \text{and} \quad \gamma_3(x_1, x_2, x_3) = (x_1, x_2, -x_3),$$

whose action is isomorphic to the usual action of $\mathbf{Z}_2 \oplus \mathbf{Z}_2 \oplus \mathbf{Z}_2$ in $\mathbf{R}^3$. This implies that the coordinate planes and axes are flow invariant; they correspond to $Fix\mathbf{Z}_2(\gamma_i)$ and $Fix(\mathbf{Z}_2(\gamma_i) \oplus \mathbf{Z}_2(\gamma_j))$, respectively $(i \neq j \in \{1, 2, 3\})$.

For $\mu_1, \mu_2, \mu_3 \in \mathbf{R}^+$ and $A_{ij} \in \mathbf{R}^-$, $i \neq j \in \{1, 2, 3\}$, making some computations, we can conclude about the existence of a unique 2-dimensional attracting and flow-invariant ellipsoid $\mathcal{S}^2$ centered at the origin, embedded as a topological manifold in $\mathbf{R}^3$. Here, the term *attracting* means that every solution with nonzero initial condition is asymptotic to the ellipsoid in forward time.

With respect to the dynamics of $\dot{X} = X_3(X)$, $X \in \mathbf{R}^3$, since $\lambda_1, \lambda_2, \lambda_3 > 0$ are the eigenvalues of DX_3 at the origin O, it follows that this equilibrium point is repelling. The intersection of $\mathcal{S}^2$ with the coordinate axes $\mathcal{O}x_i$ $(i = 1, 2, 3)$ corresponds to the set of six equilibria of saddle type $\mathcal{A} = \{\pm P_1, \pm P_2, \pm P_3\}$ (here resonances are omitted).

Assuming that:

$$\mu_1 + A_{13}\mu_3 > 0, \quad \mu_2 + A_{21}\mu_1 > 0 \quad \text{and} \quad \mu_3 + A_{32}\mu_2 > 0$$

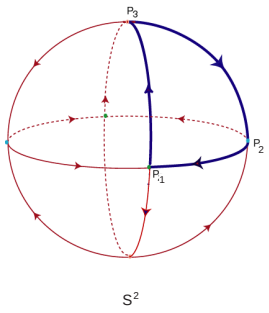

Figure 2: The network Σ_2 can be seen as the union of eight heteroclinic cycles (related by symmetry), each one lying in the boundary of the intersection between $\mathcal{S}^2$ and each octant. The network Σ_2 is the Θ-orbit of the cycle depicted on the first octant.

and

$$\mu_1 + A_{12}\mu_2 < 0, \quad \mu_2 + A_{23}\mu_3 < 0 \quad \text{and} \quad \mu_3 + A_{31}\mu_1 < 0,$$

then, associated to the set $\mathcal{A}$, there exists a heteroclinic network Σ_2. This network is the union of eight heteroclinic cycles (related by the symmetry group Θ), each one lying in the boundary of the intersection between $\mathcal{S}^2$ and each octant (see figure 2).

Moreover, we are considering that the product of the absolute value of the contracting eigenvalues at the equilibria is greater that the product of the expanding eigenvalues. This implies that the heteroclinic network is asymptotically stable - there exists an open neighbourhood V of the network such that every trajectory starting in V is forward asymptotic to the network (see Krupa and Melbourne [18] and Dos Reis [26]).

In the restriction to the first octant of the attracting sphere $\mathcal{S}^2$, the invariant manifolds of the saddles are given by:

1. $W^s(+P_1) = \mathcal{S}^2 \cap \{(x_1, x_2, x_3) \in (\mathbf{R}^+)^3 : x_3 = 0 \wedge x_1 > 0\}$;
2. $W^s(+P_2) = \mathcal{S}^2 \cap \{(x_1, x_2, x_3) \in (\mathbf{R}^+)^3 : x_1 = 0 \wedge x_3 > 0\}$;
3. $W^s(+P_3) = \mathcal{S}^2 \cap \{(x_1, x_2, x_3) \in (\mathbf{R}^+)^3 : x_2 = 0 \wedge x_2 > 0\}$.

This network is very similar to that of Dos Reis [26], who observed that it is possible to have robust cycles of non-transverse saddle-connections for a $\mathbf{Z}_2^3$-equivariant vector field. This kind of networks has also been considered by Guckenheimer and Holmes [11].

Due to the $\mathbf{Z}_2(\gamma_1)$-equivariance, the vector field X_3 is lifted by the rotation associated to the pair (x_1, ω_1), to the $\mathbf{SO(2)} \oplus \mathbf{Z}_2 \oplus \mathbf{Z}_2$-equivariant vector field $\dot{X} = X_4(X)$ where X_4 is the vector field defined in (3.4).

Using the notation of Rodrigues *et al* [27] and according to the proposition 15 of [27], the asymptotically stable heteroclinic network $\Sigma_2 \subset \mathcal{S}^2$ gives rise to an asymptotically stable heteroclinic network $\Sigma_3 \subset \mathcal{S}^3$, associated to a relative equilibrium c, with $c = \mathcal{L}(\pm P_1)$, with real Floquet multipliers and the set of four equilibria $\mathcal{B} = \{i_3(\pm P_2), i_3(\pm P_3)\}$ (two by two $\mathbf{Z}_2$-symmetric). The Floquet multipliers are precisely the eigenvalues whose eigendirections are transverse to the rotation. Here, it is important to note that c lies in the plane $Fix(\mathbf{Z}_2 \oplus \mathbf{Z}_2)$ defined by $x_2 = x_3 = 0$ and that the one-dimensional heteroclinic connections from $i_3(\pm P_2)$ to $i_3(\pm P_3)$ lie in the plane $Fix(\mathbf{SO(2)})$ defined by the equations $y_1 = y_2 = 0$ (see figure 3).

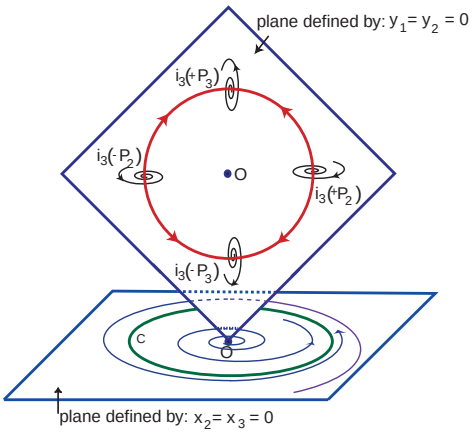

Figure 3: Representation of the two planes $Fix(\mathbf{SO(2)})$ (horizontal) and $Fix(\mathbf{Z}_2 \oplus \mathbf{Z}_2)$ (vertical), in which the invariant saddles associated to Σ_3 lie. In $Fix(\mathbf{SO(2)})$, the non trivial closed trajectory c is a sink; in $Fix(\mathbf{Z}_2 \oplus \mathbf{Z}_2)$, we observe the non robust heteroclinic connections of the network which do not involve c. Note that $\mathbf{R}^4 = Fix(\mathbf{SO(2)}) \oplus Fix(\mathbf{Z}_2 \oplus \mathbf{Z}_2)$.

Any one-dimensional heteroclinic connection lying inside $Fix(\mathbf{Z}_2(\gamma_1))$ lifts to a one-dimensional heteroclinic connection and the other become two-dimensional. To be more precise, in the restriction to $\mathcal{S}^3 \subset \mathbf{R}^4$, each heteroclinic connection involving c has dimension 2 and the others have dimension 1. All the intersections between invariant manifolds of consecutive nodes are very special: the manifolds coincide.

In the case of [23], all heteroclinic connections involving the periodic solution are two dimensional and the others involving the saddle-foci are one dimensional. After the lift by rotation, the map DX_4, at an equilibrium $i_3(\pm P_i)$ $i = 2, 3$, has four eigenvalues. The eigenvalue of $DX_3(P_i)$ whose associated eigenvector has the same direction as the rotation gives rise to two complex non-real eigenvalues: the real part is equal to that of the original linearization at each equilibrium and the imaginary part is equal to the speed of rotation ($\omega_1 \neq 0$); the other eigenvalues and the corresponding eigendirection (transverse to the lift) remain. This is a general property for the eigenvalues about the equilibria for liftings of vector fields.

The heteroclinic network Σ_3 can be decomposed into four cycles. Due to the symmetry, trajectories whose initial condition starts outside the invariant subspaces will approach in positive time one of the cycles. As we have already mentioned, the hyperplanes of equations $x_2 = 0$ and $x_3 = 0$ prevent switching and the time spent near either each equilibrium or the periodic solution increases geometrically. The limit of the ratio between consecutive times of flight inside the neighbourhoods of the saddles is related to the ratio between the real part of the eigenvalues at the corresponding saddles.

4 Analysis of the Perturbed Vector Field in $\mathbf{R}^4$

As it stands, the model given in the above section is rather unrealistic because it does not explain the reversals of the geomagnetic field. This is why it was necessary to break the equivariance of the velocity field in a way to preserve the network, allowing random itineraries around it. The perturbation may be explained by the fact that the Earth does not have exact rotational and reflectional symmetries (due to the inhomogeneities of the convection of the fluid motions inside

the Earth's core). Melbourne *et al* [23] considered the following system perturbation of X_4:

$$\begin{cases} \dot{y}_1 = y_1(\mu_1 - (y_1^2+y_2^2) + A_{12}x_2^2 + A_{13}x_3^2) - \omega_1 y_2 + \\ \quad +\varepsilon_1 y_1(y_1^4 - 10y_1^2y_2^2 + 5y_2^4) + \varepsilon_2 x_2(y_1^4 + 2y_1^2y_2^2 + y_2^4) + \varepsilon_3 y_1 x_2 x_3^3 \\ \dot{y}_2 = y_2(\mu_1 - (y_1^2+y_2^2) + A_{12}x_2^2 + A_{13}x_3^2) + \omega_1 y_1 + \\ \quad +\varepsilon_1 y_1(-5y_1^4 + 10y_1^2y_2^2 - y_2^4) + \varepsilon_3 y_2 x_2 x_3^3 \\ \dot{x}_2 = x_2(\mu_2 + A_{21}(y_1^2+y_2^2) - x_2^2 + A_{23}x_3^2) \\ \quad +\varepsilon_1 y_1(y_1^2 - 3y_2^2)x_2^2 + \varepsilon_2 y_1^5 + \varepsilon_3 x_3^5 \\ \dot{x}_3 = x_3(\mu_3 + A_{31}(y_1^2+y_2^2) + A_{32}x_2^2 - x_3^2) \\ \quad +\varepsilon_1 y_1(3y_1^2 - y_2^2)x_2 x_3 + \varepsilon_2 y_1^3 x_2 x_3 + \varepsilon_3 x_2^5 \end{cases} \tag{4.6}$$

Observe that the vector field associated to (4.6) is equivariant under the action of $-Id$, the antipodal symmetry. Since the nodes of Σ_3 are hyperbolic, they persist under small perturbations. In this section, we denote by X^ε the hyperbolic continuation of the invariant saddle X under the perturbation $\varepsilon = (\varepsilon_1, \varepsilon_2, \varepsilon_3)$. Due to the fact that the perturbation terms are not tangent to $\mathcal{S}^3$, instead of an invariant three-dimensional sphere, we can only assure that the flow has an invariant spherical shell $\mathcal{S}^3_\varepsilon$. The perturbation is done in such a way that the plane defined by the equations $y_1 = y_2 = 0$ is not broken. This means that the non-robust heteroclinic connections lying in $Fix(\mathbf{SO(2)})$ from $i_3(\pm P_2)^\varepsilon$ to $i_3(\pm P_3)^\varepsilon$ persist. This is the main difference between the present analysis and the findings of Kirk and Rucklidge [15]. In their paper, the perturbation that breaks the rotational and the reflectional equivariance does not preserve the one-dimensional connections in the heteroclinic network.

Since $i_3(\pm P_2)^\varepsilon$ and c^ε are hyperbolic, $\dim W^u(i_3(\pm P_2)^\varepsilon) = 2$ and $\dim W^s(c^\varepsilon) = 3$, then for a non-empty open set of parameters $(\varepsilon_1, \varepsilon_2, \varepsilon_3)$, the invariant manifolds meet transversely and their intersection consists of a finite number of trajectories. The same holds for the other intersections involving the saddle c^ε. Hence, generically the perturbation considered by Melbourne *et al* [23] does not destroy the heteroclinic network, which we denote by Σ_3^ε.

Using the center manifold theorem for heteroclinic cycles studied by Shaskov *et al* [29], in the context of homoclinic loops, and by Shilnikov *et al* [30], provided that the radial eigenvalue is the most contractive at all saddles, generically it is possible to reduce the interesting dynamical behaviour to a three-dimensional manifold $\mathcal{M}^3$ containing the network Σ_3^ε. More precisely, we require that:

$$-2\mu_1 < \mu_1 + A_{12}\mu_2 < 0, \quad -2\mu_2 < \mu_2 + A_{23}\mu_3 < 0 \quad \text{and} \quad -2\mu_3 < \mu_3 + A_{31}\mu_1 < 0$$

to assure the trichotomy condition (meaning that the radial component must correspond to the strong stable manifold).

Restricted to the center manifold $\mathcal{M}^3$, the heteroclinic network Σ_3^ε is of the type studied by Aguiar *et al* [3]. More precisely, the invariant saddles of the network are either periodic solutions with non zero real Floquet exponents and hyperbolic saddle-foci, and all connections that take place in 2-dimensional invariant manifolds occur as tranverse intersections. Thus, it satisfies all the hypothesis of [3] and we have:

Theorem 1 *Near $\Sigma_3^\varepsilon \cap \mathcal{M}^3$, there exists:*

(a) *a set of initial conditions with positive Lebesgue measure (on a section transverse to the network) exhibiting finite switching of any order;*

(b) infinite switching *which may be realized by infinitely many initial conditions.*

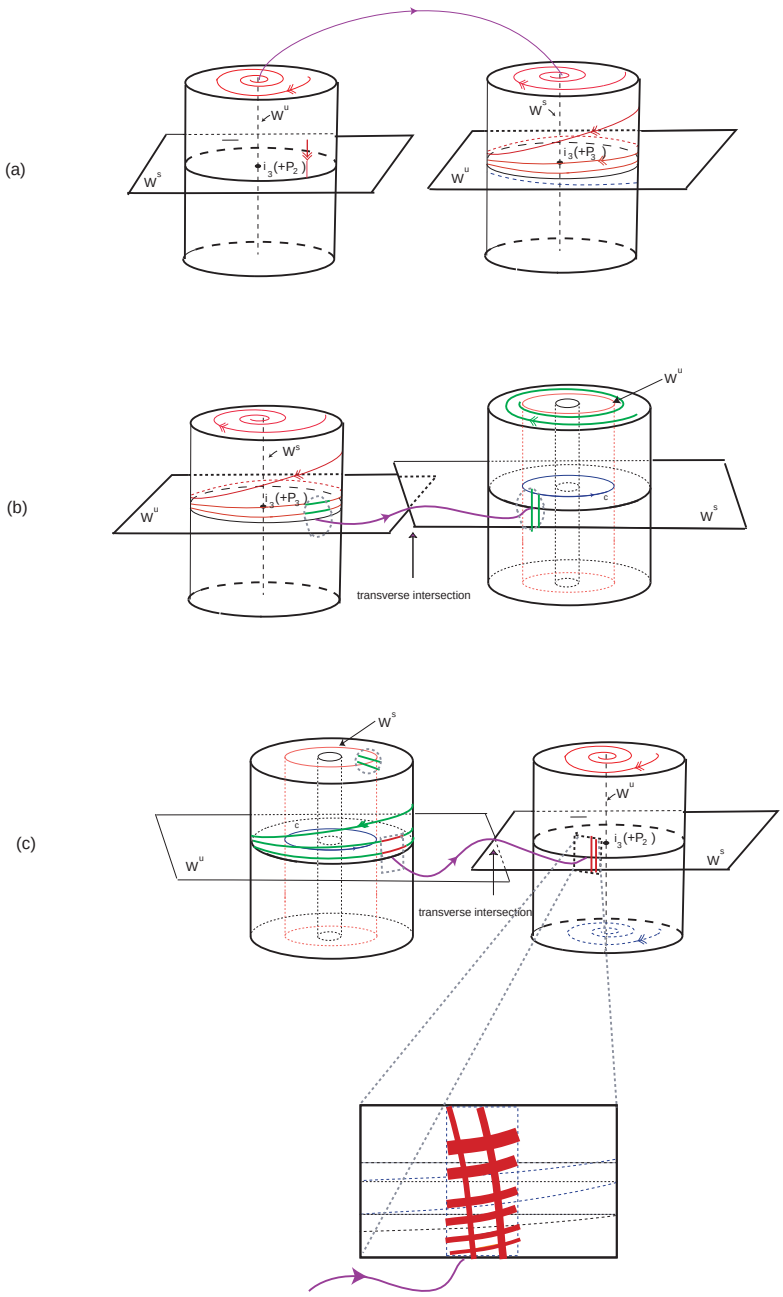

Figure 4: Cylindrical neighbourhoods around the rotating nodes of the network. (a): a segment of initial conditions lying across the stable manifold of $i_3(\pm P_2)$ is mapped, by the local map near $i_3(\pm P_2)$, into a spiral accumulating on its unstable manifold and thus on the stable manifold of $i_3(\pm P_3)$; (b): a spiral of initial conditions on the top of the neighbourhood of $i_3(\pm P_3)$ is mapped, by the local map, into a helix accumulating on the unstable manifold of $i_3(\pm P_3)$, which crosses transversely the stable manifold of c infinitely many times; (c): a segment of initial conditions lying across the stable manifold of c is mapped into a spiral accumulating on its unstable manifold. Each piece of spiral is a new segment across the stable manifold of $i_3(\pm P_2)$. In (c), it is also possible to observe the first step of the construction of the Cantor set on the wall of the cylinder.

Proof: We adapt the proof of Aguiar *et al* [1] and Aguiar *et al* [3] to our purposes. We suggest that the reader follows the proof observing figure 4.

(a) Since the vector field is smooth, using Samovol [28], the vector field may be linearised around each equilibrium point, up to a set of measure zero (resonances). Hence it is possible to obtain cylindrical neighbourhoods near each invariant saddle (hollow cylinder in the case of the non trivial closed trajectory). The boundary of each cylindrical neighbourhood forms an *isolating block*: the flow is transverse to the cylinder walls, top and bottom. We study the discrete time dinamics obtained by looking at points on the isolating block.

The initial conditions which shadow a given finite heteroclinic path are obtained by a recursive construction.

Near the saddle-foci $i_3(\pm P_2)$, the flow goes in, at the cylinder walls, and it goes out at the top and bottom. Near $i_3(\pm P_3)$, the flow goes in, at the cylinder top and bottom and it goes out at the wall. Inside the cylinder the vector field is linear, so the transition from the wall to top/bottom and top/bottom to the wall is well understood. The transition map from one isolating block to the next is, to first order, either a linear map or a rotation. The study of the local map near rotating nodes is given in sections 5 and 6 of Aguiar *et al* [3].

Any segment of initial conditions lying across the stable manifold of $i_3(\pm P_2)$ is wrapped around the isolating block. By λ-lemma it accumulates as a spiral on the unstable manifold of $i_3(\pm P_2)$ and then on the stable manifold of the next saddle, $i_3(\pm P_3)$ (see figure 4(a)).

This spiral of initial conditions on the top/bottom of the neighbourhood around $i_3(\pm P_3)$ is mapped, by the local map near $i_3(\pm P_3)$, into points lying on a helix accumulating on its unstable manifold, which crosses transversely the stable manifold of c infinitely many times (see figure 4(b)).

This is an important point in which the equilibria must be saddle-foci. The complex eigenvalues force the spreading of solutions around all the unstable manifold of $i_3(\pm P_3)$, allowing visits to all possible connections starting at $i_3(\pm P_3)$ (see figure 5 (a)). The transversality enables the existence of solutions that follow heteroclinic connections on the two different connect components of $\mathcal{M}^3 \backslash W^s(c)$, the upper and the lower part on the wall of the hollow cylinder (see figure 5 (b)).

Any curve of initial conditions lying across the stable manifold of c winds around the isolating block and accumulates, as a spiral, on its unstable manifold following all the possible heteroclinic connections starting at c. Any heteoroclinic connection is followed by a piece of spiral and it is mapped, under the transition map, into a new segment across the stable manifold of $i_3(\pm P_2)$ (see figure 4(c)), giving rise to a new segment across the stable manifold of $i_3(\pm P_3)$.

The composition of consecutive local and transition functions, maps the original segment of initial conditions lying across the stable manifold of $i_3(\pm P_2)$ into infinitely many segments with the same property. Thus, it is possible to construct recursively a nested sequence of intervals accumulating on the stable manifold of $i_3(\pm P_2)$ that follow sequences of heteroclinic connections and thus which exhibit finite switching.

Allowing some thickness on the segments, instead of a nested sequence of intervals, we construct a nested sequence of rectangles (with positive Lebesgue measure [1]) of initial conditions which shadow a given finite heteroclinic path.

[1] The heteroclinic network is embedded in $\mathbf{R}^4$.

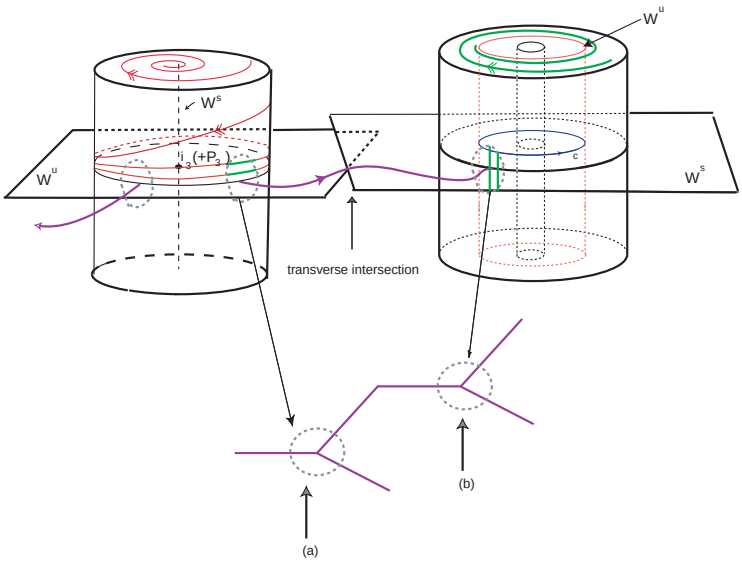

Figure 5: The mechanism for switching is related with the existence of a pair of complex eigenvalues in the linearisation of the vector field at a node and the transversal intersections of invariant manifolds. (a): Switching at the saddle-focus because of the spreading originated by the complex non real eigenvalues; (b): switching at the closed trajectory because of the transversality; here we find solutions following each connected component of $\mathcal{M}^3 \backslash W^s(c)$.

(b) The existence of infinite switching follows from the fact that the infinite intersection of a nested sequence of compact sets is non-empty. In particular, for each sequence of nested compacts, there is at least a point realizing any given infinite heteroclinic path.

□

The two main ingredients of the previous proof are the transversality and the existence of rotating nodes which forces the spreading of solutions along the unstable manifolds of the node and then along the stable manifold of the next node (see figure 5).

Remark 1 *A heteroclinic path on the network can be realized by trajectories in $W^u(c)$ since the local unstable manifold of c meets the wall of $i_3(\pm P_2)$ at a segment by transversality. In particular, there are infinitely many transverse* homoclinic connections *associated to c.*

The existence of switching near $\Sigma_3^\varepsilon \cap \mathcal{M}^3$ implies that trajectories will make repeated passes near the whole network, which may be seen as a consequence of the hyperbolic suspensed horseshoe meeting each cross section in a Cantor set, with the same shape as the whole network (the *first iteration* of the Cantor set is depicted in figure 4(c)). The sequence of heights associated to a sequence of rectangles accumulating on the network is decreasing. For details, please see Aguiar *et al* [1] and Aguiar *et al* [3].

Next result is the core of this paper: it says that the intermittency of the flow associated to perturbation referred in Melbourne *et al* [23] is closely linked with the reversals.

Corollary 2 *The geomagnetic field B changes its polarity.*

Proof: From Theorem 1 we can conclude the existence of persistent switching near Σ_3^ε, *ie* close the network, there are trajectories that visit the neighbourhoods of the saddles following all the heteroclinic connections of the network in any given order. These trajectories correspond to the evolution of the amplitude equations of (2.3). In particular, since the coefficient of the axial dipole, x_3, changes its sign then the vector field B changes its polarity. □

Theorem 1(b) also says that switching is realized by infinitely many initial conditions. The difference of the dynamics between two of these initial conditions is related with the number of revolutions inside each fixed neighbourhood with respect to a Poincaré section. The arguments of Rodrigues *et al* [27] used for non trivial periodic solutions can be slightly adapted for our case and thus we may conclude the existence of a transitive set of initial conditions with the same shape as Σ_3^ε, whose trajectories follow the network forwards and backwards and that is conjugate to a Markov shift over a finite alphabet. This set lies arbitrarily close the heteroclinic network Σ_3^ε.

A more rigorous analysis has revealed other interesting chaotic behaviour near the heteroclinic network such as infinitely many homoclinic classes associated to the relative equilibrium c^ε, suspended hyperbolic horseshoes with positive topological entropy, strange and wild attractors (Labouriau and Rodrigues [19]).

Remark 2 *The noise $(\varepsilon_1, \varepsilon_2, \varepsilon_3)$ in (4.6) is responsible for driving the dynamics far from the equilibria; nevertheless its magnitude is irrelevant for the existence of intermittency. The different parameters ε_i control the* degree *to which the symmetries (one rotational and two reflectional) are broken. The three different symmetry-breaking terms are required for the existence of switching.*

5 Switching in the context of the Geodynamo Problem and Other Consequences

The existence of switching near a general heteroclinic network implies that infinite pseudo-orbits with infinitely many discontinuities may be shadowed. In the context of this problem, switching near Σ_3^ε proved in theorem 1 implies that there are aperiodic itineraries past the various cycles in the network. Therefore the amplitude coefficients may assume any value in the center manifold $\mathcal{M}^3$ (and more importantly any sign), implying that the magnetic field B may change orientation. Theorem 1 implies that the considered model explains the irregular (in fact, chaotic) occurrence of reversals of the Earth's magnetic field (their occurrence has a non-uniform distribution). A close analysis of the equation (2.3) confirms that the occurrence of reversals requires cooperative interactions between the symmetric modes.

A magnetic reversal is generally of short duration compared with the intervals of time between reversals, during which the field remains in either the actual or the reversed polarity state. This is due to the transition between the dipole moments, which is much faster than the time trajectories spend near the nodes. This fact is consistent with other equations modelling the reversals (see for instance Kono [16] or Podvigina [24]).

Due to the chaotic behaviour induced by the presence of suspended horseshoes near the network, we may conclude that there is no satisfactory way to predict the duration of any given polarity. Beyond the existence of geomagnetic reversals, our analysis explains the intermittent behaviour between the symmetric modes and then the existence of excursions (changing of symmetric modes without changing the orientation of the magnetic field).

With our analysis, why are able to understand why the history of the geomagnetic field can be described as a strong axial dipole. This is due essentially to the fact that the contracting eigenvalue at the equilibria $i_3(\pm P_2)$ (amplitude of the axial quadripole) is much greater than the expanding eigenvalue at the equilibria $i_3(\pm P_3)$ (amplitude of the axial dipole). This relation remains under the perturbation.

According to the model presented in Melbourne *et al* [23], there is an implicit order between the symmetric modes during reversals. During the process of georeversals, equation (2.3) and time series analysis suggest that the geomagnetic field *visits* the equatorial dipole and the axial quadrupole and, at the end of the reversal, each pair of poles joins into a single pair near the opposite geographical pole. We also emphasize the pronounced asymmetry of the geomagnetic field during the reversals and the excursions. The strength of the geomagnetic field decreases drastically during these phenomena.

Although our goal is not doing numerics, we present some time series in figure 6 and the projections of a particular trajectory in figure 7 which are consistent with the analysis of the model of Melbourne, Proctor and Rucklidge [23]. The initial condition and the parameters are the same in both simulations. Figures 6 and 7 have been obtained using the dynamical systems package DSTOOL (see Guckenheimer *et al* [12])

Remark 3 *From direct measurements of Earth's dipole moment, it appears to be decaying linearly with time since the first measurements, at a rate of* 5% *per century. Recently, some scientists interpreted this decaying as a start of a reversal. Linear regressions suggest that the axial dipole moment would vanish in about 4000 (McPherron [20]).*

6 Discussion and Conclusion

Geomagnetic reversals are one of the main interesting points of the geomagnetism, one of the most challenging phenomena in geophysics. Although the details of the reversal process are not completely understood, the occurrence of reversals is well documented by studying the layered of iron-rich lava rocks, for example. Here, through theorem 1 and corollary 2, we proved that the mathematical model given by Melbourne, Proctor and Rucklidge [23] is relevant for the study of magnetohidrodynamics and that this model predicts and explains intermittent behaviour of the geomagnetic field and geo-reversals. The lengths of time intervals of constant polarity and the short duration of each reversal are consistent with those of the Earth. Also, the model explains why the geomagnetic field is predominantly axial dipolar.

As in Kirk and Rucklidge [15], we start with a heteroclinic network with reflectional and rotational symmetry. However, in contrast to their work, we study switching in a perturbation that does not break the network. The presence of the non-robust heteroclinic connection has important effects: for example, we can prove the existence of infinite switching. With the analysis of [15], since the connections $[i_3(\pm P_2) \to i_3(\pm P_3)]$ are off-centered at the top/bottom of the cylindrical neighbourhood near $i_3(\pm P_3)$, they are only able to conclude the existence of initial conditions following finite heteroclinic paths on the network.

Besides the interest from the physical point of view, the study of this model is important in the setting of dynamical systems because it describes the behaviour of a flow associated to

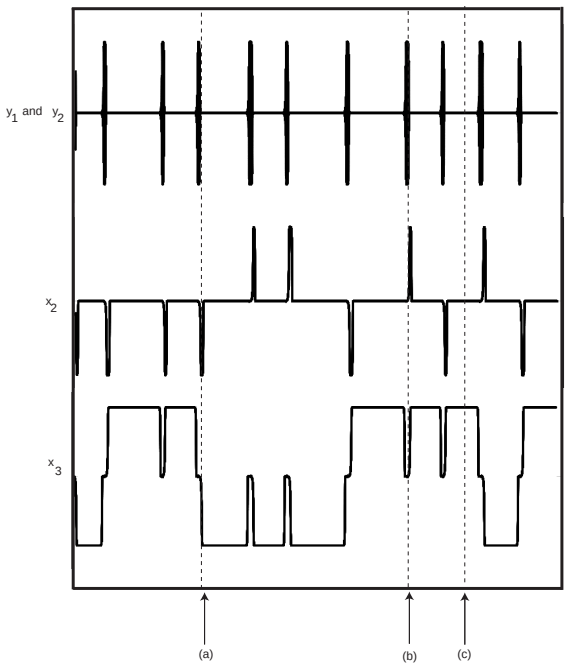

Figure 6: Time series for one trajectory for the flow associated to the differential equation (4.6), with $\mu_1 = 0.3$, $\mu_2 = 0.2$, $\mu_3 = 0.3$, $A_{12} = A_{21} = -0.33333$, $A_{13} = A_{31} = -0.5$, $A_{23} = A32 = -0.16667$, $\omega_1 = 1$, $\varepsilon_1 = 0.12$, $\varepsilon_2 = 0.1$ and $\varepsilon_3 = 0.001$. The initial condition is $(-0.5000, 0.0116, -0.1623, -0.2781)$. Caption: (a): Reversion (the vector field B change its sign); (b): Excursion (the geometry of the flow associated to B varies without changing the sign); (c): the axial dipole symmetric mode is the predominant situation.

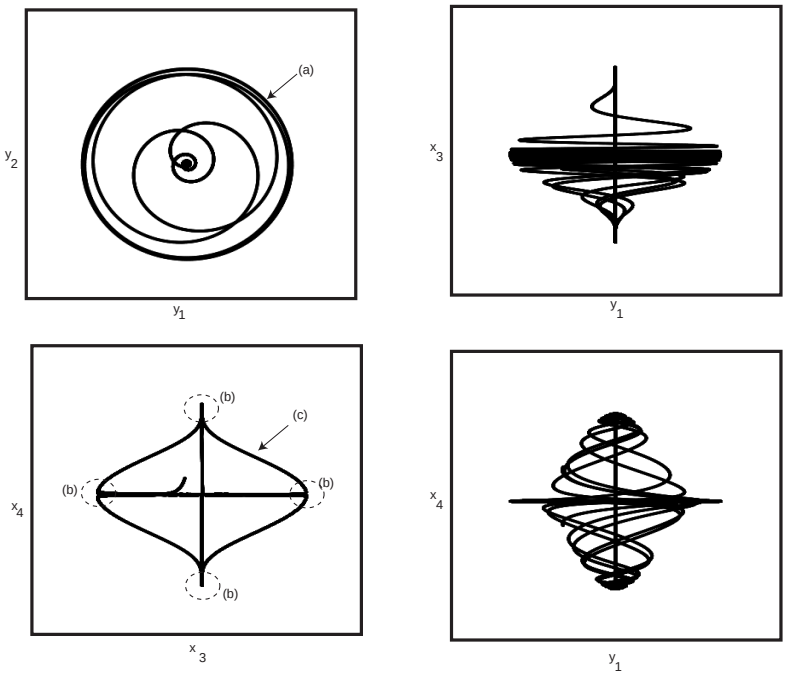

Figure 7: Projection in the (y_1, y_2), (x_3, x_4), $(y_1, x_3)$and (y_1, x_4)-planes of the trajectory with initial condition $(-0.5000, 0.0116, -0.1623, -0.2781)$ (the same as in the time series shown in figure 6) for the flow corresponding to the vector field (4.6) (same parameters as before). Caption: (a): periodic solution; (b): equilibria; (c): non robust heteroclinic orbit from $i_3(P_2)$ to $i_3(P_3)$. The interval range for all the variables is $[-3.5, 3.5]$.

a explicit vector field unfolding the symmetry breaking of an equivariant organizing center. In the fully non-equivariant case at first glance the return map is almost intractable. Here we are able to predict some qualitative features of the dynamics by assuming that X_4 is very close to X_4^ε. This is an important advantage of studying systems with some symmetry.

The ongoing discussion about the dynamics near the heteroclinic network of rotating nodes is the identification of what kind of transitive set unfolds from the attracting network. Near Σ_3^ε, there is a persistent set which is the homoclinic class of the periodic solution c^ε. The complete description of this *singular hyperbolic* set is an open question related to the J. Palis Conjecture. This answer could be used to conclude the robusteness of the shadowing property and the realization of all links and knots as periodic solutions.

Acknowledgments The author thanks the precious support, patience and corrections of Isabel Labouriau and Manuela Aguiar, without whom this paper would not have been written. Alexandre Rodrigues is also grateful to Ian Melbourne for giving the suggestion to tackle this work during their visit to University of Houston, USA. The author is also indebted to Sílvio Gama for helpful discussions and to Vlad Zheligovsky for helpful comments.

The research of the author at Centro de Matemática da Universidade do Porto (CMUP) had financial support from Fundação para a Ciência e a Tecnologia (FCT), Portugal, through the programs POCTI and POSI with European Union and national funding. A.A.P. Rodrigues was supported by the grant SFRH/BD/28936/2006 of FCT.

References

[1] M. A. D. Aguiar, S. B. Castro and I. S. Labouriau, *Dynamics near a heteroclinic network,* Nonlinearity, No. 18, 391–414, 2005

[2] M. A. D. Aguiar, S. B. S. D. Castro and I. S. Labouriau. *Simple Vector Fields with Complex Behavior*, Int. Jour. of Bif. and Chaos, Vol. 16 No. 2, 369–381, 2006

[3] M. A. D. Aguiar, I. S. Labouriau and A. A. P. Rodrigues, *Switching near a heteroclinic network of rotating nodes*, Dynamical Systems: an International Journal, Vol. 25, Issue 1, 75–95, 2010

[4] D. Armbruster , P. Chossat and I. Oprea, *Structurally stable heteroclinic cycles and the dynamo dynamics* In: Dynamo and Dynamics, a Mathematical Challenge, Kluwer Academic Publishers, 313–322, 2001

[5] P. Chossat and D. Armbruster, *Dynamics of polar reversals in spherical dynamos*, Proc. R. Soc. Lond. A, No. Vol. 459, No. 2031, 577–596, 2003

[6] P. Chossat and F. Guyard, *Heteroclinic cycles in bifurcation problems with $O(3)$ symmetry and the spherical Bénard problem*, Journal of Nonlinear Science, Vol. 6, No. 3, 201–238, 1996

[7] P. Chossat, F. Guyard and R. Lauterbach, *Generalized heteroclinic cycles in spherically invariant systems and their perturbations*, Journal of Nonlinear Sci., Vol. 9, No. 5, 479–524, 1999

[8] M. Field, *Lectures on bifurcations, dynamics and symmetry*, Pitman Research Notes in Mathematics Series, Vol. 356, Longman, 1996

[9] C. Gissinger, E. Dormy and S. Fauve, *Morphology of field reversals in turbulent dynamos*, A Letters Journal Exploring the Frontiers of Physics, EPL 90 (4), 2010

[10] D. Gubbins, C. Barber, S. Gibbonsy and J. J. Love, *Kinematic dynamo action in a sphere II - Symmetry selection*, Proc. R. Soc. Lond. A, No. 456, 1333–1353, 2000

[11] J. Guckenheimer and P. Holmes, *Structurally stable heteroclinic cycles*, Math. Proc. Camb. Phil. Soc. 103, 189–192, 1988

[12] J. Guckenheimer, M. R. Myers, F. J. Wicklin and P. A. Wolfork, *Dstool: A Dynamical System Toolkit with an Interactive Graphical Interface - Reference Manual, Center for Applied Mathematics*, Cornell Univeristy, 1995

[13] R. Holme, *Three-dimensional kinematic dynamos with equatorial symmetry: application to the magnetic fields of Uranus and Neptune*, Phys. Earth Planet. Interiors, No. 102, Issues 1–2, 105–122, 1997

[14] A. J. Homburg and J. Knobloch, *Switching homoclinic networks*, Dynamical Systems, Vol. 25, Issue 3, 351–358, 2010

[15] V. Kirk and A. Rucklidge, *The effect of symmetry breaking on the dynamics near a structurally stable heteroclinic cycle between equilibria and a periodic orbit*, Dynamical Systems: an International Journal, Vol. 23, Issue 1, 43–74, 2008

[16] M. Kono and P. Roberts, *Recent Geodynamo Simulations and Observations of the Geomagnetic Field*, Reviews of Geophysics, No. 40, 41–53, 2002

[17] M. Krupa, *Robust heteroclinic cycles*, J. Nonlin. Sci. No. 7, 129–176, 2006

[18] M. Krupa and I. Melbourne, *Asymptotic Stability of Heteroclinic Cycles in Systems with Symmetry, II,* Proc. Roy. Soc. Edinburgh, No. 134A, 1177–1197, 2004

[19] I. S. Labouriau and A. A. P. Rodrigues, *Global Generic Dynamics Close to Symmetry*, In preparation

[20] R. L. McPherron, *Solar Terrestrial Influences on Climate during Geomagnetic Reversals*, Presentation Aspen, Institute Geophysics and Planetary Physics University of California, 2010

[21] P. L. McFadden, R. T. Merril, M. W. McElhinny and S. Lee, *Reversals of the Earth's magnetic field and temporal variations of the dynamo families*, Journal of Geophysical Research, 96, 3923–3933, 1991

[22] I. Melbourne, *Intermittency as a Codimension-Three Phenomenon*, Journal of Dynamics and Differential Equations, Vol. 1, No. 4, 347–367, 1989

[23] I. Melbourne, M. R. E. Proctor and A. M. Rucklidge, *A heteroclinic model of geodynamo reversals and excursions*, Dynamo and Dynamics, a Mathematical Challenge (eds. P. Chossat, D. Armbruster and I. Oprea, Kluwer: Dordrecht, 363–370, 2001

[24] O. Podvigina, *A route to magnetic field reversals: an example of an ABC-forced non-linear dynamo*, Geophys. Astrophys. Fluid Dynamics, No. 97, 149–174, 2003

[25] C. Postlehwaite, *A new type of bifurcation from a heteroclinic cycle*, Dynamical Systems: an International Journal, Vol. 25, Issue 3, 305–322, 2010

[26] G. L. dos Reis, *Structural Stability of Equivariant Vector Fields on Two-Dimensions*, Trans. Am. Math. Soc. 283, 633–643, 1984

[27] A. Rodrigues, I. Labouriau and M. Aguiar, *Chaotic Double Cycling*, Dynamical Systems: an International Journal, Vol. 26, Issue 2, 199–233, 2011

[28] V. S. Samovol, *Linearization of a system of differential equations in the neighbourhood of a singular point,* Sov. Math. Dokl, Vol. 13, 1255–1259, 1972

[29] M. Shaskov and D. V. Turaev, *An Existence Theorem of Smooth Nonlocal Center Manifolds for Systems Close to a System with a Homoclinic Loop*, J. Nonlinear Sci., Vol. 9, 525–573, 1999

[30] L. P. Shilnikov, A. L. Shilnikov, D. M. Turaev, and L. U. Chua, *Methods of Qualitative Theory in Nonlinear Dynamics*, Part I, World Scientific Publishing Co., 1998

[31] F. Stefani, M. Xu, L. Sorriso-Valvo, G. Gerbeth, U. Gunther, *Oscillation or rotation: a comparison of two simple reversal models*, Geophysical and Astrophysical Fluid Dynamics, Vol. 101, Issues 3–4, 227–248, 2007

Article 4 – Contracting Lorenz-like attractor through the unfolding of a heteroclinic network

Submitted

Contracting Lorenz-like attractor through the unfolding of a heteroclinic network

Isabel S. Labouriau[1,2] Alexandre A. P. Rodrigues[1,2]
[1] Centro de Matemática da Universidade do Porto *
Rua do Campo Alegre, 687, 4169-007 Porto, Portugal
[2] Faculdade de Ciências, Universidade do Porto
Rua do Campo Alegre, 687, 4169-007 Porto, Portugal
islabour@fc.up.pt alexandre.rodrigues@fc.up.pt

Keywords:
Heteroclinic Network, Lorenz Attractor, Hyperbolic Dynamics, Polynomial Vector Field

AMS Subject Classifications:
Primary: 34C28; Secondary: 34C37, 37C29, 37D05, 37G35

Abstract

We construct explicitly a vector field on a three-dimensional sphere $\mathbf{S}^3$, with an attractor Λ containing two hyperbolic equilibria, a non-trivial hyperbolic basic set and heteroclinic trajectories connecting transversely the two equilibria. The vector field is the restriction to $\mathbf{S}^3$ of a polynomial vector field in $\mathbf{R}^4$ and unfolds of a heteroclinic network between two symmetric saddle-foci. Moreover, generic perturbations of this vector field will still have an attractor containing a hyperbolic basic set.

1 Introduction

A flow in a compact three-dimensional mananifold is structurally stable in the C^1 topology if and only if the flow is uniformly hyperbolic and all invariant manifolds meet transversely, as was proved in 1997, by Hayashi [25]. After the proof, the research has been centered in the study of the features of the flows which are not C^1 – structurally stable.

Arroyo *et al* [9] proved that any C^1 – vector field defined on a compact three-dimensional manifold may be approximated by a system of differential equations whose flow exhibits one of the following phenomena:

- uniform hyperbolicity;
- a heteroclinic cycle associated to, at least, one equilibrium;

*The research of the two authors at Centro de Matemática da Universidade do Porto (CMUP) had financial support from Fundação para a Ciência e a Tecnologia (FCT), Portugal. Research funded by the European Regional Development Funding FEDER through the programme COMPETE and by the Portuguese Government through the FCT – Fundação para a Ciência e a Tecnologia under the project PEst-C/MAT/UI0144/2011. A.A.P. Rodrigues was supported by the grant SFRH/BD/28936/2006 of FCT.

- a homoclinic tangency of the invariant manifolds of the periodic solutions.

In this article, we construct an explicit example of a C^∞ – vector field on the unitary sphere $\mathbf{S}^3$ that is approximated by differential equations exhibiting the first two behaviours and a non-trivial basic set. We conjecture that nearby differential equations also display the third behaviour, as well as heteroclinic tangencies of invariant manifolds of the equilibria.

Few explicit examples of vector fields whose flows contain transitive[1] but non-hyperbolic sets have been studied: the most famous example is the expanding *butterfly* proposed by E. Lorenz (1963) [30] as an approximation of the evolution equation of the atmospheric dynamics (for $\sigma = 10$, $r = 28$ and $b \approx 2.667$):

$$\begin{cases} \dot{x} = \sigma(y - x) \\ \dot{y} = rx - y - xz \\ \dot{z} = xy - bz \end{cases} . \tag{1.1}$$

The eigenvalues of the linearization of the vector field (1.1) at the origin are $\lambda_1, \lambda_2, \lambda_3 \in \mathbf{R}\backslash\{0\}$ and satisfy:

$$\lambda_2 < \lambda_3 < 0 < \lambda_1 \quad \text{and} \quad \lambda_1 + \lambda_3 > 0. \tag{1.2}$$

In order to understand the Lorenz differential equations, geometric models have been constructed independently by Afraimovich *et al* [1] in 1977 and Guckenheimer and Williams [24] two years later. The construction of these models have been based on the properties suggested by numerics. It suggested many others and an extended number of papers have been written on these piecewise smooth vector fields.

Consider a C^1 – robust attractor Λ - one that remains after any sufficiently small C^1 – pertubation of the vector field. Morales *et al* [38] proved that if such an attractor contains equilibria whose linearization has only real eigenvalues, then Λ must be *partially hyperbolic with volume expanding directions.*

The relevant notion for the general theory of robust transitive sets is the dominated splitting. A compact flow-invariant set Λ is partially hyperbolic if there is an invariant splitting $T\Lambda = E^s \oplus E^c$ for which there are $K, \lambda \in \mathbf{R}^+$ such that for $\forall t > 0, \forall x \in \Lambda$:

- $||\partial_x \phi_t|_{E^s_x}|| \leq Ke^{-\lambda t}$;
- $||\partial_x \phi_t|_{E^s_x}||.||\partial_x \phi_t|_{E^c_{\phi_t(x)}}|| \leq Ke^{-\lambda t}$.

The direction E^c of λ is *volume expanding* if $\forall t > 0, \forall x \in \Lambda, det|\partial_x \phi_t|E^c_x| \geq Ke^{\lambda t}$. The classical Lorenz model satisfies these conditions. The above result of Morales *et al* [38] unified the theory of hyperbolic dynamics and Lorenz-like flows. A good explanation about this subject may be found in chapter 3 of Araújo and Pacífico [8].

In this paper, a *persistent* behaviour is a dynamical phenomenon that occurs with positive probability on generic parametrized families through a initial flow. Clearly, having a robust attractor is persistent.

In 1993, Rovella [41] presented a persistent non-robust singular attractor in $\mathbf{R}^3$ that resemble the classical Lorenz attractor. The author started with the following variation of the geometrical Lorenz model with respect to the eigenvalues at the origin:

$$\lambda_2 < \lambda_3 < 0 < \lambda_1 \quad \text{and} \quad \lambda_1 + \lambda_3 < 0 \tag{1.3}$$

[1] It contains at least one dense trajectory.

and obtained vector fields exhibiting transitive non-hyperbolic attractors which are persistent. Rovella proved that, for an open and dense set of perturbations, the initial attractor Λ breaks up into the following: one or two periodic solutions, a hyperbolic set, the equilibrium and wandering trajectories linking them. Bonatti *et al* [14] relate this phenomenon with an interaction between Hénon-like dynamics for flows and the presence of an equilibrium.

The construction of the Rovella attractor [41] is similar to the geometric Lorenz model. Some authors constructed Lorenz-like examples through bifurcations from heteroclinic cycles and networks: for instance, Afraimovich *et al* [2] describe a codimension 1 bifurcation leading from Morse-Smale flows to Lorenz-like attractors; Morales [37] constructed a singular attractor from a hyperbolic flow, through a saddle-node bifurcation. All of these are similar to the expanding Lorenz attractor, for which condition (1.2) hold, as opposed to the contracting case.

Nowadays, particular attention is being given to the study of the dynamics near heteroclinic networks with complex behaviour, namely the construction of explicit vector fields whose flows has a specific type of sets and for which it is possible to give an analytical proof of the properties that guarantee the existence of complex behaviour (see for instance Aguiar *et al* [4, 5, 6], Kirk and Rucklidge [29], Melbourne [35], Rodrigues *et al* [40]).

Here we present a smooth vector field on $\mathbf{S}^3$ whose flow has a heteroclinic cycle with two equilibria, non-robust under generic perturbations but *almost persistent* in the definition of Rovella [41]. This is what we will call a *contracting Lorenz-like attractor*.

1.1 Organizing Center and a Framework of the Paper

A useful tool for the understanding of the dynamics associated to systems of differential equations is the determination of organizing centres as well as bifurcations they may exhibit (an example has been given in Fernandes-Sánchez *et al* [17]). In the present article, we construct an example of a polynomial vector field whose organising center has a heteroclinic network which originates a wide range of phenomena around it. More specifically, we construct an attractor set such that in generic two parameter families

$$\dot{x} = f(x, \lambda_1, \lambda_2) \quad \text{with} \quad f(*, 0) \equiv f,$$

there is a set of positive Lebesgue measure containing $(\lambda_1, \lambda_2) = (0, 0)$ for which an attractor remains (not necessarily robustly transitive).

Throughout this paper, by heteroclinic cycle we mean a set of finitely many disjoint hyperbolic equilibria p_j (also called *nodes*), $j \in \{1, \ldots, k\}$ and heteroclinic trajectories γ_j, $j \in \{1, \ldots, m\}$ such that:

$$\lim_{t \to +\infty} \gamma_j(t) = p_{j+1} = \lim_{t \to -\infty} \gamma_{j+1}(t),$$

with the understanding that $\gamma_{m+1} = \gamma_1$ and $p_{k+1} = p_1$. We also allow n-dimensional connections between two nodes p_i and p_j where $n > 1$, which can be considered as a set of solutions biasymptotic from p_i to p_j, in negative and positive time, respectively. These heteroclinic connections are what Ashwin and Chossat [11] call *continua of connections*. A heteroclinic network is a connected component of the group orbit of a heteroclinic cycle. In particular, for any pair of saddles in the network, there is a sequence of heteroclinic connections that links them (see Ashwin and Field [11] for a general definition).

We start with a structurally and asymptotically stable network associated to two saddle-foci $\mathbf{v}$ and $\mathbf{w}$. The original system has two symmetries (rotational $\mathbf{SO}(2)$ and reflectional $\mathbf{Z}_2$)

acting independently in a flow-invariant and attracting three-dimensional sphere $\mathbf{S}^3$. Restricted to $\mathbf{S}^3$, the two connections from $\mathbf{v}$ to $\mathbf{w}$ are one-dimensional and the connection from $\mathbf{w}$ to $\mathbf{v}$ is two-dimensional. A description of the flow associated to the organising center is given in section 3. In sections 4 and 5 we add the simplest possible terms that break the symmetries in specific ways. All the perturbations preserve the invariance and attraction of the sphere. The differential equations as well the perturbations were derived from Aguiar [3] and Aguiar *et al* [4].

In section 4, we consider a perturbation that breaks part of the $\mathbf{SO}(2)$-symmetry and the reflection $\mathbf{Z}_2$, splitting the two-dimensional connection into a pair of one-dimensional ones, giving rise to two Bykov cycles (also called by T-points because it corresponds to a point on the space of parameters where such cycles appears). In this paper, a *Bykov cycle* is a heteroclinic cycle with two saddle-foci of different types, in which the one-dimensional invariant manifolds coincide and the two dimensional invariant manifolds have an isolated transversal intersection. The Bykov cycles have been found in many applications of interest, ranging from the electronic oscillators [7] to magnetoconvection [42]. Such structure also appears in the flow of the Lorenz equations (for $\sigma = 10$, $r \approx 30.475$ and $b \approx 2.623$) - see Glendinning [18] for details.

Analytical proof of transverse intersection of two invariant manifolds is usually difficult but can be achieved in our example. In section 4 we give the analytical proof that the manifolds $W^u(\mathbf{v})$ and $W^s(\mathbf{w})$ meet transversely. We will make use of the Melnikov method presented in section 2, extended to heteroclinic connections.

In sections 5, we present another perturbation of the organising center which forces that the attracting heteroclinic cycles are broken but some attracting structures remain near it. Our results and conjectures are illustrated by numerical simulations, which have been obtained using the dynamical systems package DSTOOL (see Guckenheimer *et al* [23]).

2 Melnikov Method Revisited

Melnikov [36] studied a method to find the transverse intersection of the the invariant manifolds for a time periodic perturbation of a homoclinic cycle. The pioneer idea of Melnikov is to make use of the globally computable solutions of the unperturbed system the computation of perturbed solutions. This section contains a short description of the theory developed by Melnikov [36], Chow *et al* [16] and Bertozzi [12] applied to saddle-connections. For a detailed proof for the homoclinic case, see Guckenheimer and Holmes [22] (section 4.5).

If $X \in \mathbf{R}^2, t \in \mathbf{R}$ and $0 < \varepsilon \ll 1$, consider the planar system:

$$\dot{X} = f(X) + \varepsilon g(X, t) \tag{2.4}$$

such that:

- there exists $T > 0$ such that $g(X, t) = g(X, t + T)$ for all t *ie* g is T-periodic;
- for $\varepsilon = 0$, the flow has a heteroclinic connection Γ_0 associated to two hyperbolic points p_0 and p_1;
- the unstable manifold of p_0 coincides with the stable manifold of p_1.

Associated to the system (2.4), taking $S^1 \cong \mathbf{R}/T$, we define the suspended system:

$$\dot{X} = f(X) + \varepsilon g(X, \theta), \quad \dot{\theta} = 1, \quad (X, \theta) \in \mathbf{R}^2 \times S^1. \tag{2.5}$$

With the above assumptions, $p_0 \times S^1$ and $p_1 \times S^1$ are hyperbolic periodic solutions for the suspended flow, whose invariant manifolds $\Gamma_0 \times S^1$ coincide. Since the limit cycles are hyperbolic, their hyperbolic continuation is well defined for $\varepsilon \neq 0$; hereafter we denote them by $p_0^\varepsilon \times S^1$ and $p_1^\varepsilon \times S^1$. Under general conditions (without symmetry for example), the heteroclinic connection $\Gamma_0 \times S^1$ is not preserved and for a non-empty open set in the parameter space, the invariant manifolds meet transversely. Their intersection consists of a finite number of trajectories.

By parameterizing the solutions of the equations and restricting to a transverse cross section Σ, the idea of the proof of Melkinov is to define a real map which measures the infinitesimal splitting of the stable and unstable manifolds on Σ for the perturbed system. This map is known as the *Melnikov function* and it is given by:

$$M(t_0) = \int_{-\infty}^{+\infty} f(q_0(t)) \wedge g(q_0(t), t + t_0). \exp\left(\int_0^t trDf(q_0(s))ds\right) dt, \tag{2.6}$$

where $q_0(t)$ is the parametrization of the solution of the unperturbed system (2.4) starting at $t_0 = 0$ on Γ_0. Recall that the *wedge product* in $\mathbf{R}^2$ of two vectors (u_1, u_2) and (v_1, v_2) is simply given by $u_1 v_2 - u_2 v_1$. It should be clear that if f is a hamiltonian system, then $trDf(q_0(t)) = 0$ and then the Melnikov function becomes much simpler.

The main result we will use is the following:

Theorem 1 (Bertozzi [12], Melnikov [36]) *Under the above conditions, and for $\varepsilon > 0$ sufficiently small, if $M(t_0)$ has simple zeros, then $W^u(p_0^\varepsilon)$ and $W^s(p_1^\varepsilon)$ intersect transversely.*

This result is important because it allows to prove the existence of transverse homo and heteroclinic connections. The presence of this kind of transversality implies the presence of Smale's horseshoes and thus the existence of chaos. This method provides *a lower bound* for where chaotic behaviour can occur.

3 Construction of the Organising Center

We start with the differential equation in $\mathbf{R}^4$ given by:

$$\begin{aligned}
\dot{x}_1 &= x_1(1 - r^2) - \alpha_1 x_1 x_4 + \alpha_2 x_1 x_4^2 - x_2 \\
\dot{x}_2 &= x_2(1 - r^2) - \alpha_1 x_2 x_4 + \alpha_2 x_2 x_4^2 + x_1 \\
\dot{x}_3 &= x_3(1 - r^2) + \alpha_1 x_3 x_4 + \alpha_2 x_3 x_4^2 \\
\dot{x}_4 &= x_4(1 - r^2) - \alpha_1(x_3^2 - x_1^2 - x_2^2) - \alpha_2 x_4(x_1^2 + x_2^2 + x_3^2)
\end{aligned} \tag{3.7}$$

where

$$r^2 = x_1^2 + x_2^2 + x_3^2 + x_4^2, \quad \alpha_1, \alpha_2 < 0, \quad \alpha_2^2 < 8\alpha_1^2 \quad \text{and} \quad |\alpha_2| < |\alpha_1|.$$

This equation was studied by Aguiar *et al* [4]. We give here a brief description of their results. The vector field $\mathbf{X}_4$ associated to the equation (3.7) is equivariant under the action of the compact Lie group $\mathbf{SO(2)} \oplus \mathbf{Z}_2(\gamma_2)$ where $\psi_\theta \in \mathbf{SO(2)}$ acts as:

$$\psi_\theta(x_1, x_2, x_3, x_4) = (x_1 \cos(\theta) - x_2 \sin(\theta), x_1 \sin(\theta) + x_2 \cos(\theta), x_3, x_4)$$

and $\gamma_2 \in \mathbf{Z}_2(\gamma_2)$ acts as:

$$\gamma_2(x_1, x_2, x_3, x_4) = (x_1, x_2, -x_3, x_4).$$

The unitary sphere, denoted by $\mathbf{S}^3$, is globally attracting in $\mathbf{R}^4 \backslash \{\overline{0}\}$ (this means that every trajectory with nonzero initial condition is asymptotic to $\mathbf{S}^3$ in forward time). From now on, we

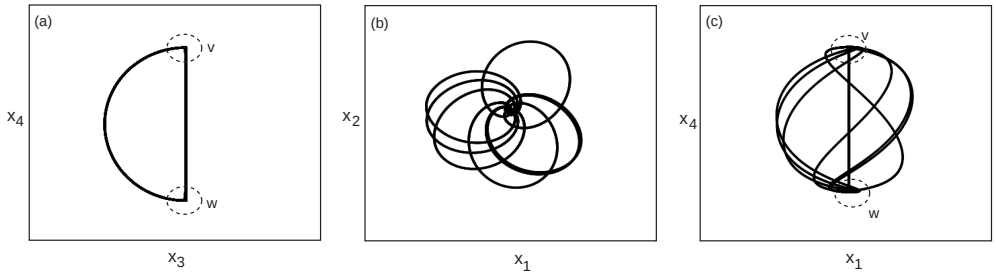

Figure 1: Projection in the (x_3, x_4), (x_1, x_2) and (x_1, x_4)-planes of the trajectory with initial condition $(-0.5000, -0.1390, -0.8807, 0.3013)$ for the flow corresponding to the equation (3.7), with $\alpha_1 = 1$ and $\alpha_2 = -0.1$.

restrict our study to this attracting three dimensional sphere where (3.7) has an asymptotically stable heteroclinic network Σ involving two hyperbolic saddle-foci given by:

$$\mathbf{v} = (0, 0, 0, +1) \quad \text{and} \quad \mathbf{w} = (0, 0, 0, -1)$$

The network is asymptotically stable by the criteria of Krupa and Melbourne [31, 32]. The equilibrium $\mathbf{v}$ (resp: $\mathbf{w}$) has one-dimensional unstable (resp: stable) manifold and two-dimensional stable (resp: unstable) manifold. The one-dimensional heteroclinic connections from $\mathbf{v}$ to $\mathbf{w}$ lie inside the invariant circle $Fix(\mathbf{SO(2)}) \cap \mathbf{S}^3$ and the two-dimensional connection from $\mathbf{w}$ to $\mathbf{v}$ lies inside the invariant two-sphere $Fix(\mathbf{Z}_2) \cap \mathbf{S}^3$. Note that all the intersections involving the invariant manifolds of $\mathbf{v}$ and $\mathbf{w}$ are very special: they coincide.

The network Σ can be decomposed into two cycles. Due to the symmetry, trajectories whose initial condition starts outside the invariant fixed point subspaces will approach in positive time one of the cycles. The fixed point hyperplanes prevent random visits to the two cycles and the time spent near each equilibrium increases geometrically. Figure 1 and the time series of figure 2 show the behaviour of a trajectory starting near Σ. Figure 1(a) and the time series of figure 2(b) emphasise that the trajectory is attracted to one of the two cycles. Observing the time series of figure 2 illustrates the increasing times spent near the equilibria.

4 Breaking the two-dimensional heteroclinic connection

In this section, we are considering a small perturbation of the vector field (3.7) that breaks the symmetry $\mathbf{SO(2)} \oplus \mathbf{Z}_2(\gamma_2)$ but is still equivariant under the action of $\gamma_1 := \psi_\pi \in \mathbf{SO(2)}$.

Theorem 2 *Consider the perturbation of* (3.7) *given by:*

$$\dot{X} = \mathbf{X}_4(X) + \lambda_1(0, 0, x_1x_2x_4, -x_1x_2x_3) = \mathbf{X}_5(X, \lambda_1) \tag{4.8}$$

that has symmetry group $\mathbf{Z}_2(\gamma_1)$ *and for which* $\mathbf{S}^3$ *is flow-invariant and globally attracting. For small* $\lambda_1 \neq 0$ *the restriction of* $\mathbf{X}_5$ *to* $\mathbf{S}^3$ *has a heteroclinic network involving the two equilibria* $\mathbf{v}$ *and* $\mathbf{w}$ *with the following properties:*

1. *the two equilibria* $\mathbf{v}$ *and* $\mathbf{w}$ *lie in* $Fix(\mathbf{Z}_2(\gamma_1)) \cap \mathbf{S}^3$ *and are hyperbolic saddle-foci;*

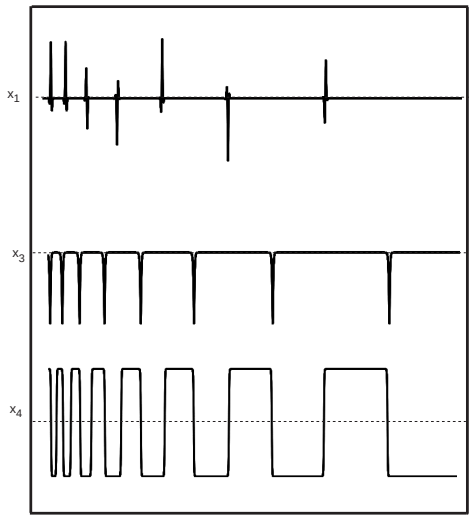

Figure 2: Time series for the trajectory with initial condition $(-0.5000, -0.1390, -0.8807, 0.3013)$ for the flow corresponding to the equation (3.7), with $\alpha_1 = 1$ and $\alpha_2 = -0.1$.

2. *there are two one-dimensional heteroclinic connections from* $\mathbf{v}$ *to* $\mathbf{w}$ *inside* $Fix(\mathbf{Z}_2(\gamma_1)) \cap \mathbf{S}^3$*;*

3. *the two-dimensional invariant manifolds of* $\mathbf{v}$ *and* $\mathbf{w}$ *intersect transversely along one-dimensional connections from* $\mathbf{w}$ *to* $\mathbf{v}$*.*

Moreover the connections from $\mathbf{v}$ *to* $\mathbf{w}$ *persist under small perturbations that preserve the symmetry.*

Proof: Clearly the perturbation term breaks all the symmetries of $\mathbf{X}_4(X)$ except γ_1. Since this perturbation is tangent to $\mathbf{S}^3$, it preserves its flow-invariance and its global attraction. It is also immediate that $\mathbf{v}$ and $\mathbf{w}$ are still the only equilibria of (4.8) and that $\gamma_1(\mathbf{v}) = \mathbf{v}$, $\gamma_1(\mathbf{w}) = \mathbf{w}$. A direct calculation shows that the perturbation does not change the eigenvalues of the linearisation at the equilibria, so they are still saddle-foci.

The circle $Fix(\mathbf{Z}_2(\gamma_1)) \cap \mathbf{S}^3$ is still flow-invariant and there are no other equilibria, thus it still consists of the two equilibria $\mathbf{v}$ and $\mathbf{w}$ and the two connections from $\mathbf{v}$ to $\mathbf{w}$. The plane $Fix(\mathbf{Z}_2(\gamma_1))$ will remain invariant under any perturbation that preserves the symmetry. Since on this plane $\mathbf{v}$ is a saddle and $\mathbf{w}$ is a sink, the connection persists under small perturbations.

Breaking the $\mathbf{Z}_2(\gamma_2)$-equivariance is necessary for the existence of transverse intersection of the manifolds $W^u(\mathbf{w})$ and $W^s(\mathbf{v})$. Nevertheless, the manifolds could intersect non transversely. The transversality of the intersection of the two-dimensional manifolds is proved in Theorem 3 below, using the Melnikov method presented in section 2. □

Theorem 3 *If* $\lambda_1 \neq 0$*, the two dimensional invariant manifolds of the equilibria* $\boldsymbol{w}$ *and* $\boldsymbol{v}$ *intersect transversely along one-dimensional orbits.*

Proof: In spherical coordinates

$$\begin{aligned} x_1 &= r\sin\phi\ \ \sin\theta\cos\varphi \\ x_2 &= r\sin\phi\ \ \sin\theta\sin\varphi \\ x_3 &= r\cos\phi\sin\theta \\ x_4 &= r\cos\theta \end{aligned}$$

equations (3.7) can be written as:

$$\begin{aligned} \dot{r} &= r(1-r^2) \\ \dot{\theta} &= \alpha_1 r\sin\theta\cos(2\phi) + \tfrac{\alpha_2}{2}r^2\sin(2\theta) + \tfrac{\lambda_1 r}{2}\sin^2(\phi)\sin^2(\theta)\cos(\phi)\sin(2\varphi) \\ \dot{\phi} &= -\alpha_1 r\cos(\theta)\sin(2\phi) - \tfrac{\lambda_1 r^2}{4}\sin^3(\phi)\sin(2\theta)\sin(2\varphi) \\ \dot{\varphi} &= 1 \end{aligned} \tag{4.9}$$

From the equation $\dot{\varphi} = 1$, we get $\varphi(t) = t$, $t \in \mathbf{R}$ and (4.9) is reduced to a three-dimensional non-autonomous differential equation. Since we are restricting our study to $\mathbf{S}^3$, the first equation may be omitted and replaced by $r = 1$. Thus, we have the following two-dimensional system of non autonomous differential equations:

$$\begin{aligned} \dot{\theta} &= \alpha_1\sin\theta\cos(2\phi) + \tfrac{\alpha_2}{2}\sin(2\theta) + \tfrac{\lambda_1}{2}\sin^2(\phi)\sin^2(\theta)\cos(\phi)\sin(2t) \\ \dot{\phi} &= -\alpha_1\cos(\theta)\sin(2\phi) - \tfrac{\lambda_1}{4}\sin^3(\phi)\sin(2\theta)\sin(2t) \end{aligned}$$

The above system of differential equations has the form:

$$\begin{aligned} \dot{\theta} &= f_1(\theta,\phi) + \lambda_1 g_1(\theta,\phi,t) \\ \dot{\phi} &= f_2(\theta,\phi) + \lambda_1 g_2(\theta,\phi,t) \end{aligned}$$

where

$$\begin{aligned} f_1(\theta,\phi) &= \alpha_1\sin\theta\cos(2\phi) + \tfrac{\alpha_2}{2}\sin(2\theta) \\ f_2(\theta,\phi) &= -\alpha_1\cos(\theta)\sin(2\phi) \\ g_1(\theta,\phi,t) &= \tfrac{1}{2}\sin^2(\phi)\sin^2(\theta)\cos(\phi)\sin(2t) \\ g_2(\theta,\phi,t) &= -\tfrac{1}{4}\sin^3(\phi)\sin(2\theta)\sin(2t) \end{aligned}$$

The maps g_1 and g_2 are periodic in t of period π. For the Melnikov function $M(t_0)$ defined in (2.6) we write $f = (f_1, f_2)$ and $g = (g_1, g_2)$. The parametrization $q_0(t)$ of the connection $[\mathbf{w} \to \mathbf{v}]$ in the unperturbed system, $\lambda_1 = 0$, is defined by $\phi = \frac{\pi}{2} + k\pi$, $k \in \{0, 1\}$. Thus, in the unperturbed system, the connections $[\mathbf{w} \to \mathbf{v}]$ are parametrized by:

$$q_0^1(t) = \left(\theta(t), \frac{\pi}{2}\right) \text{ and } q_0^2(t) = \left(\theta(t), \frac{3\pi}{2}\right).$$

Therefore, for $k \in \{0, 1\}$, we have:

$$\begin{aligned} f_1(q_0^i(t)) &= (-1)^k\alpha_1\sin(\theta(t)) + \tfrac{\alpha_2}{2}\sin(2\theta(t)) \\ f_2(q_0^i(t)) &= 0 \\ g_1(q_0^i(t), t+t_0) &= 0 \\ g_2(q_0^i(t), t+t_0) &= (-1)^{k+1}\tfrac{1}{4}\sin(2\theta(t))\sin(2(t+t_0)) \end{aligned}$$

We will show in lemma 4 below that the integral $M(t_0)$ converges and in lemma 5 that the roots of $M(t_0)$ are simple, thus completing the proof of theorem 3. □

In order to prove Lemma 4, we use the following result:

Lemma 4 *The integral $M(t_0)$ converges.*

Proof: The exterior product in the definition of the Melnikov function $M(t_0)$ is bounded since it is given by:

$$f(q_0^i(t)) \wedge g(q_0^i(t), t+t_0) = \\ = \left[-\alpha_1 \sin(\theta(t)) + (-1)^{k+1} \tfrac{\alpha_2}{2} \sin(2\theta(t))\right] \tfrac{1}{4} \sin(2\theta(t)) \sin(2(t+t_0))$$

and

$$trDf(q_0(s)) = \alpha_1 \cos(\theta(s)) + \alpha_2 \cos(2\theta(s)). \tag{4.10}$$

Since it has been shown in Aguiar *et al* [4] (lemma 16), that for any $r > 0$, the integral

$$\int_{-\infty}^{+\infty} \exp\left(-\int_0^t \alpha_2 r \cos(\theta(s)) + \alpha_3 r^2 \cos(2\theta(s)) ds\right) dt$$

converges, the convergence of $M(t_0)$ follows. □

Lemma 5 *The Melnikov integral $M(t_0)$ has simple roots.*

Proof: Using the expressions (4.10) and the expression of the *sin* of the sum, we may write $M(t_0)$ in the form:

$$M(t_0) = \cos(2t_0) \int_{-\infty}^{+\infty} [\sin(2t)]\, E(t) dt + \sin(2t_0) \int_{-\infty}^{+\infty} [\cos(2t)]\, E(t) dt.$$

where

$$E(t) = \left[-\alpha_1 \sin(\theta(t)) + (-1)^{k+1} \tfrac{\alpha_2}{2} \sin(2\theta(t))\right] \left[\tfrac{1}{4} \sin(2\theta(t))\right] \exp\left(-trDf(q_0(s)) ds\right)$$

Suppose that t_0 is a non-simple zero of $M(t_0)$. Since t_0 is a zero, we have:

$$\cos(2t_0) \int_{-\infty}^{+\infty} [\sin(2t)]\, E(t) dt + \sin(2t_0) \int_{-\infty}^{+\infty} [\cos(2t)]\, E(t) dt = 0, \tag{4.11}$$

or equivalently:

$$\tan(2t_0) = -\frac{\int_{-\infty}^{+\infty} [\sin(2t)]\, E(t) dt}{\int_{-\infty}^{+\infty} [\cos(2t)]\, E(t) dt}$$

Since t_0 is non-simple, differentiating (4.11) with respect to t_0 we must have:

$$-\sin(2t_0) \int_{-\infty}^{+\infty} [\sin(2t)]\, E(t) dt + \cos(2t_0) \int_{-\infty}^{+\infty} [\cos(2t)]\, E(t) dt = 0,$$

and thus we have

$$\tan(2t_0) = \frac{\int_{-\infty}^{+\infty} [\cos(2t)]\, E(t) dt}{\int_{-\infty}^{+\infty} [\sin(2t)]\, E(t) dt},$$

and this is a contradiction. It remains to show that $M(t_0)$ has a zero. For this, write

$$\rho e^{-i\zeta} = \int_{-\infty}^{+\infty} e^{-2it} E(t) dt \qquad \text{whence} \qquad M(t_0) = \rho \mathrm{Re}\left(e^{i(2t_0 - \zeta)}\right).$$

Thus $M(t_0)$ has zeros at $t_0 = \frac{1}{4}(\pi + 2\zeta + 2n\pi)$, $n \in \mathbf{Z}$.

□

Using the results and methods of Aguiar *et al* [5] and Aguiar *et al* [6], it follows from Theorem 2:

Theorem 6 *For any small $\lambda_1 \neq 0$ the vector field $\mathbf{X}_5(X, \lambda_1)$ is $\mathbf{Z}_2(\gamma_1)$-equivariant and has an attractor $\Lambda \subset \mathbf{S}^3$ containing the following:*

1. *two saddle-foci;*
2. *a heteroclinic network involving the saddle-foci with transverse intersection of the two-dimensional invariant manifolds;*
3. *a suspended horseshoe $\mathcal{H}$ containing the heteroclinic network on its closure.*

The attractor is robust under C^1-small perturbations that preserve the $\mathbf{Z}_2(\gamma_1)$-equivariance and if Σ is a transverse section to the suspended horseshoe, the first return map of $\mathcal{H}$ to Σ is hyperbolic at all points where the horseshoe is well defined. Moreover, there is switching on the network, i.e., *every sequence of connections in the network is shadowed by nearby trajectories. Under generic perturbations the attractor is not robust but is persistent in the C^1 topology.*

The C^1 robusteness is assured by Hirsch *et al* [26]. We illustrate the chaotic behaviour in the projeted phase portraits of figure 3 and in the time series of figure 4 corresponding to a trajectory that stays near the heteroclinic network. The figures also illustrate switching: the trajectory follows a sequence of heteroclinic connections in a random order.

Note that under generic perturbations the attractor of Theorem 6 persists but it changes its nature, since the non-transverse connections in the network disappear. The invariant sphere remains, since it is normally hyperbolic, as well as the transverse connection. On a one-parameter family of such perturbations, the vector field $\mathbf{X}_5(X, \lambda_1)$ corresponds to a *Bykov cycle*. A systematic study of the dynamics near this type of heteroclinic network is being done in Labouriau and Rodrigues [33], but at least we have the following:

Theorem 7 *There is a neighbourhood of the vector field $\mathbf{X}_5(X, \lambda_1)$ in the C^1 topology consisting of vector fields having an attracting invariant manifold diffeomorphic to $\mathbf{S}^3$ where the flow has an attractor containing the following:*

1. *two saddle-foci connected by transverse intersections of their two-dimensional invariant manifolds;*
2. *a contracting Lorenz-like attractor.*

Moreover, in this neighbourhood there is a codimension 2 set of vector fields satisfying 1.– 2.– 3. of Theorem 6. For this vector field, there is an attractor that is not robust but it persistent.

5 Breaking the one-dimensional heteroclinic connections

In this section, we consider another perturbation of system (3.7):

$$\dot{X} = \mathbf{X}_4(X) + \lambda_2(x_3^2 x_4, 0, -x_1 x_3 x_4, 0) = \mathbf{X}_6(X) \tag{5.12}$$

This perturbation breaks the **SO(2)** equivariance completely but the vector field is still equivariant under the action of γ_2. The heteroclinic cycle Σ is destroyed. When small symmetry-breaking terms destroy the non-robust heteroclinic connections, there will still be an attractor lying close to the original cycle. A good explanation using *pipes* has been given by Melbourne [34] and more recently by Golubitsky and Stewart [20] (section 8.3). Figures 5 and 6 suggest the existence of a single attracting periodic solution in each connected component $\mathbf{S}^3 \backslash [\mathbf{w} \to \mathbf{v}]$ of the phase space. Its period tends to $+\infty$ when $\lambda_2 \to 0$.

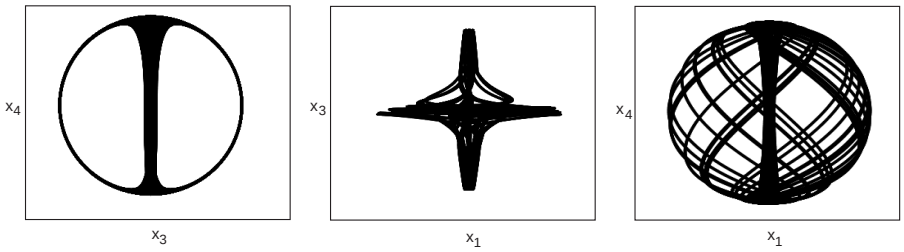

Figure 3: Projection in the (x_3, x_4), (x_1, x_3) and (x_1, x_4)-planes of the trajectory with initial condition $(-0.5000, -0.1390, -0.8807, 0.3013)$ for the flow corresponding to the equation (4.8), with $\alpha_1 = 1$ and $\alpha_2 = -0.1$.

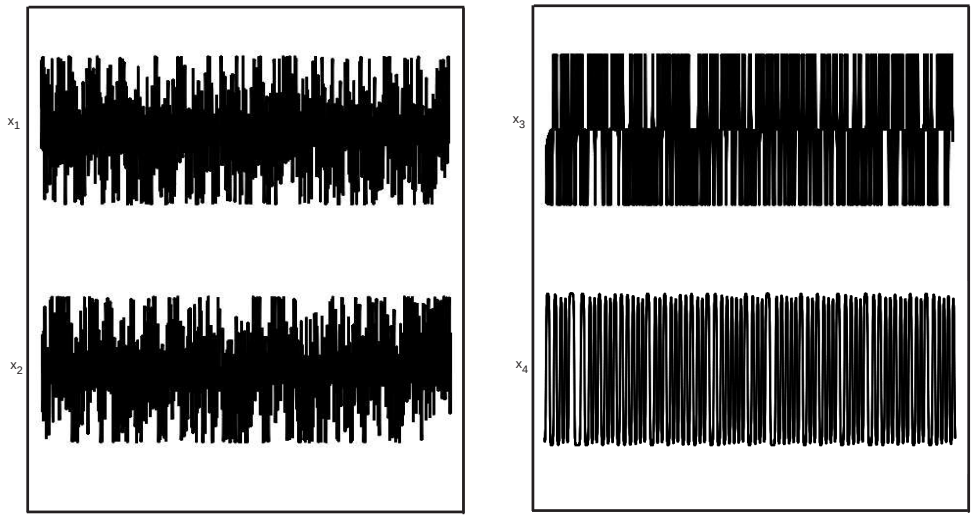

Figure 4: Time series for the trajectory with initial condition $(-0.5000, -0.1390, -0.8807, 0.3013)$ for the flow corresponding to the equation (4.8), with $\alpha_1 = 1$ and $\alpha_2 = -0.1$.

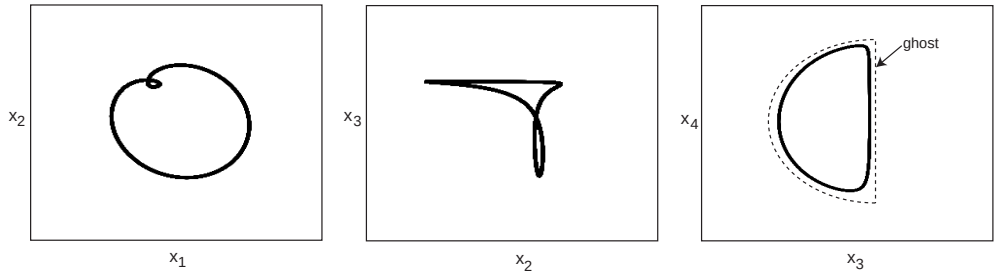

Figure 5: Projection in the (x_1, x_2), (x_2, x_3) and (x_3, x_4)-planes of the trajectory with initial condition $(-0.5000, -0.1390, -0.8807, 0.3013)$ for the flow corresponding to the equation (5.12), with $R = 1$, $\alpha_1 = 1$, $\alpha_2 = 1$, $\alpha_3 = -0.1$ and $\alpha_4 = 1$. The dotted line on the (x_3, x_4)-plane indicates the position of the original cycle.

6 Discussion - Further Work

Starting with a $\mathbf{Z}_2(\gamma_1) \oplus \mathbf{Z}_2(\gamma_2)$ vector field, it would be interesting to study the dynamics unfolds from it. It is known that breaking the two symmetries, the cycle is destroyed, giving rise to Shilnikov homoclinic orbits in the unfolding. We may also ask whether it is possible to find a curve in the bifurcation diagram (λ_1, λ_2) in which the homoclinic orbits occur.

Since the equilibria involved in the Bykov cycle are saddle-foci, then spiral curves of homoclinic cycles associated to the two equilibria emerge from the Bykov cycle in the parameter space. These structures organize a complex network of structures of bifurcations of periodic solutions. The unfolding diagram in the vicinity of a heteroclinic cycles has been already analysed, when one equilibrium is a real saddle (three real eigenvalues) and the other two are saddle-focus, by Glendinning and Sparrow [18, 19] and by Bykov [15] (the later author also considered the case *saddle-saddle*).

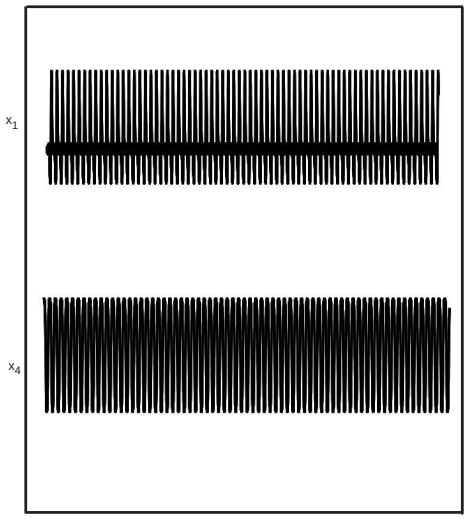

Figure 6: Time series for the trajectory with initial condition $(-0.5000, -0.1390, -0.8807, 0.3013)$ for the flow corresponding to the equation (5.12), with $R = 1$, $\alpha_1 = 1$, $\alpha_2 = 1$, $\alpha_3 = -0.1$ and $\alpha_4 = 1$.

References

[1] V. S. Afraimovich, V. V. Bykov, L. P. Shilnikov, *On the appearence and structure of the Lorenz attractor*, Dokl. Acad. Sci. USSR, No. 234, 336–339, 1977

[2] V. S. Afraimovich, S. C. Chow, W. Liu, *Lorenz-type attractors from codimension one bifurcation*, J. Dynam. Differential Equations, Vol. 7(2), 375–407, 1995

[3] M. Aguiar, *Vector Fields with heteroclinic networks,* PhD Thesis, Departamento de Matemática Aplicada, Faculdade de Ciências da Universidade do Porto, 2003

[4] M. A. D. Aguiar, S. B. S. D. Castro and I. S. Labouriau, *Simple Vector Fields with Complex Behaviour*, Int. Jour. of Bifurcation and Chaos, Vol. 16, Nr.2, 369–381 2006

[5] M. Aguiar, S. B. Castro, I. S. Labouriau, *Dynamics near a heteroclinic network,* Nonlinearity 18, 391–414, 2005

[6] M. Aguiar, I. S. Labouriau, A. Rodrigues, *Swicthing near a heteroclinic network of rotating nodes*, Dynamical Systems: an International Journal, 25(1), 75–95, 2010

[7] A. Algaba, F. Fernandez-Sánchez, E. Freire, M. Merino, and A. J. Rodriguez-Luis, *Non-transversal curves of T-points: a source of closed curves of global bifurcations*, Phys. Lett. A 303, 204–211, 2002

[8] V. Araújo, M. J. Pacífico, *Three dimensional Flows*, Ergebnisse der Mathematik und ihrer Grenzgebiete, Vol. 53, Springer, Berlin, Heidelberg, 2010

[9] A. Arroyo, F. Rodriguez-Hertz, *Homoclinic bifurcations and uniform hyperbolicity for three-dimensional flows*, Ann. Inst. H. Poincaré Anal. Non Linéaire, No. 20, 805–841, 2003

[10] P. Ashwin and P. Chossat, *Attractors for Robust Heteroclinic Cycles with Continua of Connections*, J. Nonlinear Sci., Vol. 8, No. 2, 103–129, 1998

[11] P. Ashwin and M. Field, *Heteroclinic Networks in Coupled Cell Systems* Arch. Rational Mech. Anal., Vol. 148, 107-143, 1999

[12] A. L. Bertozzi, *Heteroclinic orbits and chaotic dynamics in planar fluid flows*, SIAM J. Math. Anal, Vol. 19, No. 6, 1271–1294, 1988

[13] W. Brannath, *Heteroclinic networks on the tetrahedron*, Nonlinearity, Vol. 7, 1367-1384, 1994

[14] C. Bonatti, L. J. Díaz, M. Viana, *Dynamics beyond uniform hyperbolicity*, Springer-Verlag, Berlin, 2005

[15] V. Bykov, *Orbit Structure in a Neighbourhood of a Separatrix Cycle Containing Two Saddle-Foci*, Methods of qualitative theory of differential equations and related topics, Amer. Math. Soc., Providence, 87–97, 2000

[16] S. N. Chow, J. K. Hale, J. Mallet-Paret, *An example of bifurcation to homoclinic orbits*, J. Diff. Eqns, 37, 351–353, 1980

[17] F. Fernández-Sánchez, E. Freire, A. J. Rodríguez-Luis, *T-Points in a $\mathbf{Z}_2$-Symmetruc Electronic Oscillator. (I) Analysis*, Nonlinear Dynamics, 28, 53–69, 2002

[18] P. Glendinning and C. Sparrow, *Local and Global Behaviour near Homoclinic Orbits*, J. Stat. Phys., 35, 645–696, 1984

[19] P. Glendinning and C. Sparrow, *T-points: a codimension two heteroclinic bifurcation*, J. Stat. Phys., 43, 479–488, 1986

[20] M. Golubitsky and I. Stewart, *The Symmetry Perspective*, Birkhauser, 2000

[21] M.I. Golubitsky, I. Stewart, and D.G. Schaeffer, *Singularities and Groups in Bifurcation Theory*, Vol. II, Springer, Berlin, 2000

[22] J. Guckenheimer and P. Holmes, *Nonlinear Oscillations, Dynamical Systems, and Bifurcations of Vector Fields*, Applied Mathematical Sciences, No. 42, Springer-Verlag, 1983

[23] J. Guckenheimer, M. R. Myers, F. J. Wicklin, P. A. Wolfork, *Dstool: A Dynamical System Toolkit with an Interactive Graphical Interface - Reference Manual, Center for Applied Mathematics*, Cornell Univeristy, 1995

[24] J. Guckenheimer, R. F. Williams, *Structural stability of Lorenz attractors*, Publ. Math. IHES, No. 50, 59–72, 1979

[25] S. Hayashi, *Connecting invariant manifolds and the solution of the C^1 stability and Ω-stability conjectures for flows*, Ann. of Math., No. 2, Vol. 145 (1), 81–137, 1997

[26] M. Hirsch, C. Pugh, M. Shub, *Invariant Manifolds* Lecture Notes in Mathematics, 583, Springer-Verlag, 1977

[27] J. Hofbauer, *Heteroclinic Cycles in Ecological Differential Equations*, Tatra Mountains Math. Publ., Vol. 4, 105-116, 1994

[28] A. J. Homburg and B. Sandstede, *Homoclinic and Heteroclinic Bifurcations in Vector Fields*, Handbook of Dynamical Systems, Vol. 3, North Holland, Amsterdam, 379-524, 2010

[29] V. Kirk and A. Rucklidge, *The effect of symmetry breaking on the dynamics near a structurally stable heteroclinic cycle between equilibria and a periodic orbit*, Dynamical Systems: an International Journal, 23, Issue 1, 43–74, 2008

[30] E. N. Lorenz, *Deterministic nonperiodic flow*, J. Atmosph. Sci., No. 20, 130–141, 1963

[31] M. Krupa, and I. Melbourne, *Asymptotic Stability of Heteroclinic Cycles in Systems with Symmetry,* Ergodic Theory and Dynam. Sys., Vol. 15, 121–147, 1995

[32] M. Krupa and I. Melbourne, *Asymptotic Stability of Heteroclinic Cycles in Systems with Symmetry, II,* Proc. Roy. Soc. Edinburgh, 134A, 1177–1197, 2004

[33] I. S. Labouriau and A. A. P Rodrigues, *Global Generic Dynamics Close to Symmetry*, In conclusion

[34] I. Melbourne, *Intermittency as a codimension three phenomenon*, Journal of Dynamics and Stability of Systems, No. 1, pages 347-367, 1989

[35] I. Melbourne, *An example of a nonasymptotically stable attractor*, Nonlinearity 4(3), 835–844, 1991

[36] V. K. Melnikov, *On the stability of the center for time-periodic perturbations*, Trans. Moscow Math. Soc., Number 12, 1–57, 1963

[37] C. A. Morales, *Lorenz attractor through saddle-node bifurcations*, Ann. Inst. H. Poincaré Anal. Non Linéaire, 13, No. 5, 589–617, 1996

[38] C. A. Morales, M. J. Pacífico, E. R. Pujals, *Robust transitive singular sets for 3-flows are partially hyperbolic attractors or repellers*, Ann. of Math., No. 2, Vol. 160, 375–432, 2004

[39] A. A. P. Rodrigues, *Persistent Switching near the Heteroclinic Model for the Geodynamo Problem*, Submitted, 2011

[40] A. A. P. Rodrigues, I. S. Labouriau, M. A. D. Aguiar, *Chaotic Double Cycling*, Dynamical Systems: an International Journal, Vol. 26-2,199-233, 2011

[41] A. Rovella, *The dynamics of perturbations of contracting Lorenz maps*, Bol. Soc. Brasil. Mat. No. 24, 233-259, 1993

[42] A. M. Rucklidge, *Chaos in a low-order model of magnetoconvection*, Physica D, No. 62, 323–337, 1993

Article 5 – Global Generic Dynamics Close to Symmetry

Global Generic Dynamics Close to Symmetry

Isabel S. Labouriau[1,2] Alexandre A. P. Rodrigues[1,2]
[1] Centro de Matemática da Universidade do Porto *
Rua do Campo Alegre, 687, 4169-007 Porto, Portugal
[2] Faculdade de Ciências, Universidade do Porto
Rua do Campo Alegre, 687, 4169-007 Porto, Portugal
islabour@fc.up.pt alexandre.rodrigues@fc.up.pt

Contents

*CMUP is supported by FCT through POCI 2010 of Quadro Comunitário de Apoio III with FEDER funding.

Abstract

We characterise the nonwandering points of the dynamics of generic perturbations of a class of $(\mathbf{Z}_2 \oplus \mathbf{Z}_2)$–equivariant systems in the neighbourhood of a heteroclinic cycle containing two saddle foci of different type. In the cycle, only one of the heteroclinic connections is structurally stable. By gradually breaking the symmetry we get a wide range of well known and rich behaviour, namely the appearance of an attracting periodic trajectory, other heteroclinic trajectories, homoclinic orbits, n-pulses, horseshoes and cascades of bifurcations of periodic trajectories near an unstable homoclinicity. We also show that, generically, the coexistence of homoclinic orbits is a phenomenon of codimension 2.

1 Introduction

Symmetry has an important role in the analysis of the behaviour of some nonlinear physical systems. For instance, reflection symmetries (or $\mathbf{Z}_2$– symmetries) are relevant to a wide range of experiments in physics. These systems are idealised as having perfect symmetry, leading to the existence of invariant vector subspaces and thus to the robustness of heteroclinic cycles with respect to equivariant perturbations.

Some effects of small symmetry-breaking have already been studied by several authors and aspects related to the question of how much of the dynamics persists under the inclusion of small noise have also been considered, but details vary greatly between the different examples. For instance, Kirk and Rucklidge [28] consider small symmetry breaking for a system with an asymptotically stable heteroclinic network, Chossat [10] investigates the effect of symmetry breaking near a symmetric homoclinic cycle and Melbourne [35] analyses small perturbations near a system whose dynamics contains a heteroclinic cycle between three symmetric periodic trajectories.

In symmetric dynamics, spontaneous symmetry-breaking bifurcations occur when a state possessing high symmetry loses stability, giving rise to states with less symmetry (Krupa [29, 30]). Guckenheimer and Holmes [21] showed that robust heteroclinic cycles could arise naturally due to a low codimension symmetry-breaking bifurcation. Lauterbach and Roberts [34] proved that forced symmetry breaking, that is, slightly perturbing the equations so that some of the symmetries are broken, can naturally lead to the occurrence of robust heteroclinic cycles.

Another type of behaviour (bifurcation) occurs when the cycle is broken due to forced symmetry breaking. Typically the cycle is replaced by an invariant set contained in a small tubular neighbourhood of the cycle. The dynamics on the invariant set may be periodic, quasiperiodic or chaotic.

In this paper, we study how much the dynamics observed in a $(\mathbf{Z}_2 \oplus \mathbf{Z}_2)$–symmetric system in $\mathbf{S}^3$ persists under symmetry–breaking perturbations and we characterize the set of non wandering points. Our results appeal to generic properties of the system and are valid for any $(\mathbf{Z}_2 \oplus \mathbf{Z}_2)$–equivariant system satisfying these properties. This analysis was partially motivated by a system

constructed by Aguiar [2], whose flow contains a heteroclinic network connecting two saddle-foci of different types, where one heteroclinic connection is one dimensional and the other is two dimensional and both lie in different fixed point subspaces. Our work also forms part of a program addressing the systematic study of the dynamics near networks of equilibria, whose linearisation has a pair of conjugated and non real eigenvalues (this is what we call rotating equilibria) initialized by Bykov [7] in the eighties.

We consider f, a smooth two-parameter family of vector fields on $\mathbf{R}^n$ with flow given by the unique solution $x(t) = \varphi(t, x_0) \in \mathbf{R}^n$ of

$$\dot{x} = f(x, \lambda_1, \lambda_2) \qquad x(0) = x_0, \tag{1.1}$$

where λ_1 and λ_2 are real parameters.

Given two hyperbolic equilibria A and B, an m-dimensional *heteroclinic connection* from A to B, denoted $[A \to B]$, is an m-dimensional connected flow-invariant manifold contained in $W^u(A) \cap W^s(B)$. There may be more than one connection from A to B.

Let $\mathcal{S} = \{A_j : j \in \{1, \ldots, k\}\}$ be a finite ordered set of hyperbolic equilibria. We say that there is a *heteroclinic cycle* associated to $\mathcal{S}$ if

$$\forall j \in \{1, \ldots, k\}, W^u(A_j) \cap W^s(A_{j+1}) \neq \emptyset \pmod{k}.$$

If $k = 1$ we say that there is a *homoclinic cycle* associated to A_1. In other words, there is a connection whose trajectories tend to A_1 in both backward and forward time. A *heteroclinic network* is a finite connected union of heteroclinic cycles.

Heteroclinic networks appear frequently in the context of symmetry. Given a compact Lie group Γ acting linearly on $\mathbf{R}^n$, a vector field f is $\Gamma-$equivariant if for all $\gamma \in \Gamma$ and $x \in \mathbf{R}^n$, we have $f(\gamma x) = \gamma f(x)$. In this case $\gamma \in \Gamma$ is said to be a symmetry of f and all elements of the subgroup $\langle \gamma \rangle$ generated by γ are also symmetries of f. We refer the reader to Golubitsky, Stewart and Schaeffer [18] for more information on differential equations with symmetry.

The Γ-*orbit* of $x_0 \in \mathbf{R}^n$ is the set $\Gamma(x_0) = \{\gamma x_0, \gamma \in \Gamma\}$ that is invariant under the flow of Γ-equivariant vector fields f. In particular, if x_0 is an equilibrium of (1.1), so are the elements in its Γ-orbit.

The *isotropy subgroup* of $x_0 \in \mathbf{R}^n$ is $\Gamma_{x_0} = \{\gamma \in \Gamma, \quad \gamma x_0 = x_0\}$. For an isotropy subgroup Σ of Γ, its *fixed-point subspace* is

$$Fix(\Sigma) = \{x \in \mathbf{R}^n : \forall \gamma \in \Sigma, \gamma x = x\}.$$

If f is Γ-equivariant and Σ is a isotropy subgroup, then $Fix(\Gamma)$ is a flow-invariant vector space. This is the reason for the persistence of heteroclinic networks in symmetric flows: connections taking place inside a flow-invariant subspace may be robust to perturbations that preserve this subspace, even though they may be destroyed by more general perturbations.

2 Statement of Results

2.1 Description of the problem

The starting point of the analysis is a differential equation on the unit sphere $\mathbf{S}^3 \subset \mathbf{R}^4$

$$\dot{x} = f_0(x) \tag{2.2}$$

where $f_0 : \mathbf{S}^3 \to \mathbf{TS}^3$ is a smooth vector field with the following properties:

(P1) the organising centre f_0 is equivariant under the action of $\Gamma = \mathbf{Z}_2 \oplus \mathbf{Z}_2$ on $\mathbf{S}^3$ induced by the action on $\mathbf{R}^4$ of

$$\gamma_1(x_1, x_2, x_3, x_4) = (-x_1, -x_2, x_3, x_4)$$

and

$$\gamma_2(x_1, x_2, x_3, x_4) = (x_1, x_2, -x_3, x_4).$$

From now on, for a subgroup Δ of Γ, we denote by $Fix(\Gamma)$ the sphere

$$\{x \in \mathbf{S}^3 : \delta x = x, \forall \delta \in \Delta\}.$$

In particular,

$$Fix(\Gamma) = \{(0,0,0,1) \equiv \mathbf{v}, (0,0,0,-1) \equiv \mathbf{w}\} .$$

(P2) the equilibria $\mathbf{v}$ and $\mathbf{w}$ in $Fix(\Gamma)$ are hyperbolic saddle-foci where the eigenvalues of $df_0|_{x=X}$ are:

- $-C_{\mathbf{v}} \pm \alpha_{\mathbf{v}} i$ and $E_{\mathbf{v}}$ with $\alpha_{\mathbf{v}} \neq 0$, $C_{\mathbf{v}} > E_{\mathbf{v}} > 0$ for $X = \mathbf{v}$
- $E_{\mathbf{w}} \pm \alpha_{\mathbf{w}} i$ and $-C_{\mathbf{w}}$ with $\alpha_{\mathbf{w}} \neq 0$, $C_{\mathbf{w}} > E_{\mathbf{w}} > 0$ for $X = \mathbf{w}$.

(P3) within $Fix(\langle\gamma_1\rangle)$ the only equilibria are $\mathbf{v}$ and $\mathbf{w}$, a source and a sink, respectively. It follows that there are two heteroclinic trajectories ($\langle\gamma_2\rangle$-symmetric) from $\mathbf{v}$ to $\mathbf{w}$ (see case (a) of figure 1) that we denote by $[\mathbf{w} \to \mathbf{v}]$.

(P4) within $Fix(\langle\gamma_2\rangle)$ the only equilibria are $\mathbf{v}$ and $\mathbf{w}$, a sink and a source, respectively. Thus, there is a two-dimensional heteroclinic connection from $\mathbf{w}$ to $\mathbf{v}$ (see case (b) of figure 1). This connection together with the equilibria is the two-sphere $Fix(\langle\gamma_2\rangle)$.

Our object of study is a germ at $(\lambda_1, \lambda_2) = (0,0)$ of a two-parameter family of vector fields of $f(., \lambda_1, \lambda_2)$ that unfolds the symmetry breaking of the organizing center $f_0(x, 0, 0)$. We denote by f any of the vector fields

$$x \mapsto f(x, \lambda_1, \lambda_2),$$

when the choice of λ_1 and λ_2 is clear from the context. The parameters λ_1 and λ_2 control the type of symmetry breaking. Specifically, if $\lambda_1 \neq 0$, we are perturbing the $\mathbf{Z}_2 \oplus \mathbf{Z}_2$-equivariant vector field by breaking the symmetry γ_2 and preserving γ_1. Analogously, if $\lambda_2 \neq 0$, we destroy the equivariance under γ_1 and preserve γ_2. Throughout this article, we are assuming that these parameters act independently.

Since $\mathbf{v}$ and $\mathbf{w}$ are hyperbolic equilibria, then for each λ_1 and λ_2 close to 0, the vector field f still has two equilibria with eigenvalues satisfying (P2). When there is no loss of generality we ignore their dependence on λ_1 and λ_2. In particular, the dimensions of the local stable and unstable manifolds of $\mathbf{v}$ and $\mathbf{w}$ do not change, but generically the heteroclinic connections may be destroyed, since the fixed point subsets are no longer flow-invariant. More precisely, we are assuming:

(P5) Depending on the values of λ_1 and λ_2, the vector field f has the following symmetries:

Parameters	Symmetries preserved	Symmetries broken
$\lambda_1 = \lambda_2 = 0$	$\mathbf{Z}_2 \oplus \mathbf{Z}_2$	none
$\lambda_1 \neq 0$ and $\lambda_2 = 0$	$\langle\gamma_1\rangle$	$\langle\gamma_2\rangle$
$\lambda_1 = 0$ and $\lambda_2 \neq 0$	$\langle\gamma_2\rangle$	$\langle\gamma_1\rangle$
$\lambda_1 \neq 0$ and $\lambda_2 \neq 0$	Identity	$\mathbf{Z}_2 \oplus \mathbf{Z}_2$

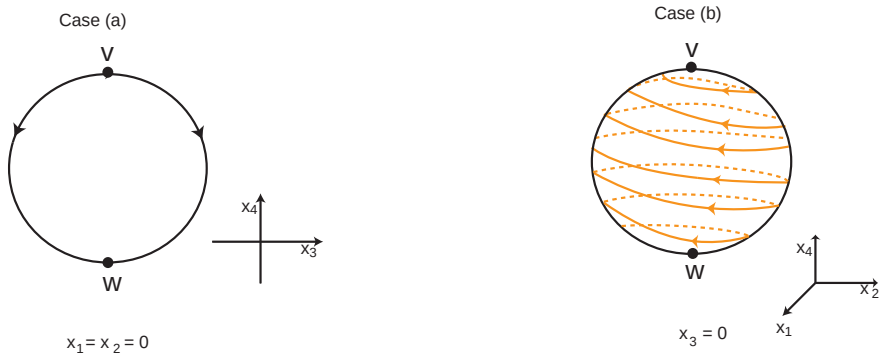

Figure 1: Heteroclinic connections for the organising center f_0. (a): from properties (P1)–(P3), the invariant circle $Fix(\langle\gamma_1\rangle)$ consists of the two equilibria $\mathbf{v}$ and $\mathbf{w}$ and two trajectories connecting them. (b): the invariant sphere $Fix(\langle\gamma_2\rangle)$ forms a two-dimensional connection $[\mathbf{v} \to \mathbf{w}]$ by property (P4). The arrows represent the coordinate system in which the heteroclinic connections lie.

The following property states that the invariant manifolds $W^u(\mathbf{w})$ and $W^s(\mathbf{v})$ meet transversely. Generically, the intersection of the manifolds consists of a finite number of trajectories.

(P6) **[Transversality]** For $\lambda_1 \neq 0$, the two dimensional manifolds $W^u(\mathbf{w})$ and $W^s(\mathbf{v})$ intersect transverselly at a finite number of trajectories.

(P7) **[Non degeneracy]** For $\lambda_2 \neq 0$, the heteroclinic connections $[\mathbf{v} \to \mathbf{w}]$ are broken.

Note that (P1)–(P4) are satisfied on a C^1-open subset of smooth Γ-equivariant vector fields on $\mathbf{S}^3$ and that (P5)–(P7) hold for a C^1 open subset of two parameter families of vector fields unfolding a Γ equivariant differential equation on the sphere. Our results are still valid on any manifold C^1-diffeomorphic to $\mathbf{S}^3$ if instead of (P2) we assume that f_0 commutes with two involutions γ_1 and γ_2 that fix, respectively, a circle and a two-sphere, that only meet at $\{\mathbf{v}, \mathbf{w}\}$.

2.2 Organising centre

When $\lambda_1 = \lambda_2 = 0$, there is a heteroclinic network (that we denote by Σ), in $\mathbf{S}^3$, associated to the two saddle-foci $\mathbf{v}$ and $\mathbf{w}$. The network Σ is the union of two heteroclinic cycles related by the γ_2 symmetry.

In order to describe the dynamics near Σ when the symmetry is broken, we start breaking part of the symmetry, as outlined in the following table:

Parameters	$\dim([\mathbf{v} \to \mathbf{w}])$	$\dim([\mathbf{w} \to \mathbf{v}])$	Section
$\lambda_1 = \lambda_2 = 0$	1	2	2.2
$\lambda_1 \neq 0$ and $\lambda_2 = 0$	1	1	4 and 2.3
$\lambda_1 = 0$ and $\lambda_2 \neq 0$	Not defined	2	5 and 2.4
$\lambda_1 \neq 0$ and $\lambda_2 \neq 0$	Not defined	1	6 and 2.5

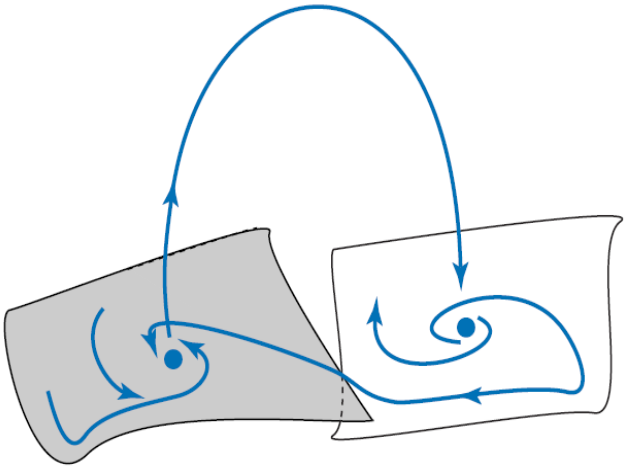

Figure 2: Bykov cycle: heteroclinic cycle associated to two saddle-foci of different types, in which the one-dimensional invariant manifolds coincide and the two dimensional invariant manifolds have a transverse intersection.

The heteroclinic connections in the network are contained in fixed point subspaces such that the hypothesis (H1) of Krupa & Melbourne [31] is satisfied. Since the inequality $C_{\mathbf{v}}C_{\mathbf{w}} > E_{\mathbf{v}}E_{\mathbf{w}}$ holds, the Krupa and Melbourne stability criterion ([31]) may be applied to Σ and we have:

Proposition 1 *Under conditions (P1)–(P4) the heteroclinic network* Σ *associated to* $\mathbf{v}$ *and* $\mathbf{w}$ *is asymptotically stable.*

The previous result means that there exists an open neighbourhood V_Σ of the network Σ such that every trajectory starting in V_Σ is forward asymptotic to the network. Due to the $\langle\gamma_2\rangle$-equivariance, trajectories whose initial condition starts outside the invariant subspaces will approach in positive time one of the cycles. The fixed point hyperplanes prevent jumps between the two cycles; in particular, random visits to both cycles require breaking the symmetry (and thus the breaking of the invariant subspaces). The time spent near each equilibrium increases geometrically. The ratio of this geometrical series is related to the eigenvalues of $df_0(x,0,0)$ at the equilibria.

2.3 Breaking the two-dimensional connection

When (P6) holds with $\lambda_2 = 0$ and $\lambda_1 \neq 0$ the network $\Sigma^\star$ consists of two copies of the simplest heteroclinic cycle between two saddle-foci, where one heteroclinic connection is structurally stable and the other is not. This cycle, called a *Bykov cycle*, has been first studied in the eighties by Bykov [7] and by Glendinning and Sparrow [17]. A Bykov cycle is a cycle with two saddle-foci of different types, in which the one-dimensional invariant manifolds coincide and the two dimensional invariant manifolds have a transversal intersection (see figure 2). It arises as a bifurcation of codimension 2. In the $\mathbf{Z}_2$-symmetric context Bykov cycles are generic.

Recently, there has been a renewal of interest in this type of heteroclinic bifurcation in different contexts (see, for instance, Ibañez and Rodriguez [25] Homburg and Natiello [24] and Sánchez *et al* [42]). Heteroclinic bifurcations of this type have been reported to arise on models

of Josephson junctions [8] and Michelson system [9]. Our approach is similar to that of Lamb *et al* [33], although they study $\mathbf{Z}_2$–reversible systems and we study the $\langle\gamma_1\rangle$-equivariant case and then break the symmetry.

2.3.1 Same orientation around the equilibria

There are two different possibilities for the geometry of the flow around Σ, depending on the direction trajectories turn around the connection $[\mathbf{v} \to \mathbf{w}]$. First we consider the case where each trajectory when close to $\mathbf{v}$ turns in the same direction as when close to $\mathbf{w}$. A simpler formulation of this will be given in subsection 3.1 below, after we have established some notation, but for the moment we are assuming:

(P8a) There are open neighbourhoods V and W of $\mathbf{v}$ and $\mathbf{w}$, respectively, such that, for any trajectory going from V to W, the direction of its turning around the connection $[\mathbf{v} \to \mathbf{w}]$ is the same in V and in W.

This is the situation in the reversible case studied by Lamb *et al* [33], where the anti-symmetry is a rotation by π. The condition would not hold if the anti-symmetry were a reflection.

In a more general setting the dynamics around heteroclinic cycles has been studied by Aguiar *et al* [5]. The main result is that, close to what remains of the network Σ after perturbation, there are trajectories that visit neighbourhoods of the saddles following all the heteroclinic connections in any given order. This is the concept of heteroclinic switching; the next paragraph gives a set-up of switching near a heteroclinic network (for more details, see Aguiar *et al* [5]). Recently, Homburg and Knobloch [23] gave an equivalent definition of switching for a heteroclinic network, using the notion of connectivity matrix (which characterizes the admissible sequences) and symbolic dynamics.

For a heteroclinic network Σ with node set $\mathcal{A}$, a *path of order k*, on Σ is a finite sequence $s^k = (c_j)_{j\in\{1,\dots,k\}}$ of connections $c_j = [A_j \to B_j]$ in Σ such that $A_j, B_j \in \mathcal{A}$ and $B_j = A_{j+1}$ *i.e.* $c_j = [A_j \to A_{j+1}]$. For an infinite path, take any $j \in \mathbf{N}$.

Let N_Σ be a neighbourhood of the network Σ and let U_A be a neighbourhood of each node A in Σ. For each heteroclinic connection in Σ, consider a point p on it and a small neighbourhood V of p. The neighbourhoods of the nodes should be pairwise disjoint, as well for those of points in connections. Given neighbourhoods as above, the point q, or its trajectory $\varphi(t)$, *follows* the finite path $s^k = (c_j)_{j\in\{1,\dots,k\}}$ of order k, if there exist two monotonically increasing sequences of times $(t_i)_{i\in\{1,\dots,k+1\}}$ and $(z_i)_{i\in\{1,\dots,k\}}$ such that for all $i \in \{1,\dots,k\}$, we have $t_i < z_i < t_{i+1}$ and:

- $\varphi(t) \subset N_\Sigma$ for all $t \in (t_1, t_{k+1})$;
- $\varphi(t_i) \in U_{A_i}$ and $\varphi(z_i) \in V_i$ and
- for all $t \in (z_i, z_{i+1})$, $\varphi(t)$ does not visit the neighbourhood of any other node except that of A_{i+1}.

There is *finite switching* near Σ if for each finite path there is a trajectory that follows it. Analogously, we define *infinite* switching near Σ by requiring that each infinite path is followed by a trajectory. In other words, for any given sequence of heteroclinic connections $(c_j)_{j\in\mathbf{N}}$ such that the ω-limit of any point in c_j coincide with the α-limit of any points in c_{j+1}, there exists at least one trajectory that remains very close to the network and follows the sequence (see figure 3).

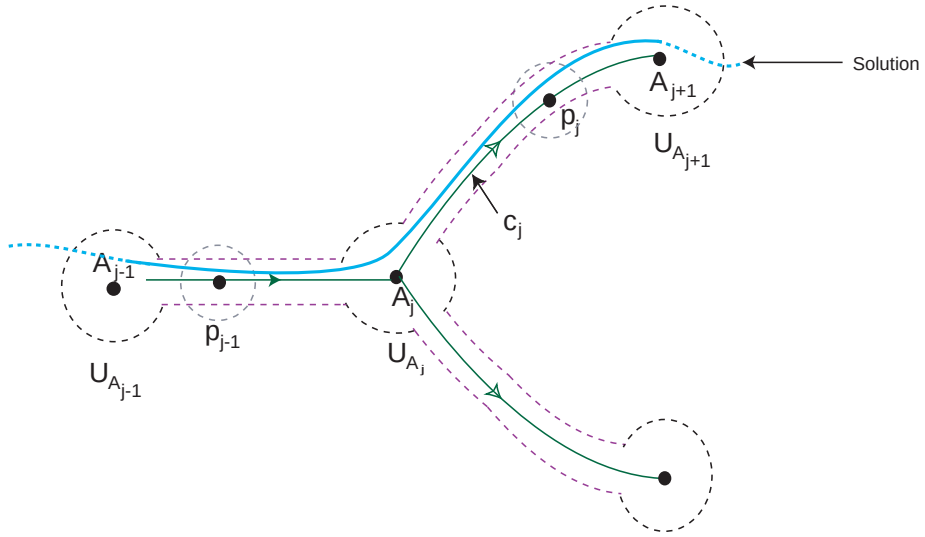

Figure 3: Trajectory shadowing two heteroclinic connections.

Proposition 2 *If a vector field f_0 satisfies (P1)–(P4) and (P8a), then the following properties are satisfied by all vector fields in an open neighbourhood of f_0 in the space of $\langle\gamma_1\rangle$-equivariant vector fields of class C^2 on $\mathbf{S}^3$:*

1. *the only heteroclinic connections from $\mathbf{v}$ to $\mathbf{w}$ are the original ones;*
2. *there are no homoclinic connections;*
3. *there is infinite switching;*
4. *the finite switching may be realised by an n-pulse heteroclinic connection $[\mathbf{w} \to \mathbf{v}]$;*
5. *there exists an increasing nested chain of a suspended uniformly hyperbolic compact sets $(G_i)_{i\in\boldsymbol{N}}$ topologically conjugate to a full shift over a finite number of symbols, which accumulates on the cycle (see figure 4).*

In the restriction to an uniformly hyperbolic invariant compact set (in a cross section) whose existence is assured by item 5 of proposition 2, the dynamics is conjugated to a full shift over a finite alphabet. In particular, since the ceiling function associated to the suspension of any horseshoe is bounded above and below (in the compact set), it follows that the topological entropy of the corresponding flow is positive (see Abramov [1]). This means that there is a positive exponential growth rate for the number of orbits, for the first return map, distinguishable with fine but finite precision (see Katok [26]).

The nested chain of horseshoes is illustrated in figure 4: a vertical rectangle in the wall of V, later called $H^{in}_{\mathbf{v}}$, first returns to the wall as several rectangles transverse to the original one. If the height of the rectangle is increased by moving its lower boundary closer to $W^s(\mathbf{v})$, then the number of returning rectangles (*legs* of the horseshoe) increases; continuing the rectangle all the way down to $W^s(\mathbf{v})$ creates infinitely many legs.

A challenge in topological dynamics is to decide whether periodic solutions can be separated by homotopies, or not. Roughly speaking, a *link* is a collection of disjoint one-spheres in $\mathbf{S}^3$. A *knot* is a link with one connected component. Two links $\mathcal{L}_1 \subset \mathbf{S}^3$ and $\mathcal{L}_2 \subset \mathbf{S}^3$ are equivalent

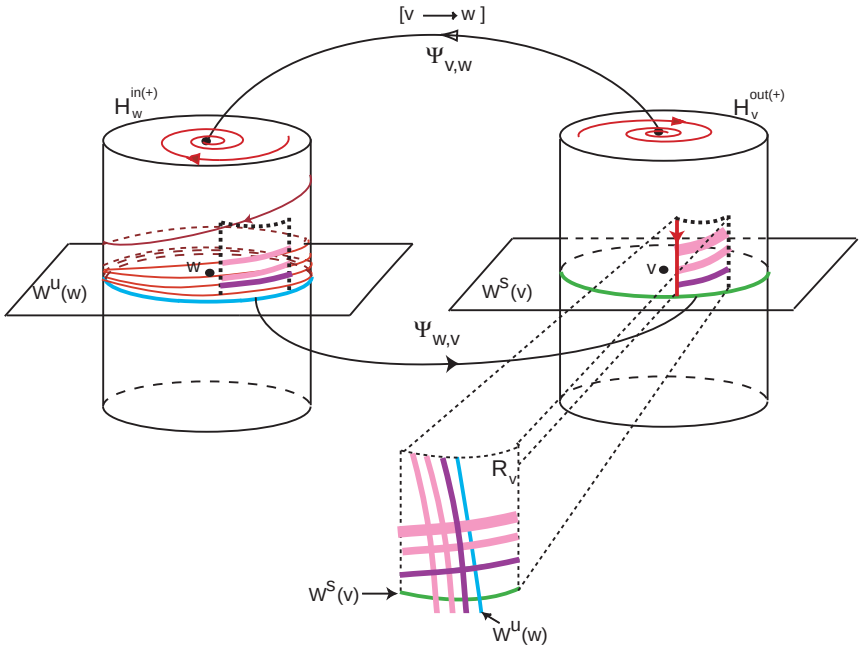

Figure 4: The presence of a transverse intersection creates a nested chain of uniformly hyperbolic horseshoes, which is accumulating on the cycle. Observe that horizontal strips s_i and their first return images by $\Psi_{\mathbf{w},\mathbf{v}} \circ \Phi_{\mathbf{w}} \circ \Psi_{\mathbf{v},\mathbf{w}} \circ \Phi_{\mathbf{v}}$ intersect in a transverse way.

if there exists an isotopy $\{\mathcal{H}_t\}_{t\in[0,1]}$ of $\mathbf{S}^3$ such that $\mathcal{H}_0 = Id_{\mathbf{S}^3}$ and $\mathcal{H}_1(\mathcal{L}_1) = \mathcal{L}_2$. We may use the following the result:

Theorem 3 (Franks and Williams [13], 1985) *If Φ_t is a C^r flow on $\mathbf{R}^3$ or $\mathbf{S}^3$ such that either:*

- *$r > 1$ and Φ_t has a hyperbolic periodic orbit with a transverse homoclinic point, or*
- *$r > 2$ and Φ_t has a compact invariant set with positive topological entropy,*

then among the closed orbits there are infinitely many distinct knot types.

It follows that among all the closed orbits which appear in the nested chain of horseshoes, there are many distinct inequivalent knot types. In particular, we may conclude that:

Corollary 4 *If f a vector field f_0 satisfies (P1)–(P4) and (P8a), then there are closed orbits linked to each of the cycles in $\Sigma^\star$ exhibiting infinitely many knot types.*

The previous result shows that among all the periodic solutions, there are many distinct inequivalent knot types. Nevertheless, we do not know if these horseshoes induce all link types. For example, neither the standard horseshoe (with two strips) nor its second iterate induces all types of links. The third iterate of the Smale horseshoe induces all link types - see Kin [27]. Based on the paper of Hirasawa and Kin [22], we solved affirmatively the problem using the concepts of *generalised horseshoes* and *twist signature*.

Corollary 5 *If f a vector field f_0 satisfies (P1)–(P4) and (P8a), then there are closed orbits linked to each of the cycles in $\Sigma^\star$ inducing all link types.*

We address the proof of corollary 5 in section 4. Observe that for each n-pulse heteroclinic connection from $\mathbf{w}$ to $\mathbf{v}$, we may define a *new* n-heteroclinic cycle and thus a *subsidiary Bykov cycle*. Hence, these *new* cycles have the same structure in their unfolding as the original cycles.

In the context of a heteroclinic cycle associated to non trivial periodic solutions, Rodrigues *et al* [40] describe the phenomenon of chaotic cycling: there are trajectories that follow the cycle making any prescribed number of turns near the periodic solutions, for any given bi-infinite sequence of turns. The rigorous definition of this concept requires an open neighourhood of Σ, V_Σ, a set of neighbourhoods of the saddles (isolating blocks) and a set of Poincaré sections near each limit cycle (counting sections). Given these sets, it is possible to code with an infinite word over a finite alphabet each trajectory that remains inside V_Σ for all time. Each repetition of a letter corresponds to a new turn inside the neighbourhood of the limit cycle; an infinite repetition (resp.: periodic word) corresponds to a trajectory lying in a invariant manifold (resp.: periodic solution).

Coding trajectories that remain for all time in the neighbourhood of Σ is beyond the scope of this paper, but we point out that this techique may be naturally applied to a heteroclinic cycle of saddle foci. Each repetition of a letter corresponds to a new turn inside the neighbourhood of $\mathbf{v}$ or $\mathbf{w}$ around the local one-dimensional invariant manifold. More precisely, it is possible to find a cross section to the heteroclinic connection $[\mathbf{v} \to \mathbf{w}]$ such that the set of initial trajectories that lie entirely in a fixed small neighbourhood may admit a complete description in the language of symbolic dynamics - in positive (resp.: negative) time, the trajectory is coded according to the number of turns inside the neighbourhood of $\mathbf{w}$ (resp.: $\mathbf{v}$) around $W^s_{loc}(\mathbf{w})$ (resp.: $W^u_{loc}(\mathbf{v})$).

2.3.2 Different orientation around equilibria

When (P8a) does not hold and (P1)–(P4) do, we have:

(P8b) There are open neighbourhoods V and W of $\mathbf{v}$ and $\mathbf{w}$, respectively, such that, for any trajectory going from V to W the direction of its turning around the connection $[\mathbf{v} \to \mathbf{w}]$ in V is the opposite of that in W.

Consider a trajectory that starts at the boundary ∂V, goes inside V where it turns several times around $[\mathbf{v} \to \mathbf{w}]$, then goes out of V, goes into W where it makes several turns again before arriving at ∂W. If (P8b) holds then it is possible to find such a trajectory with the property, that if one joins its starting point in ∂V to its end point in ∂W, one obtains a closed curve that is not linked to any of the cycles in Σ. This is in contrast to the situation where (P8b) holds, where trajectories that make a sufficiently large number of turns inside V and then move into W will necessarily yield a curve linked to one of the cycles.

In the context of a diffeomorphism containing homoclinic points, Newhouse [38] introduced the term *wild hyperbolic set* for uniformly hyperbolic sets whose invariant manifolds have a tangency. Extending the term to the case of heteroclinic tangencies, the main result of this section is the existence of a wild hyperbolic set near Σ under an open condition. Based on Bykov [7], we may conclude that:

Theorem 6 *There is an open set of vector fields f_0 satisfying (P1)–(P4) and (P8b) such that arbitrarily close to f_0, there is a $\langle\gamma_1\rangle$-equivariant vector field on $\mathbf{S}^3$ whose flow has the coexistence*

of transversality and tangencies between the two dimensional invariant manifolds $W^u(\mathbf{w})$ *and* $W^s(\mathbf{v})$.

Note that this would be the case of reversible equations where the anti-symmetry is a reflection. To the best of our knowledge, neither this situation nor the general non-reversible case has been studied.

For f_0 in the open set where Theorem 6 holds (in the C^2–topology), the first return map to a cross section, there exists a map exhibiting at least one homoclinic tangency. Using Newhouse's theory [37, 38], we can conclude the existence of a residual set $\mathcal{U}$ of vector fields exhibiting persistent heteroclinic tangencies (besides the transverse ones) and this implies the existence of non-uniformly hyperbolic dynamics which, in principle, cannot be separated from the topological horseshoes which appear near the transverse connection.

Although each individual homoclinic tangency may be eliminated either by a small perturbation or by adding noise to the system, small perturbations do not allow to remove homoclinic tangencies completely. Since we are assuming that the initial cycle is asymptotically stable, the first return map is area-contracting, and thus for all the vector fields in $\mathcal{U}$, there are infinitely many periodic attractors (see Newhouse [38]) - this is what some authors call Newhouse phenomena.

Consider now a vector field f_0 outside the open set where Theorem 6 holds for which (P1)–(P4) are satisfied and (P8a) does not . In this case, only transverse heteroclinic connections are observed in $\langle\gamma_2\rangle$-equivariant perturbations. Near these connections, dynamics of horseshoe type occurs (as in item 5 of proposition 2). The hyperbolicity of the Cantor set arising near the cycle is still assured and the set of trajectories that lie entirely in a fixed small neighbourhood may admit a complete description in the language of symbolic dynamics.

2.4 Breaking the one-dimensional connection

When (P7) holds, with $\lambda_1 = 0$ and $\lambda_2 \neq 0$, the heteroclinic cycles that existed in the fully symmetric case generically disappear. Since by (P5) we do not preserve the invariance of $Fix(\langle\gamma_2\rangle)$, we break the asymptotically stable heteroclinic network Σ but near the ghost of the original attractor there will still exist some attracting structure.

Generically each cycle is replaced by an asymptotically stable closed trajectory that lies near the original (attracting) heteroclinic cycle. One possibility would be to generate a *multi-pulse* heteroclinic connection from $\mathbf{v}$ to $\mathbf{w}$, that goes several times around close to where the original heteroclinic connection was, in a sense that will be made precise in Section 5. This is ruled out by the next result, proved in Section 5.

Theorem 7 *If a vector field* f_0 *satisfies (P1)–(P4), then the following properties are satisfied by all vector fields in an open neighbourhood of* f_0 *in the space of* $\langle\gamma_2\rangle$*-equivariant vector fields of class* C^2 *on* S^3*:*

1. *there are no multi-pulse heteroclinic connections from* $\mathbf{v}$ *to* $\mathbf{w}$*;*
2. *near each of the two cycles present in the* $\mathbf{Z}_2 \oplus \mathbf{Z}_2$*-symmetric equation, the perturbed equations have a non trivial asymptotically stable periodic solution.*

In our context, Theorem 7 may be rephrased as follows: consider a generic $\langle\gamma_2\rangle$-equivariant one-parameter perturbation $f(x, \lambda_2)$ of the $\mathbf{Z}_2 \oplus \mathbf{Z}_2$-symmetric organising centre f_0 that satisfies (P7). Then, for each small $\lambda_2 \neq 0$ there is a pair of symmetry-related non trivial asymptotically

stable periodic solutions to $\dot{x} = f(x, \lambda_2)$. As λ_2 tends to 0 the closed trajectories approach the two cycles in Σ and their period tends to $+\infty$. In local coordinates (such as will be assured by Samovol's Theorem, see Section 3 below), the limit cycle of the stable periodic trajetory winds increasingly around the local stable manifold of $\mathbf{w}$ and the time of flight inside fixed neighbourhoods of $\mathbf{v}$ and of $\mathbf{w}$ tends to $+\infty$.

2.5 Breaking the two connections

In this section we prove that breaking the Bykov cycle involving $\mathbf{v}$ and $\mathbf{w}$ may give rise to homoclinic orbits involving saddle-focus in the unfolding. These homoclinic cycles are usually called *Shilnikov homoclinic orbits* because the systematic study of the dynamics near them began with L. P. Shilnikov in 1965 (see Shilnikov [44]). The homoclinic orbits associated to a saddle-focus is one of the main sources of chaotic dynamics in three-dimensional flows. In several applications these homoclinicities play an important role.

First of all, note that under perturbation the generalized horseshoes $(G_i)_{i\in\mathbf{N}}$ which occur near the Bykov cycle in proposition 2 survive for finitely many N. For each N, G_N is uniformly hyperbolic but $\bigcup_{i\in\mathbf{N}} G_i$ is not.

2.5.1 Dynamics near Shilnikov Homoclinic Orbits

This subsection summarises some well known results about the dynamics near homoclinic orbits associated to a hyperbolic equilibrium p_0 in a three-dimensional manifold. All results will be applied in the present work. We are assuming that $\dim W^s(p_0) = 2 = \dim W^u(p_0) + 1$. For more details details, see the books Shilnikov *et al* [46]. A good recent approach has been given by Glendinning & Sparrow [16] and Wiggins [47].

In three dimensional flows, it is well known that the appearance of a Shilnikov homoclinic orbit may lead to a wide range of periodic and aperiodic motions. If p_0 is an equilibrium of (2.2) such that:

- the eigenvalues of df, at p_0, are $\lambda^s + i\omega$ and λ^u, where $-\lambda^s \neq \lambda^u$ are positive numbers and $\omega \neq 0$;
- (non-linear condition) there is a homoclinic trajectory Γ connecting p_0 to itself,

then Γ is said a *Shilnikov homoclinic connection* of p_0. It is easy to see that p_0 possesses a local two-dimensional stable manifold and a local one-dimensional unstable manifold which intersect non-transversely. If $-\lambda^s < \lambda^u$, we say that the homoclinic orbit Γ satisfies the *Shilnikov condition* (see Gaspard [14]). If Γ is a Shilnikov homoclinic connection to an equilibrium p_0 of the flow of (2.2) such that Γ:

1. *satisfies the Shilnikov condition,* then there exists a countable infinity of suspended Smale horseshoes (accumulating on the homoclinic cycle) in any small cylindrical neighbourhood of Γ. When the vector field is perturbed to break the homoclinic connection, finitely many of these horseshoes remain and there appear persistent strange attractors [36]. For each $N \in \mathbf{N}$, N-homoclinic orbits exist for infinitely many parameter values.
2. *does not satisfy the Shilnikov condition and* $-\lambda^s \neq \lambda^u$, then the homoclinic orbit is an attractor. Under small C^1– perturbations, there is one stable periodic orbit in a neighbourhood of the homoclinic orbit.

Reverting the time, dual results may be obtained for homoclinic orbits involving a saddle-focus p_0 such that $\dim W^u(p_0) = 2 = \dim W^s(p_0) + 1$.

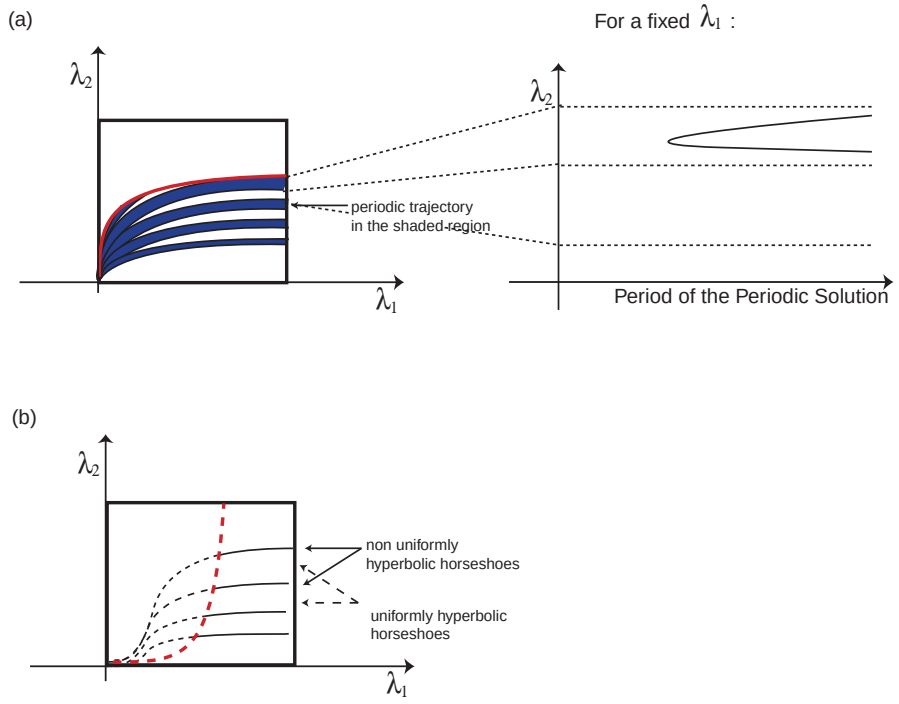

Figure 5: Bifurcation Diagrams. (a) In the bifurcation diagram (λ_1, λ_2), there are infinitely many tongues of attracting periodic trajectories accumulating on the line $\lambda_2 = 0$. These periodic trajectories are bifurcating from the attracting homoclinic orbit of $\mathbf{v}$; (b) In the bifurcation diagram (λ_1, λ_2), near each homoclinic orbit of $\mathbf{w}$, there are infinitely many non-uniformly hyperbolic horseshoes which are destroyed under small perturbations. The curves for which we observe the existence homoclinic orbits of $\mathbf{w}$ are accumulating on the line $\lambda_2 = 0$.

2.5.2 Homoclinic orbits near the network

In general, the existence of a homoclinic orbit is not a robust property. Here, we prove that the homoclinic orbits of $\mathbf{v}$ and $\mathbf{w}$ occur along lines in the two parameter space. There are two main theorems in this section: the first one characterizes the dynamics near the homoclinic orbits associated to $\mathbf{v}$ and the other states the similar results for $\mathbf{w}$. Both follow from the analysis of the bifurcation diagram depicted in figure 5.

Theorem 8 *Consider a vector field f_0 satisfying (P1)–(P4) and (P8a). A generic symmetry-breaking family f_{λ_1,λ_2} unfolding f_0 satisfies (P5)–(P7) and its dynamics, for $\lambda_1 \neq 0$ and for $\lambda_2 \neq 0$ sufficiently small satisfies:*

1. *for each $\lambda_1 > 0$, there exists a sequence of positive numbers $\lambda_2^k(\mathbf{v})$ such that if $\lambda_2 = \lambda_2^k(\mathbf{v})$ there exists an attracting homoclinic orbit associated to $\mathbf{v}$;*

2. *the homoclinic orbits which exist for $\lambda_2 = \lambda_2^k(\mathbf{v})$ and for $\lambda_2 = \lambda_2^{k+2}(\mathbf{v})$ are distinguished by the number of revolutions inside W around $W^s_{loc}(\mathbf{w})$;*

3. *for each $\lambda_1 > 0$, either for $\lambda_2^k(\mathbf{v}) < \lambda_2 < \lambda_2^{k+1}(\mathbf{v})$ or for $\lambda_2^{k+1}(\mathbf{v}) < \lambda_2 < \lambda_2^{k+2}(\mathbf{v})$, there exists an attracting periodic solution near the locus of the homoclinic orbit;*

4. *in the bifurcation diagram, the tongues for which there are no attracting limit cycles (associated to bifurcations of homoclinic orbits of* $\mathbf{v}$*) are alternated;*

5. *when* $\lambda_2 \to 0$*, the homoclinic orbits of* $\mathbf{v}$ *accumulate on the heteroclinic connection* $[\mathbf{v} \to \mathbf{w}]$.

Note that $\lambda_2^k(\mathbf{v})$ depends on λ_1. We omit this dependence to simplify the notation. From a simple analysis of the bifurcation diagram, it follows that along a vertical line $(\lambda_1 = \lambda_1^0(\mathbf{v}))$, a stable limit cycle is born from a simple homoclinic loop for $\lambda_2 = \lambda_2^k(\lambda_1^0)$; along the path, the limit cycle decreases its period and increases once again until it reaches $\lambda_2 = \lambda_2^{k+1}(\lambda_1^0)$ where the stable periodic solution becomes once again a homoclinic orbit of $\mathbf{v}$.

We have the following result concerning homoclinicities of $\mathbf{w}$:

Theorem 9 *Consider a vector field* f_0 *satisfying (P1)–(P4) and (P8a). A generic symmetry-breaking family* f_{λ_1,λ_2} *unfolding* f_0 *satisfies (P5)–(P7) and its dynamics, for* $\lambda_1 \neq 0$ *and for* $\lambda_2 \neq 0$ *sufficiently small satisfies:*

1. *for each* $\lambda_1 > 0$*, there exists a sequence of positive numbers* $\lambda_2^k, (\mathbf{w})$ *such that if* $\lambda_2 = \lambda_2^k(\mathbf{w})$ *there exists a homoclinic orbit associated to* $\mathbf{w}$*;*

2. *the homoclinic orbits which exist for* $\lambda_2 = \lambda_2^k(\mathbf{w})$ *and for* $\lambda_2 = \lambda_2^{k+2}(\mathbf{w})$ *are distinguished by the number of revolutions inside* V *around* $W^u_{loc}(\mathbf{v})$*;*

3. *if* $\lambda_2 = \lambda_2^k(\mathbf{w})$ *there exists a horseshoe with an infinite number of periodic orbits;*

4. *when* $\lambda_2 \to 0$*, the sequence of homoclinic orbits of* $\mathbf{w}$ *accumulates on the cycle.*

In the bifurcation diagram, when we follow along a vertical line $(\lambda_1 = \lambda_1^0(\mathbf{w}))$, we observe period-doubling cascade bifurcations that destabilize and restabilize the periodic orbits leadind to the full horseshoe which exists near the homoclinic orbit of $\mathbf{w}$ (see Glendinning and Sparrow [16] and Yorke and Alligood [49]). We also see the existence of a sequence of real numbers s_i such that for $\lambda_2 = s_i$ there is a double pulse homoclinic orbit exhibiting the same behaviour as the main homoclinic orbit. This double pulse follows the primary homoclinic cycle twice. We observe n-pulse homoclinic orbits $(n > 2)$.

For dissipative systems, the process of creation and destruction of horseshoes can be accompanied by unfoldings of homoclinic tangencies to hyperbolic periodic solutions. The co-existence of different types of behaviour in the flow has been investigated by many authors (see, for example, Glendinning, Abshagen & Mullin [15], Xiao-Feng & Rui-hai[48] and Bykov [7]). In the present paper, from the analysis of the bifurcation diagrams, we may conclude that:

Corollary 10 *For any family of differential equations satisfying (P1)–(P5) and (P8a) the co-existence of the homoclinic trajectories of* $\mathbf{v}$ *and* $\mathbf{w}$ *is a phenomenon of codimension 2* [1].

Note that the coexistence of homoclinic trajectories is not a *true* bifurcation since this trajectories occur in different regions of the phase space.

[1] They occur at isolated points in parameter space, accumulating at the origin.

3 Local Dynamics near the saddles

In this section, we establish local coordinates near the saddle-foci $\mathbf{v}$ and $\mathbf{w}$ and define some notation that will be used in the rest of the paper. The starting point is an application of Samovol's Theorem [41] to linearise the flow around the equilibria and to introduce cylindrical coordinates around each saddle-focus. These are used to define neighbourhoods with boundary transverse to the linearised flow. For each saddle, we obtain the expression of the local map that sends points in the boundary where the flow goes in, into points in the boundary where the flows goes out. Finally, we establish a convention for the transition maps from one neighbourhood to the other.

Note that when we refer to the stable/unstable manifold of an equilibrium point, we mean the *local* stable/unstable manifold of that equilibrium.

3.1 Linearisation near the equilibria

By Samovol's Theorem [41] (see also section 6.4 Part I of Anosov *et al* [6] and Ren & Yang [39]), around the saddle-foci, the vector field f is C^1-conjugated to its linear part, since there are no resonances of order 1. In cylindrical coordinates (ρ, θ, z) the linearisations at $\mathbf{v}$ and $\mathbf{w}$ take the form, respectively:

$$\begin{cases} \dot{\rho} = -C_{\mathbf{v}}\rho \\ \dot{\theta} = \alpha_{\mathbf{v}} \\ \dot{z} = E_{\mathbf{v}} z \end{cases} \qquad \begin{cases} \dot{\rho} = E_{\mathbf{w}}\rho \\ \dot{\theta} = \alpha_{\mathbf{w}} \\ \dot{z} = -C_{\mathbf{w}} z. \end{cases} \tag{3.3}$$

We consider cylindrical neighbourhoods of $\mathbf{v}$ and $\mathbf{w}$ in $\mathbf{S}^3$ of radius $\varepsilon > 0$ and height 2ε that we denote by V and W, respectively. Their boundaries consist of three components (see figure 6):

- The cylinder wall parametrized by $x \in \mathbf{R} \pmod{2\pi}$ and $|y| \leq \varepsilon$ with the usual cover $(x, y) \mapsto (\varepsilon, x, y) = (\rho, \theta, z)$. Here x represents the angular coordinate and y is the height of the cylinder.
- Two disks, the top and the bottom of the cylinder. We take polar coverings of these disks: $(r, \varphi) \mapsto (r, \varphi, j\varepsilon) = (\rho, \theta, z)$ where $j \in \{-, +\}$, $0 \leq r \leq \varepsilon$ and $\varphi \in \mathbf{R} \pmod{2\pi}$.

On these cross sections, we define the return maps to study the dynamics near the cycle.

Remark 1 *Property (P8a) concerning the direction of turning around the connection* $[\mathbf{v} \to \mathbf{w}]$*, may be interpreted in terms of the sign of* $\alpha_{\mathbf{v}}$ *and* $\alpha_{\mathbf{w}}$*: property (P8a) holds when they have the same signs; (P8b) holds when they have opposite signs.*

3.2 Coordinates near v

The cylinder wall is denoted by $H^{in}_{\mathbf{v}}$. Trajectories starting at interior points of $H^{in}_{\mathbf{v}}$ go into V in positive time and $H^{in}_{\mathbf{v}} \cap W^s(\mathbf{v})$ is parametrized by $y = 0$. The set of points in $H^{in}_{\mathbf{v}}$ with positive (resp. negative) second coordinate is denoted by $H^{in,+}_{\mathbf{v}}$ (resp. $H^{in,-}_{\mathbf{v}}$).

The top and the bottom of the cylinder are denoted, respectively, $H^{out,+}_{\mathbf{v}}$ and $H^{out,-}_{\mathbf{v}}$. Trajectories starting at interior points of $H^{out,+}_{\mathbf{v}}$ and $H^{out,-}_{\mathbf{v}}$ go inside the cylinder in negative time.

After linearization $W^u(\mathbf{v})$ is the z-axis, intersecting $H^{out,+}_{\mathbf{v}}$ at the origin of coordinates of $H^{out,+}_{\mathbf{v}}$. Trajectories starting at $H^{in,j}_{\mathbf{v}}$, $j \in \{+, -\}$ leave V at $H^{out,j}_{\mathbf{v}}$.

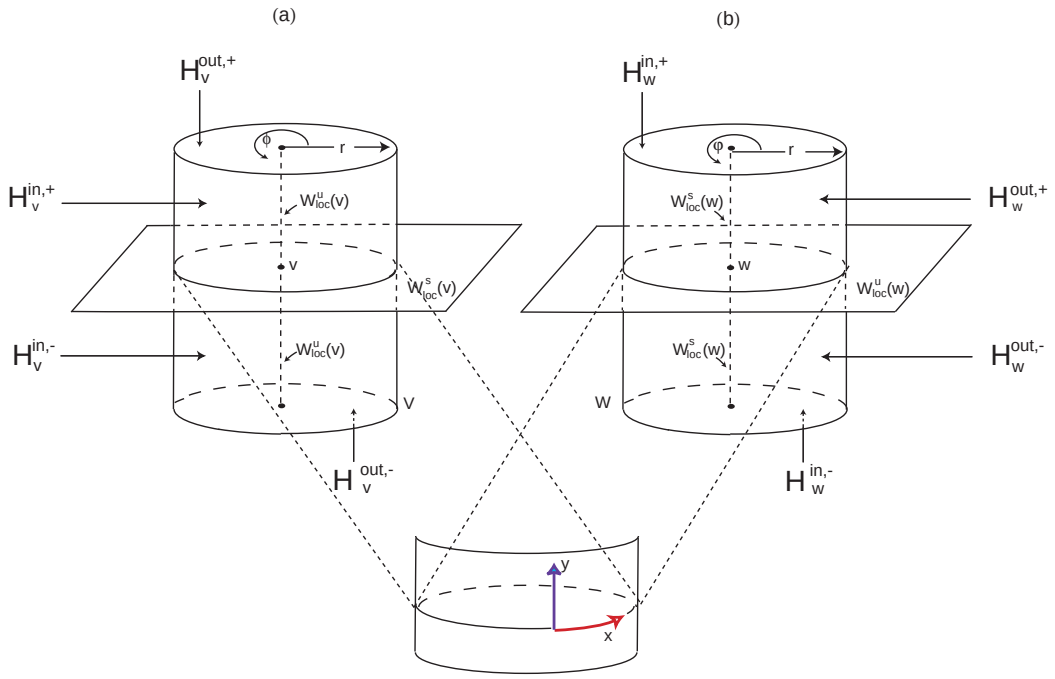

Figure 6: Neighbourhoods of the saddle-foci. (a) Once the flow goes in the cylinder V transversely across the wall $H^{in}_{\mathbf{v}}\backslash W^s(\mathbf{v})$, it leaves transversely across the top or the bottom $H^{out}_{\mathbf{v}}$; (b) Once the flow goes in the cylinder w transversely across the top or the bottom $H^{in}_{\mathbf{w}}\backslash W^s(\mathbf{w})$, it leaves transversely across the wall $H^{out}_{\mathbf{w}}$. Inside both cylinders, the vector field is linearized.

3.3 Coordinates near w

After linearization, $W^s(\mathbf{w})$ is the z -axis, intersecting the top and bottom of the cylinder at the origin of its coordinates. We denote by $H^{in,j}_{\mathbf{w}}$, $j \in \{-,+\}$, its two components. Trajectories starting at interior points of $H^{in,\pm}_{\mathbf{w}}$ go into W in positive time.

Trajectories starting at interior points of the cylinder wall $H^{out}_{\mathbf{w}}$ go into W in negative time. The set of points in $H^{out}_{\mathbf{w}}$ whose second coordinate is positive (resp. negative) is denoted $H^{out,+}_{\mathbf{w}}$ (resp. $H^{out,-}_{\mathbf{w}}$) and $H^{out}_{\mathbf{w}} \cap W^u(\mathbf{w})$ is parametrized by $y = 0$. Trajectories that start at $H^{in,j}_{\mathbf{w}}\backslash W^s(\mathbf{w})$, $j \in \{+,-\}$ leave the cylindrical neighbourhood at $H^{out,j}_{\mathbf{w}}$.

3.4 Local map near v

The local map $\Phi_{\mathbf{v}} : H^{in,+}_{\mathbf{v}} \to H^{out,+}_{\mathbf{v}}$ near $\mathbf{v}$ is given by

$$\Phi_{\mathbf{v}}(x,y) = (c_1 y^{\delta_{\mathbf{v}}}, -g_{\mathbf{v}} \ln y + x + c_2) = (r,\phi) \tag{3.4}$$

where $\delta_{\mathbf{v}}$ is the saddle index of $\mathbf{v}$,

$$\delta_v = \frac{C_{\mathbf{v}}}{E_{\mathbf{v}}} > 1, \quad c_1 = \varepsilon^{1-\delta_{\mathbf{v}}} > 0, \quad g_v = \frac{\alpha_{\mathbf{v}}}{E_{\mathbf{v}}} \quad \text{and} \quad c_2 = g_{\mathbf{v}} \ln(\varepsilon).$$

The expression for the local map from $H^{in,-}_{\mathbf{v}}$ to $H^{out,-}_{\mathbf{v}}$ we obtain for $y < 0$, $\phi_{\mathbf{v}}(x,y) = \phi_{\mathbf{v}}(x,-y)$.

3.5 Local map near w

The local map $\Phi_{\mathbf{w}} : H^{in,+}_{\mathbf{w}} \backslash W^s(\mathbf{w}) \to H^{out,+}_{\mathbf{w}}$ near $\mathbf{w}$ is given by:

$$\Phi_{\mathbf{w}}(r,\varphi) = (c_3 - g_{\mathbf{w}} \ln r + \varphi, c_4 r^{\delta_{\mathbf{w}}}) = (x,y) \ ,$$

where $\delta_{\mathbf{w}}$ is the saddle index of $\mathbf{w}$,

$$\delta_{\mathbf{w}} = \frac{C_{\mathbf{w}}}{E_{\mathbf{w}}} > 1, \quad g_{\mathbf{w}} = \frac{\alpha_{\mathbf{w}}}{E_{\mathbf{w}}}, \quad c_3 = g_{\mathbf{w}} \ln \varepsilon \quad \text{and} \quad c_4 = \varepsilon^{1-\delta_{\mathbf{w}}} > 0.$$

The same expression holds for the local map from $H^{in,-}_{\mathbf{w}} \backslash W^s(\mathbf{w})$ to $H^{out,-}_{\mathbf{w}}$.

3.6 Geometry near the saddle-foci v and w

The notation and constructions of previous subsections are now used to study the geometry associated to the local dynamics around each saddle-foci.

Definition 1 *1. A* segment β on $H^{in}_{\mathbf{v}}$ *or* $H^{out}_{\mathbf{w}}$ *is a smooth regular parametrized curve of the type* $\beta : [0,1] \to H^{in}_{\mathbf{v}}$ *or* $\beta : [0,1] \to H^{out}_{\mathbf{w}}$ *that meets* $W^s_{loc}(\mathbf{v})$ *or* $W^u_{loc}(\mathbf{w})$ *transversely at the point* $\beta(1)$ *only and such that, writing* $\beta(s) = (x(s), y(s))$*, both* x *and* y *are monotonic functions of* s*.*

2. A spiral on $H^{out}_{\mathbf{v}}$ *or* $H^{in}_{\mathbf{w}}$ around *a point* p *is a curve* $\alpha : [0,1) \to H^{out}_{\mathbf{v}}$ *or* $\alpha : [0,1) \to H^{in}_{\mathbf{w}}$ *satisfying* $\lim_{s \to 1^-} \alpha(s) = p$ *and such that, if* $\alpha(s) = (\alpha_1(s), \alpha_2(s))$ *are its expressions in polar coordinates* (ρ, θ) *around* p*, then* α_1 *and* α_2 *are monotonic, with* $\lim_{s\to 1^-} |\alpha_2(s)| = +\infty$*.*

3. Let $a, b \in \mathbf{R}$ *such that* $a < b$ *and let* $H^{out}_{\mathbf{w}}$ *be a surface parametrized by a covering* $(\theta, h) \in \mathbf{R} \times [a,b]$ *where* θ *is periodic. A* helix on $H^{out}_{\mathbf{w}}$ accumulating on the circle $h = h_0$ *is a curve* $\gamma : [0,1) \to H$ *such that its coordinates* $(\theta(s), h(s))$ *are monotonic functions of* s *with* $\lim_{s\to 1^-} h(s) = h_0$ *abd* $\lim_{s\to 1^-} |\theta(s)| = +\infty$*.*

At the item 2 of the previous definition, p will be the intersection of the one dimensional local stable/unstable manifold of $\mathbf{v}$ or $\mathbf{w}$ with the considered cross section. At the item 3, the curve is the intersection of the two dimensional local unstable manifold of $\mathbf{w}$ with the cross section $H^{out}_{\mathbf{w}}$. Observing figure 7, the definitions become clear. The next lemma summarises some basic technical results about the geometry near the saddle-foci. The proof may be found in section 6 of Aguiar *et al* [5] - this is why it will be omitted.

Lemma 11 *1. For* $j \in \{+,-\}$*, a segment* β *on* $H^{in,j}_{\mathbf{v}}$ *is mapped by* $\phi_{\mathbf{v}}$ *into a spiral on* $H^{out,j}_{\mathbf{v}}$ *around* $W^u(\mathbf{v})$*;*

2. For $j \in \{+,-\}$*, a segment* β *on* $H^{out,j}_{\mathbf{w}}$ *is mapped by* $\phi^{-1}_{\mathbf{w}}$ *into a spiral on* $H^{in,j}_{\mathbf{w}}$ *around* $W^s(\mathbf{w})$*;*

3. For $j \in \{+,-\}$*, a spiral on* $H^{in,j}_{\mathbf{w}}$ *around* $W^s(\mathbf{w})$ *is mapped by* ϕ_w *into a helix on* $H^{out,j}_{\mathbf{w}}$ *accumulating on the circle* $H^{out}_{\mathbf{w}} \cap W^u(\mathbf{w})$*.*

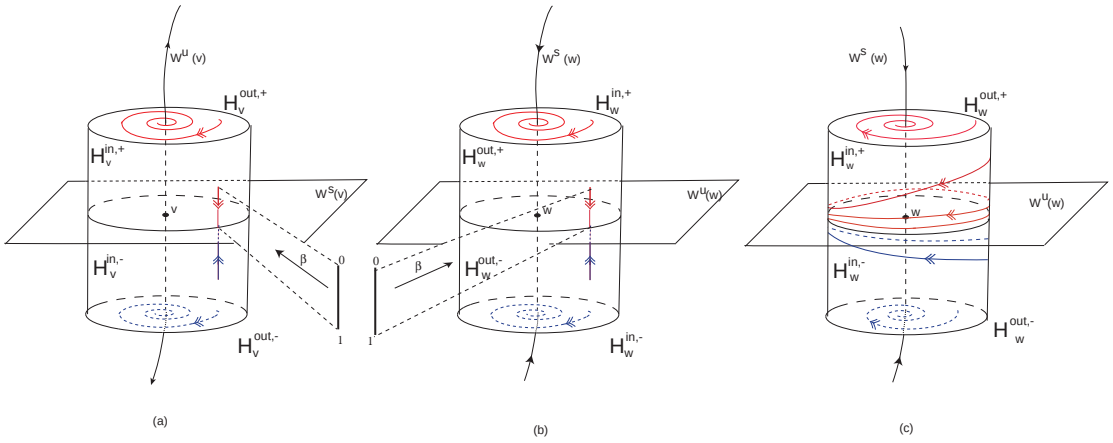

Figure 7: Smooth structures referred in lemma 11. (a): a segment β on $H^{in,j}_{\mathbf{v}}$ is mapped by $\phi_{\mathbf{v}}$ into a spiral on $H^{out,j}_{\mathbf{v}}$ around $W^u(\mathbf{v})$; (b): a segment β on $H^{out,j}_{\mathbf{w}}$ is mapped by $\phi^{-1}_{\mathbf{w}}$ into a spiral on $H^{in,j}_{\mathbf{w}}$ around $W^s(\mathbf{w})$; (c): a spiral on $H^{in,j}_{\mathbf{w}}$ around $W^s(\mathbf{w})$ is mapped by ϕ_w into a helix on $H^{out,j}_{\mathbf{w}}$ accumulating on the circle $H^{out}_{\mathbf{w}} \cap W^u(\mathbf{w})$.

3.7 Transition Maps

In the rest of this paper, we study the Poincaré first return map on the boundaries defined in this section. Consider the transition maps

$$\Psi_{\mathbf{v},\mathbf{w}} : H^{out,j}_{\mathbf{v}} \longrightarrow H^{in,j}_{\mathbf{w}} \qquad j = +,- \quad \text{and} \quad \Psi_{\mathbf{w},\mathbf{v}} : H^{out}_{\mathbf{w}} \longrightarrow H^{in}_{\mathbf{v}}.$$

For $\lambda_1 = 0$, the map $\Psi_{\mathbf{w},\mathbf{v}}$ may be taken to be the identity. For $\lambda_1 \neq 0$, the map can be seen as a rotation by an angle $\alpha(\lambda_1)$ with $\alpha(0) = 0$. Without loss of generality, we use $\alpha = \frac{\pi}{2}$, that simplifies the expressions used.

For $\lambda_2 = 0$ one of the connections $[\mathbf{w} \to \mathbf{v}]$ goes from $H^{out,+}_{\mathbf{v}}$ to $H^{in,+}_{\mathbf{w}}$. For $\lambda_2 = 0$, the linear part of the map $\Psi_{\mathbf{v},\mathbf{w}}$ may be represented (in rectangular coordinates) as the composition of a rotation of the coordinate axes and a change of scales. As in Bykov [7], after a rotation and a uniform rescaling of the coordinates, we may assume without loss of generality that for $\lambda_2 \neq 0$, $\Psi_{\mathbf{v},\mathbf{w}}$ is given by the map $T(x,y) + L(x,y)$, where:

$$T(x,y) = \begin{pmatrix} \lambda_2 \\ 0 \end{pmatrix} \qquad \text{and} \qquad L(x,y) = \begin{pmatrix} a & 0 \\ 0 & \frac{1}{a} \end{pmatrix} \qquad a \in \mathbf{R}^+ \backslash \{1\}$$

Note that the map $\Psi_{\mathbf{v},\mathbf{w}}$ is given in rectangular coordinates. To compose this map with $\Phi_{\mathbf{v}}$, it is required to change the coordinates. We address this issue later in section 5. We summarise the above information in the table below:

Parameters	Symmetries preserved	$\Psi_{\mathbf{v},\mathbf{w}}$	$\Psi_{\mathbf{w},\mathbf{v}}$
$\lambda_1 = \lambda_2 = 0$	γ_1, γ_2	L	Identity
$\lambda_1 \neq 0$ and $\lambda_2 = 0$	γ_1	L	Rotation
$\lambda_1 = 0$ and $\lambda_2 \neq 0$	γ_2	$T \circ L$	Identity
$\lambda_1 \neq 0$ and $\lambda_2 \neq 0$	Identity	$T \circ L$	Rotation

With this choice of local coordinates the maps $\Phi_{\mathbf{v}}$ and $\Phi_{\mathbf{w}}$ do not depend on λ_1, λ_2. The transition map $\Psi_{\mathbf{w},\mathbf{v}}$ may be taken to depend on λ_1 but not on λ_2 and is written as $\Psi_{\mathbf{w},\mathbf{v}}(x, y, \lambda_1)$.

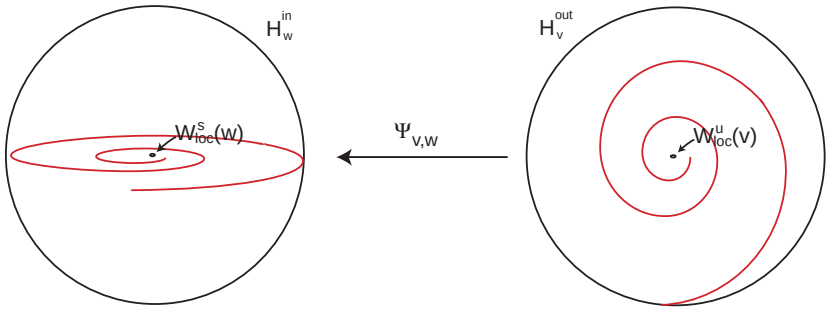

Figure 8: The transition map from $\mathbf{v}$ to $\mathbf{w}$. We set that the transition map from $\mathbf{v}$ to $\mathbf{w}$ may be approximated by a diagonal map.

The other transition map $\Psi_{\mathbf{v},\mathbf{w}}$ may be taken to depend on λ_2 but not on λ_1 and is written as $\Psi_{\mathbf{v},\mathbf{w}}(r, \varphi, \lambda_2)$.

4 Transverse Intersection of 2-dimensional manifolds

In this section, when we break the $\mathbf{Z}_2(\gamma_1)$ equivariance, using property (P6), we are assuming that the heteroclinic connection between $\mathbf{w}$ and $\mathbf{v}$ becomes transverse and one-dimensional. We still have a heteroclinic network of a different nature, which will be denoted by $\Sigma^\star$.

4.1 Same orientaton around equilibria (P8a)

4.1.1 Proof of Proposition 2

Items 1 and 2 of proposition 2 follows from the three facts:

- the equilibria are hyperbolic;
- the fixed point subspace that contains the two connections $[\mathbf{v} \to \mathbf{w}]$ remains invariant;
- dim $W^u(\mathbf{v}) = 1$ and $W^u(\mathbf{v}) \subset Fix\,\langle\gamma_1\rangle$.

Item 3 is a direct consequence of the main result about finite and infinite switching of Aguiar *et al* [5]. Item 4 follows straightforwardly from the referred paper picking the segment β as $W^u(\mathbf{w})$.

In order to prove item 5, we start with some terminology about horizontal and vertical strips. Given a rectangular region $\mathcal{R}$ in $H^{in}_{\mathbf{v}}$ or in $H^{out}_{\mathbf{w}}$ parametrized by a rectangle $R = [w_1, w_2]\times[z_1, z_2]$, a *horizontal strip* in $\mathcal{R}$ will be parametrized by:

$$\mathcal{H} = \{(x, y) : x \in [w_1, w_2], y \in [u_1(x), u_2(x)]\},$$

where

$$u_1, u_2 : [w_1, w_2] \to [z_1, z_2]$$

are Lipschitz functions such that $u_1(x) < u_2(x)$. The *horizontal boundaries* of the strip are the lines parametrized by the graphs of the u_i, the *vertical boundaries* are the lines $\{w_i\} \times [u_1(w_i), u_2(w_i)]$ and its *heigth* is

$$h = \max_{x\in[w_1,w_2]} (u_2(x) - u_1(x)) .$$

When both $u_1(x)$ and $u_2(x)$ are constant functions we call $\mathcal{H}$ a *horizontal rectangle across* $\mathcal{R}$. A *vertical strip across* $\mathcal{R}$, its *width* and a *vertical rectangle* have similar definitions, with the roles of x and y reversed.

Item 5 follows from the construction of the Cantor sets presented in Aguiar *et al* [3] – if $R_{\mathbf{v}} \subset H^{in}_{\mathbf{v}}$ is a rectangle containing $[\mathbf{w} \to \mathbf{v}] \cap H^{in}_{\mathbf{v}}$ on its border, the initial conditions that returns to $H^{in}_{\mathbf{v}}$ are contained in a sequence of horizontal strips accumulating on the stable manifold of $\mathbf{v}$, whose heights tend to zero. Each one of these horizontal strips lying on the rectangle $R_{\mathbf{v}} \subset H^{in}_{\mathbf{v}}$, is mapped by $\Phi_{\mathbf{w}} \circ \Psi_{\mathbf{v},\mathbf{w}} \circ \Phi_{\mathbf{v}}$ into a horizontal strip across $H^{out}_{\mathbf{w}}$. By (P6), they are mapped by $\Psi_{\mathbf{v},\mathbf{w}}$ into vertical strips across $R_{\mathbf{w}}$ crossing transversely the original. This gives rise to a nested chain of uniformly hyperbolic horseshoes, accumulating on the heteroclinic connection, each one with positive topological entropy [13]. An illustration of the way these horseshoes are appearing is given in figure 4.

4.1.2 Proof of Corollary 5

The proof of Corollary 5 is connected with the geometry of the horseshoe G_n which arises near the cycle (see item 5 of proposition 2). Each horizontal strip in $H^{in}_{\mathbf{v}}$ is mapped by the first return map into a vertical strip. This vertical strip intersects transverselly n times the original horizontal strip. As in Hirasawa *et al* [22], denoting the consecutive intersection points by $p_1, \ldots, p_n$, we are able to construct the *twist signature* of the horseshoe associated to G_n: is a finite sequence of integers $(a_i)_{i\in\{1,\ldots,n\}}$ satisfying the following conditions:

- $a_1 = 0$;
- $a_i = a_{i-1} + 1$ if the oriented segment $[p_{i-1}, p_i]$ goes around the counterclockwise direction;
- $a_i = a_{i-1} - 1$ if the oriented segment $[p_{i-1}, p_i]$ goes around the clockwise direction.

We will use the following result of Hirasawa and Kin [22] [adapted]:

Theorem 12 *Let G a generalized horseshoe map with twist signature $(a_1, a_2, \ldots, a_n)$. Then G induces all link types if and only if one of the following is satisfied:*

- *each $a_i \geq 0$ and $\max\{a_i\} \geq 3$.*
- *each $a_i \leq 0$ and $\max\{a_i\} \geq -3$.*

For $n > 2$, the generalised horseshoe G_n induces all links because the admissible signatures are of the type $(0, 1, 2, 3, \ldots, n)$ or $(0, -1, -2, -3, \ldots, -n)$ (the intersection of the horseshoes is clear in the arrows in figure 9).

4.2 Opposite Orientation around equilibria (P8b)

In this section, we give a more precise formulation of Theorem 6 and prove it. Consider the conditions

$$\alpha_{\mathbf{v}} > 0 \quad \text{and} \quad \frac{1}{2}\sqrt{\frac{\eta^2}{1+\eta^2}}\left[\frac{1}{a^2} - a^2\right] > g_{\mathbf{w}}^{-1} + \eta^{-1}\left[a^2\frac{1-\sqrt{\frac{1}{1+\eta^2}}}{2} + \frac{1}{a^2}\frac{1+\sqrt{\frac{1}{1+\eta^2}}}{2}\right] \tag{4.5}$$

and

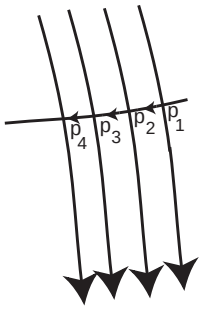

Figure 9: Pleated Diagram associated to G_n, the spine of the generalized horseshoe: given two oriented horizontal and vertical boundaries in $R_{\mathbf{v}}$, h and v respectively, the pleated diagram associated to the horseshoe is the union of the oriented arcs $v \cup \Psi_{\mathbf{w},\mathbf{v}} \circ \Phi_{\mathbf{w}} \circ \Psi_{\mathbf{v},\mathbf{w}} \circ \Phi_{\mathbf{v}}(h)$ (see definition 2.11 of Hirasawa and Kin [22]).

$$\alpha_{\mathbf{v}} < 0 \quad \text{and} \quad -\frac{1}{2}\sqrt{\frac{\eta^2}{1+\eta^2}}\left[\frac{1}{a^2} - a^2\right] < g_{\mathbf{w}}^{-1} + \eta^{-1}\left[a^2\frac{1-\sqrt{\frac{1}{1+\eta^2}}}{2} + \frac{1}{a^2}\frac{1+\sqrt{\frac{1}{1+\eta^2}}}{2}\right]. \quad (4.6)$$

where $\eta = \frac{\alpha_{\mathbf{v}}}{C_{\mathbf{v}}}$ and $a > 1$ is the parameter appearing in the transition map $\Psi_{\mathbf{v},\mathbf{w}}$. Clearly, the set of vector fields that satisfy (P1)–(P4) and (P8b) and either (4.5) or (4.6) is open in the C^2–topology. For these vector fields, given a neighbourhood $\mathcal{U}$ in $H^{in}_{\mathbf{v}}$ of $p \in W^u(\mathbf{w}) \cap W^s(\mathbf{v}) \cap H^{in}_{\mathbf{v}}$, let ξ be the connected component of $W^u(\mathbf{w}) \cap H^{in}_{\mathbf{v}}$ containing p, with a choice of orientation on this curve. Then $\Phi_{\mathbf{w}} \circ \Psi_{\mathbf{v},\mathbf{w}} \circ \Phi_{\mathbf{v}}(\xi)$ defines an oriented curve in $H^{out}_{\mathbf{w}}$. This curve changes the direction of its turning around the cylinder wall $H^{out}_{\mathbf{w}}$ at points where it has vertical tangent.

Definition 2 *We say that the vector field has the* dense reversals property *if for any neighbourhood $\mathcal{U}$ of p the projection into $W^u_{loc}(\mathbf{w})$ of the points where $\Phi_{\mathbf{w}} \circ \Psi_{\mathbf{v},\mathbf{w}} \circ \Phi_{\mathbf{v}}(\xi)$ has a vertical tangent is dense in $W^u_{loc}(\mathbf{w})$.*

Proposition 13 *In a generic one parameter family f_{λ_1} of smooth $\langle\gamma_1\rangle$-equivariant vector fields on $\mathbf{S}^3$ satisfying (P1)–(P4), (P8b) and either (4.5) or (4.6), with C^2 dependence of parameter λ_1, all the vector fields f_{λ_1} have the dense reversals property, except for a countable set of values of λ_1.*

Proof: Without loss of generality, we are assuming that $W^u(\mathbf{w}) \cap H^{in}_{\mathbf{v}}$ is a segment parametrized by $(s, \lambda_1 s)$ with $0 < s \ll 1$. The image of $W^u(\mathbf{w}) \cap H^{in}_{\mathbf{v}}$ by the local map near $\mathbf{v}$, $\Phi_{\mathbf{v}}$, is given by:

$$\Phi_{\mathbf{v}}(s, \lambda_1 s) = (c_1^\star s^{\delta_{\mathbf{v}}}, s - g_{\mathbf{v}} \ln s + c_2^\star) = (r, \varphi), \quad (4.7)$$

where $c_1^\star$ and $c_2^\star$ depend on λ_1. By lemma 11 of section 3.6, this curve is a spiral accumulating on $W^u_{loc}(\mathbf{v}) \cap H^{out}_{\mathbf{v}}$. Transforming the polar coordinates of $\Phi_{\mathbf{v}}(s, \lambda_1 s)$ into rectangular coordinates, it yields:

$$\begin{cases} x = r\cos(\varphi) \\ y = r\sin(\varphi) \end{cases} \quad (4.8)$$

Since we are considering that the transition map $\Psi_{\mathbf{v},\mathbf{w}}$ from $H^{out}_{\mathbf{v}}$ to $H^{in}_{\mathbf{w}}$ may be approximated by the linear map $\Psi_{\mathbf{v},\mathbf{w}}(x, y) = \left(ax, \frac{1}{a}y\right)$, with $a > 1$ (see figure 8). Note that if the argument

of $L(x,y)$ lies in the interval $\left(\frac{k\pi}{2}, \frac{(k+1)\pi}{2}\right)$, then the argument of $\Psi_{\mathbf{v},\mathbf{w}}(x,y)$ lies in the same interval. This, we may write $\Psi_{\mathbf{v},\mathbf{w}} \circ \Phi_{\mathbf{v}}(s, \lambda_1 s)$ in polar coordinates as

$$\begin{cases} R = \sqrt{a^2 r^2 \cos^2(\varphi) + \frac{1}{a^2} r^2 \sin^2(\varphi)} & \\ \Phi = \arctan\left(\frac{1}{a^2}\tan(\varphi)\right) & \text{if} \quad \varphi \in \left(\frac{-\pi}{2}, \frac{\pi}{2}\right) \\ \Phi = \operatorname{arccotan}\left(a^2 \operatorname{cotan}(\varphi)\right) & \text{if} \quad \varphi \in (0, \pi) \\ \Phi = \arctan\left(\frac{1}{a^2}\tan(\varphi)\right) + \pi & \text{if} \quad \varphi \in \left(\frac{\pi}{2}, \frac{3\pi}{2}\right) \\ \Phi = \operatorname{arccotan}\left(a^2 \operatorname{cotan}(\varphi)\right) + \pi & \text{if} \quad \varphi \in (\pi, 2\pi) \end{cases} \tag{4.9}$$

Note that the radial component may be written as:

$$R = r\sqrt{a^2 \cos^2(\varphi) + \frac{1}{a^2}\sin^2(\varphi)}.$$

Using the expression of the local map near $\mathbf{w}$, $\Phi_{\mathbf{w}}$, it follows that $\Phi_{\mathbf{w}} \circ \Psi_{\mathbf{v},\mathbf{w}} \circ \Phi_{\mathbf{v}}(s, \lambda_1 s)$ is given by:

$$\begin{cases} x = c_3 - g_{\mathbf{w}} \ln\left(r\sqrt{a^2\cos^2(\varphi) + \frac{1}{a^2}\sin^2(\varphi)}\right) + \Phi \\ y = c_4 r^{\delta_{\mathbf{w}}} \left(a^2\cos^2(\varphi) + \frac{1}{a^2}\sin^2(\varphi)\right)^{\frac{\delta_{\mathbf{w}}}{2}} \end{cases} \tag{4.10}$$

Of course, x and y depend on r and φ, which depend on s. The curve $(x(s), y(s))$ will not correspond to a helix on $H^{out}_{\mathbf{w}}$ because the angular angular component $x(s)$ may not be monotonic although the height tends to zero. The angular coordinate $x_{\mathbf{w}}(s)$ of $\Phi_{\mathbf{w}} \circ \Psi_{\mathbf{v},\mathbf{w}} \circ \Phi_{\mathbf{v}}(s, \lambda_1 s)$ may be written as:

$$c_3 - g_{\mathbf{w}} \ln r - \frac{g_{\mathbf{w}}}{2} \ln\left(a^2\cos^2(\varphi) + \frac{1}{a^2}\sin^2(\varphi)\right) + \Phi$$

where (r, φ) are given in (4.7). First of all, we would like to find the zeros of its derivative. Generically, they will correspond to the points where the curve $(x(s), y(s))$ changes the orientation on the wall. Let

$$C(\varphi) = a^2\cos^2(\varphi) + \frac{1}{a^2}\sin^2(\varphi).$$

The derivative of $x_{\mathbf{w}}(s)$ does not depend on the choice of branch in (4.9) and is given by:

$$\frac{dx_{\mathbf{w}}}{ds}(s) = \frac{1}{s}\left[-g_{\mathbf{w}}\delta_{\mathbf{v}} + \frac{g_{\mathbf{v}} g_{\mathbf{w}}}{2}\left(\frac{1}{a^2} - a^2\right)\frac{\sin(2\varphi)}{C(\varphi)} - \frac{g_{\mathbf{v}}}{C(\varphi)}\right] + \tag{4.11}$$

$$+\frac{1}{C(\varphi)}\left[\frac{-g_{\mathbf{v}} g_{\mathbf{w}}}{2}\left[\frac{1}{a^2} - a^2\right]\sin(2\varphi) + 1\right].$$

We show in Lemma 15 below that this derivative is zero at two sequences s_n with

$$\lim_{n\to\infty} s_n = 0 \quad \text{and} \quad x_{\mathbf{w}}(s_n) \approx \frac{g_{\mathbf{w}}\delta_{\mathbf{v}} n\pi}{g_{\mathbf{v}}} + c_3^\star, \tag{4.12}$$

where $c_3^\star$ depends continuously on λ_1, on a and on the eigenvalues of the linearization of the vector field at $\mathbf{v}$ and $\mathbf{w}$. □

Lemma 14 *Let k and t be continuous maps defined on $\boldsymbol{R}_0^+$ such that:*

1. *there is a sequence s_j such that $k(s)$ changes sign at s_j and $\lim_{j\in\boldsymbol{N}} s_j = 0$;*

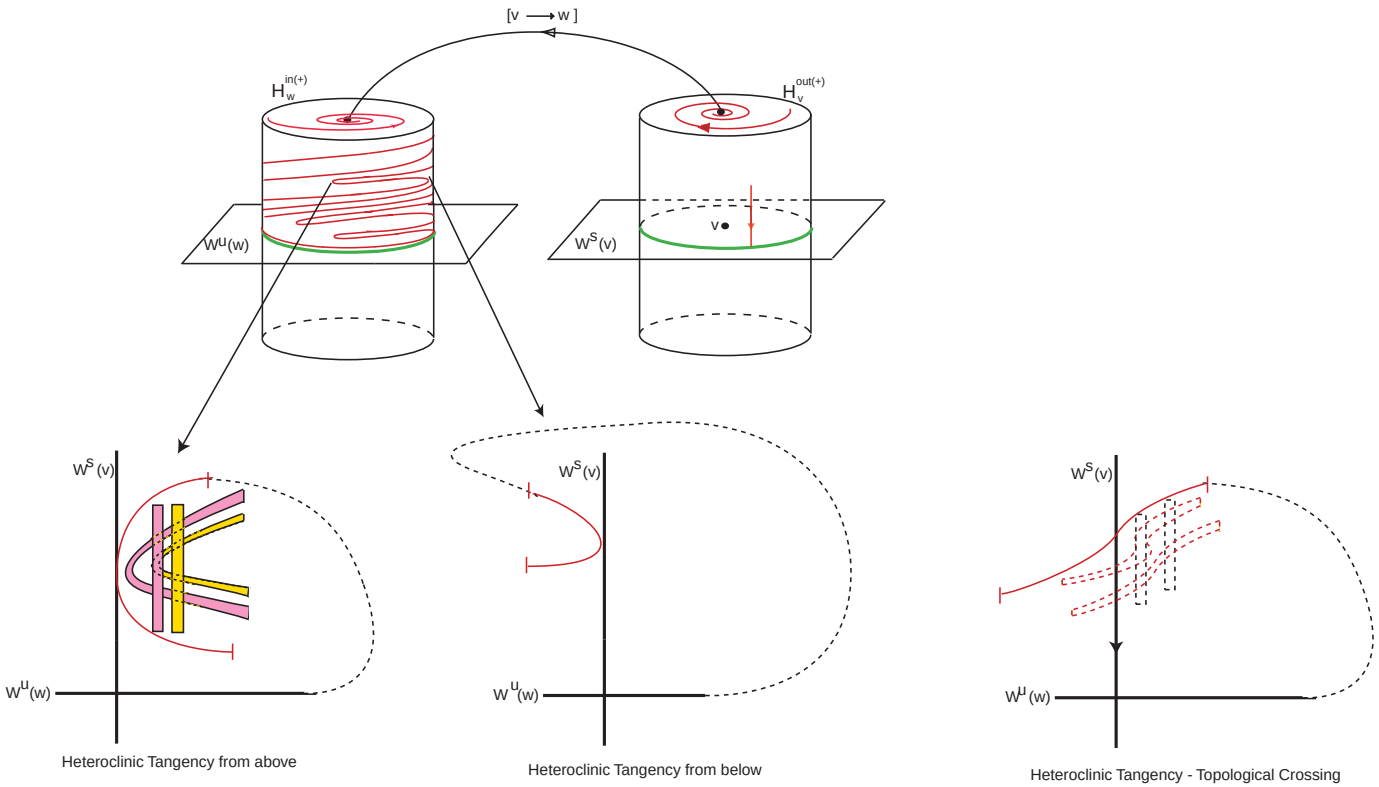

Figure 10: On the cross section $H^{out}_{\mathbf{w}}$ (on left), we see the curve reversing the orientation of its angular coordinate.

2. if a and b are two zeros of k, then there exists $x_{a,b} \in (a,b)$ such that $|k(x_{a,b})| > |t(x_{a,b})|$.

Then there is a sequence σ_j such that $\lim_{j\to\infty} \sigma_j = 0$, of points where $f(s) = \frac{k(s)}{s} + t(s)$ changes sign, satisfying

$$s_{2j+2} < \sigma_j < s_{2j}.$$

Proof: First of all, note that if $s > 0$ then:

$$sign(f) = sign\left(\frac{k(s)}{s} + t(s)\right) = sign(k(s) + s.t(s)). \tag{4.13}$$

Since k has infinitely many changes of sign near zero, then there exists infinitely many terns (a,b,c), such that:

- $0 < a < b < c$;
- $k(a) = k(b) = k(c) = 0$;
- $\forall s \in (a,b), k(s) > 0$;
- $\forall s \in (b,c), k(s) < 0$.

From the hypothesis (2), we know that there exists $x_{a,b} \in (a,b)$ and $x_{b,c} \in (b,c)$ such that $|k(x_{a,b})| > |t(x_{a,b})|$ and $-k(x_{b,c}) > |t(x_{b,c})|$. Using equality (4.13), this means that $sign(f)$ changes in (a,c). From the existence of infinitely many terns (a,b,c) as above, then f has infinitely many changes of sign. The existence of infinitely many zeros of f follows by its continuity in $\mathbf{R}_0^+$. □

Lemma 15 *Under the hypothesis of proposition 13, there are two sequences $(s_n)_n$ such that $s_n > 0$, $\lim_{n\to\infty} s_n = 0$ and*

$$\frac{dx_{\mathbf{w}}}{ds}(s_n) = 0 \quad with \quad x_{\mathbf{w}}(s_n) \approx \frac{g_{\mathbf{w}}\delta_{\mathbf{v}} n\pi}{g_{\mathbf{v}}} + c_3^\star,$$

where $c_3^\star$ is a constant that, for each sequence $(s_n)_n$, depends on λ_1, on the eigenvalues of the linearization of the vector field around $\mathbf{v}$ and $\mathbf{w}$ and on the transition map $\Psi_{\mathbf{v},\mathbf{w}}$.

Proof: Using lemma 14, to show that the equation $\frac{dx_{\mathbf{w}}}{ds}(s) = 0$ has infinitely many zeros is equivalent to prove that the equation

$$\sin(2\varphi) = \frac{g_{\mathbf{v}} + g_{\mathbf{w}}\delta_{\mathbf{v}} C(\varphi)}{\frac{g_{\mathbf{v}} g_{\mathbf{w}}}{2}\left(\frac{1}{a^2} - a^2\right)} \tag{4.14}$$

has infinitely many solutions. The equation (4.14) is equivalent to:

$$\frac{1}{2}\sin(2\varphi)\left[\frac{1}{a^2} - a^2\right] = \frac{E_{\mathbf{w}}}{\alpha_{\mathbf{w}}} + \frac{C_{\mathbf{v}}}{\alpha_{\mathbf{v}}} C(\varphi). \tag{4.15}$$

Note that the solutions of $\frac{dx_{\mathbf{w}}}{ds}(s) = 0$ and those of equation (4.15) are arbitrarily close, when s is close to zero. We want to write these solutions as functions of s of lemma 16, *ie*, we want to solve (for s) the equations:

$$-g_{\mathbf{v}} \ln(s_n) + s_n + c_2^\star = \phi_1 + n\pi \quad \text{and} \quad -g_{\mathbf{v}} \ln(s_n) + s_n + c_2^\star = \phi_2 + n\pi.$$

Taking into account that $s \approx 0$, then we may write:

$$s_n(\phi_1) \approx \exp\left[\frac{\phi_1 + n\pi - c_2^\star}{-g_{\mathbf{v}}}\right] \quad \text{and} \quad s_n(\phi_2) \approx \exp\left[\frac{\phi_2 + n\pi - c_2^\star}{-g_{\mathbf{v}}}\right].$$

The expression of $x_{\mathbf{w}}$ evaluated at $s_n(\phi_1) \equiv s_n$ is given by:

$$x_{\mathbf{w}}(s_n) = c_3 - g_{\mathbf{w}} \ln(c_1^\star s_n^{\delta_{\mathbf{v}}}) - \frac{g_{\mathbf{w}}}{2} \ln(a^2 \cos^2(\varphi_n^\star(\phi_1)) + \frac{1}{a^2} \sin^2(\varphi_n^\star(\phi_1))) + \arctan\left(\frac{1}{a^2} \tan(\varphi_n^\star(\phi_1))\right)$$

Recalling that $\varphi_n^\star(\phi_1) = \phi_1 + n\pi$, $C(\varphi)$ and tan are π-periodic and using the expression of $s_n(\phi_1)$, it follows that the only term in $x_{\mathbf{w}}(s_n)$ that depends on n is $-g_{\mathbf{w}} \ln(c_1^\star s_n^{\delta_{\mathbf{v}}}(\phi_1))$. Grouping the terms that do not depend on n into a constant $c_3^\star \in \mathbf{R}$, we get:

$$x_{\mathbf{w}}(s_n) = \frac{g_{\mathbf{w}} \delta_{\mathbf{v}} n\pi}{g_{\mathbf{v}}} + c_3^\star.$$

□

Lemma 16 *Under the hypothesis of Proposition 13, the equation*

$$\frac{1}{2} \sin(2\varphi) \left[\frac{1}{a^2} - a^2\right] = \frac{E_{\mathbf{w}}}{\alpha_{\mathbf{w}}} + \frac{C_{\mathbf{v}}}{\alpha_{\mathbf{v}}} C(\varphi)$$

has two solutions $\phi_1, \phi_2 \in [0, \pi]$.

Proof: We are going to study the maps which appear in the two members of equation (4.15), whose graphs are depicted in figure 12:

$$g_1(\varphi) = \frac{1}{2} \sin(2\varphi) \left[\frac{1}{a^2} - a^2\right] \quad \text{and} \quad g_2(\varphi) = g_{\mathbf{w}}^{-1} + \frac{C_{\mathbf{v}}}{\alpha_{\mathbf{v}}} C(\varphi).$$

Note that since $a > 1$, then $\left[\frac{1}{a^2} - a^2\right] < 0$. Also note that if $\alpha_{\mathbf{v}} > 0$ (resp.: $\alpha_{\mathbf{v}} < 0$), the equation has solutions if $\varphi \in \left[\frac{\pi}{2}, \frac{3\pi}{4}\right] + k\pi$ (resp.: $\varphi \in \left[\frac{\pi}{4}, \frac{\pi}{2}\right] + k\pi$), $k \in \mathbf{Z}$ (see figure 12).

The graphs of g_1 and g_2 have a tangency if they have the same derivative (necessary condition but not sufficient). The equality $g_1'(\varphi) = g_2'(\varphi)$ is equivalent to:

$$\cos(2\varphi) \left[\frac{1}{a^2} - a^2\right] = \frac{C_{\mathbf{v}}}{\alpha_{\mathbf{v}}} \left[\frac{1}{a^2} - a^2\right] \sin(2\varphi)$$

and then it follows immediately that $\tan(2\varphi) = \eta$ where $\eta = \frac{\alpha_{\mathbf{v}}}{C_{\mathbf{v}}}$. Denote by φ_n^* the solutions of the equation $g_1'(\varphi) = g_2'(\varphi)$ where the graphs g_1 and g_2 have the same slope. Now, we want to compute the image of $g_1(\varphi^*)$ and $g_2(\varphi^*)$ and impose that $g_1(\varphi^*) > g_2(\varphi^*)$ if $\alpha_v > 0$ and $g_1(\varphi^*) < g(\varphi^*)$ if $\alpha_v < 0$. Using trigonometric identities and the fact that $\tan(2\varphi^\star) = \eta$, it follows that

$$cos^2(2\varphi^\star) = \frac{1}{1+\eta^2} \quad \text{and} \quad sin^2(2\varphi^\star) = \frac{\eta^2}{1+\eta^2}$$

and

$$cos^2(\varphi^\star) = \frac{1 - \cos(2\varphi)}{2} \quad \text{and} \quad sin^2(\varphi^\star) = \frac{1 + \cos(2\varphi)}{2}$$

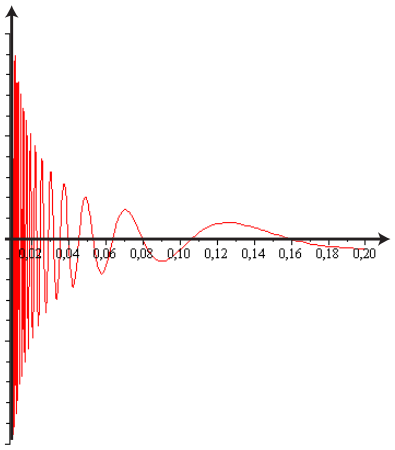

Figure 11: Graph of $\frac{1}{s}\left[-g_{\mathbf{w}}\delta_{\mathbf{v}} + \frac{g_{\mathbf{v}}g_{\mathbf{w}}}{2}\left(\frac{1}{a^2} - a^2\right)\frac{\sin(2\varphi)}{C(\varphi)} - \frac{g_{\mathbf{v}}}{C(\varphi)}\right]$ as a function of s, under the condition that equation (4.15) has solutions.

If $\alpha_{\mathbf{v}} > 0$ then both $\alpha_{\mathbf{w}}$ and $g_{\mathbf{w}}$ are negative by (P8b) and

$$g_1(\varphi^*) = \frac{1}{2}\sqrt{\frac{\eta^2}{1+\eta^2}}\left[\frac{1}{a^2} - a^2\right] > g_{\mathbf{w}}^{-1} + \eta^{-1}\left[a^2\frac{1-\sqrt{\frac{1}{1+\eta^2}}}{2} + \frac{1}{a^2}\frac{1+\sqrt{\frac{1}{1+\eta^2}}}{2}\right] = g_2(\varphi^*),$$

then the graphs g_1 and g intersect transverselly at a pair of points, meaning that $x_{\mathbf{w}}(s)$ changes the orientation. Analogously, if $\alpha_{\mathbf{v}} < 0$ then both $\alpha_{\mathbf{w}}$ and $g_{\mathbf{w}}$ are negative and

$$g_1(\varphi^*) = -\frac{1}{2}\sqrt{\frac{\eta^2}{1+\eta^2}}\left[\frac{1}{a^2} - a^2\right] < g_{\mathbf{w}}^{-1} + \eta^{-1}\left[a^2\frac{1-\sqrt{\frac{1}{1+\eta^2}}}{2} + \frac{1}{a^2}\frac{1+\sqrt{\frac{1}{1+\eta^2}}}{2}\right] = g_2(\varphi^*),$$

then the graphs g_1 and g_2 intersect transverselly into a pair of points. Since g_1 ang g_2 are π-periodic, the solutions of the equation $g_1(\varphi) = g_2(\varphi)$ (when they exist) are of the form

$$\varphi_n(\phi_1) := \phi_1 + n\pi \quad \text{and} \quad \varphi_n(\phi_2) := \phi_2 + n\pi,$$

with $n \in \mathbf{Z}$. □

Note that if (P8a) holds then for $\alpha_{\mathbf{v}} > 0$, we have $g_1(\varphi^*) < 0$ and $g_2(\varphi^*) > 0$, so $W^u_{loc}(\mathbf{w}) \cap H^{in}_v$ is mapped by $\Phi_{\mathbf{w}} \circ \Psi_{\mathbf{v},\mathbf{w}} \circ \Phi_{\mathbf{v}}$ into a helix in $H^{out}_{\mathbf{w}}$, since the curve $\Phi_{\mathbf{w}} \circ \Psi_{\mathbf{v},\mathbf{w}} \circ \Phi_{\mathbf{v}}(s, \lambda_1 s)$ never has a vertical tangency. Similarly, if $\alpha_{\mathbf{v}} > 0$ and (P8a) holds, then for $g_1(\varphi^*) > 0$ and $g_2(\varphi^*) < 0$ the same conclusion holds.

5 Proof of Theorem 7: existence of periodic trajectories

In this section, we treat the case $\lambda_1 = 0$ and $\lambda_2 \neq 0$, when the two-dimensional manifolds $W^u(\mathbf{w})$ and $W^s(\mathbf{v})$ coincide. We prove theorem 7 - the existence of a non-trivial closed trajectory - by finding a fixed point of the Poincaré first return map R in $H^{in}_{\mathbf{w}}$.

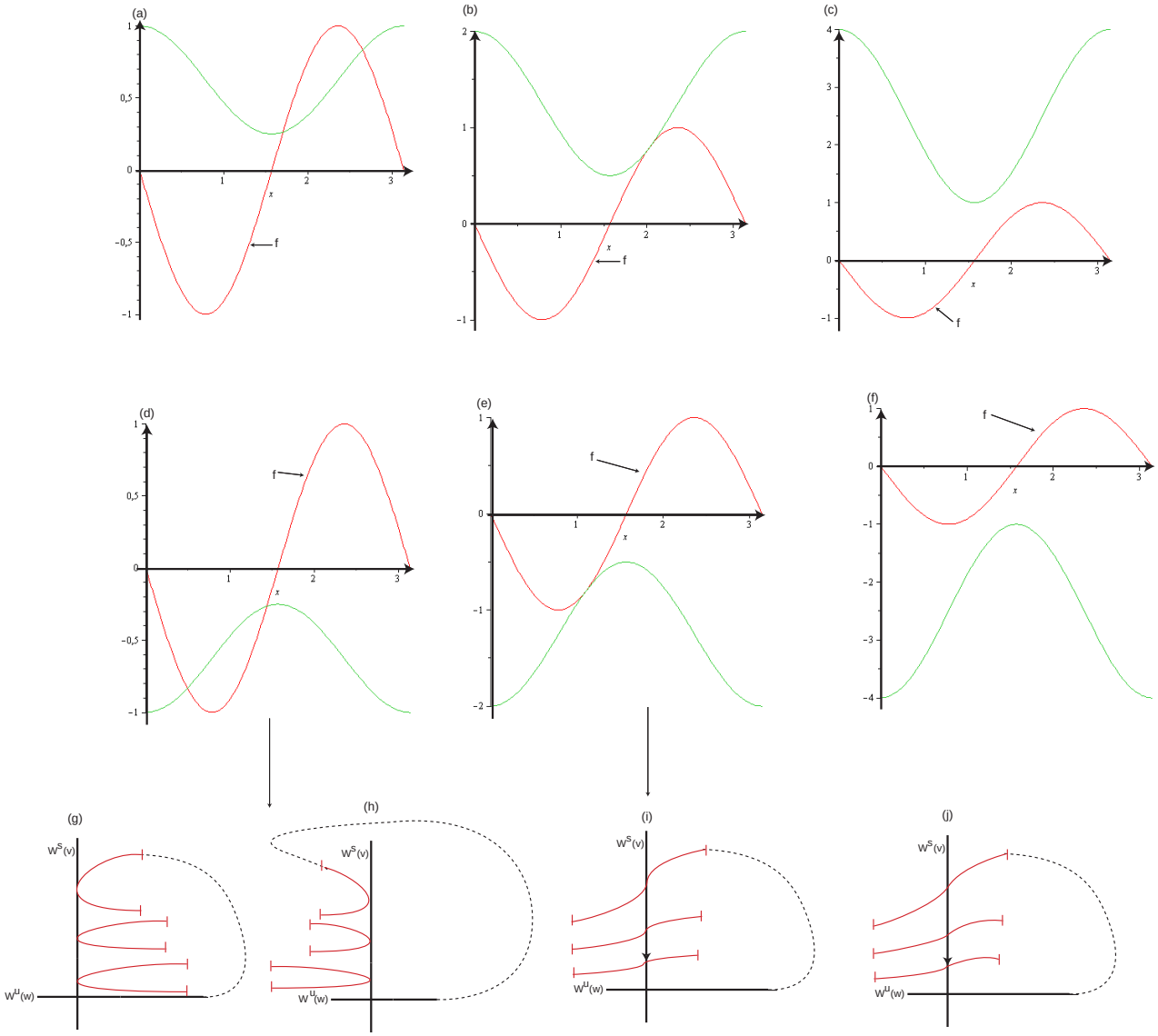

Figure 12: Plots of g_1 and g_2 referred in lemma 16. (a)-(c): $\alpha_{\mathbf{v}} > 0$;(d)-(f): $\alpha_{\mathbf{v}} < 0$. If g_1 and g_2 intersect as in figures (a) and (d), the homoclinic tangencies appear as in figures (g) and (h). If g_1 and g_2 have a tangency as in (b) and (e) we observe a topological crossing (i). If g_1 and g_2 do not intersect as in (c) and (f), then all invariant manifolds $W^u(\mathbf{w})$ and $W^s(\mathbf{v})$ meet transversely as depicted in figure (j).

5.1 Poincaré Map

Since $\lambda_1 = 0$, then $\Psi_{\mathbf{w},\mathbf{v}}$ is the identity. The symmetry γ_2 is preserved and thus the two half-spheres in $\mathbf{S}^3 \backslash Fix(\langle\gamma_2\rangle)$ are flow-invariant with symmetric dynamics. We look at one of them, where for $\lambda_2 = 0$ the connection goes from $H^{out,+}_{\mathbf{v}}$ to $H^{in,+}_{\mathbf{w}}$, omitting the redundant + signs to lighten the notation. Consider the map:

$$R_* = \Phi_{\mathbf{v}} \circ \Psi_{\mathbf{w},\mathbf{v}} \circ \Phi_{\mathbf{w}} : H^{in}_{\mathbf{w}} \backslash W^u_{loc}(\mathbf{w}) \quad \longrightarrow \quad H^{out}_{\mathbf{v}}$$

that in polar coordinates is given by

$$R_*(r,\varphi) = \Big(c_5 r^{\delta}, c_6 + \varphi - c_7 \ln(r)\Big) = (\rho,\theta) \tag{5.16}$$

where

$$c_5 = c_1 c_4^{\delta_{\mathbf{v}}} = \varepsilon^{1-\delta}, \quad \delta = \delta_{\mathbf{v}}\delta_{\mathbf{w}} \quad c_6 = -g_{\mathbf{v}} \ln(c_4) + c_2 + c_3 \quad c_7 = g_{\mathbf{v}}\delta_{\mathbf{w}} + g_{\mathbf{w}}$$

and, due to (P2), we have:

$$\delta = \delta_{\mathbf{v}}\delta_{\mathbf{w}} = \frac{C_{\mathbf{v}} C_{\mathbf{w}}}{E_{\mathbf{v}} E_{\mathbf{w}}} > 1. \tag{5.17}$$

It is worth noting that:

$$c_7 = g_{\mathbf{v}}\delta_{\mathbf{w}} + g_{\mathbf{w}} > 0.$$

In Cartesian coordinates, we have $R_*(r,\varphi) = (\rho\cos\theta, \rho\sin\theta) = (x,y)$.

The Poincaré first return map is λ_2-dependent and given by $R(r,\varphi) = \Psi_{\mathbf{w},\mathbf{v}}(R_*(r,\varphi),\lambda_2)$, where $\Psi_{\mathbf{w},\mathbf{v}} : H^{out}_{\mathbf{v}} \longrightarrow H^{in}_{\mathbf{w}}$ is given by $\Psi_{\mathbf{w},\mathbf{v}}(x,y) = (x+\lambda_2, y)$.

5.2 There are no multi-pulse heteroclinic connections $[\mathbf{v} \to \mathbf{w}]$

In this section, we will prove the first assertion of theorem 7. We start by making its statement more precise:

Definition 3 *Let $A \subset \mathcal{V}_{\mathbf{v}}$ be a cross-section to the flow meeting $W^u(\mathbf{v})$. A one-dimensional connection $[\mathbf{v} \to \mathbf{w}]$ that meets A at precisely k points is called a* k-pulse heteroclinic connection *with respect to A. If $k > 1$ we call it a multi-pulse heteroclinic connection. A similar definition holds for a cross-section $B \subset V_{\mathbf{w}}$ and for pairs of cross-sections A, B.*

We intend to show that generically in a one-parameter unfolding satisfying (P1)–(P5) and (P7), with $\lambda_1 = 0$, there are no multi-pulse heteroclinic connections with respect to $A = H^{out}_{\mathbf{v}}$. Then a 2-pulse heteroclinic connection occurs for $\lambda_2 = \lambda_*$ whenever R maps $\Psi_{\mathbf{v},\mathbf{w}}(0,0,\lambda_*) \in H^{in}_{\mathbf{w}}$ into the origin of $H^{out}_{\mathbf{w}}$. A k-pulse connection arises when $R^k\left(\Psi_{\mathbf{v},\mathbf{w}}(0,0,\lambda_*)\right) = (0,0)$ and $R^j\left(\Psi_{\mathbf{v},\mathbf{w}}(0,0,\lambda_*)\right) \neq (0,0)$ for $0 < j < k$.

Thus, in order to find a value λ_* where there is a multi-pulse connection one has to solve the two equations $R^k\left(\Psi_{\mathbf{v},\mathbf{w}}(0,0,\lambda_*)\right) = (0,0)$ for λ_*. Generically the two equations do not have a common solution.

Note that for two-parameter families, i.e. $\lambda_2 \in \mathbf{R}^2$, generically there would be isolated values λ_k for which there would be k-pulse connections. In order to get branches of multi-pulses arbitrariliy close to $\lambda_2 = 0$, one would need three parameters. This codimension 3 behaviour is beyond the scope of this paper.

5.3 Existence of a fixed point of the Poincaré map

We start by finding the radial coordinate of the fixed point. For this we consider the maps $g^{\pm} : (0, \varepsilon) \longrightarrow \mathbf{R}$ (see figure 13)

$$g^+(r) = r + \varepsilon \left(\frac{r}{\varepsilon}\right)^{\delta} \qquad g^-(r) = r - \varepsilon \left(\frac{r}{\varepsilon}\right)^{\delta} .$$

Since $\delta > 1$ both maps are of class C^1 and

$$\frac{dg^+}{dr}(0) = \frac{dg^-}{dr}(0) = 1. \tag{5.18}$$

Lemma 17 *If C is a circle of centre $(0,0)$ and radius r_0 in $H^{in}_{\mathbf{w}}$, with $0 < r_0 < \varepsilon$, then $R(C, \lambda_2)$ is a circle of centre $(\lambda_2, 0)$ and radius $c_5 r_0^{\delta} < r_0$. Moreover:*

- *if $\lambda_2 \in (g^-(r_0), g^+(r_0))$, then $R(C, \lambda_2) \cap C$ contains exactly two points;*
- *if either $\lambda_2 = g^+(r_0)$ or $\lambda_2 = g^-(r_0)$, then $R(C, \lambda_2)$ is tangent to C and thus $R(C, \lambda_2) \cap C$ contains a single point;*
- *if λ_2 lies outside the interval $[g^-(r_0), g^+(r_0)]$, then $R(C, \lambda_2) \cap C$ is empty.*

Proof: Write C in polar coordinates as (r_0, φ), where $\varphi \in [0, 2\pi)$, $r_0 \in \mathbf{R}_0^+$ is fixed, and let $R_*(r_0, \varphi) = (\rho, \theta)$. Then $\rho = c_5 r_0^{\delta}$ is constant and $\theta = \varphi + c_6 - c_7 \ln(r_0)$ varies in an interval of length 2π. Hence, $R_*(C)$ is a circle with centre $(0,0)$ and therefore, $R(C, \lambda_2) = \Psi_{\mathbf{w},\mathbf{v}} \circ R_*(C)$ is a circle with centre $(\lambda_2, 0)$ and radius $\varepsilon \left(\frac{r_0}{\varepsilon}\right)^{\delta}$. Since $r_0 < \varepsilon$ and $\delta > 1$, then this radius is less that r_0.

For $\lambda_2 = 0$, the two circles C and $R(C, \lambda_2)$ are concentric. For a fixed $r_0 > 0$, as λ_2 increases from zero, $R(C, \lambda_2)$ moves to the right and is contained in $H^{in}_{\mathbf{w}}$ as long as $\lambda_2 \leq \varepsilon \left(1 - \left(\frac{r_0}{\varepsilon}\right)^{\delta}\right)$. As $R(C, \lambda_2)$ moves to the right it has first an internal tangency to C at $\lambda_2 = g^+(r_0)$, then the two circles meet at exactly two points and at $\lambda_2 = g^-(r_0)$ they two points come together as C and $R(C, \lambda_2)$ have an external tangency (figure 13). □

Let $a(\lambda_2)$, $b(\lambda_2)$ be the inverses of the maps $\lambda_2 = g^+(r)$ and $\lambda_2 = g^-(r)$, respectively. Since g^- has a maximum at some point $r^* \in (0, \varepsilon)$ with $g^-(r^*) = \lambda_2^*$, then $b(\lambda_2)$ is defined only for $0 < \lambda_2 < \lambda_2^*$ (see figure 13). For each $r \in (a(\lambda_2), b(\lambda_2))$, in the circle C with centre at the origin and radius r there are two points whose images by R lie in the same circle. These points $P^+(r)$ and $P^-(r)$ are symmetrically placed with respect to the line that contains the centres of C and of $R(C, \lambda_2)$. In proposition 18 we show that for at least one of these points the angular coordinate is also fixed by R and that this happens for each $\lambda_2 < \lambda_2^*$.

Proposition 18 *For any λ_2 with $0 < \lambda_2 \leq \lambda_2^*$ there is a point $P \in H^{in}_{\mathbf{w}}$ such that $R(P, \lambda_2) = P$.*

Proof: Consider a fixed $\lambda_2 \in [0, \lambda_2^*]$. For this proof, we need two systems of polar coordinates in $H^{in}_{\mathbf{w}}$: one centered at $W^s(\mathbf{w}) \cap H^{in}_{\mathbf{w}}$ (that we call S_1, coordinates (r, θ)) and the other centered at $W^u(\mathbf{v}) \cap H^{in}_{\mathbf{w}}$ (that we will call S_2, coordinates (ρ, φ)). The angular component of both systems of coordinates starts at the line through the two centres; for S_1 at the half-line that contains the centre of S_2, for S_2 at the half-line that does not contain the centre of S_1 (see figure 14). Both angular coordinates φ and θ are taken in $[-\pi, \pi]$ ($\mathbf{R}$ (mod 2π)).

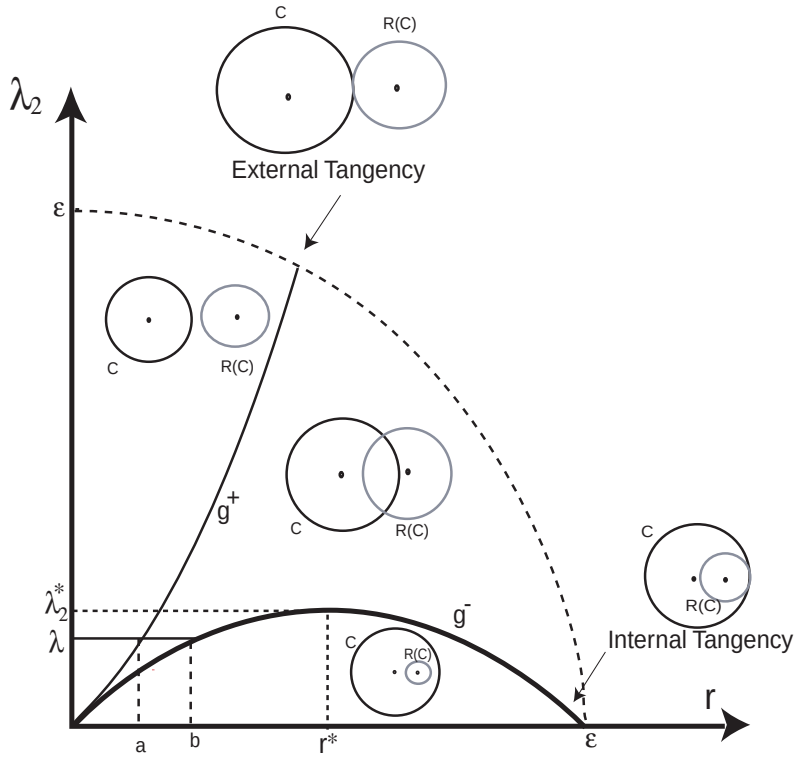

Figure 13: Thin line: graph of $g^+(r) = r + \varepsilon \left(\frac{r}{\varepsilon}\right)^\delta$ where the circle C of radius r and the circle $R(C, \lambda_2)$ have an external tangency; thick line: graph of $g^-(r) = r - \varepsilon \left(\frac{r}{\varepsilon}\right)^\delta$ where C and $R(C, \lambda_2)$ have an internal tangency. Inside the wedge-shaped region between the two curves, C meets $R(C, \lambda_2)$ at two points, outside it $C \cap R(C, \lambda_2) = \emptyset$.

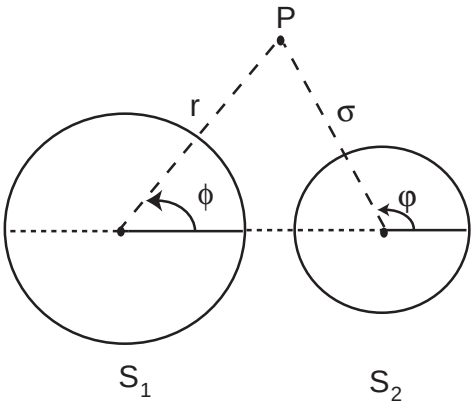

Figure 14: The two coordinate systems S_1 and S_2.

We begin by measuring the angular component of the two intersection points P^+ and P^- of the circles C and $R(C, \lambda_2)$. Let $\varphi^+(r)$ and $\varphi^-(r)$ stand for the angular coordinates $\varphi^+(r) = \varphi^+(P^+(r))$ and $\varphi^-(r) = \varphi^-(P^-(r))$, in the reference frame S_2. Then the functions

$$\varphi^+ : [a(\lambda_2), b(\lambda_2)] \longrightarrow [0, \pi] \qquad \varphi^- : [a(\lambda_2), b(\lambda_2)] \longrightarrow [-\pi, 0]$$

are both monotonic and satisfy

$$\varphi^+(a(\lambda_2)) = \pi \qquad \varphi^+(b(\lambda_2)) = 0 \qquad \varphi^-(a(\lambda_2)) = -\pi \qquad \varphi^-(b(\lambda_2)) = 0 \ . \tag{5.19}$$

Similarly, $\theta^+(r) = \theta^+(P^+(r))$ and $\theta^-(r) = \theta^-(P^-(r))$ are measured in the reference frame S_1 and define monotonic functions

$$\theta^+ : [a(\lambda_2), b(\lambda_2)] \longrightarrow [0, \pi] \qquad \theta^- : [a(\lambda_2), b(\lambda_2)] \longrightarrow [-\pi, 0]$$

such that

$$\theta^+(a(\lambda_2)) = \theta^+(b(\lambda_2)) = \theta^-(a(\lambda_2)) = \theta^-(b(\lambda_2)) = 0 \ . \tag{5.20}$$

Finally, denoting by $\Psi(r, \theta) = c_6 + \theta - c_7 \ln r$ the angular coordinate of $R(r, \theta)$ measured in S_2, with θ measured in S_1, let $\Psi^+,\ \Psi^- : [a(\lambda_2), b(\lambda_2)] \longrightarrow \mathbf{R}$ be given by

$$\Psi^+(r) = \Psi(r, \theta^+(r)) \qquad \Psi^-(r) = \Psi(r, \theta^-(r)) \ .$$

Again, these are monotonic functions and they satisfy:

$$\Psi^+(a(\lambda_2)) = \Psi^-(a(\lambda_2)) \qquad \text{and} \qquad \Psi^+(b(\lambda_2)) = \Psi^-(b(\lambda_2)) \ . \tag{5.21}$$

With this notation, if for some $r_0 \in [a(\lambda_2), b(\lambda_2)]$ we have $\varphi^+(r_0) = \Psi^+(r_0) \pmod{2\pi}$ then the point with S_2 coordinates $(r_0, \varphi^+(r_0))$ is a fixed point for R. Similarly, $\varphi^-(r_0) = \Psi^-(r_0) \pmod{2\pi}$ implies that $(r_0, \varphi^-(r_0))$ is a fixed point for R.

Note that by (5.19) the union of the graphs of φ^+ and φ^- is a connected curve and this curve divides the strip $[a(\lambda_2), b(\lambda_2)] \times \mathbf{R}$ in three connected components. The limited component contains the segment $\{a(\lambda_2)\} \times (-\pi, \pi)$; each one of the unlimited components contains one of the half-lines $\{b(\lambda_2)\} \times (0, +\infty)$ and $\{b(\lambda_2)\} \times (-\infty, 0)$. If either $\Psi^+(a(\lambda_2)) = (2k+1)\pi$ or

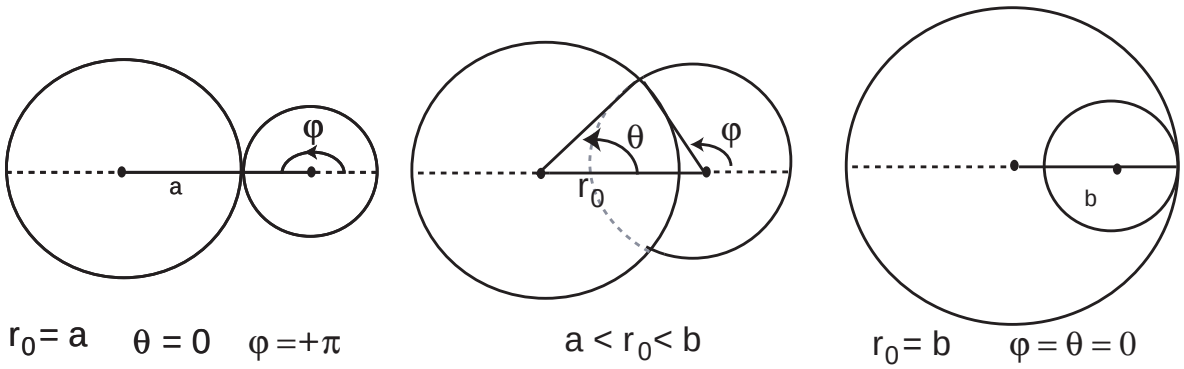

Figure 15: For a fixed $\lambda_2 < \lambda_2^*$, and for $r = a(\lambda_2) = a$, the circles C and $R(C, \lambda_2)$ have an external tangency (left). In this case, the intersection point has angular coordinate $\theta^+ = \theta^- = 0$ in S_1 and $\varphi^+ = \pi$, $\varphi^- = -\pi$ in S_2. For $r = b(\lambda_2) = b$, the circles C and $R(C, \lambda_2)$ have an internal tangency (right). Here, the intersection point has angular coordinate 0 in both coordinate systems. At the centre: for $r \in (a(\lambda_2), b(\lambda_2))$, the angular coordinate in S_2 of the upper (lower) intersection point decreases (increases) to 0 as r increases.

$\Psi^+(b(\lambda_2)) = 2k\pi$ for some $k \in \mathbf{Z}$ then either $(a(\lambda_2), \varphi^+(a(\lambda_2)))$ or $(b(\lambda_2), \varphi^+(b(\lambda_2)))$, respectively, is fixed by R. When this is not the case, let N be an integer such that $\Psi^+(a(\lambda_2)) + 2N\pi \in (-\pi, \pi)$, so $(a(\lambda_2), \Psi^+(a(\lambda_2)) + 2N\pi)$ lies in the limited component of the strip. Since

$$(b(\lambda_2), \Psi^+(b(\lambda_2)) + 2N\pi) = (b(\lambda_2), \Psi^-(b(\lambda_2)) + 2N\pi)$$

lies in one of the unlimited components, then the graphs of Ψ^+ and of Ψ^- must cross the union of the graphs of φ^+ and φ^- (see figure 16). If $(b(\lambda_2), \Psi^+(b(\lambda_2)) + 2N\pi)$ lies in $\{b(\lambda_2)\} \times (0, +\infty)$, then the graph of $\Psi^+(r)) + 2N\pi$ crosses the graph of $\varphi^+(r)$, otherwise the graphs of $\Psi^-(r)) + 2N\pi$ and of $\varphi^-(r)$ must cross. □

Several periodic trajectories may occur in two ways: first, there may be trajectories that make more than one loop around the place where the original cycle was, appearing as fixed points of some higher iterate R^N of the Poincaré map R; second, the graphs of $\Psi^\pm$ may cross the graphs of $\varphi^\pm$ several times $\pmod{2\pi}$, giving rise to several fixed points of the Poincaré map R. We show next that the second possibility does not take place for small λ_2.

Proposition 19 *For small $\lambda_2 > 0$ the Poincaré map has only one fixed point in $H^{in}_{\mathbf{w}}$.*

Proof: For the map Ψ^+ defined in the proof of proposition 18, using (5.20), we have

$$\Psi^+(b(\lambda_2)) - \Psi^+(a(\lambda_2)) = c_6 + \theta^j(b(\lambda_2)) - c_7 \ln b(\lambda_2) - c_6 - \theta^j(a(\lambda_2)) + c_7 \ln a(\lambda_2) = c_7 \ln \frac{a(\lambda_2)}{b(\lambda_2)} .$$

Then, since by (5.18),

$$\lim_{\lambda_2 \to 0} a(\lambda_2) = \lim_{\lambda_2 \to 0} b(\lambda_2) = 0 \quad \text{and} \quad \lim_{\lambda_2 \to 0} \frac{da}{d\lambda_2}(\lambda_2) = \lim_{\lambda_2 \to 0} \frac{db}{d\lambda_2} = 1$$

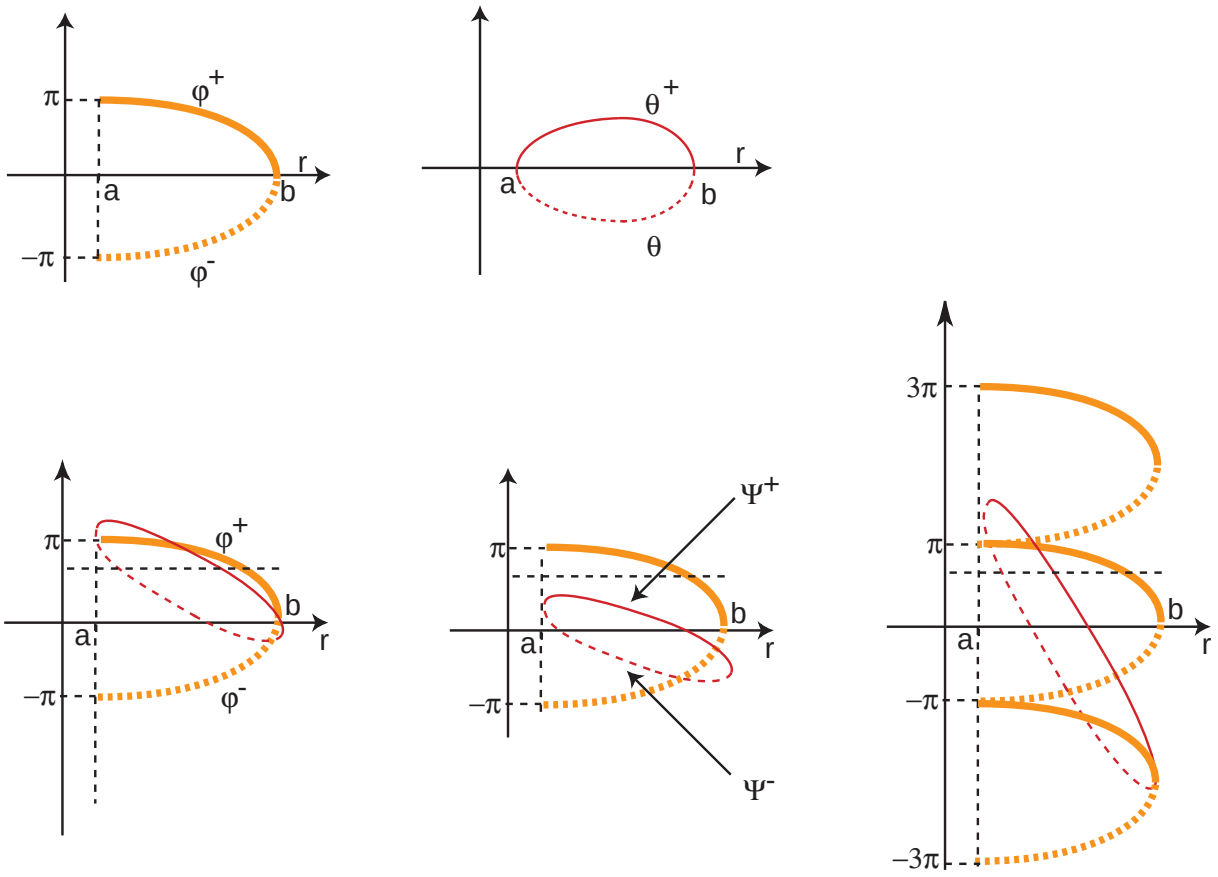

Figure 16: When either $\varphi^+(r) = \Psi^+(r) \pmod{2\pi}$ or $\varphi^-(r) = \Psi^-(r) \pmod{2\pi}$ there is a fixed point for the first return map R. Graphs are: thick lines for $\varphi^\pm$, thin for $\Psi^\pm$, solid lines for +, dashed for -, with $\Psi^+(a(\lambda_2)) \in (-\pi, \pi)$. Left: when $\Psi^+(b(\lambda_2)) > 0$ the graphs of φ^+ and Ψ^+ must cross. At the centre, crossing of the graphs of φ^- and Ψ^- when $\Psi^+(b(\lambda_2)) < 0$. Right: for large λ_2 new fixed points appear in pairs as the graphs of $\Psi^\pm$ cross the graphs of $\varphi^\pm$ several times $\pmod{2\pi}$.

we get

$$\lim_{\lambda_2 \to 0} \left(\Psi^+(b(\lambda_2)) - \Psi^+(a(\lambda_2)) \right) = 0$$

even though, since $c_7 > 0$

$$\lim_{\lambda_2 \to 0} \Psi^+(b(\lambda_2)) = \lim_{\lambda_2 \to 0} \Psi^+(a(\lambda_2)) = \infty \ .$$

It follows that $|\Psi^+(b(\lambda_2)) - \Psi^+(a(\lambda_2))| \ll \pi$ for small $\lambda_2 > 0$ and thus, since $\Psi^\pm$ and $\varphi^\pm$ are monotonic, there is only one crossing $\pmod{2\pi}$ of either the graphs of Ψ^+ and φ^+ or of the graphs of Ψ^- and φ^-. Therefore the fixed point of the Poincaré map is unique. □

5.4 Stability of the fixed point

Proposition 20 *For small $\lambda_2 > 0$ the periodic solution corresponding to the unique fixed point of Poincaré map in $H^{in}_{\mathbf{w}}$ of Proposition 19 is asymptotically stable.*

Proof: We want to estimate the eigenvalues of the derivative $DR(X)$ of the Poincaré map $R : H^{in}_{\mathbf{w}} \longrightarrow H^{in}_{\mathbf{w}}$. To do this we write R as a composition of maps

$$R(X) = P \circ R_* \circ h^{-1}(X)$$

where $R_* = (\rho(r,\varphi), \theta(r,\varphi))$ is the expression (5.16) in polar coordinates, $h(r,\varphi) = (r\cos\varphi, r\sin\varphi)$ and $P(\rho,\theta) = (\rho\cos\theta + \lambda_2, \rho\sin\theta)$. For $X \in H^{in}_{\mathbf{w}}$, $X \neq (0,0)$ we write $h^{-1}(X) = (r(X), \varphi(X))$.

From the derivatives

$$DP(\rho,\theta) = \begin{pmatrix} \cos\theta & -\rho\sin\theta \\ \\ \sin\theta & \rho\cos\theta \end{pmatrix} \qquad DR_*(r,\varphi) = \begin{pmatrix} c_5\delta r^{\delta-1} & 0 \\ \\ -\dfrac{c_7}{r} & 1 \end{pmatrix}$$

$$Dh^{-1}(X) = \begin{pmatrix} \cos\varphi(X) & \sin\varphi(X) \\ \\ -\dfrac{\sin\varphi(X)}{r(X)} & \dfrac{\cos\varphi(X)}{r(X)} \end{pmatrix}$$

it follows that $DR(X)$ does not depend explicitly on λ_2. Then, at $X = h^{-1}(r,\varphi)$ we have

$$\det DR(X) = c_5^2\delta r^{2\delta-2}(X) \ .$$

The trace $\operatorname{tr} DR(X)$, omiting the dependence on X, is given by

$$\operatorname{tr} DR(X) = \left(c_5\delta r^{\delta-1} + \frac{\rho}{r} \right)(\cos\theta\cos\varphi + \sin\theta\sin\varphi) + \frac{c_7\rho}{r}(\sin\theta\cos\varphi - \cos\theta\sin\varphi) \ .$$

We want to estimate $\det DR$ and $\operatorname{tr} DR$ at points $X(\lambda_2)$ where $R(X(\lambda_2)) = X(\lambda_2)$ for small $\lambda_2 > 0$. In polar coordinates we get $h^{-1}(X(\lambda_2)) = (r(\lambda_2), \varphi(\lambda_2))$ and we know that $\lim_{\lambda_2 \to 0} r(\lambda_2) = 0$. Then from the expression above, and since by (5.17) we have $\delta > 1$,

$$\lim_{\lambda_2 \to 0} \det DR(X)(\lambda_2)) = 0 \ .$$

For the trace, substituting the value of $\rho(r,\varphi) = c_5 r^\delta$ obtained in (5.16) we get

$$\lim_{r \to 0} \frac{\rho(r,\varphi)}{r} = \lim_{r \to 0} c_5 r^{\delta-1} = 0$$

since $\delta > 1$. Then at the limit cycle $\lim_{\lambda_2 \to 0} \operatorname{tr} DR(X(\lambda_2)) = 0$. It follows that the eigenvalues of $DR(X(\lambda_2))$ also tend to zero and thus for small λ_2 they lie within the disk of radius 1. $\square$

6 Proof of theorem 8

In this section, we are assuming that both symmetries $\mathbf{Z}_2(\gamma_1)$ and $\mathbf{Z}_2(\gamma_2)$ are broken (ie $\lambda_1 \neq 0$ and $\lambda_2 \neq 0$) and that property (P8a) is satisfied. Without loss of generality, we assume that the transition map from $\mathbf{v}$ to $\mathbf{w}$ is just a translation along the horizontal axis. Recall that the parameter λ_2 controls the splitting of the heteroclinic orbit $[\mathbf{v} \to \mathbf{w}]$ and λ_1 is the parameter controling the angle in $H^{in}_{\mathbf{v}}$ of the transverse intersection $W^u(\mathbf{w})$ and $W^s(\mathbf{v})$.

Near the heteroclinic network $\Sigma^\star$ which exists for $\lambda_1 \neq 0$ and $\lambda_2 = 0$, there exists an invariant Cantor set topologically equivalent to a full shift with an infinite countable set of periodic solutions. It corresponds to infinitely many intersections of a vertical rectangle $\mathcal{R}_{\mathbf{v}}$ in $H^{in}_{\mathbf{v}}$ with its image, under the first return map to $H^{in}_{\mathbf{v}}$. Only a finite number of them will survive, under a small perturbation (ie, the horseshoes which exist for $\lambda_2 = 0$ lose infinitely many legs).

If $\lambda_1 \neq 0 \neq \lambda_2$, the tips of the spirals $\Phi^{-1}_{\mathbf{w}}(W^s(\mathbf{v})) \cap H^{in}_{\mathbf{w}}$ and $\Psi_{\mathbf{v},\mathbf{w}} \circ \Phi_{\mathbf{v}}(W^u(\mathbf{w})) \cap H^{in}_{\mathbf{w}}$ are separated and generically the center of the first curve does not intersect the second spiral. Thus, the spirals have only a finite number of intersections. Thus, the number of heteroclinic connections from $\mathbf{v}$ to $\mathbf{w}$ is finite.

For $\lambda_1 \neq 0 \neq \lambda_2$, besides the existence of uniformly hyperbolic horseshoes, there are homoclinic orbits of $\mathbf{v}$ and $\mathbf{w}$, whose coexistence we address in the present section. The existence of these homoclinic loops in a phenomenon which depends on the right combination of the parameters (λ_1, λ_2) that shall be discussed here.

We start by a global description of $\Phi^{-1}_{\mathbf{w}}(W^s(\mathbf{v})) \cap H^{in}_{\mathbf{w}}$. The homoclinic connections are then discussed separately: those in $\mathbf{v}$ in section 6.1 and those in $\mathbf{w}$ in section 6.2. For λ_1 close to zero, we are assuming that $W^s(\mathbf{v})$ intersects the wall $H^{out}_{\mathbf{w}}$ of the cylinder W in an ellipsis. This is the expected unfolding from the coincidence of the invariant manifolds of the equilibria (see figure 17).

We are assuming that $W^u(\mathbf{w}) \cap W^s(\mathbf{v}) \cap H^{out}_{\mathbf{w}}$ consists of two points P_1 and P_2 (see figure 17). Each of these points $W^s(\mathbf{v}) \cap H^{out}_{\mathbf{w}}$ defines a segment and each segment may be approximated by a line of slope $\pm\lambda_1$ parametrized by s (see figure 18) with either $s \in (0, \varepsilon^*)$ or $s \in (\pi - \varepsilon^*, \pi)$, respectively, where $\varepsilon^* \in (0, \varepsilon)$).

Near P_1, the slope is λ_1; near P_2, the slope is $-\lambda_1$. When $\lambda_1 = 0$ the invariant manifolds coincide; when $\lambda_1 \neq 0$, these two segments appear automatically. For assumption, we have:

$$\lim_{s \to 0^+} s_1(s) = P_1 \quad \text{and} \quad \lim_{s \to \pi^-} s_2(s) = P_2.$$

By lemma 11, locally the curves $\Phi^{-1}_{\mathbf{w}}(s_1(s))$ and $\Phi^{-1}_{\mathbf{w}}(s_2(s))$ are disjoint spirals in H^{in}_w accumulating on the point $W^s_{loc}(\mathbf{w}) \cap H^{in}_{\mathbf{w}}$.

Globally, $W^s(\mathbf{v}) \cap H^{out}_{\mathbf{w}}$ is a closed curve $(x(s), y(s))$, $s \in [0, 2\pi]$, with two arcs where $y(s)$ is monotonic (figure 17). Each arc is mapped diffeomorphically by $\Phi^{-1}_{\mathbf{w}}$ into a spiral and the two spirals meet at the image of the maximum of $y(s)$ (see figure 19).

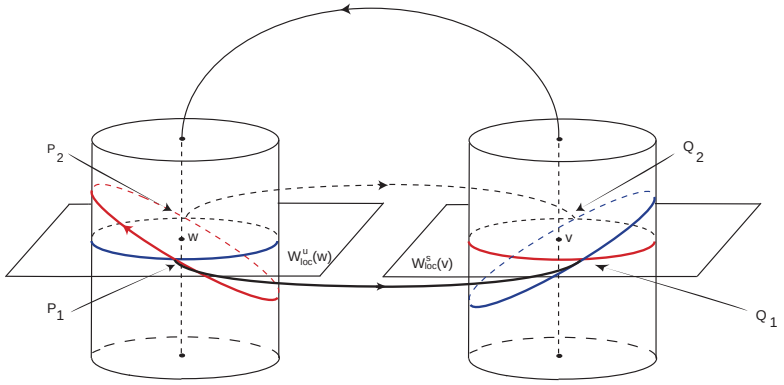

Figure 17: Both $W^s(\mathbf{v}) \cap H^{out}_{\mathbf{w}}$ and $W^u(\mathbf{w}) \cap H^{in}_{\mathbf{v}}$ are closed curves, approximated by ellipses for small λ_1.

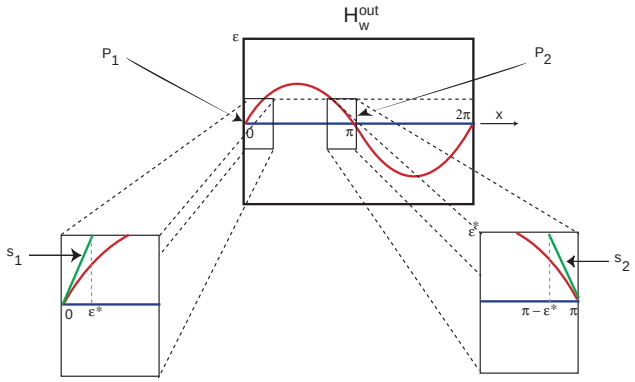

Figure 18: The cylinder $H^{out}_{\mathbf{w}}$ is shown here opened into a rectangle to emphasize the fact that locally $W^s(\mathbf{v})$ defines two lines on this wall.

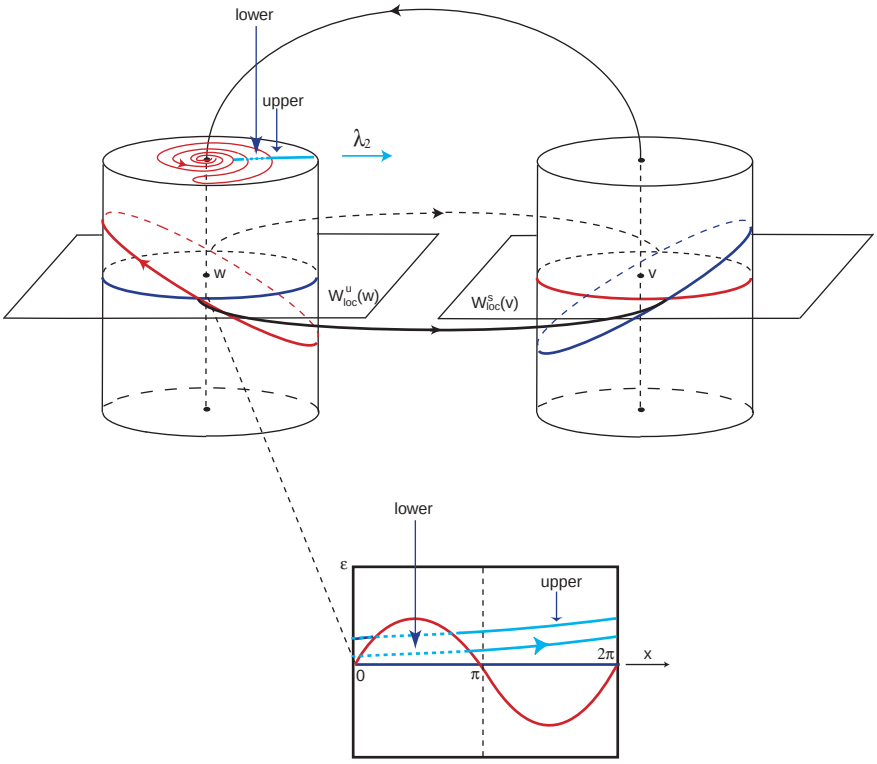

Figure 19: The backwards iterate $\Phi_{\mathbf{w}}^{-1}(W^s(\mathbf{v}))$ consists of two joined-up spirals in $H_{\mathbf{w}}^{in}$ shown in red, that divide $H_{\mathbf{w}}^{in}$ in two components, mapped into the upper and lower parts of $H_{\mathbf{v}}^{in}$. As λ_2 increases from zero, $W^u(\mathbf{v}) \cap H_{\mathbf{w}}^{in}$ moves along the blue line, whose image by $\Phi_{\mathbf{w}}$ describes a helix in $H_{\mathbf{w}}^{out}$. Arrows on $W^s(\mathbf{v})$ and on the blue line are just indications of orientation, not of flow.

6.1 Homoclinic connections of v - Tongues of Attracting Periodic Trajectories

Note that we are assuming that $\alpha_{\mathbf{v}}, \alpha_{\mathbf{w}} > 0$ since hypothesis (P8a) is satisfied. The primary homoclinicity of $\mathbf{v}$ occurs when the unstable manifold of $\mathbf{v}$ has a successful encounter with the stable manifold of the same equilibrium on $H^{in}_{\mathbf{w}}$. Here, we will find the values $\lambda_2(\mathbf{v})$ of the parameter λ_2 for which system (2.2) has a homoclinic connection of $\mathbf{v}$. This happens when $\lambda_1 > 0$ and either:

$$\lambda_2(\mathbf{v}) = \left(\frac{\lambda_1 s}{c_4}\right)^{\frac{1}{\delta_{\mathbf{w}}}} \quad \text{and} \quad s - c_3 + \left(\frac{\alpha_{\mathbf{w}}}{C_{\mathbf{w}}}\right) \ln\left(\frac{\lambda_1 s}{c_4}\right) = 2k\pi, k \in \mathbf{Z} \tag{6.22}$$

or

$$\lambda_2(\mathbf{v}) = \left(-\frac{\lambda_1(s-\pi)}{c_4}\right)^{\frac{1}{\delta_{\mathbf{w}}}} \quad \text{and} \quad s - c_3 + \left(\frac{\alpha_{\mathbf{w}}}{C_{\mathbf{w}}}\right) \ln\left(\frac{-\lambda_1(s-\pi)}{c_4}\right) = 2k\pi, \quad k \in \mathbf{Z}. \tag{6.23}$$

Using the above equations and the approximated for of $W^s(\mathbf{v}) \cap H^{out,+}_{\mathbf{w}}$, we may write the parameter λ_1^k as function of λ_2:

$$\lambda_1^k(\lambda_2) = \frac{c_4 \lambda_2^{\delta_{\mathbf{w}}}}{2k\pi + c_3 - \frac{\alpha_{\mathbf{w}}}{E_{\mathbf{w}}} \ln(\lambda_2)} \quad \text{and} \quad s \in (0, \varepsilon^\star) \tag{6.24}$$

or

$$\lambda_1^k(\lambda_2) = \frac{c_4 \lambda_2^{\delta_{\mathbf{w}}}}{\pi + 2k\pi + c_3 - \frac{\alpha_{\mathbf{w}}}{E_{\mathbf{w}}} \ln(\lambda_2)} \quad \text{and} \quad s \in (\pi - \varepsilon^\star, \pi) \tag{6.25}$$

Both equations (6.24) and (6.25) may be simplified as:

$$\lambda_1^k(\lambda_2) = \frac{c_4 \lambda_2^{\delta_{\mathbf{w}}}}{k\pi + c_3 - \frac{\alpha_{\mathbf{w}}}{E_{\mathbf{w}}} \ln(\lambda_2)}$$

where the denominator is either the value of s or of $\pi - s$ and only has meaning when it lies in the interval $(0, \varepsilon^*)$. For $\lambda_2 > 0$, define:

$$k_0(\lambda_2) = \min\left\{k \in \mathbf{Z} : 2k\pi + c_3 - \frac{\alpha_{\mathbf{w}}}{E_{\mathbf{w}}} \ln(\lambda_2) > 0\right\}.$$

Lemma 21 *1.* $\lim_{\lambda_2 \to 0} k_0(\lambda_2) = -\infty$

2. $\forall k > k_0, \quad \frac{d\lambda_1^k}{d\lambda_2}(0) = 0$*;*

Proof:

1. It is immediate from the fact that when $\lambda_2 \to 0$, $\ln(\lambda_2) \to -\infty$.

2. Observe that:

$$\frac{d\lambda_1^k}{d\lambda_2}(\lambda_2) = \frac{c_4 \lambda_2^{\delta_{\mathbf{w}}-1}}{k\pi + c_3 - \frac{\alpha_{\mathbf{w}}}{E_{\mathbf{w}}} \ln(\lambda_2)} + \frac{c_4 \lambda_2^{\delta_{\mathbf{w}}-1} \frac{\alpha_{\mathbf{w}}}{E_{\mathbf{w}}}}{\left(k\pi + c_3 - \frac{\alpha_{\mathbf{w}}}{E_{\mathbf{w}}} \ln(\lambda_2)\right)^2}.$$

When $\lambda_2 \to 0$, the above expression tends to zero.

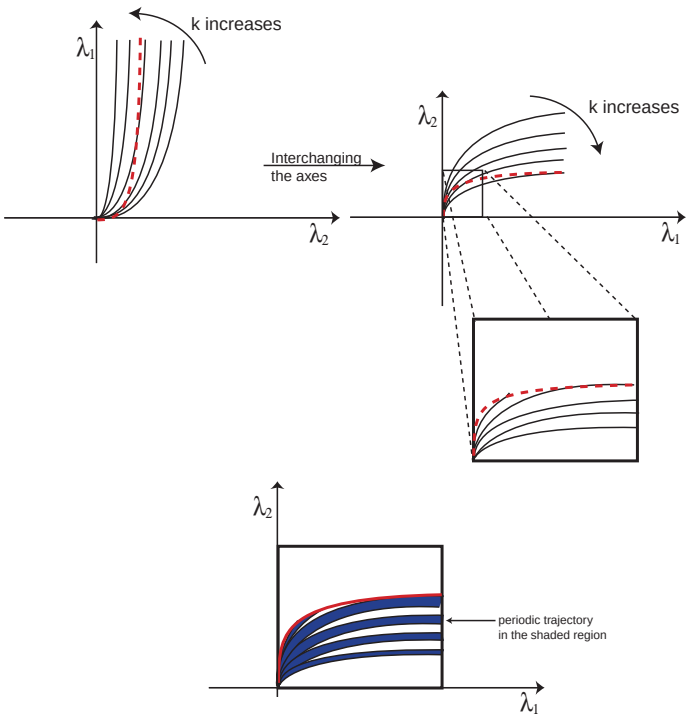

Figure 20: Top: solid lines are the curves $(\lambda_1^k(\lambda_2), \lambda_2)$ where there is a homoclinic connection to $\mathbf{v}$, dashed line is the limit $s = \varepsilon^*$ for the linear approximation of $W^s(\mathbf{v}) \cap H^{out}_{\mathbf{w}}$. Bottom: Pairs of these lines delimitate a tongue where there is a periodic trajectory.

□

In a neighbourhood of the singular point $(\lambda_1, \lambda_2) = (0, 0)$, the graph of λ_1 as function of λ_2 is depicted in figure 20, for different values of $k > k_0$. Recall that $s \in [0, \varepsilon^\star]$; in particular, the end points of the graphs coincide with the intersection of the graphs of $\lambda_1^k(\lambda_2)$ with that of $\lambda_1(\lambda_2) = \frac{c_4 \lambda_2^{\delta_{\mathbf{w}}}}{\varepsilon^\star}$ (which represents the evolution of the end point of s_i of the linear approximation of $W^s(\mathbf{v}) \cap H^{out,+}_{\mathbf{w}}$). When $\lambda_2 \to 0^+$, the equation

$$k\pi + c_3 - \frac{\alpha_{\mathbf{w}}}{E_{\mathbf{w}}} \ln(\lambda_2) = 0$$

has infinitely many solutions (one for each k). In particular:

Lemma 22 *For all k sufficiently large, there exists $\lambda_2^\star(k)$ such that*

$$\lim_{\lambda_2 \to \lambda_2^\star(k)} \lambda_1^k(\lambda_2) = +\infty$$

and moreover $\lim_{k \to +\infty} \lambda_2^\star(k) = 0$. *In other words, the graph of $\lambda_1^k(\lambda_2)$ has a vertical asymptote for $\lambda_2 = \lambda_2^\star(k)$.*

From the bifurcation diagram, it follows that for a fixed λ_2, there are finitely many λ_1 for which we observe homoclinic connections of $\mathbf{v}$. We also conclude that for a fixed λ_2, there exists a $\lambda_1^\star$, such that for $\lambda_1 < \lambda_1^\star$, there are no more homoclinic connections.

Theorem 23 *1. for each $\lambda_1 > 0$, if $\lambda_2 = \lambda_2^k(\lambda_1)$, there exists an attracting homoclinic orbit associated to $\mathbf{v}$;*

2. the homoclinic orbits which exist for $\lambda_2 = \lambda_2^k(\lambda_1)$ and for $\lambda_2 = \lambda_2^{k+2}(\lambda_1)$ are distinguished by the number of revolutions inside $\mathcal{V}_w$ around $W^s_{loc}(\mathbf{w})$;

3. for each $\lambda_1 > 0$, either for $\lambda_2^k(\lambda_1) < \lambda_2 < \lambda_2^{k+1}(\lambda_1)$ or for $\lambda_2^{k+1}(\lambda_1) < \lambda_2 < \lambda_2^{k+2}(\lambda_1)$, there exists an attracting periodic solution near the locus of the homoclinic orbit;

4. in the bifurcation diagram, the regions for which there are no attracting limit cycles (associated to bifurcations of homoclinic orbits of $\mathbf{v}$) are alternate with the regions containing limit cycles;

5. along a vertical line ($\lambda_1 = \lambda_1^0$), a stable limit cycle is born from a simple homoclinic loop for $\lambda_2 = \lambda_2^k(\lambda_1^0)$; away from the path, the limit cycle decreases its period and then increases again until it reaches $\lambda_2 = \lambda_2^{k+1}(\lambda_1^0)$ in which the stable periodic solution becomes once again a homoclinic orbit of $\mathbf{v}$.

We have proved assertions 1 and 2. The other assertions follow from the results of Shilnikov [44], Glendinning and Sparrow [16] and Shilnikov *et al* [45, 46].

Corollary 24 *In the bifurcation diagram (λ_1, λ_2), there are infinitely many tongues of attracting periodic trajectories accumulating on the line $\lambda_2 = 0$. These periodic trajectories are bifurcating from the attracting homoclinic orbit of $\mathbf{v}$.*

Corollary 25 *When $\lambda_2 \to 0$, the homoclinic orbits of $\mathbf{v}$ accumulate on the heteroclinic connection $[\mathbf{v} \to \mathbf{w}]$.*

6.2 Homoclinic orbits of w - A cascade of horseshoes is only a participating part!

Using the same argument as before, we assume the existence of two segments r_1 and r_2 (parametrized by s) which correspond to a linear approximation of $W^u(\mathbf{w}) \cap H^{in}_{\mathbf{v}}$, in a neighbourhood of the points $W^s(\mathbf{v}) \cap W^u(\mathbf{w}) \cap H^{in}_{\mathbf{v}}$ (Q_1 and Q_2). The parameter $\lambda_1 > 0$ is the absolute value of the slope of r_1 and r_2; (near Q_1, the slope is λ_1; near Q_2, the slope is -λ_1). Their parametrizations are given by:

$$r_1 : \quad r_1(s) = (s, \lambda_1 s), \quad \text{for} \quad s \in [0, \varepsilon^\star]$$

and

$$r_2 : \quad r_2(s) = (s, -\lambda_1(s - \pi)), \quad \text{for} \quad s \in [\pi - \varepsilon^\star, \pi].$$

As before, we have:

Lemma 26 *If $\lambda_1 \neq 0$, then $\phi_v(r_1(s))$ and $\phi_v(r_2(s))$ are disjoint logarithmic spirals in $H^{out}_{\mathbf{v}}$ accumulating on the point $W^u_{loc}(\boldsymbol{v}) \cap H^{out}_{\mathbf{v}}$.*

Observing that:

$$\phi_{\mathbf{v}}(r_1(s)) = \phi_{\mathbf{v}}(s, \lambda_1 s) = (c_1(\lambda_1 s)^{\delta_{\mathbf{v}}}; -g_v \ln(\lambda_1 s) + s + c_2) = (\sigma, \phi)$$

and

$$\phi_{\mathbf{v}}(r_2(s)) = \phi_{\mathbf{v}}(s, -\lambda_1(s - \pi)) = (c_1(-\lambda_1(s - \pi))^{\delta_{\mathbf{v}}}; -g_v \ln(-\lambda_1(s - \pi)) + s + c_2) = (\sigma, \phi),$$

the homoclinic orbit associated to $\mathbf{w}$ (investigated on H_w^{in}) exists if and only if either

$$\lambda_2(\mathbf{w}) = c_1(\lambda_1 s)^{\delta_\mathbf{v}} \quad \text{and} \quad s + c_2 - \left(\frac{\alpha_v}{E_v}\right)\ln(\lambda_1 s) = 2k\pi, k \in \mathbf{Z} \tag{6.26}$$

or

$$\lambda_2(\mathbf{v}) = c_1\left(-\lambda_1(s-\pi)\right)^{\delta_v} \quad \text{and} \quad s + c_2 - \left(\frac{\alpha_v}{C_v}\right)\ln(-\lambda_1(s-\pi)) = 2k\pi, k \in \mathbf{Z}. \tag{6.27}$$

Using the above equations, we may write the parameter λ_1^k as function of λ_2 as either:

$$\lambda_1^k(\lambda_2) = \frac{c_1^\star \lambda_2^{\frac{1}{\delta_v}}}{2k\pi + c_2 - \frac{\alpha_v}{E_v}\ln(\lambda_2)} \quad \text{and} \quad s \in (0, \varepsilon^\star)$$

or

$$\lambda_1^k(\lambda_2) = \frac{c_1^\star \lambda_2^{\frac{1}{\delta_v}}}{\pi + 2k\pi + c_2 - \frac{\alpha_v}{E_v}\ln(\lambda_2)} \quad \text{and} \quad s \in (0, \varepsilon^\star)$$

The proof of theorem 9 proceeds as that of Theorem 8, except that the curves $(\lambda_1^k(\lambda_2), \lambda_2)$ are tangent to the λ_1-axis. It follows from results of Shilnikov [44] and Glendinning and Sparrow [16], that a horseshoe bifurcates from each homoclinic connection. In the neighbourhood of these homoclinic orbits, infinitely many periodic solutions of saddle type occur. These solutions are contained in suspended horseshoes that accumulate on the homoclinic cycle.

References

[1] L. Abramov, *On the entropy of a flow* (Russian), Dokl. Akad. Nauk. SSSR 128, 873–875, 1959

[2] M. Aguiar, *Vector Fields with heteroclinic networks,* PhD Thesis, Departamento de Matemática Aplicada, Faculdade de Ciências da Universidade do Porto, 2003

[3] M. Aguiar, S. B. Castro and I. S. Labouriau, *Dynamics near a heteroclinic network,* Nonlinearity, No. 18, 391–414, 2005

[4] M. Aguiar, S. B. Castro and I. S. Labouriau, *Simple Vector Fields with Complex Behaviour*, Int. Jour. of Bifurcation and Chaos, Vol. 16, No. 2, 369–381, 2006

[5] M. Aguiar, I. S. Labouriau and A. Rodrigues, *Swicthing near a heteroclinic network of rotating nodes*, Dynamical Systems: an International Journal, Vol. 25, Issue 1, 75–95, 2010

[6] D. V. Anosov, S. Kh. Aranson, V. I. Arnold, I. U. Bronshtein, V. Z. Grines and Yu. S. Il'yashenko, *Ordinary Differential Equations and Smooth Dynamical Systems*, Springer, 1988

[7] V. V. Bykov, *Orbit Structure in a Neighbourhood of a Separatrix Cycle Containing Two Saddle-Foci*, Amer. Math. Soc. Transl, Vol. 200, 87–97, 2000

[8] J. B. van den Berg, S. A. van Gils and T. P. P. Visser, *Parameter dependence of homoclinic solutions in a single long Josepson junction*, Nonlinearity, No. 16(2), 707–717, 2003

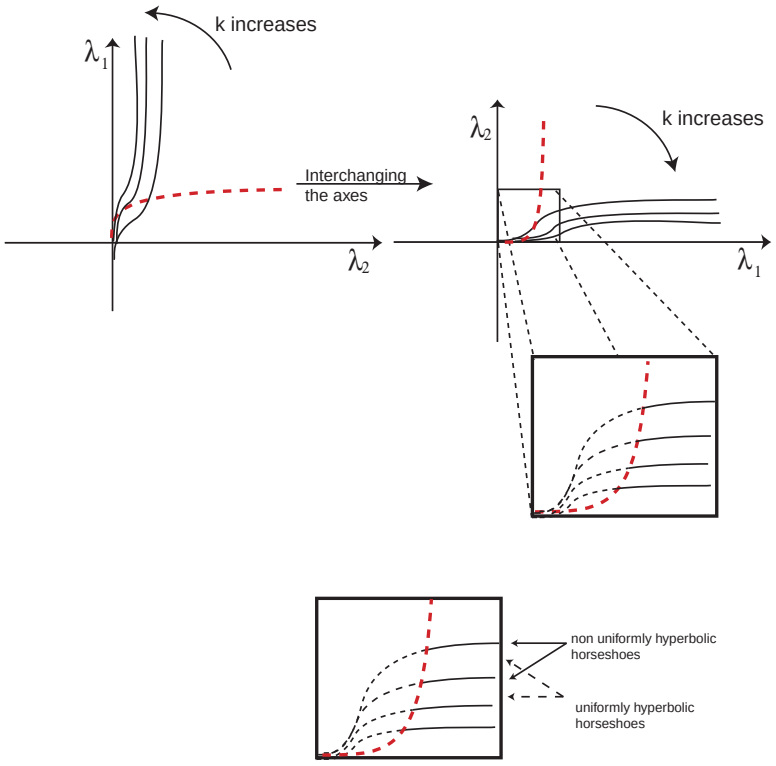

Figure 21: Top: Solid lines are the curves $(\lambda_1^k(\lambda_2), \lambda_2)$ where there is a homoclinic connection to $\mathbf{w}$, dashed line is the limit $s = \varepsilon^*$ for the linear approximation of $W^u(\mathbf{w}) \cap H^{in}_{\mathbf{v}}$. Bottom: at each one of these lines a horseshoe is created.

[9] V. Carmona, F. F. Sánchez and A. E. Teruel, *Existence of a reversible T-point heteroclinic cylce in a piecewise linear version of the Michelson system*, SIAM J. Applied Dynamical Systems, 1032–1048, 2008

[10] P. Chossat, *Forced reflectional symmetry breaking of an O(2)-symmetric homoclinic cycle*, Nonlinearity, Vol. 70, Issue 2, 297–310, 1996

[11] F. Dumortier, S. Ibánez, H. Kokubu, *New aspects in the unfolding of the nilpotent singularity of codimension three*, Dynamical Systems, Vol. 16, No. 1, 63–95, 2001

[12] M. Field, *Lectures on bifurcations, dynamics and symmetry*, Pitman Research Notes in Mathematics Series, Vol. 356, Longman, 1996

[13] J. Franks and R. F. Williams, *Entropy and Knots*, Transactions of the American Mathematical Society, Vol. 291, No. 1, 241–253, 1985

[14] P. Gaspard, *Generation of a countable set of homoclinic flows through bifurcation*, Phys. Letters, 97 A, Issues 1–2, 1–4 , 1983

[15] P. Glendinning, J. Abshagen and T. Mullin, *Imperfect Homoclinic Bifurcation*, Phys. Rev. E 64, 036208–036215, 2001

[16] P. Glendinning and C. Sparrow, *Local and global behavior near homoclinic orbits*, J. Stat. Phys., 35, 645–696, 1984

[17] P. Glendinning and C. Sparrow, *T-points: A codimension Two Heteroclinic Bifurcation*, J. Stat. Phys., 43, No. 3–4, 479–488, 1986

[18] M. I. Golubitsky, I. Stewart, and D. G. Schaeffer, *Singularities and Groups in Bifurcation Theory* , Vol. II, Springer, 2000

[19] R. W. Ghrist, P. J. Holmes and M. C. Sullivan, *Knots and Links in Three-Dimensional Flows*, Lectures Notes in Mathematics, 1654, Springer, 1997

[20] J. Guckenheimer and P. Holmes, *Nonlinear Oscillations, Dynamical Systems and Bifurcations of Vector Fields*, Springer-Verlag, 1983

[21] J. Guckenheimer and P. Holmes, *Structurally stable heteroclinic cycles*, Math. Proc. Camb. Phil. Soc, 103, 189–192, 1988

[22] M. Hirasawa and E. Kin, *Determination of generalized horseshoe map inducing all links*, Topology and its Applications, 139, No. 1–3, 261–277, 2004

[23] A. J. Homburg and J. Knobloch, *Switching homoclinic networks*, Dynamical Systems: an International Journal, Vol. 25, Issue 3, 351–358, 2010

[24] A. J. Homburg and M. A. Natiello, *Accumulations of T-points in a model for solitary pulses in an excitable reaction-diffusion medium*, Physica D, Vol. 201, No. 3–4, 212–229, 2005

[25] S. Ibáñez and J. A. Rodríguez, *Shilnikov configurations in any generic unfolding of the nilpotent singularity of codimension three in* $\boldsymbol{R}^3$, Journal of Differential Equations, 208, 147–175, 2008

[26] A. Katok and B. Hasselblatt, *Introduction to the Modern Theory of Dynamical Systems*, Cambridge University Press, Cambridge, 1995

[27] E. Kin, *The third power of the Smale horseshoe induces all link types*, J. Knot Theory Ramifications, Vol. 9, No. 7, 939–953, 2000

[28] V. Kirk and A. M. Rucklidge, *The effect of symmetry breaking on the dynamics near a structurally stable heteroclinic cycle between equilibria and a periodic orbit,* Dynamical Systems: An International Journal, Vol. 23, Nr.1, 41–83, 2008

[29] M. Krupa, *Bifurcations of relative equilibria*, SIAM J. Math. Anal, Vol. 21, No. 6, 1453–1486, 1990

[30] M. Krupa, *Robust Heteroclinic Cycles*, J. Nonlinear Sci., 129–176, 1997

[31] M. Krupa, and I. Melbourne, *Asymptotic Stability of Heteroclinic Cycles in Systems with Symmetry,* Ergodic Theory and Dynam. Sys., Vol. 15, 121–147, 1995

[32] M. Krupa and I. Melbourne, *Asymptotic Stability of Heteroclinic Cycles in Systems with Symmetry, II,* Proc. Roy. Soc. Edinburgh, 134A, 1177–1197, 2004

[33] J. S. W. Lamb, M. A. Teixeira, Kevin N. Webster *Heteroclinic bifurcations near Hopf-zero bifurcation in reversible vector fields in* $\mathbf{R}^3$, Journal of Differential Equations, 219, 78–115, 2005

[34] R. Lauterbach and M. Roberts, *Heteroclinic cyles in Dynamical Systems with Broken Spherical Symmetry*, Journal of Differential Equations, Vol. 100(1), 22–48, 1992

[35] I. Melbourne, *Intermittency as a codimension three phenomenon*, J. Dyn. Stab. Syst., 1, 347–367, 1989

[36] L. Mora, M. Viana, *Abundance of strange attractors*, Acta Math. 171, 1–71, 1993

[37] S. E. Newhouse, *Diffeomorphisms with infinitely many sinks*, Topology, 13, 9–18, 1974

[38] S. E. Newhouse, *The abundance of Wild Hyperbolic Sets and Non-Smooth Stable Sets for Diffeomorphisms*, Publ. Math. Inst. Hautes Études Sci., Vol. 50, 101–151, 1979

[39] Z. Ren and J. Yang, *On the* C^1*–normal forms for hyperbolic vector fields*, C. R. Acad. Sci. Paris, Ser.I 336, Issue 9, 709–712, 2003

[40] A. A. P. Rodrigues, I. S. Labouriau, M. A. D. Aguiar, *Chaotic Double Cycling*, Dynamical Systems: an International Journal, Vol. 26, Issue 2, 199–233, 2011

[41] V. S. Samovol, *Linearization of a system of differential equations in the neighbourhood of a singular point,* Sov. Math. Dokl, Vol. 13, 1255–1959, 1972

[42] F. Fernández-Sánchez, E. Freire and A. J. Rodríguez-Luis, *T-Points in a* $\mathbf{Z}_2$*-Symmetruc Electronic Oscillator. (I) Analysis*, Nonlinear Dynamics, 28, 53–69, 2002

[43] F. Fernández-Sánchez, E. Freire and A. J. Rodríguez-Luis, *Analysis of the T-point-Hopf bifurcation*, Physica D, 237, 292–305, 2008

[44] L. P. Shilnikov, *A case of the existence of a countable number of periodic motions*, Sov. Math. Dokl., 6, 163–166, 1965

[45] L. P. Shilnikov, A. L. Shilnikov, D. M. Turaev, and L. U. Chua, *Methods of Qualitative Theory in Nonlinear Dynamics*, Part I, World Scientific Publishing Co., 1998

[46] L. P. Shilnikov, A. L. Shilnikov, D. M. Turaev, and L. U. Chua, *Methods of Qualitative Theory in Nonlinear Dynamics*, Part II, World Scientific Publishing Co., 2001

[47] S. Wiggins, *Global Bifurcations and Chaos: Analytical Methods*, Springer-Verlag, 1988

[48] Y. Xiao-feng, G. Rui-hai, *Coexistence of the Chaos and the Periodic Solutions in Planar Fluids Flows*, Applied Mathematics and Mechanics (English version), Vol. 12, N. 12, 1135–1142, 1991

[49] J. A. Yorke, K. T. Alligood, *Period-Doubling Cascade of Attractors: A prerequisite for Horseshoes*, Communications in Mathematical Physics, 101, 305–321, 1985

Article 6 – Dynamics near the Product of Planar Heteroclinic Attractors

Accepted for Publication in Dynamical Systems: an International Journal (2011)

DYNAMICS NEAR THE PRODUCT OF PLANAR HETEROCLINIC ATTRACTORS

NIKITA AGARWAL, ALEXANDRE RODRIGUES, MICHAEL FIELD

Abstract. Motivated by problems in equivariant dynamics and connection selection in heteroclinic networks, Ashwin and Field investigated the product of planar dynamics where one at least of the factors was a planar homoclinic attractor. However, they were only able to obtain partial results in the case of a product of two planar homoclinic attractors. We give general results for the product of planar homoclinic and heteroclinic attractors. We show that the likely limit set of the basin of attraction of the product of two planar heteroclinic attractors is always the unique one-dimensional heteroclinic network which covers the heteroclinic attractors in the factors. The method we use is general and likely to apply to products of higher dimensional heteroclinic attractors as well as to situations where the product structure is broken but the cycles are preserved.

1. Introduction

One way of analyzing the dynamics of coupled dynamical systems is to first understand the dynamics of product systems (that is, uncoupled systems) and then perturb by adding coupling. In the case of two uncoupled dynamical systems, the perturbation could be to a skew product system where the base system weakly forces the second system. Motivated by problems in equivariant dynamics and coupled systems, Ashwin and Field [4] made a preliminary study of product dynamics when one of the factors was a (planar) homoclinic attractor. Strong results were obtained when the other factor was an attracting limit cycle — perhaps not so surprisingly, the main result (that the product was a minimal Milnor attractor [4, Theorem 1.2]) depended on non-trivial results from metric number theory. Strong results were also found when the second factor was a basic hyperbolic set. However, if both factors were planar homoclinic attractors, results were only obtained for a very restricted model [4, §6, Theorem 6.13].

In this paper we give quite general results about the *likely limit sets* of products of two-dimensional homoclinic and heteroclinic attractors. Although we restrict to products of two-dimensional systems, we believe that the methods we use have much wider applicability both to higher dimensional systems and to systems which are perturbations of a product.

Before stating our main result and giving examples, we need to recall the definition of the 'likely limit set' (details and references are given in the next section). Let M be a compact manifold, possibly with boundary, with measure ℓ which we assume is locally equivalent to Lebesgue measure. Suppose that X is a compact indecomposable attractor for the flow $\Phi_t : M \to M$ and that X has basin of attraction $\mathcal{B}(X)$ which we assume has strictly positive measure. It may be the case that ℓ-almost all points in $\mathcal{B}(X)$ are forward asymptotic to a proper subset of X. We capture this idea by defining the likely limit set of $\mathcal{B}(X)$ to be the smallest compact flow invariant subset Z of X with the property that for ℓ-almost all points $x \in \mathcal{B}(X)$, the omega limit set $\omega(x) \subset Z$.

Research of NA, MF and AR supported in part by NSF Grant DMS-0806321, research of AR supported in part by Centro de Matemática da Universidade do Porto (CMUP) and Fundação para a Ciência e Tecnologia (FCT), Portugal, through the programs POCTI and POSI with European Union and national fundings and also by the grant SFRH/BD/28936/2006 of FCT.

Suppose that Φ_t is a C^1 flow on the compact surface M, possibly with boundary. A *heteroclinic network* for the flow ϕ_t consists of a closed connected 1-dimensional Φ_t-invariant subset Σ of M which is the union of a finite set $\mathcal{E}(\Sigma) = \mathcal{E}$ of hyperbolic saddle points and a finite set of Φ_t-trajectories connecting equilibria in $\mathcal{E}$ such that the graph defined by equilibria (vertices) and trajectories (edges) is strongly connected (given two equilibria $\mathbf{p}, \mathbf{q} \in \mathcal{E}$, there exists a finite chain of trajectories in Σ joining $\mathbf{p}$ to $\mathbf{q}$). The simplest example of a heteroclinic network is a homoclinic loop consisting of one equilibrium and one trajectory (see below). We say that the heteroclinic network Σ is a *heteroclinic attractor* if the basin of attraction of Σ is a neighbourhood of Σ in M (below we allow for one-sided attractors, such as a homoclinic loop).

Theorem 1.1. *Let M_1, M_2 be compact surfaces and $\Sigma_1 \subset M_1$, $\Sigma_2 \subset M_2$ be heteroclinic attractors for C^2 flows $\phi_t^i : M_i \to M_i$, $i = 1, 2$. The likely limit set of $\mathcal{B}(\Sigma_1 \times \Sigma_2)$ for the product flow $\phi_t^1 \times \phi_t^2$ is the heteroclinic network*

$$(\Sigma_1 \times \mathcal{E}(\Sigma_2)) \cup (\mathcal{E}(\Sigma_1) \times \Sigma_2) \subset M_1 \times M_2.$$

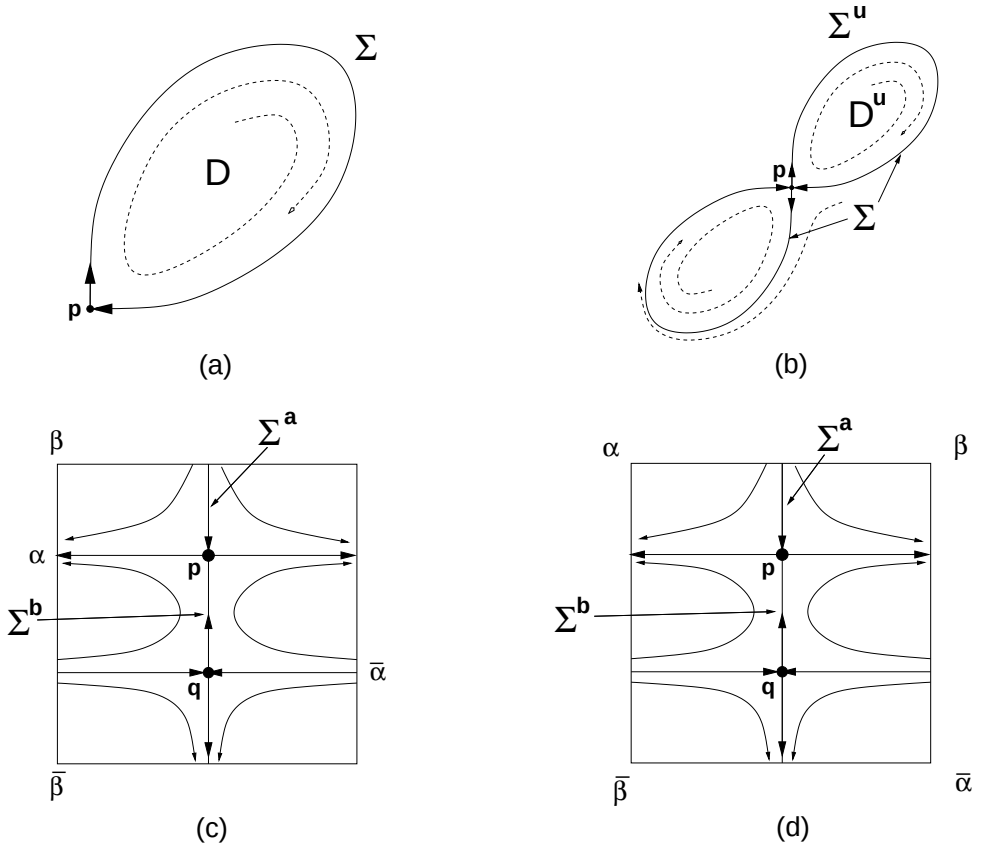

FIGURE 1. Homoclinic attractors on surfaces. (a) One sided homoclinic attractor, (b) figure-of-eight homoclinic attractor, (c) heteroclinic attractor on the Klein bottle, (d) heteroclinic attractor on projective space

.

In figure 1 we show a number of examples of homoclinic and heteroclinic attractors.

The attracting planar homoclinic loop $\Sigma \subset D$ shown in figure 1(a) is the simplest example of a planar homoclinic attractor. In this case the single equilibrium point $\mathbf{p}$ on the loop is a saddle point with contraction dominating the expansion. This loop is a one-sided attractor — nothing is said about the dynamics on the complement of the region D enclosed by the loop. If we take

two such attracting planar homoclinic loops $\Sigma_1 \subset D_1$, $\Sigma_2 \subset D_2$, with corresponding equilibria $\mathbf{p}_1$, $\mathbf{p}_2$, then it is a consequence of results in [4] that the only possibilities for the likely limit set of $\mathcal{B}(\Sigma_1 \times \Sigma_2) \subset D_1 \times D_2$ are either $\Sigma_1 \times \Sigma_2$ or the homoclinic network $(\Sigma_1 \times \{\mathbf{p}_2\}) \cup (\{\mathbf{p}_1\} \times \Sigma_2)$. It follows from theorem 1.1 that the second case is the only possibility.

The figure of eight homoclinic attractor Σ shown in figure 1(b) is attracting on both sides provided that the single equilibrium point $\mathbf{p}$ on the loop is a saddle point with contraction dominating the expansion. We consider the product of two loops of this type or the product with a one-sided homoclinic attractor of the type shown in figure 1(a). For example, if we take the product of figure of eight loops Σ_1, Σ_2, then theorem 1.1 implies that the likely limit set of $\mathcal{B}(\Sigma_1 \times \Sigma_2)$ is always the homoclinic network $(\Sigma_1 \times \{\mathbf{p}_2\}) \cup (\{\mathbf{p}_1\} \times \Sigma_2)$. In this case, there is a richer structure present as if we look at the product of $\mathcal{B}(\Sigma_1^u)$ (see figure 1) with that part of the basin of attraction of Σ_2 exterior to the loop, then the likely limit set is $(\Sigma_1^u \times \{\mathbf{p}_2\}) \cup (\{\mathbf{p}_1\} \times \Sigma_2)$.

In figure 1(c,d), we show two simple examples of heteroclinic attractors defined on the Klein bottle (c) and 2-dimensional real projective space (d). In both figures we identify opposite edges of the square so that α is identified with $\bar{\alpha}$, β with $\bar{\beta}$. The vector field on the Klein bottle has two saddle point equilibria $\mathbf{p}, \mathbf{q}$ on the heteroclinic network $\Sigma = \Sigma^a \cup \Sigma^b$, where in figure 1(c) we have indicated the unique edge of the heteroclinic cycle Σ^b (respectively, Σ^a), which is not common to Σ^a (respectively, Σ^b).

The vector field on projective space also has two saddle point equilibria $\mathbf{p}, \mathbf{q}$ on the heteroclinic network $\Sigma = \Sigma^a \cup \Sigma^b$. In this case the complement of the network has *three* connected regions.

If we take the product of the heteroclinic attractor Σ_1 on the Klein bottle with that the heteroclinic attractor Σ_2 on projective space, then it follows from theorem 1.1 that the likely limit set of $\mathcal{B}(\Sigma_1 \times \Sigma_2)$ is the heteroclinic network $\Sigma = (\Sigma_1 \times \{\mathbf{p}_2, \mathbf{q}_2\}) \cup (\{\mathbf{p}_1, \mathbf{q}_1\} \times \Sigma_2)$.

Remarks 1.2. (1) For general attracting heteroclinic networks, we expect the presence of *essentially asymptotically stable* subnetworks (see Brannath [6] and Melbourne [19]). More precisely, if Σ is an attracting heteroclinic network associated to a finite number of equilibria with only real eigenvalues, then the connections associated to the strongest expanding eigenvalues determine a possibly smaller attractor. If the attractor is a heteroclinic cycle then it is essentially asymptotically stable (in a neighbourhood of the network, almost all orbits converge to the cycle). An explicit example of this phenomenon was given by Kirk and Silber [16]. Given an asymptotically stable heteroclinic network Σ, define the principal out-connection of a saddle to be the heteroclinic connection corresponding to the most positive expanding eigenvalue of the linearization at the node. Ashwin and Chossat [5] conjectured the existence of an essentially asymptotically stable subnetwork $\Sigma^\star \subset \Sigma$ containing the principal connections that forms part of the attractor Σ. A general proof of essential asymptotic stability can be based on the Strong Lambda Lemma of Deng [8] but this result lies beyond the scope of the present paper. By contrast, products of heteroclinic attractors generally lead to heteroclinic networks without proper essentially asymptotically stable subnetworks. This is irrespective of the relative strength of eigenvalues at the equilibria. In all of the examples described above, the likely limit sets contain no proper essentially asymptotically stable heteroclinic cycles.
(2) For a product of planar heteroclinic cycles, the invariant subspaces forced by the product structure are least codimension two. In the absence of proper essentially asymptotically stable cycles, it is natural to ask whether switching (in the sense described by Aguiar *et al.* [2] and Homburg *et al.* [13]) can occur. We briefly address the study of this phenomenon at the end of section 3.

At the suggestion of a referee, we include some heuristic comments about the main result.

Suppose that the planar flows ϕ_t^1, ϕ_t^2 have homoclinic attractors Σ_1, Σ_2 respectively. Consider a segment γ_1 of a trajectory of ϕ_t^1, with initial condition $x \notin \Sigma_1$, that starts at $a \in A$ and makes one circuit of the loop, arriving back at c (see figure 2). Choose times t_a, t_b, t_c such that

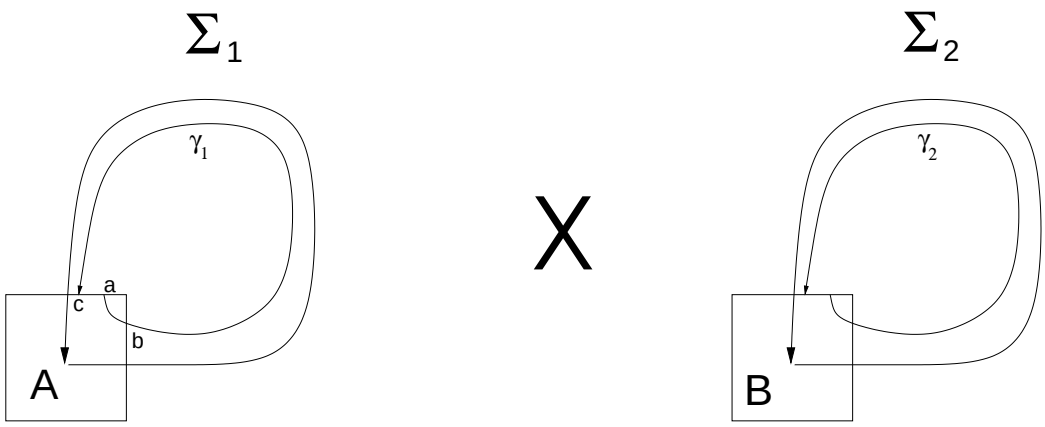

FIGURE 2. A product of homoclinic attractors

$a = \phi^1_{t_a}(x)$, $b = \phi^1_{t_b}(x)$, $c = \phi^1_{t_c}(x)$, If we assume the flow is linear on A, then it is easy to show that $t_b - t_a = O(|\log a|)$ and so $t_b - t_a \to \infty$ as $a \to 0$. On the other hand $t_c - t_b$ will be uniformly bounded above. If we pick a random time $t \in [t_a, t_c]$, then the probability p that $\phi^1_t(x) \notin A$ is $(t_c - t_b)/(t_c - t_a)$ and so $p \to 0$ as $a \to 0$. Similar comments hold for circuits γ_2 of the second system. If we assume the events of lying outside A and B are independent, then it follows that for almost all initial conditions (x, y), $\omega(x, y)$ contains no points of $(\Sigma_1 \setminus A) \times (\Sigma_2 \setminus B)$. The required result on the likely limit set would then follow by letting the diameters of A and B decrease to zero. However, since we are dealing with a deterministic system, we cannot assume independence of events (though we can expect a 'decay of correlations'). In practice, what we have to do is show that for almost all initial conditions (x, y), we can find a future time $T = T(x, y)$ such that for $t \geq T$, either $\phi^1_t(x) \in A$ or $\phi^2_t(y) \in B$. This in turn implies that for almost all initial conditions (x, y), $\omega(x, y)$ contains no points of $(\Sigma_1 \setminus A) \times (\Sigma_2 \setminus B)$. Our basic argument depends on obtaining precise estimates on the times t for which we can have $\phi^1_t(x) \notin A$ and $\phi^2_t(y) \notin B$ and then applying the Borel-Cantelli lemma (the part that does not require independence of events!) The analysis is fairly straightforward if we assume linear connection maps. However, the general case is tricky and does *not* follow directly from the special case. This, in itself, is a caution about making linearity assumptions on connection maps in heteroclinic networks: the nonlinearities are highly significant. To obtain our general results, we require flows to be at least C^2. *Our methods fail completely if the flows are only C^1 (or $C^{1+\varepsilon}$) even if we assume C^1 linearizability at the equilibria.* Indeed, it is quite possible that our results do not hold if the flows are only C^1.

We describe the contents of the paper by section. In section 2, we review basic definitions and results on Milnor attractors and the likely limit set. We also establish some conventions for our subsequent analysis of planar and surface attracting homoclinic and heteroclinic cycles. In section 3, we establish notational conventions and outline the strategy of the proof of the main result for the case of the product of two planar attracting homoclinic loops. The key and new ingredient is the use of the Borel-Cantelli lemma. In section 4 we give the proof for the product of two planar attracting homoclinic loops subject only to a restriction on the connection maps — we assume they are linear. In section 5, we show how our methods easily extend to general products of heteroclinic attractors, including figure eight homoclinic cycles and attracting heteroclinic cycles. We continue to assume the linearity restriction on connection maps. In section 6, we remove the linearity assumption on connection maps. The resulting analysis is delicate, especially in the resonant case where we assume that both heteroclinic

cycles have the same asymptotic attractivity (for a product of homoclinic loops, this amounts to the ratio of the eigenvalues at the equilibria being equal). We present the details only in the case of a product of attracting homoclinic loops but the extension of our methods and results to the general case is clear. At first reading, we would advise (and expect) most readers to omit the details in section 6. Overall these three sections illustrate how we use our argument based on the Borel-Cantelli lemma in a technically simple situation (section 4); how we extend to more general networks (section 5) and finally how we handle the arguments in the technically more demanding case when we make no simplifying assumptions on connection maps (section 6).

In sections 7 and 8, we show the results of numerical simulations of product systems as well as consider cases where we break homoclinic connections but preserve the product structure. We conclude with a brief discussion of possible generalizations and extensions of our results.

2. Preliminaries

2.1. **Milnor attractors and the likely limit set.** Let M be a differential manifold, possibly with boundary, and let ℓ denote a measure on M locally equivalent to the Lebesgue measure on charts (for example, if M is an orientable Riemannian manifold, then ℓ can be the measure defined by the Riemannian volume form). If Z is a measurable subset of M with $\ell(Z) \neq 0$, we let $\mathcal{F}(Z)$ denote the set of measurable subsets Z' of Z such that $\ell(Z \smallsetminus Z') = 0$.

Suppose that $\Phi_t : M \to M$ is a C^1 flow (or semi-flow) on M. Given $x \in M$, let

$$\omega(x) = \cap_{T>0}\overline{\{\Phi_t(x) \mid t \geq T\}}$$

denote the ω-limit set of the trajectory through x.

If X is a compact invariant subset of M, we let $\mathcal{B}(X) = \{x \in M \mid \omega(x) \subset X\}$ denote the *basin of attraction* of X. We recall the definitions of a Milnor attractor and minimal Milnor attractor (for more details we refer to Milnor [20]).

Definition 2.1 (Milnor [20])**.** A compact invariant subset X of M is a *Milnor attractor* if

(1) $\ell(\mathcal{B}(X)) > 0$;
(2) for any proper compact invariant subset Y of X, $\ell(\mathcal{B}(X) \smallsetminus \mathcal{B}(Y)) > 0$.

We say X is a *minimal (Milnor) attractor* if for all proper compact invariant subsets Y of X, $\ell(\mathcal{B}(Y)) = 0$.

Remark 2.2. A Milnor attractor X is minimal iff there is a full measure subset B of $\mathcal{B}(X)$ such that $\omega(x) = X$ for all $x \in B$.

Definition 2.3 (cf. Milnor [20])**.** Let $Z \subset M$ be measurable with $\ell(Z) > 0$, and Z forward Φ_t-invariant. The *likely limit set* $\mathcal{L}(Z)$ *of* Z is the smallest closed Φ_t-invariant subset of Z that contains all ω-limit sets except for a subset of Z of zero measure. That is,

$$\mathcal{L}(Z) = \cap_{Z' \in \mathcal{F}(Z)}\overline{\{\omega(x) \mid x \in Z'\}}.$$

Remarks 2.4. (1) If Z is relatively compact, then $\mathcal{L}(Z)$ is a non-empty, compact Φ_t-invariant subset of M.
(2) The definition of the likely limit set applies to measurable subsets $Z \subset M$ with $\ell(Z) > 0$ that are not necessarily forward Φ_t-invariant: since the flow is assumed C^1, it preserves measure zero sets and from this it follows straightforwardly that $\mathcal{L}(Z) = \mathcal{L}(\cup_{t\geq 0}\Phi_t(Z))$. (Of course, $\mathcal{L}(Z)$ may be empty if $\cup_{t\geq 0}\Phi_t(Z)$ is not relatively compact.)

We recall two results from [4] about likely limit sets.

Lemma 2.5 (Ashwin & Field [4, Lemma 2.3])**.** *Let $Z \subset M$ be measurable with $\ell(Z) > 0$, and Z forward Φ_t-invariant.*

(1) *$x \in \mathcal{L}(Z)$ iff for all $\varepsilon > 0$ and all $Z' \in \mathcal{F}(Z)$ there exists $a \in Z'$ such that $B_\varepsilon(x) \cap \omega(a) \neq \emptyset$ ($B_\varepsilon(x)$ denotes the ε ball about x);*

(2) $\mathcal{L}(Z)$ *is a minimal Milnor attractor iff for all* $x \in \mathcal{L}(Z)$ *and all* $\varepsilon > 0$ *and all* $H \subset Z$ *with* $\ell(H) > 0$, *we have*

$$\ell(\{a \in H \mid B_\varepsilon(x) \cap \omega(a) \neq \emptyset\}) > 0.$$

Theorem 2.6 (cf. Ashwin & Field [4, Theorem 1.1])**.** *Let* M_1, M_2 *be compact manifolds, possibly with boundary and* $\Phi_t = (\phi_t^1, \phi_t^2)$ *be a product of* C^1 *flows on* $M_1 \times M_2$. *Suppose that* $X_i \subset M_i$ *are forward* ϕ_t^i*-invariant measurable subsets of* M_i *of strictly positive measure,* $i = 1, 2$. *Then* $\mathcal{L}(X_1 \times X_2)$ *is invariant under the* $\mathbb{R}^2$ *action defined by* (ϕ_t^1, ϕ_s^2), $t, s \in \mathbb{R}^2$.

Proof. It is no loss of generality to assume that the X_i are ϕ_t^i-invariant subsets of M_i (replace X_i by $\cup_{t\in\mathbb{R}}\phi_t^i(X_i)$). The proof given in [4] for the case $X_i = M_i$, $i = 1, 2$, extends trivially to the case where the $X_i \subset M_i$ are ϕ_t^i-invariant measurable subsets of M_i of strictly positive measure – the crucial point is that the flows ϕ_t^i preserve sets of measure zero. □

2.2. **Planar homoclinic attractors.** Suppose that we are given a C^2 semi-flow Φ_t defined on some region $D^\star$ of $\mathbb{R}^2$ containing the origin. We assume that the origin is a hyperbolic saddle with associated eigenvalues $-\mu < 0 < \lambda$ and eigen-directions the x- and y-axes of $\mathbb{R}^2$ respectively. We also assume that there is a homoclinic cycle $\Sigma \subset D^\star$ connecting the origin (see figure 3).

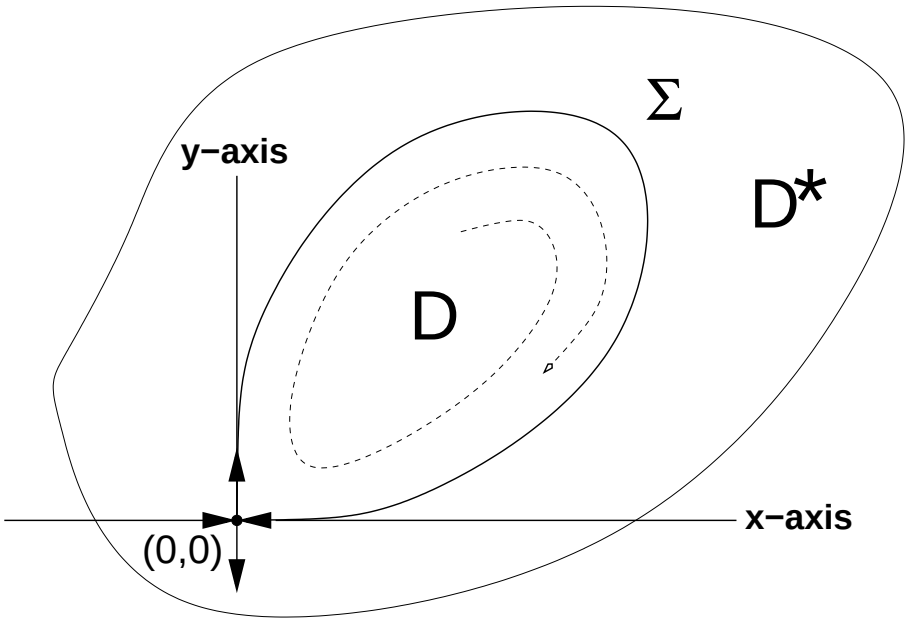

FIGURE 3. Attracting homoclinic loop in region $D^\star \subset \mathbb{R}^2$. Inside the region bounded by the homoclinic cycle Σ, trajectories approach the cycle. Outside this region, trajectories eventually go away from the cycle.

If $\mu > \lambda$, then it is well known that Σ is a (one-sided) attracting homoclinic cycle. More precisely, if we let $D \subset D^\star$ be the compact region in $\mathbb{R}^2$ with boundary Σ, then there exists an open neighbourhood N of Σ in D such that for all $x \in N \setminus \Sigma$, $\omega(x) = \Sigma$. We may choose N so that N is forward Φ_t-invariant with smooth interior boundary ∂N and such that the trajectories of Φ_t intersect ∂N transversally (see figure 4 and note that if $x \notin D$, then $\omega(x) \not\subset \Sigma$).

Given the setup shown in figure 4, N is a subset of the basin of attraction $\mathcal{B}(\Sigma)$ of Σ and, of course, $\mathcal{L}(N) = \mathcal{L}(\mathcal{B}(\Sigma)) = \Sigma$. In future, we always assume that a homoclinic cycle Σ of this type is the boundary of a compact region $D \subset \mathbb{R}^2$ and comes with a choice of neighbourhood N satisfying the properties described above. We denote by the quadruple (Σ, Φ_t, D, N).

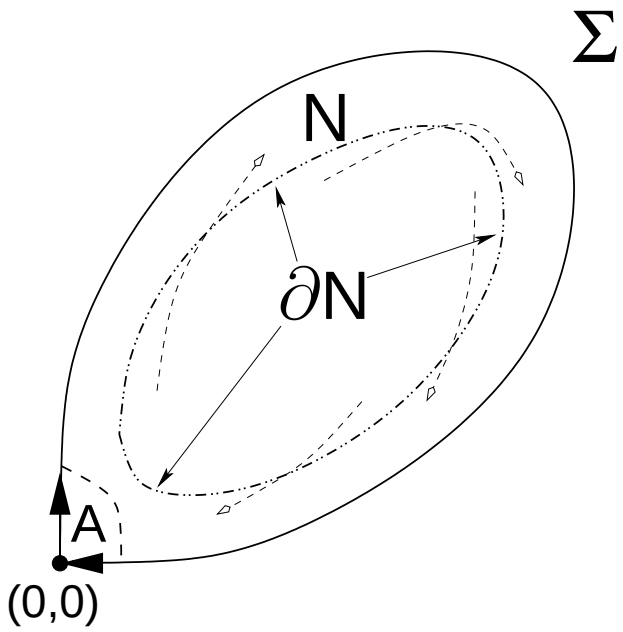

FIGURE 4. Interior neighbourhood N of Σ. Note that N is constructed in such a way that it is forward flow invariant and trajectories of Φ_t intersect ∂N transversely.

Remark 2.7. Noting remarks 2.4(2), if A is an open interior neighbourhood of $(0,0)$ (see figure 4), then $\mathcal{L}(A) = \Sigma$.

We may carry out a similar process for an attracting 'figure of eight' homoclinic cycle in the plane or, more generally an attracting planar heteroclinic cycle such as the Guckenheimer-Holmes cycle [11], [10, §5.2] or the heteroclinic cycles on the Klein bottle and projective space shown in figure 1.

3. Products of planar attracting homoclinic loops

For the next two sections we assume that $(\Sigma_i, \phi_t^i, D_i, N_i)$, $i = 1, 2$, are planar attracting homoclinic loops ('homoclinic attractors'). Recall that we assume $\partial D_i = \Sigma_i$, ϕ_i^t is a C^2 flow on D_i, and $N_i \subset \mathcal{B}(\Sigma_i)$ is a forward ϕ_i^t-invariant open interior neighbourhood of Σ_i. We assume that both homoclinic attractors have a saddle point at $(0,0)$, and corresponding eigenvalues $-\mu_i < 0 < \lambda_i$, where $\rho_i = \mu_i/\lambda_i > 1$, $i = 1, 2$ (in the terminology of L Shilnikov, the ρ_i are the *saddle indices* of the homoclinic loops [22, Chapter 13]). Set $\Sigma = (\Sigma_1 \times \{(0,0)\}) \cup (\{0,0\} \times \Sigma_2) \subset D_1 \times D_2 \subset \mathbb{R}^4$ and let $\mathbf{0} = (0,0,0,0) \in \Sigma$ denote the unique equilibrium for the product flow in $N_1 \times N_2$. Let $\Phi_t = (\phi_t^1, \phi_t^2)$ denote the product flow on $D_1 \times D_2$.

Using theorem 2.6, it was shown in Ashwin & Field [4, Theorem 6.1] that either $\mathcal{L}(N_1 \times N_2) = \Sigma$ or $\mathcal{L}(N_1 \times N_2) = \Sigma_1 \times \Sigma_2$. Our aim is to prove that we always have $\mathcal{L}(N_1 \times N_2) = \Sigma$. For the remainder of this section, we outline the strategy that we use for the proof as well as establish notational conventions.

Since $(0,0)$ is a hyperbolic saddle point of a C^2 *planar* flow, it follows by a result of Hartman [12] that we can always choose a C^1-linearization of ϕ_t^i on some closed neighbourhood A_i of $(0,0)$, $i = 1, 2$ (the C^2 regularity of the flow will play a key role in section 6). Linearly rescaling coordinates, we may assume that $A_i = [0,1] \times [0,1] \subset N$. Let $A_i^\circ = [0,1) \times [0,1)$ denote the interior of A_i in D_i. We may choose the A_i so that the forward ϕ_t^i-trajectory through $(1,1)$ meets $\{1\} \times [0,1] \subset \partial A_i$ after one circuit of the loop (see figure 5).

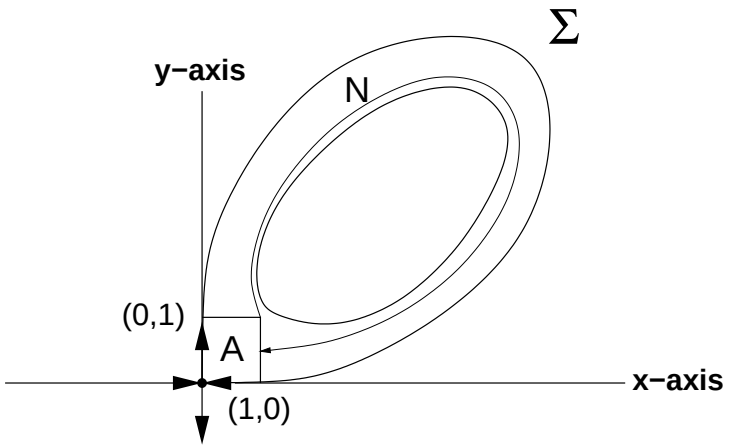

FIGURE 5. Linearizing coordinates at the origin.

Given $i \in \{1,2\}$, let $U_i = \{1\}\times[0,1]$, $V_i = [0,1]\times\{1\} \subset \partial A_i$ denote the vertical and horizontal interior boundaries of A_i (see figure 6).

We adopt the convention that if $y \in [0,1] \approx U_i$, then $\phi_t^i(y)$ is defined to be $\phi_t^i(1,y)$. We similarly identify a point $(x,1) \in V_i$ with $x \in [0,1]$.

We have a C^1 time of first return map $T_i : V_i \to \mathbb{R}$ and associated C^1 connection map $C_i : V_i \to U_i$ defined by $C_i(x) = \phi^i_{T_i(x)}(x)$, $x \in V_i$.

Let $\tau_i^+ = \sup_{x\in V_i} T_i(x)$, $\tau_i^- = \inf_{x\in V_i} T_i(x)$. Obviously, $\tau_i^+ \geq \tau_i^- > 0$. Since the time it takes for a trajectory starting at $y \in U_i$ to exit A_i though V_i grows without bound as $y \to 0^+$, it is easy to verify that every trajectory in $N_1 \times N_2$ passes through $A_1 \times A_2$. From this it follows that $\mathcal{L}(A_1 \times A_2) = \mathcal{L}(N_1 \times N_2)$.

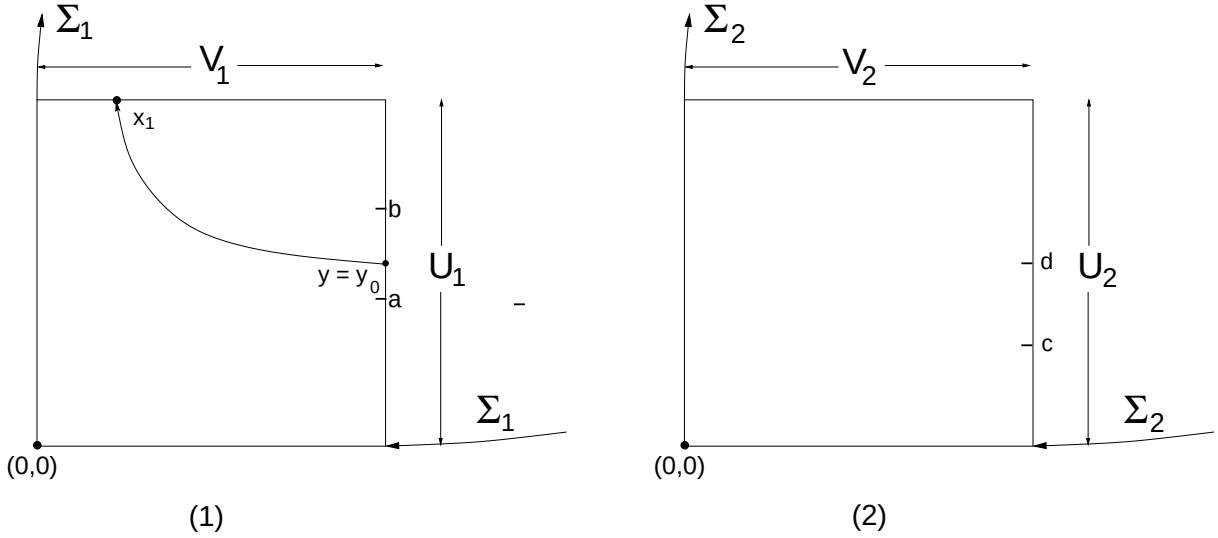

FIGURE 6. Notation and setup for the sets A_1, A_2: all trajectories with initial conditions on $U_i \smallsetminus \{(1,1)\}$ (respectively $V_i \smallsetminus \{(1,1)\}$), are inside A_i for small strictly positive (respectively, negative) time.

Given $b \in U_1$, $b > 0$, let $a < b$ denote the first point of intersection of the forward ϕ_t^1-trajectory through b with U_1. Similarly, given $d \in U_2$, $d > 0$, define $c < d$ to be the first point of intersection of the forward ϕ_t^2-trajectory through d with U_2. (See figure 6.)

Given $y \in [a, b]$, let $0 < s_1^y(1) < s_1^y(2) < \cdots$ denote the sequence of positive times t at which $\phi_t^1(y) \in V_1$ and $0 = t_1^y(0) < t_1^y(1) < t_1^y(2) < \cdots$ denote the sequence of positive times t at which $\phi_t^1(y) \in U_1$. Observe that $t_1^y(n) - s_1^y(n) \in [\tau_1^-, \tau_1^+]$.

Let $(x_n^1) \subset V_1$ be the decreasing sequence of points of intersection of the forward trajectory through $y \in [a, b]$ with V_1 and (y_n^1) be the corresponding sequence of points of intersection with U_1. We have

$$\begin{aligned} y_n^1 &= \phi^1_{T_1(x_n^1)}(x_n^1), \\ x_n^1 &= \phi^1_{s_1^y(n)}(y) = \phi^1_{s_1^y(n)-s_1^y(1)}(x_1^1), \\ y_n^1 &= \phi^1_{t_1^y(n)}(y) = \phi^1_{s_1^y(n)+T_1(x_n^1)}(y), \\ s_1^y(n+1) - t_1^y(n) &= \lambda_1^{-1} \log(y_n^1)^{-1}, \\ x_{n+1}^1 &= (y_n^1)^{\mu_1/\lambda_1} = (y_n^1)^{\rho_1}, \end{aligned}$$

where the last two statements use the linearity of the flow ϕ_t^1 on A_1 and hold for $n \geq 0$. Similar statements hold for ϕ_t^2.

Definition 3.1. Given $n \in \mathbb{N}$, $y \in [a, b]$, we say $t > 0$ is *n-singular* for A_1 if $t \in [s_1^y(n), t_1^y(n)]$. If $t \geq s_1^y(n)$, we say the trajectory $\phi_t^1(y)$ has made at least n-turns about the homoclinic cycle Σ_1.

Remarks 3.2. (1) If t is n-singular for A_1, then $\phi_t^1(y) \notin A_1^\circ$.
(2) The definition of making at least n-terms about Σ_1 implicitly depends on A_1.

Let $\mathcal{C} \subset \Sigma_1 \times \Sigma_2$ consist of all pairs $(p, q) \in \Sigma_1 \times \Sigma_2$ such that $p, q \notin [0, 1) \times \{0\} \cup \{0\} \times [0, 1)$. If we let $\kappa_i \subset \Sigma_i$ be the closed arcs defined by $\kappa_i = \Sigma_i \setminus A_i^\circ$, then $\mathcal{C} = \kappa_1 \times \kappa_2$.

Definition 3.3. Given A_1, A_2 as defined above, a point $(X, Y) \in A_1 \times A_2$ is a *bad point* if $\omega(X, Y) \cap \mathcal{C}^\circ \neq \emptyset$ ($\mathcal{C}^\circ$ denotes the interior of $\mathcal{C}$ in $\Sigma_1 \times \Sigma_2$).

Remark 3.4. We shall show that the set of bad points in $A_1 \times A_2$ has measure zero. It then follows immediately from theorem 2.6 that $\mathcal{L}(A_1 \times A_2) = \Sigma$.

Let $E = [a, b] \times [c, d] \subset U_1 \times U_2$. For $n \in \mathbb{N}$, define $E_n \subset E$ by

$$E_n = \{(y, z) \in E \mid \exists t \in [s_1^y(n), t_1^y(n)] \text{ such that } \phi_t^2(z) \notin A_2^\circ\}.$$

We refer to points of E_n as the *n-bad points of E*. Observe that $(y, z) \in E_n$ if and only if there exists $t > 0$, $m \in \mathbb{N}$ such that t is n-singular for A_1 and m-singular for A_2. In particular, $\phi_t^2(z) \notin A_2^\circ$. If, for $m \in \mathbb{N}$, we define

$$E_{n,m} = \{(y, z) \in E \mid [s_1^y(n), t_1^y(n)] \cap [s_2^z(m), t_2^z(m)] \neq \emptyset\},$$

then $E_n = \cup_{m \geq 1} E_{n,m}$.

Lemma 3.5. *If $(y, z) \in E$, then a point $(p, q) \in \mathcal{C}^\circ \cap \omega(y, z)$ only if there exists an infinite increasing sequence $n_1 < n_2 < \cdots$ ... such that $(y, z) \in \cap_{j \geq 1} E_{n_j}$. Conversely, if there exists an infinite increasing sequence $n_1 < n_2 < \cdots$ ... such that $(y, z) \in \cap_{j \geq 1} E_{n_j}$, then $(p, q) \in \mathcal{C} \cap \omega(y, z)$.*

Proof. If there exists $N \in \mathbb{N}$ such that $(y, z) \notin E_n$, $n \geq N$, then all the limit points of the Φ_t-trajectory through (y, z) must lie in $(A_1 \times \Sigma_2) \cup (\Sigma_1 \times A_2)$ which is disjoint from $\mathcal{C}^\circ$. Conversely, suppose $(y, z) \in \cap_{j \geq 1} E_{n_j}$. Using the compactness of $\Sigma_1 \times \Sigma_2$, we can pick a subsequence (m_j) of (n_j) and sequence $t_{m_1} < t_{m_2} < \cdots$ with $t_{m_j} \in [s_1^y(m_j), t_1^y(m_j)]$ and $\phi^2_{t_{m_j}}(z) \notin A_2^\circ$, such that $(\Phi_{t_{m_j}}(y, z))$ converges to a point in $\mathcal{C}$. $\square$

Applying the Borel-Cantelli lemma. Let E_∞ denote the subset of E consisting of points (y, z) such that there exists an infinite increasing sequence (n_j) such that $(y, z) \in \cap_{j\geq 1} E_{n_j}$. We have $E_\infty = \cap_{N\geq 1} \cup_{n\geq N} E_n$. It follows from lemma 3.5 that the bad points of E are a subset of E_∞. Take Lebesgue measure ℓ_2 on E. Our main work will be to show $\sum_{n=1}^{\infty} \ell_2(E_n) < \infty$. It then follows from the Borel-Cantelli lemma that $\ell_2(E_\infty) = 0$ and so there is a full measure subset E' of E such that $\omega(y, z) \cap \mathcal{C}^\circ = \emptyset$ for all $(y, z) \in E'$.

The proof we give for the convergence of $\sum_{n=1}^{\infty} \ell_2(E_n)$ applies to all products $E = [a, b] \times [c, d] \subset (0, 1] \times (0, 1] \subset U_1 \times U_2$, where a, c are the points of first return. Since $(0, 1] \times (0, 1]$ can written as a countable union of such products, it follows by the σ-additivity of ℓ_2 that the set of bad points in $U_1 \times U_2$ has zero measure.

Furthermore, we are able to show that our arguments do not depend on the particular choice of linearizing neighbourhood $A_1 \times A_2$: we can replace $E = (\{1\} \times [a, b]) \times (\{1\} \times [c, d])$ by any product of vertical intervals from $A_1 \times A_2$. That is, suppose $x, x', b, d \in (0, 1]$, and define corresponding intervals $I_x = \{x\} \times [a, b] \subset A_1$, $I_{x'} = \{x'\} \times [c, d] \subset A_2$ such that a is the first point of intersection of the forward ϕ_t^1-orbit through (x, b) with $\{x\} \times [0, 1]$, and similarly for c. Set $E = I_x \times I_{x'}$. Now linearly rescale the horizontal coordinates to obtain a new box linearizing neighbourhood $A_1^\star \times A_2^\star \subset A_1 \times A_2$ such that in the new coordinates $A_1^\star, A_2^\star = [0, 1] \times [0, 1]$ and $I_x = [a, b] \subset \{1\} \times (0, 1]$, $I_{x'} = [c, d] \subset \{1\} \times (0, 1]$ (note that the vertical coordinates are unchanged). By the original argument, it follows there is a full measure subset E' of E such that $\omega(y, z) \cap \mathcal{C}^\circ = \emptyset$ for all $(y, z) \in E'$ ($\mathcal{C}$ is expanded when we use the smaller box $A_1^\star \times A_2^\star$ so we can safely take the *original* $\mathcal{C}$ for this argument). Using the argument of the previous paragraph, we deduce that the bad points are a measure zero subset of $(\{x\} \times (0, 1]) \times (\{x'\} \times [0, 1]) \subset A_1 \times A_2$ for all $x, x' \in (0, 1]$. Since the set of bad points in $A_1 \times A_2$ is easily seen to be measurable, it follows by Fubini's theorem that the set of bad points form a measure zero subset of $A_1 \times A_2$. Therefore there is a full-measure subset A' of $A_1 \times A_2$ for which $\omega(y, z) \cap \mathcal{C}^\circ = \emptyset$ for all $(y, z) \in A'$ proving that $\mathcal{L}(A_1 \times A_2) \neq \Sigma_1 \times \Sigma_2$. Hence, $\mathcal{L}(N_1 \times N_2) = \Sigma$.

Remark 3.6. The final step uses the $\mathbb{R}^2$-invariance of the likely limit set (theorem 2.6). However, we could have avoided this by observing that our arguments show the existence of a full-measure subset A' of $A_1 \times A_2$ for which $\omega(y, z) \cap \mathcal{C}^\circ = \emptyset$ for all $(y, z) \in A'$. Since this holds for a base of box neighbourhoods $A_1 \times A_2$ of $\mathbf{0}$, we deduce that $\mathcal{L}(N_1 \times N_2) \subset \Sigma$. Of course, for product dynamics we can infer equality. However, in other situations where the product structure is broken but the attracting homoclinic loops persist, the inclusion $\mathcal{L}(N_1 \times N_2) \subset \Sigma$ may be strict (this is of particular interest for products of planar 'figure of eight' attracting homoclinic loops.)

4. Products of homoclinic loops: proof of a special case

In this section, we present the proof for products of planar attracting homoclinic loops under a simplifying assumption on the connection maps $C_i : V_i \to U_i$. We assume that for both flows ϕ_t^i, there exist strictly positive constants τ_1, τ_2, m_1, m_2 such that

$$T_i(x) = \tau_i,\ C_i(x) = m_i x,\ x \in U_i. \tag{4.1}$$

We give the proof for general connection maps in section 6.

Remarks 4.1. (1) Since we are assuming $A_i = [0, 1] \times [0, 1] \subset N_i$, we always have $m_i < 1$, $i = 1, 2$ (else N_i would contain a limit cycle).
(2)

Observe that (4.1) continues to hold, though generally with different constants τ_1, τ_2, m_1, m_2, if we replace A_1, A_2 by smaller rectangular neighbourhoods $A_1^\star, A_2^\star$ (relative to the same choice of linearizing coordinates). Referring to figure 7, suppose we linearly rescale coordinates on $A^\star$ so that, in the rescaled coordinates, $A^\star = [0, 1] \times [0, 1]$ (we omit the subscript i). We may choose

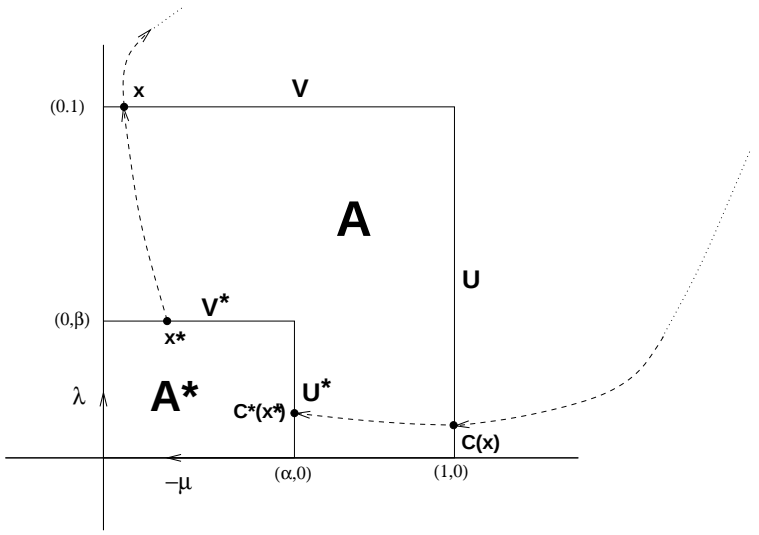

FIGURE 7. Rescaling coordinates and the connection map.

unique $T, S \geq 0$ such that $\alpha = e^{-\mu S}$, $\beta = e^{-\lambda T}$. In coordinates $(x^\star, y^\star)$ on $A^\star = [0,1] \times [0,1]$, the connection map $C^\star : V^\star \to U^\star$ is given by

$$C^\star(x^\star) = e^{(T+S)\lambda} C(e^{-\mu(T+S)} x^\star) \tag{4.2}$$

In particular, if $C(x) = mx$, then in rescaled coordinates, we have

$$C^\star(x^\star) = e^{(T+S)(\lambda-\mu)} m x^\star.$$

Since $\lambda - \mu < 0$, $e^{(T+S)(\lambda-\mu)} m < m$, if $T + S > 0$.

As in the previous section, we choose $E = [a,b] \times [c,d] \subset U_1 \times U_2$.

Lemma 4.2. *Let $(y,z) \in E$, $n \in \mathbb{N}$. We have*

(1) $t_1^y(n) = s_1^y(n) + \tau_1$ *and* $t_2^z(n) = s_2^z(n) + \tau_2$.
(2) $t_1^y(n) = n\tau_1 - \frac{1}{\lambda_1}(\alpha_n \log y + \pi_n \log m_1)$, *where* $\alpha_n = \frac{\rho_1^n - 1}{\rho_1 - 1}$, *and* $\pi_n = \frac{\rho_1^n - n\rho_1 + (n-1)}{(\rho_1 - 1)^2}$.
(3) $t_2^z(n) = n\tau_2 - \frac{1}{\lambda_2}(\beta_n \log z + \theta_n \log m_2)$, *where* $\beta_n = \frac{\rho_2^n - 1}{\rho_2 - 1}$, *and* $\theta_n = \frac{\rho_2^n - n\rho_2 + (n-1)}{(\rho_2 - 1)^2}$.

Proof. (1) Immediate from (4.1) and the definitions of $t_1^y(n)$, $s_1^y(n)$.
(2,3) We prove (2), the proof of (3) is identical. Let $y_0 = y, y_1, \cdots$ and $x_1, x_2, \cdots$ denote the successive points of intersection of the forward trajectory through y with U_1 and V_1 respectively. We have $s_1^y(n) - t_1^y(n) = -\frac{1}{\lambda_1} \log y_n$, $x_n = y_n^{\rho_1}$, and $y_{n+1} = m_1 x_n = m_1 y_n^{\rho_1}$. Substituting and summing the finite sums gives the result. □

We will need the estimate on the ratios π_n/α_n, θ_n/β_n given by the next lemma.

Lemma 4.3. *(Notation as above.) For all $n \in \mathbb{N}$ we have*

$$0 \leq \frac{\pi_n}{\alpha_n} \leq \frac{1}{\rho_1 - 1}, \quad 0 \leq \frac{\theta_n}{\beta_n} \leq \frac{1}{\rho_2 - 1}.$$

Proof. Computing we find that

$$\frac{\pi_n}{\alpha_n} = \frac{\rho_1^n - n\rho_1 + (n-1)}{(\rho_1 - 1)(\rho_1^n - 1)} = \frac{1}{\rho_1 - 1}\left(1 - \frac{n}{\sum_{j=1}^{n-1} \rho_1^j}\right).$$

Since $\rho_1^j \geq 1$, $j \geq 0$, the result follows. □

Definition 4.4. Given $n, m \in \mathbb{N}$ and $y \in [a, b]$, we define the closed subinterval $[Z_m^1(y, n), Z_m^2(y, n)]$ of $[c, d]$ by

$$[Z_m^1(y, n), Z_m^2(y, n)] = \{z \in [c, d] \mid (y, z) \in E_{n,m}\}.$$

We refer to $[Z_m^1(y, n), Z_m^2(y, n)]$ as a *bad subinterval*.

Lemma 4.5. *If $n, m \in \mathbb{N}$, $y \in [a, b]$ and $[Z_m^1(y, n), Z_m^2(y, n)] \neq \emptyset$, then $Z_m^1(y, n)$ is given as the maximum of c and the unique solution of $s_2^z(m) = s_1^y(n) + \tau_1$ and $Z_m^2(y, n)$ as the minimum of d and the unique solution of $s_2^z(m) = s_1^y(n) - \tau_2$.*

Proof. The result follows by noting that $s_2^z(m)$ is a decreasing function of $z \in [c, d]$ and that the endpoints of the bad interval are given as the intersection of $[c, d]$ with the interval with endpoints determined by the equations $s_2^z(m) = s_1^y(n) - \tau_2, s_1^y(n) + \tau_1$. □

Proposition 4.6. *Every bad subinterval $[Z_m^1(y, n), Z_m^2(y, n)]$ of $[c, d]$ is contained in the interval $[\overline{Z}_m^1(y, n), \overline{Z}_m^2(y, n)]$ where,*

$$\begin{aligned}
\overline{Z}_m^2(y, n) &= e^{\frac{\lambda_2}{\beta_m}(m\tau_2 - (n-1)\tau_1)} y^{\frac{\lambda_2 \alpha_n}{\lambda_1 \beta_m}} m_1^{\frac{\lambda_2 \pi_n}{\lambda_1 \theta_m}} m_2^{-\frac{\theta_m}{\beta_m}} \\
\overline{Z}_m^1(y, n) &= e^{\frac{\lambda_2}{\beta_m}((m-1)\tau_2 - n\tau_1)} y^{\frac{\lambda_2 \alpha_n}{\lambda_1 \beta_m}} m_1^{\frac{\lambda_2 \pi_n}{\lambda_1 \theta_m}} m_2^{-\frac{\theta_m}{\beta_m}} < \overline{Z}_m^2(y, n)
\end{aligned}$$

Proof. By lemma 4.5, $[Z_m^1(y, n), Z_m^2(y, n)]$ is contained in an interval with end points given by the solution of $s_2^z(m) = s_1^y(n) + \tau_1, s_1^y(n) - \tau_2$. Solving for z, using lemma 4.2, gives the result. □

Remark 4.7. We have $\overline{Z}_m^1(y, n) = e^{\frac{-\lambda_2}{\beta_m}(\tau_1 + \tau_2)} \overline{Z}_m^2(y, n)$.

Let $y \in [a, b]$, $n \in \mathbb{N}$ and $t \in [s_1^y(n), s_1^y(n) + 1]$. The number of turns of $\phi_t^2(z)$ is an increasing function of $z \in [c, d]$. In particular, the maximum number of turns is made when $z = d$. If we let $M_E(n, y)$ denote the number of turns taken by d around Σ_2 in time $s_1^y(n) + 1$, we have

$$M_E(n, y) = \min\{m \mid s_2^d(m + 1) > s_1^y(n) + 1\}, \tag{4.3}$$

Define $M_E(n) = \sup_{y \in [a,b]} M(n, y)$.

Lemma 4.8. *(Notation and assumptions as above.) If $n \in \mathbb{N}$, we have*

1. *$M_E(n) < \infty$.*
2. *If $t > 0$ is n-singular for A_1, then the number of turns of $\phi_t^2(z)$ about Σ_2 is at most $M_E(n)$.*

4.1. **The ℓ_2 measure of E_∞.** We start by estimating $\ell_2(E_n)$.

Lemma 4.9. *There exists $C > 0$ such that for all $n \in \mathbb{N}$,*

$$\ell_2(E_n) \leq C \sum_{m=1}^{\infty} \frac{1}{\lambda_1 \beta_m + \lambda_2 \alpha_n} e^{\frac{\lambda_2}{\beta_m}(\tau_2 m - \tau_1(n-1))}.$$

Proof. Let $n \in \mathbb{N}$. We have

$$\begin{aligned}
\ell_2(E_n) &\leq \int_a^b \sum_{m=1}^{M_E(n)} (\overline{Z}_m^2(y, n) - \overline{Z}_m^1(y, n))\, dy \\
&= \int_a^b \sum_{m=1}^{M_E(n)} e^{\frac{\lambda_2}{\beta_m}(\tau_2 m - \tau_1(n-1))} (1 - e^{\frac{-\lambda_2}{\beta_m}(\tau_1 + \tau_2)}) y^{\frac{\lambda_2 \alpha_n}{\lambda_1 \beta_m}} m_1^{\frac{\lambda_2 \pi_n}{\lambda_1 \theta_m}} m_2^{-\frac{\theta_m}{\beta_m}}\, dy, \\
&= \sum_{m=1}^{M_E(n)} e^{\frac{\lambda_2}{\beta_m}(\tau_2 m - \tau_1(n-1))} (1 - e^{\frac{-\lambda_2}{\beta_m}(\tau_1 + \tau_2)}) m_1^{\frac{\lambda_2 \pi_n}{\lambda_1 \theta_m}} m_2^{-\frac{\theta_m}{\beta_m}} \left(\int_a^b y^{\frac{\lambda_2 \alpha_n}{\lambda_1 \beta_m}}\, dy \right).
\end{aligned}$$

By lemma 4.3, there exists $C_1 = C_1(m_2) > 0$ such that $m_2^{-\frac{\theta_m}{\beta_m}} \leq C_1$, for all $m \in \mathbb{N}$. Since $m_1 < 1$, we have $m_1^{\frac{\lambda_2\pi_n}{\lambda_1\theta_m}} \leq 1$, for all $m, n \in \mathbb{N}$. We also have

$$\int_a^b y^{\frac{\lambda_2\alpha_n}{\lambda_1\beta_m}}\, dy \leq \int_0^1 y^{\frac{\lambda_2\alpha_n}{\lambda_1\beta_m}}\, dy = \frac{\lambda_1\beta_m}{\lambda_1\beta_m + \lambda_2\alpha_n}.$$

Hence

$$\begin{aligned}\ell_2(E_n) &\leq C_1 \sum_{m=1}^{M_E(n)} \frac{\lambda_1\beta_m}{\lambda_1\beta_m + \lambda_2\alpha_n} e^{\frac{\lambda_2}{\beta_m}(\tau_2 m - \tau_1(n-1))}(1 - e^{\frac{-\lambda_2}{\beta_m}(\tau_1+\tau_2)}) \\ &\leq C_1 \sum_{m=1}^{M_E(n)} \frac{\lambda_1\lambda_2(\tau_1+\tau_2)}{\lambda_1\beta_m + \lambda_2\alpha_n} e^{\frac{\lambda_2}{\beta_m}(\tau_2 m - \tau_1(n-1))},\end{aligned}$$

where we have used $(1 - e^{\frac{-\lambda_2}{\beta_m}(\tau_1+\tau_2)}) \leq (\tau_1+\tau_2)\frac{\lambda_2}{\beta_m}$. Hence we have the estimate

$$\ell_2(E_n) \leq C \sum_{m=1}^{\infty} \frac{1}{\lambda_1\beta_m + \lambda_2\alpha_n} e^{\frac{\lambda_2}{\beta_m}(\tau_2 m - \tau_1(n-1))}.$$

where $C = \lambda_1\lambda_2 C_1(\tau_1+\tau_2)$. □

Lemma 4.10. $\ell_2(E_\infty) = 0$.

Proof. We start by proving that $\sum_{n=1}^{\infty} \ell_2(E_n) < \infty$. By lemma 4.9, it suffices to prove that $\sum_{n,m=1}^{\infty} \frac{1}{\lambda_1\beta_m+\lambda_2\alpha_n} e^{\frac{\lambda_2}{\beta_m}(\tau_2 m - \tau_1(n-1))}$ converges. By the arithmetic-geometric mean inequality we have the estimate

$$\frac{1}{\lambda_1\beta_m + \lambda_2\alpha_n} \leq 1/(2\sqrt{\lambda_1\lambda_2}\sqrt{\beta_m\alpha_n}),\ m, n \geq 1.$$

It follows easily from the definition of α_n, β_m that there exists $C > 0$ such that

$$\frac{1}{\lambda_1\beta_m + \lambda_2\alpha_n} \leq C\rho_1^{-n/2}\rho_2^{-m/2}, m, n \geq 1. \tag{4.4}$$

Observe that if $\tau_2 m - \tau_1(n-1) \leq 0$, then $e^{\frac{\lambda_2}{\beta_m}(\tau_2 m - \tau_1(n-1))} \leq 1$. On the other hand if $\tau_2 m - \tau_1(n-1) > 0$, then $(\tau_2 m - \tau_1(n-1))/\beta_m \leq \tau_2$, since $\beta_m \geq m$, and so $e^{\frac{\lambda_2}{\beta_m}(\tau_2 m - \tau_1(n-1))} \leq e^{\tau_2\lambda_2}$. Hence we have a uniform bound on $e^{\frac{\lambda_2}{\beta_m}(\tau_2 m - \tau_1(n-1))}$ and the convergence of the double sum follows from (4.4). Since $\sum_{n=1}^{\infty} \ell_2(E_n) < \infty$, it follows by the Borel-Cantelli lemma [15, Theorem 13.1], that $\ell_2(E_\infty) = 0$. □

Theorem 4.11. *The likely limit set of the product of two planar homoclinic attractors* (Σ_1, ϕ_t^1) *and* (Σ_2, ϕ_t^2) *is* Σ.

Proof. Our argument for the vanishing of $\ell_2(E_\infty)$ did not depend on our choices of $b, d \in [0, 1]$. We now follow the arguments given at the end of section 3: by σ-additivity of ℓ_2, the set of bad points in $(\{1\} \times [0, 1]) \times (\{1\} \times [0, 1])$ has measure zero. Using the rescaling argument given in section 3, we deduce that the set of bad points in $(\{x\} \times [0, 1]) \times (\{x'\} \times [0, 1])$ has measure zero for all $x, x' \in (0, 1]$. It follows by Fubini's theorem that the set of bad points in $A_1 \times A_2$ has measure zero. Hence $\mathcal{L}(A_1 \times A_2) = \mathcal{L}(N_1 \times N_2) \neq \Sigma_1 \times \Sigma_2$. and the result follows by theorem 2.6. □

Remark 4.12. Neither of the cycles in the network $\Sigma \subset \mathbb{R}^4$ is essentially asymptotically stable: for all points (not lying on the stable manifolds), the associated trajectory makes infinitely many traversals arbitrarily close to both homoclinic cycles, even when $\rho_1 = \rho_2$.

4.2. **Switching.** In the remainder of the section, we briefly indicate why we cannot expect switching in the network Σ.

Following the notation of Homburg *et al.* [13], let $\gamma_1 = \Sigma_1 \times \{(0,0)\}$ and $\gamma_2 = \{(0,0)\} \times \Sigma_2$ denote the homoclinic orbits which define the heteroclinic network Σ. Let U_Σ be a tubular neighbourhood of Σ and $U_{\mathbf{0}} \subset U_\Sigma$ be a small neighbourhood of $\mathbf{0}$. Let S_1 and S_2 be two mutually disjoint cross sections transverse to γ_1 and γ_2 respectively. We suppose $S_1, S_2 \subset U_\Sigma \setminus U_{\mathbf{0}}$.

Let $\kappa = (k_i) \in \{1,2\}^{\mathbb{N}}$ be a symbolic sequence. We say that the trajectory with initial condition $\overline{x}$ is a forward realization of κ if the forward trajectory of $\overline{x}$ is contained in U_Σ and there exists an increasing sequence of times $(t_i)_{i\in\mathbb{Z}^+}$, with $t_0 = 0$, such that:

- $\phi^1_{t_i} \times \phi^2_{t_i}(\overline{x}) \in S_{k_i}, i \in \mathbb{N}$;
- $\phi^1_{t_i} \times \phi^2_{t_i}(\overline{x}) \notin S_1 \cup S_2$, all $t \in (t_i, t_{i+1})$, $i \in \mathbb{N}$;
- for $t \in (t_i, t_{i+1})$, the trajectory visits $U_{\mathbf{0}}$ exactly once, $i \in \mathbb{N}$.

In other words, a realization of κ is a trajectory that, after an initial transient, follows the homoclinic connections γ_{k_i} in the order prescribed by κ. Our next definition is based on that of Aguiar *et al.* [2] adapted to our context.

Definition 4.13. The product of two homoclinic cycles is *switching* if for each symbolic sequence $\kappa \in \{1,2\}^{\mathbb{N}}$, there exists a forward realization of κ in U_Σ.

Remarks 4.14. (1) The product of two homoclinic cycles is *finite switching* if the previous set-up holds for finite sequences κ (instead of infinite sequences).
(2) In the obvious way, switching can be defined for the product of two heteroclinic attractors.

Proposition 4.15. *The network in $\Sigma \subset \mathbb{R}^4$ is not switching or finite switching.*

Proof. It suffices to prove that Σ is not finite switching. Without loss of generality, suppose that $U_{\mathbf{0}} \subset A_1 \times A_2$ and $K \subset U_{\mathbf{0}}$ is compact and disjoint from Σ. Given $\overline{x} = (y,z) \in U_{\mathbf{0}}$, suppose that $t > 0$ is n-singular for A_1 (that is, the ϕ^1_t trajectory through y). The number of turns of $\phi^2_t(z)$ about Σ_2 is at most $M_K(n) < \infty$, where we may choose $M_K(n)$ independent of $\overline{x} \in K$, as in lemma 4.8. All we have to do now is choose a finite sequence where the proportion of 2's grows at a rate faster than $M(n)/n$. For example, if we assume $\rho_1 \leq \rho_2$, then it is easy to show that there exists $N \in \mathbb{N}$, such that $M_K(n) < 2n$, for $n \geq N$. It follows that if we define the finite block κ by concatenating (1222) sufficiently many times, then κ has no realization. □.

5. Products of heteroclinic attractors

In this section, we study the product of two heteroclinic attractors, both contained in a compact surface. These attractors may be homoclinic cycles, *figure eight* homoclinic cycles, heteroclinic cycles or heteroclinic networks. We only provide provide detailed computations for the cases where one heteroclinic attractor is a homoclinic loop and the other is either a heteroclinic cycle with two equilibria or a figure eight homoclinic cycle. The general case is proved along very similar lines (though with more notation).

As we did in the previous section, we assume a simplifying condition on the connection maps (which we remove in section 6).

Let M_1, M_2 denote compact surfaces (possibly with boundary). Suppose that $\Sigma_1 \subset M_1$, $\Sigma_2 \subset M_2$ are heteroclinic attractors. Denote the set of equilibria of Σ_i by $\mathcal{E}_i$, $i = 1,2$. Set $\Sigma = (\Sigma_1 \times \mathcal{E}_2) \cup (\mathcal{E}_1 \times \Sigma_2)$.

Theorem 5.1. *(Notation and assumptions as above.) The likely limit set of $\mathcal{B}(\Sigma_1 \times \Sigma_2)$ is the heteroclinic network Σ.*

In order to prove this result it suffices to take the product of any pair of heteroclinic cycles $\Sigma_1^\star \subset \Sigma_1$, $\Sigma_2^\star \subset \Sigma_2$ and show that the likely limit set of $\mathcal{B}(\Sigma_1^\star \times \Sigma_2^\star)$ is the heteroclinic network

$\Sigma^\star = (\Sigma_1^\star \times \mathcal{E}_2^\star) \cup (\mathcal{E}_1^\star \times \Sigma_2^\star)$, where $\mathcal{E}_i^\star \subset \Sigma_i$ is the set of saddle points on Σ_i, $i = 1, 2$. Note that we allow for the basin of attraction to be an interior or exterior neighbourhood of the cycle and as well as the cycle being a single homoclinic loop or a figure eight homoclinic cycle. We remark that if $\Sigma^\star$ is a subset of the connected surface M, then $M \setminus \Sigma^\star$ has either two or three connected components. (The complement of the figure eight homoclinic cycle, figure 1(b), has three connected components as do the sub-cycles of the network shown in figure 1(d). If we allow the underlying manifold to have as its boundary the cycle — allowing corners — then the complement can have one component.)

As indicated above, we only give detailed arguments for the case when $\Sigma_1^\star$ is a planar homoclinic loop and $\Sigma_2^\star$ is either a planar heteroclinic cycle with two equilibria or a planar figure eight homoclinic cycle. Our analysis covers all of the issues that arise in the general case.

5.1. **Product of a homoclinic loop and heteroclinic cycle.** Let $(\Sigma_1, \phi_t^1, D_1, N_1)$ be a planar attracting homoclinic loop and follow all the notational conventions used in the previous two sections. In particular, N_1 will be an interior neighbourhood of Σ_1 and Σ_1 will have a hyperbolic saddle point $\{(0,0)\} \in \mathbb{R}^2$. We assume that $(\Sigma_2, \phi_t^2, D_2, N_2)$ is a planar attracting heteroclinic cycle with hyperbolic equilibria $\mathbf{p}_1, \mathbf{p}_2$ – see figure 8. As we have drawn this, N_2 will be an interior neighbourhood of Σ_2. Denote the connections between $\mathbf{p}_1$ and $\mathbf{p}_2$ by Σ_{21}, Σ_{22} so that $\Sigma_2 = \Sigma_{21} \cup \Sigma_{22}$.

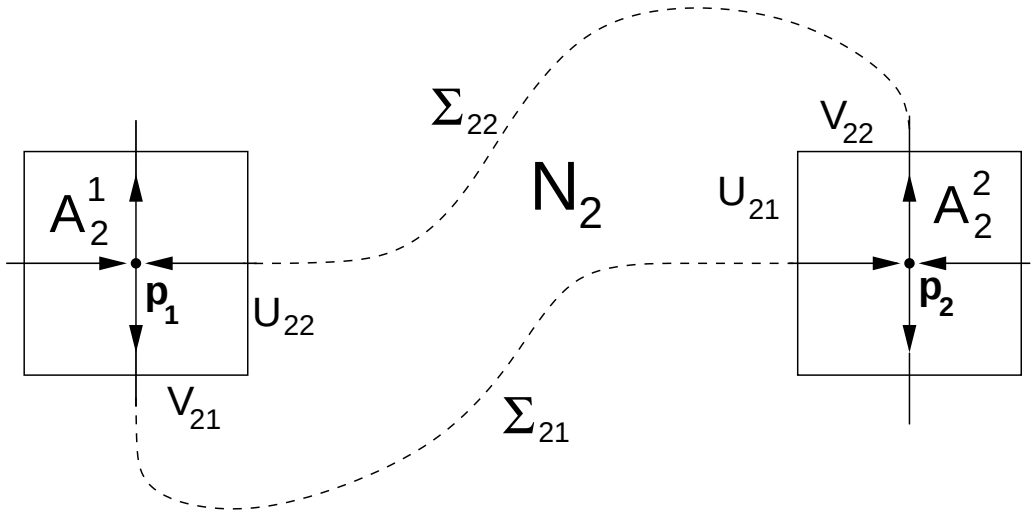

FIGURE 8. Notational conventions for heteroclinic attractor Σ_2

Suppose the hyperbolic saddle at $\mathbf{p_j}$ has eigenvalues $-\mu_2^j < 0 < \lambda_2^j$, and set $\eta_1 = \mu_2^1/\lambda_2^1$, $\eta_2 = \mu_2^2/\lambda_2^2$. We assume $\rho_2 = \eta_1\eta_2 > 1$ so that Σ_2 is attracting. Since $\mathbf{p}_1, \mathbf{p}_2$ are hyperbolic saddle points for a C^2 planar flow, we may C^1-linearize the flow ϕ_t^2 on box neighbourhoods A_2^1 of $\mathbf{p}_1$ and A_2^2 of $\mathbf{p}_2$. Set $A_2 = A_2^1 \cup A_2^2$. We assume coordinates on A_2^1, A_2^2 are chosen so that equilibria correspond to the origin $(0,0) \in \mathbb{R}^2$ and the stable manifold at $(0,0)$ is tangent to the x-axis, the unstable manifold to the y-axis and $A_2^j = [-1,1] \times [-1,1]$, $j = 1, 2$. Define

$$U_{21} = \{-1\} \times [0,1]\,, \quad V_{21} = [0,1] \times \{-1\},$$
$$U_{22} = \{1\} \times [-1,0]\,, \quad V_{22} = [-1,0] \times \{1\}.$$

(See figure 8 and note that $(V_{21} \times U_{22}) \cup (V_{22} \times U_{21}) \subset N_2$.) We have C^1 time of first return maps $T_{21} : V_{21} \to \mathbb{R}$, $T_{22} : V_{22} \to \mathbb{R}$ and associated C^1 connection maps $C_{21} : V_{21} \to U_{21}$,

$C_{22} : V_{22} \to U_{22}$. For this section we assume there are strictly positive constants $\tau_{21}, \tau_{22}, m_{21}, m_{22}$ such that

$$T_{21}(x) = \tau_{21},\ T_{22}(x) = \tau_{22},\ C_{21}(x) = m_{21}x,\ C_{22}(x) = m_{22}x. \tag{5.5}$$

After linearly rescaling one coordinate direction if necessary, we may always assume that $m_{21}, m_{22} < 1$. In particular, the connection maps C_{21}, C_{22} are defined on all of V_{21}, V_{22}.

Remark 5.2. If we are given a finite set of planar linear flows ϕ_t^j, each with a hyperbolic saddle point at the origin, box neighbourhoods $A^j \approx [-1,1]\times[-1,1]$, C^1 connection maps $C_j : V_j \to U_j$, and C^1 time of first return maps $T_j : V_j \to \mathbb{R}$, $j = 1, \cdots, r$, where each product $V_j \times U_j$ determines a quadrant of A^j, then this data determines a heteroclinic cycle Σ between r equilibria. In general, Σ will be defined on a surface, possibly non-orientable. We have chosen the particular configuration shown in figure 8 because it extends naturally to the exterior of a figure eight attracting homoclinic cycle.

Given $d \in U_{22} \approx [-1, 0]$, let $c > d$ denote the first point of intersection of the forward ϕ_t^2-trajectory through d with U_{22}. Necessarily $[d, c] \subset U_{22}$. Given $z \in [d, c]$, we define strictly monotone increasing sequences $(t_2^{z,2}(n))_{n\geq 0}$, $(s_2^{z,1}(n))_{n\geq 1}$, $(t_2^{z,1}(n))_{n\geq 1}$, $(s_2^{z,2}(n))_{n\geq 1}$ by

(1) $t_2^{z,2}(0) = 0$ and for $n > 0$, $t_2^{z,j}(n)$ is the time to the nth intersection of the forward ϕ_t^2 trajectory through z with U_{2j}, $j = 1, 2$.
(2) $s_2^{z,j}(n)$ is the time to the nth intersection of the forward ϕ_t^2 trajectory through z with V_{2j}, $j = 1, 2$.

We have

$$0 = t_2^{z,2}(0) < s_2^{z,1}(1) < t_2^{z,1}(1) < s_2^{z,2}(1) < t_2^{z,2}(1) < s_2^{z,1}(2) < \cdots$$

Set $z = z^2(0)$ and for $n \geq 1$, let $z^2(n)$ denote the successive points of intersection of the forward trajectory through z with U_{22} ($z^2(n) = \phi_{t_2^{z,2}(n)}(z)$). We similarly let $z^1(n)$ denote the nth point of intersection of the forward trajectory through z with U_{21} ($z^1(n) = \phi_{t_2^{z,1}(n)}(z)$). A straightforward computation shows that

$$\begin{aligned} z^1(n) &= m_{21}^{(1+\cdots+\rho_2^{n-1})} m_{22}^{\eta_1(1+\cdots+\rho_2^{n-2})} z^{\eta_1\rho_2^{n-1}}, \\ z^2(n) &= m_{21}^{\eta_2(1+\cdots+\rho_2^{n-1})} m_{22}^{(1+\cdots+\rho_2^{n-1})} z^{\rho_2^n}. \end{aligned}$$

As we did in the previous section, it is now straightforward to compute the sequences $(s_2^{z,j}(n))$, $(t_2^{z,j}(n))$, $j = 1, 2$.

Lemma 5.3. *For $n \geq 1$ we have*

$$t_2^{z,1}(n) = s_2^{z,1}(n) + \tau_{21}.$$
$$t_2^{z,2}(n) = s_2^{z,2}(n) + \tau_{22}.$$

$$t_2^{z,1}(n) = n\tau_{21} + (n-1)\tau_{22} - \frac{1}{\lambda_2^1}(\sum_{j=0}^{n-1} \log z^2(j)) - \frac{1}{\lambda_2^2}(\sum_{j=1}^{n-1} \log z^1(j)).$$

$$t_2^{z,2}(n) = n(\tau_{21} + \tau_{22}) - \frac{1}{\lambda_2^1}(\sum_{j=0}^{n-1} \log z^2(j)) - \frac{1}{\lambda_2^2}(\sum_{j=1}^{n} \log z^1(j)).$$

For $\rho > 1$, $n \geq 0$, define

$$\begin{aligned} \pi_n(\rho) &= \frac{\rho^n - n\rho + n - 1}{(\rho-1)^2}, \\ \alpha_n(\rho) &= \frac{\rho^n - 1}{\rho - 1}. \end{aligned}$$

We have the following expressions for the summations in lemma 5.3.

$$\begin{aligned}\sum_{j=0}^{n-1}\log z^2(j) &= \eta_2\pi_n(\rho_2)\log m_{21}+\pi_n(\rho_2)\log m_{22}+\alpha_n(\rho_2)\log z\\ \sum_{j=1}^{n-1}\log z^1(j) &= \pi_n(\rho_2)\log m_{21}+\eta_1\pi_{n-1}(\rho_2)\log m_{22}+\eta_1\alpha_{n-1}(\rho_2)\log z\end{aligned}$$

Definition 5.4. We say $t>0$ is *m-singular* for Σ_2 if

$$t\in[s_2^{z,1}(m),t_2^{z,1}(m)]\cup[s_2^{z,2}(m),t_2^{z,2}(m)].$$

Note that if t is m-singular for Σ_2, then $\phi_t^2(z)\notin A_2^\circ$.

Set $E=[a,b]\times[d,c]\subset U_1\times U_{22}$ (the interval $[a,b]$ is as defined in the previous section). For $n,m\in\mathbb{N}$, $j=1,2$, define

$$\begin{aligned}E_{m,n}^j &= \{(y,z)\in E\mid\exists t\in[s_1^y(n),t_1^y(n)]\cap[s_2^{z,j}(n),t_2^{z,j}(n)\},\\ E_n^j &= \cup_{m=1}^\infty E_{m,n}^j,\\ E_n &= E_n^1\cup E_n^2.\end{aligned}$$

A point $(y,z)\in E_n$ if there exists $t>0$ such that t is n-singular for Σ_1 and there exists $m\in\mathbb{N}$ such that t is m-singular for Σ_2. We refer to the points of E_n as the n-bad points of E.

Fix $y\in[a,b]$. For $m,n\in\mathbb{N}$, $j=1,2$, define (possibly empty) closed subintervals $[Z_{j,m}^1(y,n),Z_{j,m}^2(y,n)]$ of $[d,c]$ by

$$[Z_{j,m}^1(y,n),Z_{j,m}^2(y,n)]=\{z\in[d,c]\mid(y,z)\in E_{m,n}^j\}.$$

We refer to $[Z_{j,m}^1(y,n),Z_{j,m}^2(y,n)]$ as a bad subinterval.

Proposition 5.5. *Let $y\in[a,b]$. Given $m,n\in\mathbb{N}$ and $j=1,2$, we have $[Z_{j,m}^1(y,n),Z_{j,m}^2(y,n)]\subset[\overline{Z}_{j,m}^1(y,n),\overline{Z}_{j,m}^2(y,n)]$, where*

$$\begin{aligned}\overline{Z}_{1,m}^2(y,n) &= e^{\frac{1}{u_m}(-(n-1)\tau_1+(m-1)(\tau_{21}+\tau_{22})+\tau_{21})}y^{\frac{\alpha_n}{u_m\lambda_1}}m_1^{\frac{\pi_n}{u_m\lambda_1}}m_{21}^{-\frac{a_m}{u_m}}m_{22}^{-\frac{b_m}{u_m}},\\ \overline{Z}_{2,m}^2(y,n) &= e^{\frac{1}{v_m}(-(n-1)\tau_1+m(\tau_{21}+\tau_{22}))}y^{\frac{\alpha_n}{v_m\lambda_1}}m_1^{\frac{\pi_n}{v_m\lambda_1}}m_{21}^{-\frac{c_m}{v_m}}m_{22}^{-\frac{d_m}{v_m}},\\ \overline{Z}_{1,m}^1(y,n) &= e^{-\frac{1}{u_m}(\tau_1+\tau_{21})}\overline{Z}_{1,m}^2(y,n),\\ \overline{Z}_{2,m}^1(y,n) &= e^{-\frac{1}{v_m}(\tau_1+\tau_{22})}\overline{Z}_{2,m}^2(y,n),\end{aligned}$$

and

$$\begin{aligned}u_m &= \tfrac{\alpha_m(\rho_2)}{\lambda_2^1}+\tfrac{\eta_1\alpha_{m-1}(\rho_2)}{\lambda_2^2}, & v_m &= \tfrac{\alpha_m(\rho_2)}{\lambda_2^1}+\tfrac{\eta_1\alpha_m(\rho_2)}{\lambda_2^2},\\ a_m &= \tfrac{\eta_2\pi_m(\rho_2)}{\lambda_2^1}+\tfrac{\pi_m(\rho_2)}{\lambda_2^2}, & b_m &= \tfrac{\pi_m(\rho_2)}{\lambda_2^1}+\tfrac{\eta_1\pi_{m-1}(\rho_2)}{\lambda_2^2},\\ c_m &= \tfrac{\eta_2\pi_m(\rho_2)}{\lambda_2^1}+\tfrac{\pi_{m+1}(\rho_2)}{\lambda_2^2}, & d_m &= \tfrac{\pi_m(\rho_2)}{\lambda_2^1}+\tfrac{\eta_1\pi_m(\rho_2)}{\lambda_2^2}.\end{aligned}$$

Proof. For $j=1,2$, the interval $[\overline{Z}_{j,m}^1(y,n),\overline{Z}_{j,m}^2(y,n)]$ is contained in an interval with end points given by the solution of $s_2^{z,j}(m)=s_1^y(n)+\tau_1,s_1^y(n)-\tau_{2j}$. Solving for z, using lemma 5.3, gives the result. □

Lemma 5.6. *If we define*

$$\begin{aligned}S_1 &= \sum_{m=1}^\infty\frac{1}{u_m\lambda_1+\alpha_n}e^{\frac{1}{u_m}(-(n-1)\tau_1+(m-1)(\tau_{21}+\tau_{22})+\tau_{21})},\\ S_2 &= \sum_{m=1}^\infty\frac{1}{v_m\lambda_1+\alpha_n}e^{\frac{1}{v_m}(-(n-1)\tau_1+m(\tau_{21}+\tau_{22}))},\end{aligned}$$

then there exists $C > 0$ such that for all $n \in \mathbb{N}$,

$$\ell_2(E_n) \leq C\,(S_1 + S_2)\,.$$

Proof. As in lemma 4.9, we have

$$\ell_2(E_n) = \ell_1(E_n^1) + \ell_2(E_n^2) \leq \sum_{j=1}^{2} \int_a^b \sum_{m=1}^{\infty} \left(\overline{Z}_{j,m}^2(y,n) - \overline{Z}_{j,m}^1(y,n) \right).$$

By lemma 4.3, we have $0 \leq \frac{a_m}{u_m}, \frac{b_m}{u_m} \leq K_1 \frac{\pi_m(\rho_2)}{\alpha_m(\rho_2)} \leq K_1 \frac{1}{\rho_2 - 1}$, $0 \leq \frac{c_m}{v_m}, \frac{d_m}{v_m} \leq K_2 \frac{\pi_m(\rho_2)}{\alpha_m(\rho_2)} \leq K_2 \frac{1}{\rho_2 - 1}$, for some constants $K_1, K_2 > 0$. Therefore, there exists $C_1 = C_1(m_1, m_{21}, m_{22}) > 0$ such that $m_1^{\frac{\pi_n}{u_m \lambda_1}} m_{21}^{-\frac{a_m}{u_m}} m_{22}^{-\frac{b_m}{u_m}} \leq C_1$, $m_1^{\frac{\pi_n}{v_m \lambda_1}} m_{21}^{-\frac{c_m}{v_m}} m_{22}^{-\frac{d_m}{v_m}} \leq C_1$, for all $m, n \in \mathbb{N}$. The remainder of the proof follows that of lemma 4.9. □

Lemma 5.7. $\ell_2(E_\infty) = 0$.

Proof. It is easy to see that $u_m, v_m \geq \frac{\alpha_m(\rho_2)}{\lambda_2^1}$. Hence for some constant $C > 0$

$$\frac{1}{u_m \lambda_1 + \alpha_n}, \frac{1}{v_m \lambda_1 + \alpha_n} \leq \frac{\lambda_2^1}{\alpha_m(\rho_2)\lambda_1 + \alpha_n \lambda_2^1} \leq C \rho_1^{-n/2} \rho_2^{-m/2}$$

Along similar lines to the proof of lemma 4.1, we show that $\sum_{n=1}^{\infty} \ell_2(E_n) < \infty$. It follows by the Borel-Cantelli lemma that $\ell_2(E_\infty) = 0$. □

We have the following special case of theorem 5.1.

Proposition 5.8. *The likely limit set of the product of the planar homoclinic cycle (Σ_1, ϕ_t^1) and the attracting planar heteroclinic cycle (Σ_2, ϕ_t^2) is Σ.*

Proof. Similar to that of theorem 4.11. □

5.2. **Product of a homoclinic loop and a figure eight cycle.** We now consider the case where $(\Sigma_2, \phi_t^2, D_2, N_2)$ is an attracting figure eight homoclinic cycle. Write $N_2 = N_2^- \cup N_2^+$ where $N_2^- = N_{21}^- \cup N_{22}^-$ is an interior neighbourhood of Σ_2 in $\mathbb{R}^2$ and N_2^+ is an exterior neighbourhood of Σ_2 in $\mathbb{R}^2$ (see figure 9). We may write Σ_2 as the union of two attracting homoclinic loops Σ_{21}, Σ_{22}.

It follows from the results of section 3 applied to the products $\Sigma_1 \times \Sigma_{21}$ and $\Sigma_1 \times \Sigma_{22}$, that $\mathcal{L}(N_1 \times N_2^-) = \Sigma$. It remains to show that $\mathcal{L}(N_1 \times N_2^+) = \Sigma$.

We suppose that the hyperbolic saddle at $(0,0)$ has associated eigenvalues $-\mu_2 < 0 < \lambda_2$. Set $\rho_2 = \mu_2/\lambda_2$ and assume $\rho_2 > 1$ so that Σ_2 is an attracting homoclinic cycle. Since $(0,0)$ is a hyperbolic saddle point for a C^2 planar flow, we may C^1-linearize the flow ϕ_t^2 on a box neighbourhood $A_2 \subset N_2$ of $(0,0)$. We assume coordinates are chosen so that the stable manifold at $(0,0)$ is tangent to the x-axis, the unstable manifold to the y-axis and $A_2 = [-1,1] \times [-1,1]$. Define

$$U_{21} = \{-1\} \times [0,1]\,, \quad V_{21} = [0,1] \times \{-1\},$$
$$U_{22} = \{1\} \times [-1,0]\,, \quad V_{22} = [-1,0] \times \{1\}.$$

(See inset to figure 9.)

But now we are exactly in the situation described by figure 8. Our previous results extend immediately (with $\lambda_2 = \lambda_2^1 = \lambda_2^2$, $\mu_2 = \mu_2^1 = \mu_2^2$ and the terms η_1, η_2 replaced by $\rho_2 = \mu_2/\lambda_2$, and ρ_2 by ρ_2^2, $m_2 = m_{21} = m_{22}$, $\tau_2 = \tau_{21} = \tau_{22}$).

Summarizing, we have shown

Proposition 5.9. *The likely limit set of the product of a planar homoclinic attractor (Σ_1, ϕ_t^1) and an attracting planar figure eight cycle (Σ_2, ϕ_t^2), is Σ.*

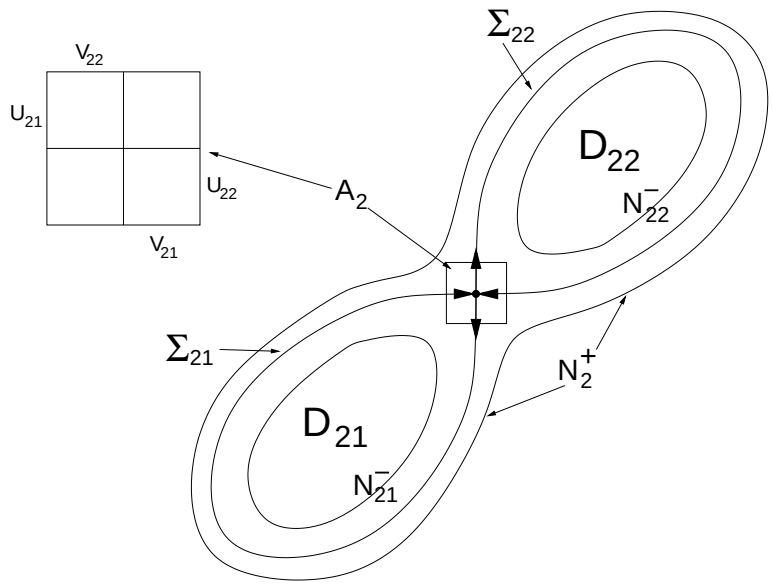

FIGURE 9. Notational conventions for figure eight homoclinic attractor Σ_2

6. General Global maps

In the previous sections, we assumed that the connection maps $C : V \to U$ were linear and the associated time maps $T : V \to \mathbb{R}$ were constant. In this section, we remove this restriction and show that our results continue to hold. We give the details only for product of two attracting homoclinic loops (details for the general case of products of heteroclinic attractors are similar and use the same methods). As far as possible we follow the notational conventions of sections 3, 4. The reader should note that a particular concern is to obtain results where we can use the rescaling strategy described at the end of section 3.

Since we are assuming flows are at least C^2, the maps $C_i : V_i \to U_i$, $T_i : V_i \to \mathbb{R}$ defined in section 3 are C^2 (see Wiggins [24, Section 10.3]). Hence for $i = 1, 2$ we may write

$$C_i(x) = \gamma^i(x)x \tag{6.6}$$

$$T_i(x) = \tau_i + O(|x|), \tag{6.7}$$

where γ^i is C^1, $m_i = \gamma^i(0) \in (0, 1)$ and $\tau_i = T_i(0)$.

Variation in the time maps T_i causes only minor problems. However, the case of general connection maps is delicate — this is already evident in the analysis given in [4, §3] for the product of a homoclinic loop and limit cycle. We start with an analysis of the case when $\rho_1 \neq \rho_2$ and conclude with the harder case $\rho_1 = \rho_2$. Note that the results in the first part of the section hold with no restriction on ρ_1, ρ_2 (> 1). We indicate in the text results which do not hold with $\rho_1 = \rho_2$.

Rescaling. We start with an analysis of how the connection map changes when we restrict to a smaller rectangular $\hat{A} \subset A$ (we omit subscripts in what follows). Let $A = [0, 1] \times [0, 1]$ and $\hat{A} = [0, \alpha] \times [0, \beta] \subset A$. Let $\alpha = e^{-\mu S}$, $\beta = e^{-\lambda T}$. Linearly rescale coordinates on A so that, in the new coordinates $(\hat{x}, \hat{y})$, $\hat{A} = [0, 1] \times [0, 1]$. If we let $\hat{C} : V^\star \to U^\star$ denote the connection map associated to $\hat{A}$, we have

$$\hat{C}(\hat{x}) = e^{(T+S)\lambda} C(e^{-\mu(T+S)}\hat{x})$$

(See remarks 4.1(2).) Writing $C(x) = \gamma(x)x$, gives

$$\hat{\gamma}(\hat{x}) = e^{(T+S)(\lambda-\mu)}\gamma(e^{-(T+S)\mu}\hat{x}) \tag{6.8}$$

$$\frac{\hat{\gamma}'(\hat{x})}{\hat{\gamma}(\hat{x})} = e^{-(T+S)\mu}\frac{\gamma'(e^{-(T+S)\mu}\hat{x})}{\gamma(e^{-(T+S)\mu}\hat{x})} \tag{6.9}$$

Let $c_1 = \sup_{x\in[0,1]} |\gamma'(x)|$.

Lemma 6.1. *Let $T, S \geq 0$ and define $\hat{m} = \hat{\gamma}(0)$, $\hat{m}^+ = \sup_{\hat{x}\in[0,1]} \hat{\gamma}(\hat{x})$, $\hat{m}^- = \inf_{\hat{x}\in[0,1]} \hat{\gamma}(\hat{x})$. We have*

1. $\hat{m} = e^{(T+S)(\lambda-\mu)}m$.
2. $\hat{m}(1 - \frac{c_1}{m}e^{-\mu(T+S)}) \leq \hat{m}^- \leq \hat{m}^+ \leq \hat{m}(1 + \frac{c_1}{m}e^{-\mu(T+S)})$.

These estimates continue to hold if we increase either T or S.

Proof. The estimates follow straightforwardly from (6.8,6.9). □

Define $\varepsilon_0 > 0$ by

$$\varepsilon_0 = \min\{1/4, (\rho_2 - 1)/4\}.$$

It follows from lemma 6.1 and (6.9) that we can choose A_2 so that

$$m_2^+ \leq \min\{\rho_2^{-2/\rho_2}, 2^{-3}\}. \tag{6.10}$$

$$\left|\frac{\gamma'(x)}{\gamma(x)}\right| \leq \frac{\varepsilon_0}{2}. \tag{6.11}$$

Shrinking A_i if necessary, we can assume that there exist $\tau_i^-, \tau_i^+ > 0$ so that $\tau_i^- \leq T_i(x) \leq \tau_i^+$, for all $x \in V_i$.

Remarks 6.2. (1) If we shrink A_2 further then (6.10,6.11) continue to hold — m_2^+ is a decreasing function of $T + S$.
(2) If we shrink A_i, $\tau_i^\pm$ increase, $i = 1, 2$.

Defining the sequences. Exactly as in section 3, choose a rectangle $E = [a, b] \times [c, d] \subset U_1 \times U_2$. Given $y = y_0 \in U_1$, $z = z_0 \in U_2$ let (y_n) and (z_n) denote the successive points of intersection of the forward trajectories through y_0 with U_1 and through z_0 with U_2. For $n \geq 1$, we have

$$y_n = \gamma^1(y_{n-1}^{\rho_1})y_{n-1}^{\rho_1}, \qquad z_n = \gamma^2(z_{n-1}^{\rho_2})z_{n-1}^{\rho_2}.$$

For $n \geq 0$ define $\gamma_n^1(y) = \gamma^1(y_n)$, $\gamma_n^2(y) = \gamma^2(z_n)$.

We have a straightforward generalization of lemma 4.2.

Lemma 6.3. *Let $(y, z) \in E$, $n \in \mathbb{N}$. We have*

1. $t_1^y(n) = s_1^y(n) + T_1(y_n^{\rho_1})$ *and* $t_2^z(n) = s_2^z(n) + T_2(z_n^{\rho_2})$.
2. $t_1^y(n) = \sum_{i=0}^{n-1} T_1(y_i^{\rho_1}) - \frac{1}{\lambda_1}(\alpha_n \log y + \log \prod_{j=0}^{n-2} \left(\gamma_j^1(y)\right)^{\alpha_{n-1-j}})$.
3. $t_2^z(n) = \sum_{i=0}^{n-1} T_2(z_i^{\rho_2}) - \frac{1}{\lambda_2}(\beta_n \log z + \log \prod_{j=0}^{n-2} \left(\gamma_j^2(z)\right)^{\beta_{n-1-j}})$.

Remark 6.4. If we assume the connection maps are linear, $\gamma^i = m_i$, $i = 1, 2$, we find that

$$\prod_{j=0}^{n-2} \left(\gamma_j^1(y)\right)^{\alpha_{n-1-j}} = m_1^{\sum_{j=0}^{n-2} \alpha_{n-1-j}} = m_1^{\pi_n},$$

with a similar expression for $\prod_{j=0}^{n-2} \left(\gamma_j^2(z)\right)^{\beta_{n-1-j}}$. These are the terms that appear in lemma 4.2.

The main estimate. In this section we derive the main estimate on $|(\gamma_n^2)'(z)/\gamma_n^2(z)|$ that we use for our proof of convergence of $\sum \ell_2(E_n)$. So as to simplify the notation, we generally drop the identifying subscript 2 from γ_j^2, γ_2 and ρ_2. Given $n \in \mathbb{N}$, define $\overline{\gamma}_n : [c,d] \to \mathbb{R}$ by

$$z_n = \overline{\gamma}_n(z) z^{\rho^n},\ z \in [c,d].$$

Since we have $\gamma(x)x \le m^+ x$, for all $x \in (0,1]$, we have the easy estimate

$$z_n \le (m^+)^{\beta_n} z^{\rho^n},\ n \ge 1, \tag{6.12}$$

where $\beta_n = \sum_{j=0}^{n-1} \rho^j$.

Lemma 6.5. *For $n \ge 1$ we have*

(1) $\left|\frac{\overline{\gamma}_n'(z)}{\overline{\gamma}_n(z)}\right| \le \varepsilon_0 \rho^n$.

(2) $\left|\frac{\gamma_n'(z)}{\gamma_n(z)}\right| \le \varepsilon_0$.

If $S \ge 0$ and we linearly rescale coordinates in the x-direction so that $e^{-\mu S}$ is rescaled to 1, then estimate (2) changes to

$$\left|\frac{\gamma_n'(z)}{\gamma_n(z)}\right| \le e^{-\mu S}\varepsilon_0.$$

Proof. The proof of (1) is very similar to that of lemma 3.4 in [4] and we only indicate the main points. The proof goes by induction on n with the hypothesis at step n being

$$\left|\frac{\overline{\gamma}_n'(z)}{\overline{\gamma}_n(z)}\right| \le \varepsilon_0(1-2^{-n})\rho^n.$$

When $n=1$, we have $\overline{\gamma}_1(z) = \gamma(z^\rho)$ and differentiating gives

$$\frac{\overline{\gamma}_1'(z)}{\overline{\gamma}_1(z)} = \rho z^{\rho-1}\frac{\gamma'(z^\rho)}{\gamma(z^\rho)}.$$

Hence by (6.11), we have $|\rho z^{\rho-1}\frac{\gamma'(z^\rho)}{\gamma(z^\rho)}| \le \varepsilon_0 \frac{\rho}{2} z^{\rho-1} \le \varepsilon_0 \frac{\rho}{2}$, since $z \in (0,1]$. This verifies the result when $n=1$. Given the truth of the statement for $n-1$, the proof of step n proceeds by estimating the derivative $\overline{\gamma}_n'$ and uses the bound $m_2^+ \le 2^{-3}$ (see (6.10)) and (6.12).

Turning to (2), we have $z_n = \overline{\gamma}_n(z) z^{\rho^n}$ and differentiating with respect to z gives

$$z_n' = \overline{\gamma}_n'(z) z^{\rho^n} + \overline{\gamma}_n(z)\rho^n z^{\rho^n - 1}.$$

We have $\gamma_n(z) = \gamma(z_n^\rho)$. Differentiating and dividing by $\gamma_n(z)$,

$$\begin{aligned}\frac{\gamma_n'(z)}{\gamma_n(z)} &= \frac{\gamma'(z_n^\rho)}{\gamma(z_n^\rho)}\rho z_n^{\rho-1} z_n', \\ &= \frac{\gamma'(z_n^\rho)}{\gamma(z_n^\rho)}\rho z_n^{\rho-1}\left(\overline{\gamma}_n'(z) z^{\rho^n} + \overline{\gamma}_n(z)\rho^n z^{\rho^n-1}\right).\end{aligned}$$

By (6.11), we have

$$\left|\frac{\gamma_n'(z)}{\gamma_n(z)}\right| \le \varepsilon_0 \frac{\rho z_n^{\rho-1}}{2}\left(\left|\overline{\gamma}_n'(z) z^{\rho^n}\right| + \left|\overline{\gamma}_n(z)\rho^n z^{\rho^n-1}\right|\right).$$

By (1) and choice of ε_0, we have $|\overline{\gamma}_n'(z)| \le \varepsilon_0 \rho^n \overline{\gamma}_n(z) \le \rho^n \overline{\gamma}_n(z)$ and so

$$\begin{aligned}\frac{\rho z_n^{\rho-1}}{2}\left|\overline{\gamma}_n'(z) z^{\rho^n}\right| &\le \frac{\rho z_n^{\rho-1}}{2}\rho^n \overline{\gamma}_n(z) z^{\rho^n}, \\ &= \frac{\rho^{n+1} z_n^\rho}{2}, \\ &\le \frac{\rho^{n+1}(m^+)^{\rho\beta_n}}{2}.\end{aligned}$$

Turning to the second term, we have

$$\begin{aligned}\frac{\rho z_n^{\rho-1}}{2}\left|\overline{\gamma}_n(z)\rho^n z^{\rho^n-1}\right| &= \frac{z_n^\rho \rho^{n+1}}{2z},\\ &\leq \frac{(m^+)^{\rho\beta_n} z^{\rho^{n+1}} \rho^{n+1}}{2z},\\ &\leq \frac{\rho^{n+1}(m^+)^{\rho\beta_n}}{2}.\end{aligned}$$

Using the bound $m^+ \leq \rho^{-2/\rho}$ (see (6.10)), we get $\rho^{n+1}(m^+)^{\rho\beta_n} \leq 1$.

The final statement is immediate from (6.9). □

Remarks 6.6. (1) Lemma 6.5 continues to hold, with the smaller constants, if we shrink A_2. (2) Estimate (2) of lemma 6.10 will more than suffice to handle the situation when $\rho_1 \neq \rho_2$. The final statement will be crucial for the analysis when $\rho_1 = \rho_2$.

Estimating $\ell_2(E_n)$ when $\rho_2 > \rho_1$. For this section we assume $\rho_2 \neq \rho_1$. Without loss of generality we suppose $\rho_2 > \rho_1$. Under these conditions, we prove that there exists $N \in \mathbb{N}$, $C > 0$ such that for all $n \geq N$,

$$\ell_2(E_n) \leq C\frac{n}{\alpha_n} \tag{6.13}$$

Since $\sum_{n\geq 1} \frac{n}{\alpha_n} < \infty$, this implies that $\sum_{n\geq 1} \ell_2(E_n) < \infty$ and so $\ell_2(E_\infty) = 0$.

We continue to assume $(y, z) \in E = [a, b] \times [c, d]$. Define

$$M_1 = M_1(n, y) = \prod_{j=0}^{n-2} (\gamma_j^1(y))^{\alpha_{n-1-j}}, \quad M_2(n, z) = \prod_{j=0}^{n-2} (\gamma_j^2(z))^{\beta_{n-1-j}}$$

$$N_1 = N_1(n, y) = \sum_{i=0}^{n-2} T_1(y_i^{\rho_1}), \quad N_2(n, z) = \sum_{i=0}^{n-2} T_2(z_i^{\rho_2})$$

The bad intervals are contained in intervals $[Z_m^1(y, n), Z_m^2(y, n)]$ which have nonempty intersection with $[c, d]$. The points of $Z_m^1(y, n), Z_m^2(y, n)$ are obtained by solving the following equations for z

$$s_1^y(n) = s_2^z(m) + T_2(z_m^{\rho_2}), \quad s_1^y(n) = s_2^z(m) - T_1(y_n^{\rho_1}). \tag{6.14}$$

For $i = 1, 2$ define

$$N_{2i} = N_2(m, Z_m^i(y, n)), \quad M_{2i} = M_2(m, Z_m^i(y, n)) \tag{6.15}$$

Using (6.14), we find that

$$\begin{aligned}Z_m^1(y, n) &= e^{\frac{\lambda_2}{\beta_m}(N_{21}-N_1+T_2(z_m^{\rho_2}))} y^{\frac{\lambda_2\alpha_n}{\lambda_1\beta_m}} M_1^{\frac{\lambda_2}{\lambda_1\beta_m}} M_{21}^{-\frac{1}{\beta_m}}\\ Z_m^2(y, n) &= e^{\frac{\lambda_2}{\beta_m}(N_{22}-N_1-T_1(y_n^{\rho_1}))} y^{\frac{\lambda_2\alpha_n}{\lambda_1\beta_m}} M_1^{\frac{\lambda_2}{\lambda_1\beta_m}} M_{22}^{-\frac{1}{\beta_m}}\end{aligned}$$

The maximum number of turns around Σ_2 in time $s_1^y(n) + \tau_1^+$ is taken when $z = d$, and is estimated by

$$M_E(n, y) = \min\{m \mid s_2^d(m + 1) > s_1^y(n) + \tau_1^+\} \tag{6.16}$$

Define $M_E(n) = \sup_{y\in[a,b]} M_E(n, y)$. Choose $r > 0$ such that $\rho_2^r < \rho_1$.

Lemma 6.7. *There exists $N_1 \in \mathbb{N}$ such that $M_E(n) \leq rn$ for all $n \geq N_1$.*

Proof. By definition, $s_2^d(M_E(n)+1) > s_1^y(n) + \tau_1^+$. The result now follows by a straightforward computation using the expressions for $s_2^d(M_E(n)+1)$ and $s_1^y(n)$ given by lemma 6.3. Indeed, the condition $\rho_2 > \rho_1$ implies that $\lim_{n\to\infty} M_E(n)/n = 0$. □

Let $J(n) = \{m \in \mathbb{N} \mid [Z_m^1(y,n), Z_m^2(y,n)] \cap [c,d] \neq \emptyset\}$. For $n \in \mathbb{N}$, define

$$K_n = \sup_{m\in J(n)} \{e^{-\frac{\lambda_2}{\beta_m}\left((n-1)\tau_1^- - m\tau_2^+\right)} (m_1^+)^{\frac{\pi_n\lambda_2}{\lambda_1\beta_m}} (m_2^-)^{-\frac{\theta_m}{\beta_m}}\}$$

Lemma 6.8. *There exists $N \geq N_1$ such that*

$$K_n \leq 2,\ n \geq N. \tag{6.17}$$

Proof. If $n \geq N_1$, then for all $m \in J(n)$, $m \leq rn$. It follows easily from the condition $\rho_2^r < \rho_1$ and lemma 4.3 that $\lim_{n\to\infty} K_n = 0$. □

Remark 6.9. Lemma 6.8 does not extend to the case when $\rho_2 = \rho_1$. The difficulty lies with the term $(m_2^-)^{-\frac{\theta_m}{\beta_m}}$ which we can only bound by $(m_2^-)^{-\frac{1}{\rho_2 - 1}}$ (lemma 4.3). We handle this problem at the end of the section.

For $n \in \mathbb{N}$, $m \in J(n)$ set $D_{m,n}^y = Z_m^2(n,y) - Z_m^1(n,y)$, $m \in J(n)$. We have

$$\ell_2(E_n) \leq \int_a^b \sum_{m=1}^{M_E(n)} D_{m,n}^y \, dy$$

Lemma 6.10. *For $n \in \mathbb{N}, m \in J(n)$*

$$D_{m,n}^y \leq (I_1 + I_2 + I_3) y^{\frac{\lambda_2\alpha_n}{\lambda_1\beta_m}} \tag{6.18}$$

where

$$I_1 = K_n \frac{\lambda_2}{\beta_m}(m-1)(\tau_2^- - \tau_2^+),\ I_2 = K_n \frac{\lambda_2}{\beta_m}(\tau_1^+ + \tau_2^+)\ I_3 = K_n \left|\log\left(\frac{M_{22}}{M_{21}}\right)\right|.$$

Proof. We have

$$\begin{aligned}
D_{m,n}^y &\leq e^{-\frac{\lambda_2}{\beta_m}N_1} y^{\frac{\lambda_2\alpha_n}{\lambda_1\beta_m}} M_1^{\frac{\lambda_2}{\lambda_1\beta_m}} e^{\frac{\lambda_2}{\beta_m}((m-1)\tau_2^+)} e^{\frac{\lambda_2}{\beta_m}\tau_2^+} (M_{21})^{-\frac{1}{\beta_m}} \\
&\quad - e^{-\frac{\lambda_2}{\beta_m}N_1} y^{\frac{\lambda_2\alpha_n}{\lambda_1\beta_m}} M_1^{\frac{\lambda_2}{\lambda_1\beta_m}} e^{\frac{\lambda_2}{\beta_m}((m-1)\tau_2^-)} e^{-\frac{\lambda_2}{\beta_m}\tau_1^+} (M_{22})^{-\frac{1}{\beta_m}} \\
&\leq e^{-\frac{\lambda_2}{\beta_m}N_1} y^{\frac{\lambda_2\alpha_n}{\lambda_1\beta_m}} (m_1^+)^{\frac{\pi_n\lambda_2}{\lambda_1\beta_m}} e^{\frac{\lambda_2}{\beta_m}((m-1)\tau_2^+)} e^{\frac{\lambda_2}{\beta_m}\tau_2^+} (m_2^-)^{-\frac{\theta_m}{\beta_m}} \\
&\quad \times \left(1 - e^{\frac{\lambda_2}{\beta_m}\left((m-1)(\tau_2^- - \tau_2^+) - (\tau_1^+ + \tau_2^+)\right)} \left(\frac{M_{22}}{M_{21}}\right)^{-\frac{1}{\beta_m}}\right) \\
&\leq K_n \left(\frac{\lambda_2}{\beta_m}\left((m-1)(\tau_2^+ - \tau_2^-) + (\tau_1^+ + \tau_2^+)\right) + \frac{1}{\beta_m}\log\left(\frac{M_{22}}{M_{21}}\right)\right) y^{\frac{\lambda_2\alpha_n}{\lambda_1\beta_m}}
\end{aligned}$$

By separating the three terms, we obtain the result. □

Remark 6.11. In the case when $\tau_2^+ = \tau_2^- = \tau_2$, $M_{21} = M_{22} = m_2^{\theta_m}$, the terms I_1 and I_3 vanish, and we are only left with I_2 which is precisely the term in lemma 4.9. The crucial term we have to estimate is $\left|\log\left(\frac{M_{22}}{M_{21}}\right)\right|$ in I_3.

Lemma 6.12. *We have $\left|\log\left(\frac{M_{22}}{M_{21}}\right)\right| \leq \varepsilon_0 \frac{\beta_m}{\rho_2 - 1} D_{m,n}^y$.*

Proof. Using (6.15), we get

$$\begin{aligned}
\left|\log\left(\frac{M_{22}}{M_{21}}\right)\right| &= \left|\log\prod_{j=0}^{m-2}\left(\frac{\gamma_j(Z_m^2(n,y))}{\gamma_j(Z_m^1(n,y))}\right)^{\beta_{m-j-1}}\right|,\\
&\leq \sum_{j=0}^{m-2}\beta_{m-j-1}\left|\log\frac{\gamma_j(Z_m^2(n,y))}{\gamma_j(Z_m^1(n,y))}\right|,\\
&\leq \sum_{j=0}^{m-2}\beta_{m-j-1}\left|\frac{\gamma_j'(w)}{\gamma_j(w)}\right| D_{m,n}^y,\\
&\leq \varepsilon_0\sum_{j=0}^{m-2}\beta_{m-j-1}\, D_{m,n}^y, \quad \text{(lemma 6.5)},\\
&= \varepsilon_0\frac{1}{\rho_2-1}\sum_{j=0}^{m-2}\left(\rho_2^{m-j-1}-1\right) D_{m,n}^y\\
&\leq \varepsilon_0\frac{1}{\rho_2-1}\sum_{j=0}^{m-2}\rho_2^{m-j-1}\, D_{m,n}^y,\\
&\leq \varepsilon_0\frac{\beta_m}{\rho_2-1}\, D_{m,n}^y.
\end{aligned}$$

The second inequality is obtained by using mean value theorem on the interval $[Z_m^1(n,y), Z_m^2(n,y)]$, $w \in (Z_m^1(n,y), Z_m^2(n,y))$. □

Lemma 6.13. *For $n \geq N$, there exists $C > 0$ such that*

$$\ell_2(E_n) \leq C\frac{n}{\alpha_n}$$

Proof. We have

$$I_1 \leq C_1\,\frac{m}{\beta_m}\; y^{\frac{\lambda_2\alpha_n}{\lambda_1\beta_m}},\; I_2 = C_2\;\frac{1}{\beta_m}\; y^{\frac{\lambda_2\alpha_n}{\lambda_1\beta_m}},\; I_3 \leq C_3\, y^{\frac{\lambda_2\alpha_n}{\lambda_1\beta_m}}\, D_{m,n}^y,$$

where $C_1 = K_n\lambda_2(\tau_2^+ - \tau_2^-)$, $C_2 = K_n\lambda_2(\tau_1^+ + \tau_2^+)$, $C_3 = \varepsilon_0 K_n/(\rho_2 - 1)$.

Proof. Since $D_{m,n}^y \leq I_1 + I_2 + I_3$ we have

$$\begin{aligned}
D_{m,n}^y &\leq (mC_1 + C_2)\frac{1}{\beta_m}\, y^{\frac{\lambda_2\alpha_n}{\lambda_1\beta_m}} + C_3 y^{\frac{\lambda_2\alpha_n}{\lambda_1\beta_m}}\, D_{m,n}^y\\
&\leq (C_1 + C_2)\frac{m}{\beta_m}\, y^{\frac{\lambda_2\alpha_n}{\lambda_1\beta_m}} + C_3 y^{\frac{\lambda_2\alpha_n}{\lambda_1\beta_m}}\, D_{m,n}^y\\
&\leq (C_1 + C_2)\frac{m}{\beta_m}\, y^{\frac{\lambda_2\alpha_n}{\lambda_1\beta_m}} + \frac{1}{2} y^{\frac{\lambda_2\alpha_n}{\lambda_1\beta_m}}\, D_{m,n}^y,
\end{aligned}$$

where the last inequality holds by lemma 6.8 for $n \geq N$ and our choice of $\varepsilon_0 = \min\{1/4, (\rho_2 - 1)/4\}$. Hence for $n \geq N$, we have the estimate

$$\begin{aligned}
D_{m,n}^y &\leq (C_1 + C_2)\frac{m}{\beta_m}\frac{y^{\frac{\lambda_2\alpha_n}{\lambda_1\beta_m}}}{1 - y^{\frac{\lambda_2\alpha_n}{\lambda_1\beta_m}}/2}\\
&\leq \left(\frac{2m\lambda_1(C_1 + C_2)}{\lambda_2\alpha_n}\right)\frac{\frac{\lambda_2\alpha_n}{\lambda_1\beta_m} y^{\frac{\lambda_2\alpha_n}{\lambda_1\beta_m}-1}/2}{1 - y^{\frac{\lambda_2\alpha_n}{\lambda_1\beta_m}}/2}
\end{aligned}$$

Integrating, we get

$$\begin{aligned}\int_{y=a}^{b} D^y_{m,n}\,dy &\leq \int_0^1 D^y_{m,n}\,dy\\ &= \left(\frac{2m\lambda_1(C_1+C_2)}{\lambda_2\alpha_n}\right)\log 2\\ &\leq C\frac{n}{\alpha_n}.\end{aligned}$$

where $C = \frac{2r\lambda_1(C_1+C_2)}{\lambda_2}$. □

Remark 6.14. Our arguments extend immediately to the case of rectangles $E \subset (\{x\}\times[0,1])\times(\{x'\}\times[0,1])$, where $x \in V_1, x' \in V_2$. The key observation is that lemma 6.7 continues to hold and so our arguments all continue to apply with the *same* ε_0.

Estimating $\ell_2(E_n)$ when $\rho_2 = \rho_1$. Assume that $\rho_1 = \rho_2 = \rho$. We need replacements for lemmas 6.7, 6.8. Following our earlier notation, we may choose $N_1 = N(\rho, \lambda_2, \tau_1^-, \tau^+) \in \mathbb{N}$ such that

$$\sup_{n\geq N_1} K_n \leq 2(m_2^-)^{-\frac{1}{\rho-1}}.$$

Set $k = m_2^-$. Linearly rescale A_2 in the x-direction by $e^{-\mu_2 S}$, where S is chosen so that

$$e^{S(\lambda_2-\mu_2)}k^{-\frac{1}{\rho-1}} \leq 1. \tag{6.19}$$

If we let $\hat{A}_2 = [0, e^{-\mu_2 S}]\times[0,1]$, then a lower bound for $\hat{m}_2^-$ on $\hat{A}_2$ is $e^{S(\lambda_2-\mu_2)}k$ and the constant ε_0 in lemma 6.5 rescales to $\hat{\varepsilon}_0 = \varepsilon_0 e^{-\mu S}$.

Replace A_2 by $\hat{A}_2$. On the rescaled A_2 we have

$$\begin{aligned}(m_2^-)^{-\frac{1}{\rho-1}} &\leq (ke^{S(\lambda_2-\mu_2)})^{-\frac{1}{\rho-1}} = k^{-\frac{1}{\rho-1}}e^{S\lambda_2},\\ \varepsilon_0 &= e^{-\mu S}\min\{\frac{1}{4}, \frac{\rho-1}{4}\},\\ \sup_{n\geq N_1} K_n &\leq 2k^{-\frac{1}{\rho-1}}e^{S\lambda_2}.\end{aligned}$$

Lemma 6.12 holds without any assumptions on ρ_1, ρ_2 and so we still have $\left|\log\left(\frac{M_{22}}{M_{21}}\right)\right| \leq \varepsilon_0\frac{\beta_m}{\rho-1}D^y_{m,n}$. We have the following straightforward variation on lemma 6.7.

Lemma 6.15. *If $\rho_1 = \rho_2$, there exists $N \geq N_1$ such that*

$$M_E(n) \leq 2n,\ n \geq N.$$

Finally, for lemma 6.13 to hold, it is enough that $\varepsilon_0 K_n/(\rho-1) \leq \frac{1}{2}$, $n \geq N$. Computing, we find that

$$\begin{aligned}\varepsilon_0 K_n/(\rho-1) &\leq 2\min\{\frac{1}{4}, \frac{\rho-1}{4}\}e^{-\mu_2 S}k^{-\frac{1}{\rho-1}}e^{S\lambda_2}/(\rho_2-1)\\ &\leq \frac{2}{\rho-1}\min\{\frac{1}{4}, \frac{\rho-1}{4}\},\ \text{by (6.19)},\\ &\leq \frac{1}{2}.\end{aligned}$$

Remark 6.16. Of course, we could use our argument for the resonant case $\rho_1 = \rho_2$ in the general case. However, we prefer to present the arguments separately as we feel both arguments have intrinsic interest and may be relevant in problems where product structure is broken.

7. Simulations

In this section, we present numerical simulations which illustrate our results on the likely limit set for the product flow of two attracting homoclinic orbits. We consider the product of identical dynamical systems given by

$$x' = y - x + (x-a)^2, \tag{7.20}$$

$$y' = y + 3x - x^3, \tag{7.21}$$

where $a = 1.7611050$. The two-dimensional system has an attracting homoclinic cycle Σ_1 associated to the saddle point $p = (0.452, -1.263)$ (see figure 10). Since the attractors are identical for the product system, we see that if the initial conditions are equal then the ω-limit set will be the diagonal $\{(u,u), u \in \Sigma_1\} \subset \Sigma_1 \times \Sigma_1$. We look at the ω-limit set of the trajectory with initial condition $((x_1,y_1),(x_2,y_2)) = ((2,2.1),(1.7,1))$. Ignoring the initial transient, we show the projections of this trajectory on the (x_1,x_2)- and (y_1,y_2)-planes in figures 11 and 12.

The projections of the product flow on the (x_1,x_2)- and (y_1,y_2)-planes are illustrated in figures 11 and 12. It is clear from figures that when the (x_1,y_1) components of the trajectory are in the neighbourhood of p then the (x_2,y_2) components of the trajectory visits each point of the homoclinic orbit, and vice-a-versa. The results of the simulation are consistent with the ω-limit being equal to Σ and not $\Sigma_1 \times \Sigma_1$. (Simulations were performed using XPPAUT software [9].)

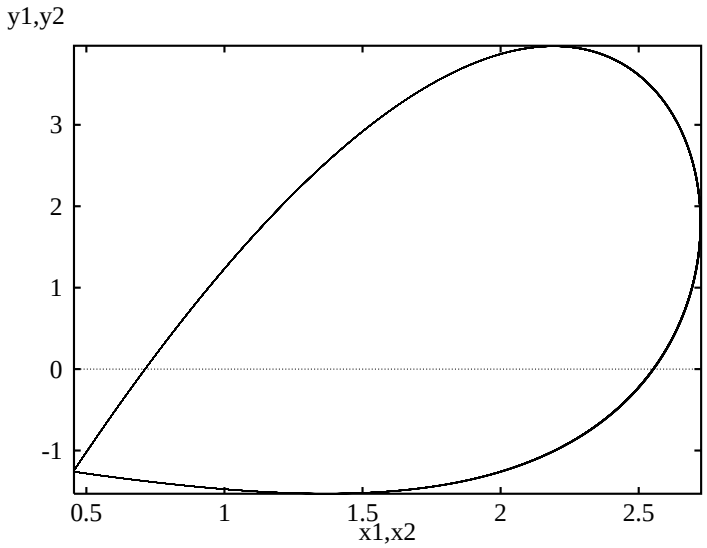

Figure 10. Projection of ω-limit set onto x_1, y_1 plane.

8. Bifurcations near the Product of Attractors

Consider the product dynamics for two planar attracting homoclinic loops $\Sigma_1, \Sigma_2 \subset \mathbb{R}^2$ (for example, the loops associated to the differential equations (7.20,7.21) described in the previous section). We investigate bifurcations that occur when we break either or both of the homoclinic connections but preserve the product structure. We will make use of the Andronov-Leontovich theorem and assume the presence of a splitting parameter (for background and more details we refer to Kuznetsov [18, §6.2], Wiggins [23] or Andronov *et al.* [3]).

Specifically, for $i = 1, 2$, we assume that ξ_i is the splitting parameter governing the homoclinic cycle Σ_i, so that (see figure 13)

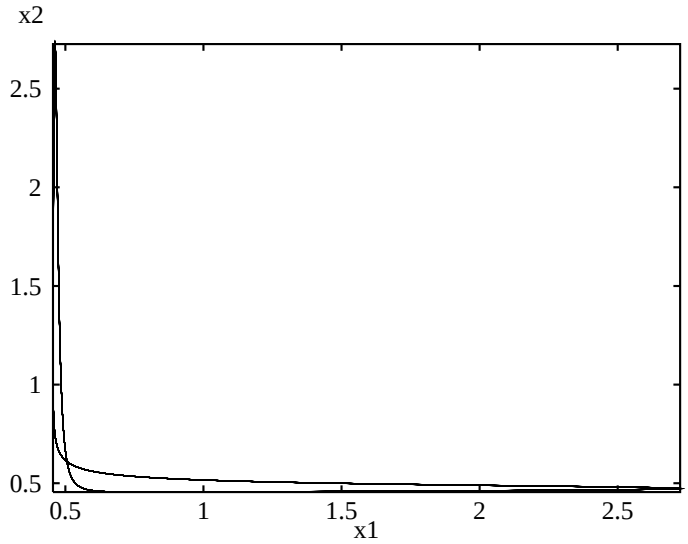

FIGURE 11. Projection of ω-limit set onto x_1, x_2 plane.

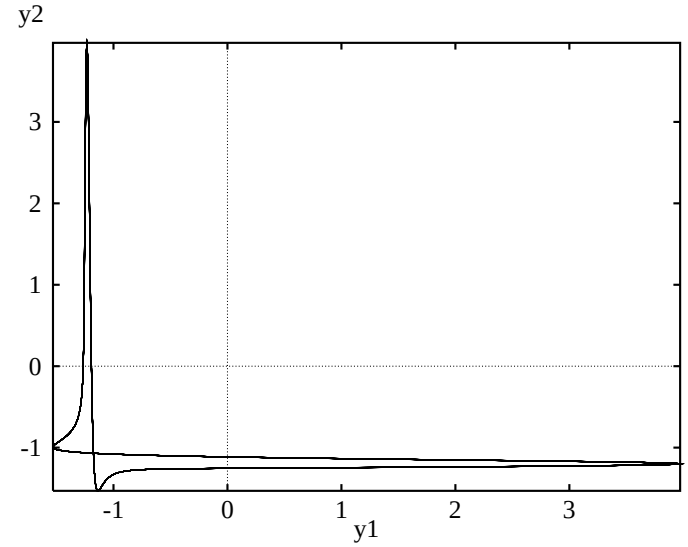

FIGURE 12. Projection of ω-limit set onto y_1, y_2 plane.

(a) for $\xi_i < 0$, the stable manifold lies inside the unstable manifold;
(b) for $\xi_i = 0$, the stable manifold coincides with the unstable manifold giving the homoclinic cycle Σ_i;
(c) for $\xi_i > 0$, the stable manifold lies outside the unstable manifold.

Since the cycles $\Sigma_i \subset \mathbb{R}^2$ are attracting, it follows by the Andronov-Leontovich theorem [3, 18, 23] that for sufficiently small $\xi_i > 0$, there exists a unique stable (hyperbolic) limit cycle $C_i(\xi_i) \subset N_i$ such that as $\xi_i \to 0^+$, the limit cycle $C_i(\xi_i)$ approaches the locus of Σ_i and its period $P_i(\xi_i)$ tends to $+\infty$.

Keeping our earlier notation for the eigenvalues of the linearization at the equilibrium $\mathbf{p}_i$ of Σ_i, we assume that

(NR) $\frac{\mu_2}{\lambda_2} \notin \left\{\frac{3}{2}, 2, 3, 4\right\}$ and

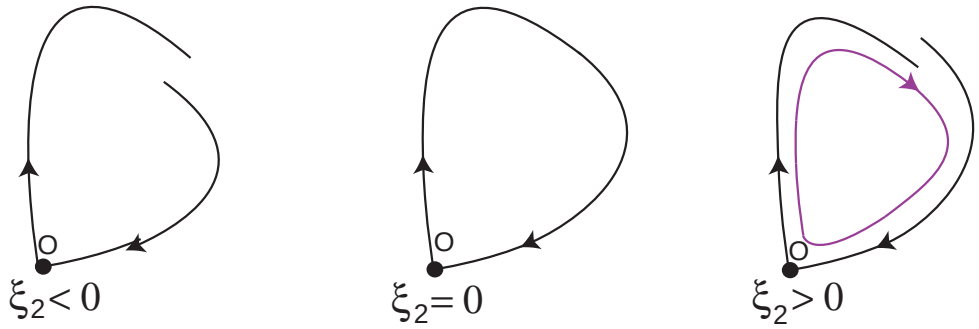

FIGURE 13. Phase plane as splitting parameter is varied

(DI) ϕ_t^2 is at least C^7,

(Conditions (NR,DI) imply that the flow ϕ_t^2 is C^3-linearizable at $\mathbf{p}_2$.) Keeping $\xi_2 = 0$ (so the cycle Σ_2 persists), we break the cycle Σ_1 by varying ξ_1. By Andronov-Leontovich theorem, there exists $\delta_1 > 0$ such that for all $\xi_1 \in (0, \delta)$, there exists a unique stable limit cycle $C_1(\xi_1) \subset N_1$. Applying theorem 1.2 of Ashwin and Field [4], it follows that the minimal Milnor attractor for the product system $\Phi_t^{\xi_1,0} = (\phi_t^{1,\xi_1}, \phi_t^{2,0})$ is the topological torus $C_1(\xi_1) \times \Sigma_2$.

Remark 8.1. Theorem 1.2 of Ashwin and Field is stated for the case when the flow ψ_t on the limit cycle is linear. That is, $\psi_t(\theta) = \theta + \omega t$. However, the result extends immediately to general C^1-flows on a limit cycle. Return times to a section transverse to the homoclinic loop, will be equidistributed, modulo the period. However, points of intersection with the section will generally not be equidistributed.

The torus $C_1(\xi_1) \times \Sigma_2$ is the minimal Milnor attractor that appears along the horizontal axis of the bifurcation diagram depicted in figure 14(a). We have a similar argument when we fix the first system at $\xi_1 = 0$ and perturb the second one.

Moreover, if we set $\mathcal{A} = (0, \delta_1) \times (0, \delta_2)$, then for all $(\xi_1, \xi_2) \in \mathcal{A}$, the likely limit set of $N_1 \times N_2$ is the attracting normally hyperbolic two dimensional torus $\mathbb{T}(\boldsymbol{\xi}) = C_1(\xi_1) \times C_2(\xi_2)$. Note that $\mathbb{T}(\boldsymbol{\xi})$ will be a minimal Milnor attractor if $P_1(\xi_1)/P_2(\xi_1)$ is irrational — this will happen on a full measure subset of $\mathcal{A}$. If the ratio is rational, then the induced flow on $\mathbb{T}(\boldsymbol{\xi})$ is a rational torus flow and so $\mathbb{T}(\boldsymbol{\xi})$ is not even a Milnor attractor.

If the vector field associated to the flow ϕ_t^2 is equivariant under the group $\mathbb{Z}_2(-I)$ generated by $-I(x, y) = (-x, -y)$, then the set $\gamma(\Sigma_2) \neq \Sigma_2$ is also a homoclinic orbit associated to the origin and $\widetilde{\Sigma}_2 = \Sigma_2 \cup \gamma(\Sigma_2)$ defines a figure of eight homoclinic cycle (see section 5). Homoclinic cycles of this type appear often in the literature on the bifurcation theory of planar systems (for example, Dangelmayr & Guckenheimer [7]).

Just as above, we can break the connections for either of the homoclinic loops contained in $\widetilde{\Sigma}_2$. Furthermore, if we analyze the first return map to a cross section in the external part of an attracting figure of eight, we can show the existence of a stable fixed point for $\xi_2 < 0$. That is, a periodic orbit surrounding the figure of eight bifurcates for $\xi_2 < 0$, as shown in figure 15 (see Guckenheimer & Holmes [11], Wiggins [23]).

Next we consider the unfolding of the product of an attracting homoclinic cycle and an attracting figure of eight (see figure 16).

Along the ξ_1 axis (where we break the homoclinic cycle Σ_1), the likely limit set consists of two two-dimensional topological tori $C_1(\xi_1) \times \widetilde{\Sigma}_2$, which intersect in a topological circle. This will be a Milnor attractor, but not minimal. Along the positive ξ_2-axis (where we break the figure of

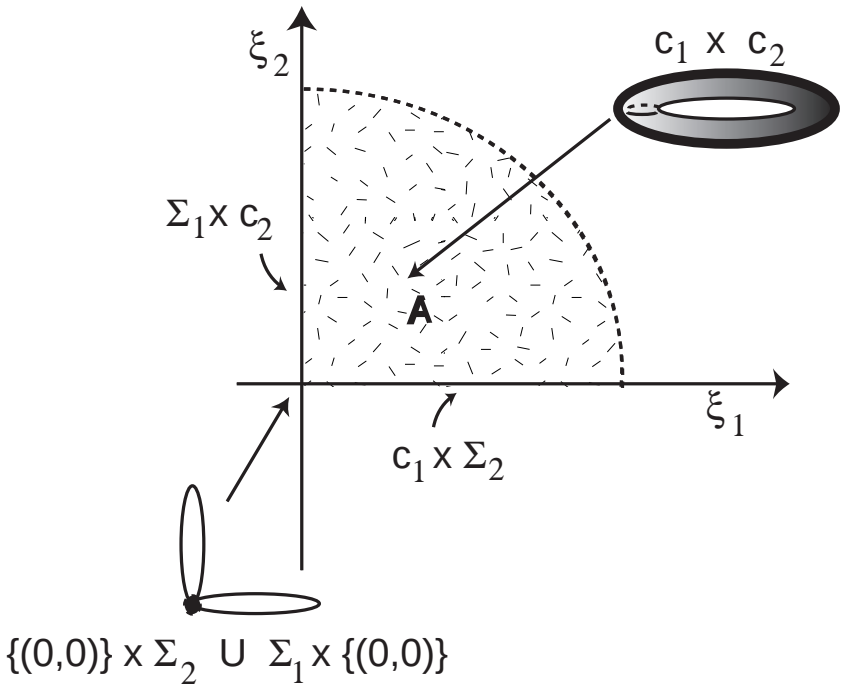

FIGURE 14. Bifurcation diagram for the likely limit set of $N_1 \times N_2$ for a product of homoclinic attractors.

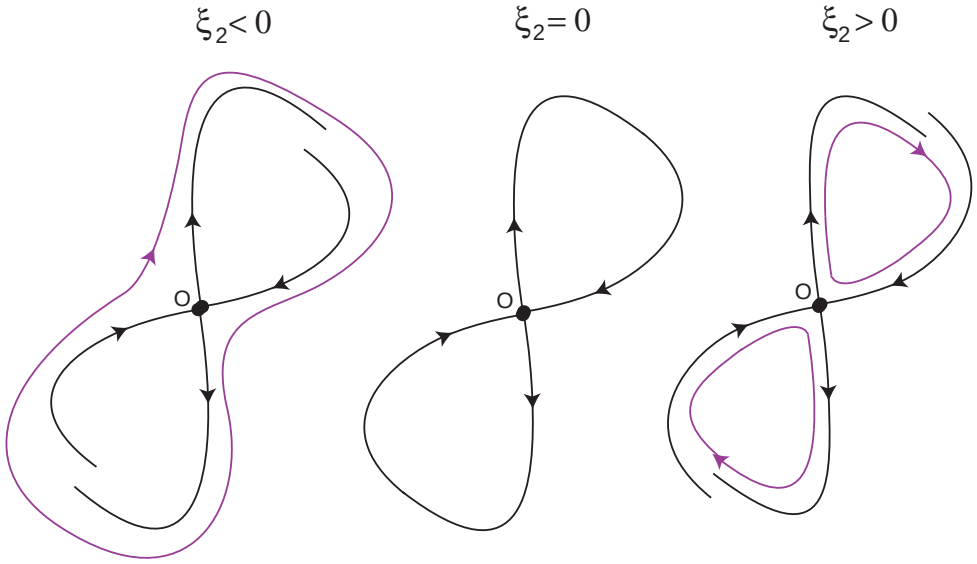

FIGURE 15. Bifurcations to periodic solutions near an attracting figure of eight cycle.

eight $\widetilde{\Sigma}_2$), the Milnor attractor has two connected components $(\Sigma_1 \times C_{12}(\xi_2)) \cup (\Sigma_1 \times C_{22}(\xi_2))$, each of which is a minimal Milnor attractor. Along the negative ξ_2-axis, the minimal Milnor attractor is the product of Σ_1 and the attracting limit cycle that appears outside $\widetilde{\Sigma}_2$. In the

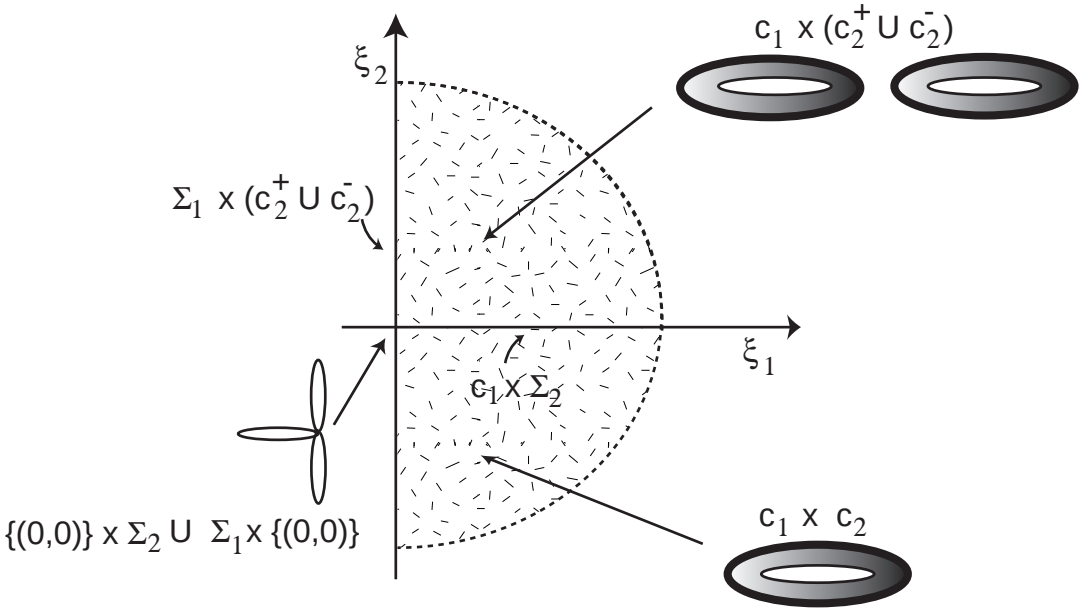

FIGURE 16. Bifurcation diagram for the likely limit set of $N_1 \times N_2$ for the product of a homoclinic attractor and an attracting figure of eight cycle.

first quadrant of the bifurcation diagram there will be two tori which are the likely limit sets for $N_1 \times N_2$. These will be minimal Milnor attractors if the induced flows are irrational torus flows.

Finally, we briefly consider the product of a single homoclinic orbit and a heteroclinic attractor consisting of two equilibria and two connections. The analysis is similar to what we did for the product of two single homoclinic attractors because at least one attracting limit cycle bifurcates from the heteroclinic cycle if the interior connection is broken (see figure 17). Given the heteroclinic network shown in figure 17, a characteristic situation is that there is a unique unstable equilibrium enclosed by each cycle (when $\xi = 0$). When we break the interior heteroclinic connection from A to B, an attracting limit cycle is created. We show a typical scenario in figure 17.

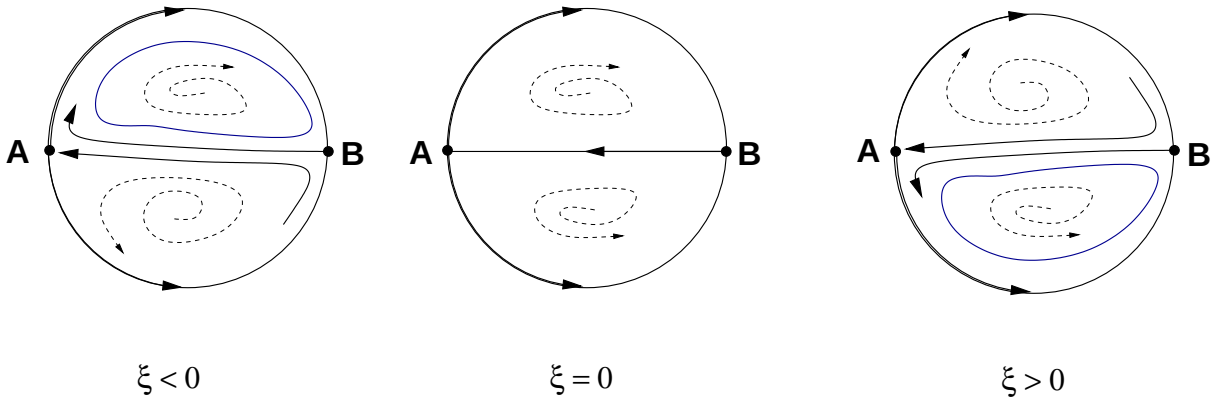

FIGURE 17. An unfolding of a heteroclinic cycle.

9. Discussion and Conclusion

Motivated by the partial results in Ashwin and Field [4] and supported by numerical simulations, we have proved that the likely limit set of the product of two planar heteroclinic attractors is the one-dimensional heteroclinic network which covers the attracting networks in the factors. The result implies that generically two independent trajectories around the heteroclinic connections are forward asynchronous. Following the analysis presented here, it is not difficult to prove that the likely limit set of the product of a finite number of heteroclinic attractors is also the 1-dimensional heteroclinic network which covers the attracting networks in the factors.

For the proof of our main result we needed to assume that the flow was at least C^2. The situation when the flow is only C^1 is far from clear, especially in the resonant case when $\rho_1 = \rho_2$. Since theorem 2.6 holds for C^1-flows, a counterexample in the C^1-case would give the likely limit set as the product of heteroclinic attractors and would likely depend on large fluctuations in the derivative of the connection maps. Similar issues of differentiability arise in the case of the product of a homoclinic attractor and a limit cycle (the result in Ashin and Field [4] required the homoclinic flow to be C^7) and it is not clear whether or not the product of a homoclinic attractor and a limit cycle is a minimal Milnor attractor if the flow (for the homoclinic factor) is less regular, for example C^2.

In the context of game theory and the replicator equation, Sato *et al.* [21] studied numerical examples of heteroclinic networks in the product of simplices. In the case of the Rock-Scissors-Paper game, the dynamics is dependent on the payoff matrices between the players. Under some conditions, numerical evidence was found for the existence of complicated behaviour near the product network. There remain questions about the heteroclinic network which appears in the product dynamics. One candidate heteroclinic network for the product is the product of the heteroclinic networks for each simplex. However, only some cycles might be observable and these may depend on the interaction between the players. This is one reason why we believe our result may have interesting applications outside of equivariant dynamics and network dynamics [1, §5] and why it would be worthwhile generalizing to products of two heteroclinic cycles in higher dimensions. In dimensions greater than 2, issues such as the orientability of the homoclinic connection and the existence of degenerate cases of homoclinic cycles, such as orbit flip and inclination flip, complicate the study. There is also the question of considering the product of a homoclinic cycle with a *butterfly* or *bellows*. We refer to the recent survey by Homburg and Sandstede [14] for more details on these types of cycle as well as issues connected to bifurcation theory and the breakdown of hyperbolicity at the saddle point.

The outstanding question is undoubtedly to obtain quantitative results about the effects of perturbations breaking the product structure to, for example, a skew product structure but keeping the heteroclinic cycles. Does the loss of the product structure lead to phenomena related to essential asymptotic stability or do the likely limit set results persist for small enough perturbations? Put another way, is it possible to find cycle preserving perturbations that make a pre-specified subnetwork essentially asymptotically stable?

References

[1] M Aguiar, P Ashwin, Dias and M Field. 'Dynamics of coupled cell networks: synchrony, heteroclinic cycles and inflation', *Journal of Nonlinear Science*, to appear.

[2] M A D Aguiar, I S Labouriau and A A P Rodrigues. 'Switching near a network of rotating nodes', *Dynamical Systems: an International Journal* **25**(1) (2010), 75–95.

[3] A A Andronov, E A Leontovich, I I Gordon, A G Maier. *Theory of Bifurcations of Dynamical Systems on a Plane* (Israel Program of Scientific Translations, Jerusalem, 1973).

[4] P Ashwin and M Field. 'Product dynamics for homoclinic attractors', *Proceedings of Royal Society, Series A* **461** (2005), 155–177.

[5] P Ashwin and P Chossat, 'Attractors for Robust Heteroclinic Cycles with Continua of Connections', *J. Nonlinear Sci.* **8** (1998), 103–129.

[6] W Brannath. 'Heteroclinic networks on the tetrahedron', Nonlinearity **7** (1994), 1367–1384.
[7] G Dangelmayr and J. Guckenheimer, 'On a four parameter family of planar vector fields', *Arch. Rational Mech. Anal.* **97** (1987), 321–352.
[8] B Deng. 'The Shilnikov problem, exponential expansion, strong λ-lemma, C^1-linearization, and homoclinic bifurcations', *Journal of Differential Equations*, **79** (1989), 189–231.
[9] B Ermentrout. *Simulating, Analyzing, and Animating Dynamical Systems: A Guide to XPPAUT for Researchers and Students* (SIAM, Philadelphia, USA 2003).
[10] M Field. *Dynamics and Symmetry* (Imperial College Press Advanced Texts in Mathematics – Vol. 3, 2007.)
[11] J Guckenheimer and P Holmes, 'Structurally stable heteroclinic cycles', *Math. Proc. Camb. Phil. Soc.* **103** (1988), 189–192.
[12] P Hartman. 'On local homeomorphisms of Euclidean spaces', *Bol. Soc.Mat.Mexicana* **2**(5) (1960), 220-241.
[13] A J Homburg and J Knobloch. 'Switching homoclinic networks', *Dynamical Systems* **23** (2010), 351–358.
[14] A J Homburg and B Sandstede. 'Homoclinic and Heteroclinic Bifurcations in Vector Fields' (Chapter 8 in *Handbook of Dynamical Systems*, vol. 3, Elsevier, 2010).
[15] J F C Kingman and S J Taylor. *Introduction to Measure and Probability*, (Cambridge University Press, 1966).
[16] V Kirk and M Silber. 'A Competition Between Heteroclinic Cycles', *Nonlinearity* **7** (1994), 1605–1621.
[17] M Krupa and I Melbourne. 'Asymptotic Stability of Heteroclinic Cycles in Systems with Symmetry, II,' *Proc. Roy. Soc. Edinburgh* **134A** (2004), 1177–1197.
[18] Yuri A Kuznetsov. *Elements of Applied Bifurcation Theory* (Applied Mathematical Sciences **112**, Spring-Verlag, 1995).
[19] I Melbourne. 'An example of a non-asymptotically stable attractor', *Nonlinearity* **4** (1991), 835–844.
[20] J Milnor. 'On the concept of attractor', *Commun. Math. Phy.* **99** (1985), 177–195.
[21] Y Sato, E Akiyama and J P Crutchfield, 'Stability and Diversity in Collective Adaptation', *Physica D* **210** (2005), 21–57.
[22] L S Shilnikov. *Methods of Qualitative Theory in Nonlinear Dynamics, Part II* (World Scientic Publ. Co. Ltd., Singapore, 2001).
[23] S Wiggins. *Global Bifurcations and Chaos: Analytical Methods* (Springer-Verlag, 1988).
[24] S Wiggins. *Introduction to Applied Nonlinear Dynamical Systems and Chaos* (Springer-Verlag, 2003).

Nikita Agarwal, Department of Mathematics, University of Houston, Houston, TX 77204-3008, USA
E-mail address: nagarwal@math.uh.edu

Alexandre Rodrigues, Centro de Matemática da Universidade do Porto and Faculdade de Ciências da Universidade do Porto, Rua do Campo Alegre 687, 4169-007 Porto, Portugal
E-mail address: alexandre.rodrigues@fc.up.pt

Michael Field, Department of Mathematics, University of Houston, Houston, TX 77204-3008, USA
E-mail address: mf@uh.edu

Discussion and Future Work

The case for my life, then, or for that of anyone else who has been a mathematician in the same sense in which I have been one, is this: that I have added something to knowledge, and helped others to add more; and that these somethings have a value which differs in degree only, and not in kind, from that of the creations of the great mathematicians, or of any of the other artists, great or small, who have left some kind of memorial behind them.

G. Hardy, A Mathematician's Apology

The six works in this thesis have investigated the dynamics near heteroclinic cycles and networks; in articles [1-5] the nodes of the heteroclinic cycles and networks networks are either saddle-foci or non-trivial periodic solutions. In article 6, we give a contribution to the study of the dynamics near the product of *uncoupled* attracting planar systems.

In article 1, besides a rigorous definition of *switching*, we describe a mechanism which provides switching near a heteroclinic network embedded in a three-dimensional manifold without boundary, exhibiting infinitely many initial conditions following any prescribed infinite heteroclinic path. This phenomenon is generated by the presence of rotating nodes and the fact that all connections that take place in two-dimensional invariant manifolds occur as transverse intersections.

In three-dimensions this seems to be the only possible mechanism for the existence of *infinite switching*. This mechanism also works in higher dimensions if we can capture the heteroclinic network inside a three-dimensional manifold. This may be achieved using either the *center manifold of heteroclinic cycles* [**74, 75**] or the *normal hyperbolicity* [**31**] of a three-dimensional flow-invariant set.

In n-dimensional smooth manifolds ($n > 3$), there are other mechanisms for the existence of forward switching: for example, in Kirk *et al* [**40**] the *transversality* is not necessary; switching holds just by the the presence of spiralling due to complex eigenvalues in the linearized flow about one of the nodes *common to all* cycles in the network. For conservative systems, in the context of game theory, Aguiar [**2**] and Aguiar and Castro [**4**] proved switching without neither rotating nodes nor transversality.

Switching and the associated dynamics near the network are *independent* on the ratio between the real part of the contracting and the real part of the expanding eigenvalues [6]; the only condition we require is the non-resonance C^1–condition of Samovol [**66**]. At the first glance, there is no guarantee that this condition will hold for small perturbations since the condition for resonances seems to be dense in $\mathbf{R}$ (see section 2.9 of Shilnikov *et al* [**74**]). Nevertheless we have been able to prove that in three dimensional smooth manifolds, this does not occur. More precisely, if $\tilde{f}$ is a smooth hyperbolic germ of a vector field f defined on a three-dimensional smooth manifold, at an equilibrium point p, whose linearization has a real eigenvalue μ and two complex non-real conjugate eigenvalues of the form $\lambda + \omega i$, such that $|\mu| \neq |\lambda|$ and $\mu\lambda < 0$, then $\tilde{f}$ is C^1 –conjugated to $df(p)$.

Using the results of Aguiar *el al* [**5**], we may also conclude that the existence of switching is accompanied by chaotic dynamics namely the existence of a *nested chain* of suspended horseshoes accumulating on the network, with the same shape as it. Switching may also be realised by periodic trajectories (if the heteroclinic path is periodic) as well as by the invariant manifolds involved in the transverse intersection.

Article 1 also contains an example (constructed in Aguiar [**1**]), satisfying the conditions which entail switching. As in Kirk and Rucklidge [**42**], we start with a heteroclinic network with reflectional and rotational symmetry. However, in contrast to [**42**], we prove switching in a perturbation that does not break completely the network. Since the non-robust connections do not coincide, in [**42**] the authors were only able to conclude the existence of initial conditions following *finite* heteroclinic paths on the network.

The trajectory shadowing the heteroclinic network is far from being unique. Paper 2 is a good tool to understand the difference between two different solutions that shadow the same heteroclinic path: they differ on the number of revolutions around the *rotating* nodes.

In article 2, asking again for transverse intersection of the invariant manifolds of successive nodes, we investigate a way to code all trajectories that remain forever close to a heteroclinic cycle associated to a finite number of periodic solutions. Given a set of Poincaré sections (associated to a set of isolating blocks), we conclude about the existence of a *robust* and *transitive* set Λ of initial conditions whose trajectories follow the cycle for negative and positive times. Usind techiques developed by Alekseev [**8**] and by Shilnikov [**70**], we prove that the dynamics of the discretization of the flow (in Λ) is conjugated to a Markov shift over a finite alphabet . This conjugacy codes *all* trajectories lying in the nonwandering set associated to the cycle. The particular and remarkable point is that the *word* associated to each trajectory can be interpreted as the number of turns around the limit cycles. Our explicit conjugacy allows us to prove that the set of heteroclinic

[6] With respect to article 1, we are able to prove the existence of an invariant set near the perturbed heteroclinic network, even when the unperturbed network is completely repelling.

connections is dense in the *nonwandering* set associated to the original cycle. Following Alekseev [**8**], we also prove that the discretization of the flow is a *quasirandom* system, *ie*, we prove that there exists an invariant set with positive Lebesgue measure with positive *topological entropy*, which implies the existence of infinitely many distinct knot types for the flow (Franks and Williams [**23**]) An obvious continuation of this work is to generalise the result for heteroclinic networks involving saddle-foci. This analysis should be more tricky since, if we allow the presence of equilibria in the network, the transversality of all consecutive nodes is not possible.

The Cantor sets found near the heteroclinic network described in articles 1 and 2 are seccionaly hyperbolic and they admit an invariant splitting over the whole set (where the first return is well defined). Our current problem is to identify and determine the structure of the attractors that persist after perturbation of the network. This is why several people are interested in accurate numerical methods which allow the capture of the complex dynamics in such systems.

At this point, it would be fruitful to see the difference between our horseshoes and those of Labarca and Pacífico [**47**]; they found singular hyperbolic sets near heteroclinic cycles defined on compact manifolds with boundary. In both cases, the equilibrium is accumulated by periodic solutions of saddle type. The nonwandering trajectories near the heteroclinic cycle associated to periodic trajectories must contain an uniformly hyperbolic horseshoe. When at least one node of the cycle is a saddle-focus, the horseshoe cannot be uniformly hyperbolic since the hyperbolic splitting cannot be extended continuously to equilibria. We guess the existence of a non-robust partially hyperbolic set (together with hyperbolic sets) with a very complex spiralling structure. Understand completely the nonwandering set associated to this kind of heteroclinic cycles and networks is far from being done.

Heteroclinic networks appear in several mathematical models of physical systems near symmetry. This is the case of article 3, in which we proved analitically that the model for the geomagnetic field given by Melbourne, Proctor and Rucklidge [**54**] explains excursions and reversals of the Earth's magnetic field.

Although the details of the reversal process are not completely understood, the occurrence of reversals is well documented by studying for example, layers of iron-rich lava rocks. In article 3, using the concepts of switching and cycling of articles 1 and 2, we prove that the mathematical model given by Melbourne, Proctor and Rucklidge [**54**] is relevant for the study of magnetohidrodynamics and that this model *predicts* and explains intermittent behaviour of the geomagnetic field and geo-reversals. The lengths of time intervals of constant polarity and the short duration of each reversal are consistent with

those of the Earth. Also, the model explains why the geomagnetic field is predominantly axial dipolar.

Due to the chaotic behaviour induced by the presence of suspended horseshoes near the network, we may conclude that there is no satisfactory way to predict the duration of any given polarity.

In general, the capture of all trajectories that remain in the neighbourhood of the network (or what remains from it) is very complicated. Articles 4 and 5 can be understood as an attempt to describe the effect of small symmetry-breaking on the dynamics near two $\mathbf{Z}_2 \oplus \mathbf{Z}_2$ – equivariant heteroclinic cycles associated to two saddle-foci of different type, whose heteroclinic connections coincide. Breaking one $\mathbf{Z}_2$ – symmetry, we found in paper 4, an attractor containing two saddle-foci (Bykov cycle), heteroclinic trajectories connecting transversely them and a non-trivial hyperbolic basic set near the network. This attractor is *non-robust* under generic perturbations. Breaking the other symmetry, the network disappears but near the *ghost* of each cycle, there will appear a unique hyperbolic periodic solution. The stability of this orbit is related to the stability of the original network. An interaction between the parameters that govern the symmetries allowed us to plot a bifurcation diagram where a sequence of homoclinic orbits with different stabilities coexists with topological horseshoes. The study of this type of homoclinic bifurcations is one of the most important global bifurcation phenomena which occurs in many applications (see for example Medrano *et al* [**51**] who applied these bifurcations to a survey about the *double-scroll circuit*).

A surprising phenomenon found in article 5 is the existence of heteroclinic tangencies. The capture of these tangencies has been possible because we did not assume the transition map $\Psi_{\mathbf{v}\to\mathbf{w}}$ to be the identity. In the presence of heteroclinic tangencies, for a set of parameters having positive Lebesgue measure, it occurs shift dynamics with respect to arbitrarily many symbols together with wild hyperbolic sets and infinitely many *Newhouse* sinks (see Champneys *et al* [**19**] and Shilnikov [**73**]). Our study can also contribute to the understanding of bifurcations involving these structures. Due to the existence of folds between the heteroclinic manifolds, we conjecture the existence of *Hénon-like strange attractors* near the heteroclinic cycles.

In article 6, using a delicate and tricky analysis of the time of flight of a trajectory near a fixed neighbourhood of the saddle equilibria and around a planar homoclinic cycle, we proved the conjecture of Ashwin and Field [**12**] (on the plane) which states that the likely limit set of the product of two attracting heteroclinic cycles is the network defined as the union of the attracting sets. For general attracting heteroclinic networks whose nodes are not rotating, we expect the presence of *essentially asymptotically stable* subnetworks. The product of homoclinic attractors studied in article 6 is completely

unexpected because it leads to heteroclinic networks in which the above property does not hold and simultaneously it does not have *switching*. Following the analysis presented, it is not difficult to prove that the likely limit set of a finite number of heteroclinic attractors is also the *union* of the cycles. Our result may be generalized for the product of two heteroclinic cycles in higher dimensions.

The distant future of trajectories near a heteroclinic network is practically inaccessible and may only be described in average, in probabilistic and ergodic terms. A good problem related to our work is about the convergence of *times-averages* associated to trajectories that remain near the network for all time (see Takens [**79**] for a setup of this notion). Gaunersdorfer [**24**] and Takens [**78**] showed that each orbit in the domain of an attracting heteroclinic cycle has historic behaviour. A discrete orbit $\{x, \phi(x), \phi^2(x), \phi^3(x), \ldots\}$ has historic behaviour if for some continuous map $f : X \to \mathbf{R}$, the average $\lim_n \frac{1}{n+1} \sum_{i=0}^{n} f(\phi^n(x))$ does not exist. In [**79**], the author explains why this definition has been adopted. It would be interesting to generalise this result for higher dimensions and investigate whether, in the case of a heteroclinic network of rotating nodes, almost all trajectories have historic behaviour.

In summary, in this thesis we attempted to give a useful contribution to the understanding of the dynamics near general heteroclinic networks but a lot more needs to be done before the dynamics is completely understood.

Bibliography

[1] M. A. D. Aguiar, *Vector fields with heteroclinic networks*, Phd thesis, Departamento de Matemática Aplicada, Faculdade de Ciências da Universidade do Porto, 2003

[2] M. A. D. Aguiar, *Is there switching for replicator dynamics and bimatrix games?*, Physica D: Nonlinear Phenomena, 240 1475–1488, 2011

[3] M. A. D. Aguiar, P. Ashwin, A. P. S. Dias and M. Field, *Dynamics of coupled cell networks: Synchrony, heteroclinic cycles and inflation*, Journal of Nonlinear Science, No. 21, Issue 2, 271–323, 2011

[4] M. A. D. Aguiar and S. Castro, *Chaotic switching in a two-person game*, Physica D, 239, 1598–1609, 2010

[5] M. A. D. Aguiar, S. Castro, and I. Labouriau, *Dynamics near a heteroclinic network*, Nonlinearity, 18, 391–414, 2005

[6] M. A. D. Aguiar, S. B. S. D. Castro and I. S. Labouriau, *Simple Vector Fields with Complex Behavior*, Int. Jour. of Bif. and Chaos, Vol. 16 No. 2, 369–381, 2006

[7] V. S. Afraimovich, V. V. Bykov, L. P. Shilnikov, *On the appearence and structure of the Lorenz attractor*, Dokl. Acad. Sci. USSR, No. 234, 336–339, 1977

[8] V. Alekseev, *Quasirandom dynamical systems. I. Quasirandom diffeomorphisms*, Mat. Sbornik, Tom 76 (118), No. 1, 72–134, 1968

[9] V. Araújo and M. J. Paciífico, *Three-Dimensional Flows*, Vol. 53 of Ergebnisse der Mathematik und ihrer Grenzgebiete, Springer, 2010

[10] D. Armbruster, E. Stone and V. Kirk, *Noisy heteroclinic networks*, Chaos, No. 13, 73–128, 2003

[11] P. Ashwin and P. Chossat, *Attractors for Robust Heteroclinic Cycles with Continua of Connections*, J. Nonlinear Sci., Vol. 8, 103–129, 1998

[12] P. Ashwin and M. Field, *Heteroclinic networks in coupled cell systems*, Arch. Ration. Mech. Anal., No. 148, 107–143, 1999

[13] P. Ashwin and M. Field, *Product dynamics for homoclinic attractors*, Proceedings of Royal Society, Series A 461 , 155–177, 2005

[14] P. Ashwin, A. Rucklidge, and R. Sturman, *Two-state intermittency near a symmetric interaction of saddle-node and Hopf bifurcations: a case study from dynamo theory*, Physica D, 194, 30–48, 2004

[15] F. Busse and R. Clever, *Nonstationary convection in a rotating system*, Recent Developments in Theoretical and Experimental Fluid Mechanics, Springer-Verlag, Berlin, 1979

[16] V. Bykov, *Orbit Structure in a Neighbourhood of a Separatrix Cycle Containing Two Saddle-Foci*, Methods of qualitative theory of differential equations and related topics, Amer. Math. Soc., Providence, No. 200, 87–97, 2000

[17] W. Brannath, *Heteroclinic networks on the tetrahedron*, Nonlinearity 7, 1367–1384, 1994

[18] S. Castro, I. Labouriau and O. Podvigina, *A heteroclinic network in mode interaction with symmetry*, Dynamical Systems: an international journal, Vol. 25, Issue 3, 359–396, 2010

[19] A. Champneys, V. Kirk, E. Knobloch, B. Oldeman, J. Rademacher, *Unfolding a Tangent Equilibrium-to-Periodic Heteroclinic Cycle*, SIAM J. Appl. Dyn. Syst., No. 8, 1261–1304, 2009

[20] P. Channell, G. Cymbalyuk and A. Shilnikov, *Origin of Bursting through Homoclinic Spike Adding in a Neuron Model*, Physical Review Letters, PRL 98, 134101–134105, 2007

[21] M. Field, *Lectures on bifurcations, dynamics and symmetry*, Pitman Research Notes in Mathematics Series, Vol. 356, Longman, 1996

[22] M. Field, *Dynamics and Symmetry (Imperial College Press Advanced Texts in Mathematics)*, Vol. 3, 2007

[23] J. Franks and R. F. Williams, *Entropy and Knots*, Transactions of the American Mathematical Society, Vol. 291, No. 1, 241–253, 1985

[24] A. Gaunersdorfer, *Time averages for heteroclinic attractors*, SIAM J. Math. Anal. 52, 1476–1489, 1992

[25] P. Glendinning and C. Sparrow, *Local and Global Behaviour near Homoclinic Orbits*, J. Stat. Phys., 35, 645–696, 1984

[26] P. Glendinning and C. Sparrow, *T-points: a codimension two heteroclinic bifurcation*, J. Stat. Phys., 43, 479–488, 1986

[27] M. Golubitsky and I. Stewart, *The Symmetry Perspective*, Birkhauser, 2000

[28] S. Gonchenko, D. Turaev and L. Shilnikov, *Homoclinic Tangencies of an Arbitrary Order in Newhouse Domains*, Journal of Mathematical Sciences, Vol. 105, No. 1, 69–128, 2001

[29] S. Gonchenko, D. Turaev and L. Shilnikov, *Homoclinic Tangencies of Arbitrarily High Orders in Conservative and Dissipative Two-Dimensional Maps*, Nonlinearity, 20, 241–271, 2007

[30] J. Guckenheimer and R. F. Williams, *Structural stability of Lorenz attractors*, Publ. Math. IHES, No. 50, 59–72, 1979

[31] M. W. Hirsch, C. C. Pugh and M. Shub, *Invariant Manifolds*, Lecture Notes in Mathematics, 583, Springer-Verlag, 1977

[32] J. Hofbauer and K. Sigmund, *Evolutionary Game Dynamics*, Bulletin of the American Mathematical Society, Vol. 40, 2003

[33] J. Hofbauer, *Heteroclinic cycles in ecological differential equations*, Tatra Mount. Math. Publ. 4, 105–116, 1994

[34] P. Holmes, *A strange family of three-dimensional vector fields near a degenerate singularity*, J. Diff. Eqns, 37, 382–403, 1980

[35] A. J. Homburg, *Global Aspects of Homoclinic Bifurcations in Vector Fields*, Memoirs of the American Mathematical Society, Vol. 121, No. 578, American Mathematical Society, 1996

[36] A.J. Homburg and J. Knobloch, *Multiple homoclinic orbits in conservative and reversible systems*, Transactions Amer. Math. Soc. 358, 1715–1740, 2006

[37] A.J. Homburg and J. Knobloch, *Switching homoclinic networks*, Dynamical Systems: an International Journal, Vol. 25, Issue 3, 351–358, 2010

[38] A. J. Homburg and B. Sandstede, *Homoclinic and Heteroclinic Bifurcations in Vector Fields*, Chapter 8 in Handbook of Dynamical Systems, Vol. 3, Elsevier, 2010

[39] A. Jukes, *Homoclinic Bifurcations*, PhD Thesis, Imperial College of London, 2006

[40] V. Kirk, E. Lane, C. Postlethwaite, A. Rucklidge and M. Silber, *A mechanism for switching near a heteroclinic network*, Dynamical Systems: An International Journal, Vol. 25, Issue 3, 323–349, 2010

[41] V. Kirk and M. Silber, *A Competition Between Heteroclinic Cycles*, Nonlinearity 7, 1605–1621, 1994

[42] V. Kirk and A. Rucklidge, *The effect of symmetry breaking on the dynamics near a structurally stable heteroclinic cycle between equilibria and a periodic orbit*, Dynamical Systems: an International Journal, Vol. 23, Issue 2, 42–74, 2008

[43] J. Knobloch, *Bifurcation of degenerate homoclinics in reversible and conservative systems*, J. Dynam. Differential Equations, Vol. 9, 427–444, 1997

[44] W. Koon, M. Lo, J. Marsden and S. Ross, *Heteroclinic Connections between Periodic Orbits and Resonance Transition in Celestial Mechanics*, Control and Dynamical Systems Seminar (California Institute of Technology), 1999

[45] M. Krupa and I. Melbourne, *Asymptotic stability of heteroclinic cycles in systems with symmetry*, Ergod. Th. & Dynam. Sys., 15, 121–147, 1995

[46] M. Krupa and I. Melbourne, *Asymptotic Stability of Heteroclinic Cycles in Systems with Symmetry II*, Proc. Roy. Soc. Edinburgh, No. 134A, 219–232, 2004

[47] R. Labarca and M. Pacífico, *Stability of singular horseshoes*, Topology 25, 1986

[48] J. Lamb, M. Teixeira and K. Webster, *Heteroclinic bifurcations near Hopfzero bifurcation in reversible vector fields in* $\boldsymbol{R}^3$, Journal of Differential Equations, 219, 78–115, 2005

[49] X. B. Lin, *Using Melnikov's method to solve Shilnikov's problem*, Proc. Roy. Soc. Edinburgh, No. 116 A, 295–325, 1990

[50] E. N. Lorenz, *Deterministic nonperiodic flow*, J. Atmosph. Sci., No. 20, 130–141, 1963

[51] R. Medrano, M. Baptista and I. Caldas, *Homoclinic orbits in a piecewise system and their relation with invariant sets*, Physica D, 186, 133–147, 2003

[52] I. Melbourne, *Intermittency as a codimension three phenomenon*, J. Dyn. Diff. Eqn. Vol. 1, No. 4, 347–367, 1989

[53] I. Melbourne, *An example of a nonasymptotically stable attractor*, Nonlinearity 4, 835–844, 1991

[54] I. Melbourne, M. R. E. Proctor and A. M. Rucklidge, *A heteroclinic model of geodynamo reversals and excursions*, Dynamo and Dynamics, a Mathematical Challenge (eds. P. Chossat, D. Armbruster and I. Oprea, Kluwer: Dordrecht, 363–370, 2001

[55] R. Moeckel, *Chaotic Orbits in the Three Body Problem*, in P.H. Rabinowitz, A. Ambrosetti, I. Ekeland and E.J. Zehnder (eds.) Periodic Solutions of Hamiltonian Systems and Related Topics (Il Ciocco 1986) NATO ASI Ser. C 209, Reidel, Dordrecht, 203–219, 1987

[56] C. A. Morales, M. J. Pacífico and E. R. Pujals, *Robust transitive singular sets for 3-flows are partially hyperbolic attractors or repellers*, Ann. of Math., No. 2, Vol. 160, 375–432, 2004

[57] H. K. Ngueyen and A. J. Homburg, *Resonant heteroclinic cycles and Lorenz type attractors in models for skewed varicose instability*, Nonlinearity, No. 18, 155–173, 2005

[58] A. Palacios and H. Juarez, *Criptography with Cycling Chaos*, Physics Letters A, Vol. 303, Issues 5-6, 345–351, 2002

[59] C. Postlethwaite, *A new mechanism for stability loss from a heteroclinic cycle*, Dynamical Systems: An International Journal, Vol. 25, Issue 3,305–322, 2010

[60] C. Postlethwaite and J. Dawes, *A codimension two resonant bifurcation from a heteroclinic cycle with complex eigenvalues*, Dynamical Systems: An international Journal, 21, 313–336, 2006

[61] J. Rademacher, *Homoclinic orbits near heteroclinic cycles with one equilibrium and one periodic orbit.* J. Differential Equations 218, 390–443, 2005

[62] J. Rademacher, *Homoclinic Bifurcation from Heteroclinic Cycles with Periodic Orbits and Tracefiring of Pulses*, PhD Thesis, Faculty of Graduate School of the University of Minnesota, 2004

[63] G. L. dos Reis, *Structural Stability of Equivariant Vector Fields on Two-Dimensions*, Trans. Am. Math. Soc. 283, 633–643, 1984

[64] A. Rovella, *The dynamics of perturbations of contracting Lorenz maps*, Bol. Soc. Brasil. Mat. No. 24, 233–259, 1993

[65] B. Sandstede and A. Scheel, *Forced Symmetry Breaking of Homoclinic Cycles*, Nonlinearity 8, 333–365, 1995

[66] V. Samovol, *Linearization of a system of differential equations in the neighbourhood of a singular point*, Sov. Math. Dokl, Vol. 13, 1255–1259, 1972

[67] Y. Sato, E. Akiyama and J Farmer, *Chaos in learning a simple two-person game*, *PNAS* 997, 4748–4751, 2002

[68] M. Shashkov and D. V. Turaev, *An Existence Theorem of Smooth Nonlocal Center Manifolds for Systems Close to a System with a Homoclinic Loop*, J. Nonlinear Sci., Vol. 9, 525–573, 1999

[69] L. Shilnikov, *A case of the existence of a denumerable set of periodic motions*, Sov. Math. Dokl. 6, 163–166, 1965

[70] L. Shilnikov, *A Poincaré-Birkhoff problem*, Mat. Sb. 74, 378–397, 1967

[71] L. Shilnikov, *On the generation of a periodic motion from trajectories doubly asymptotic to an equilibrium state of saddle type*, Math. USSR Sbornik 77(119), 461–472, 1968

[72] L. Shilnikov, *A contribution to the problem of the structure of an extended neighborhood of a rough state of saddle-focus type*, Math. USSR Sbornik 81(123), 92–103, 1970

[73] L. Shilnikov, *Bifurcations and Strange Attractors*, Proceeding of the ICM, Beijing, Vol. 3, 349–372, 2002

[74] L. Shilnikov, A. Shilnikov, D. Turaev, and L. Chua, *Methods of Qualitative Theory in Nonlinear Dynamics 1*, World Scientific Publishing Co., 1998

[75] L. Shilnikov, A. Shilnikov, D. Turaev, and L. Chua, *Methods of Qualitative Theory in Nonlinear Dynamics 2*, World Scientific Publishing Co., 1998

[76] S. Smale, *Diffeomorphisms with many periodic points*. Diffential and Combinatorial Topology (symposium in honor of Marston Morse, 63–80, Princeton, 1965

[77] S. Smale, *Differentiable dynamical systems*, Bull. Am. Math. Soc., No. 73, 747–817, 1967

[78] F. Takens, *Heteroclinic attractors: time averages and moduli of topological stability* Bol. Soc. Bras. Mat. 25, 107–120, 1994

[79] F. Takens, *Orbits with historic behaviour, or non-existence of averages – Open Problem*, Nonlinearity, 21, 33–36, 2008

[80] C. Tresser, *About some theorems by L. P. Shilnikov*, Ann. Inst. Henri Poincaré, 40, 441–461, 1984

[81] W. Tucker, *The Lorenz attractor exists*, C. R. Acad. Sci. Paris Sér. I Math. No. 328, 1197–1202, 1999